INFORMATION TO USERS

This manuscript has been reproduced from the microfilm master. UMI films the text directly from the original or copy submitted. Thus, some thesis and dissertation copies are in typewriter face, while others may be from any type of computer printer.

The quality of this reproduction is dependent upon the quality of the copy submitted. Broken or indistinct print, colored or poor quality illustrations and photographs, print bleedthrough, substandard margins, and improper alignment can adversely affect reproduction.

In the unlikely event that the author did not send UMI a complete manuscript and there are missing pages, these will be noted. Also, if unauthorized copyright material had to be removed, a note will indicate the deletion.

Oversize materials (e.g., maps, drawings, charts) are reproduced by sectioning the original, beginning at the upper left-hand corner and continuing from left to right in equal sections with small overlaps.

ProQuest Information and Learning
300 North Zeeb Road, Ann Arbor, MI 48106-1346 USA
800-521-0600

The Assessment of Reinforcing Steel Corrosion in the South Section of the Dickson Bridge

by

François Laplante

Department of Civil Engineering and Applied Mechanics
McGill University
Montreal, Canada
July 2000

A THESIS SUBMITTED TO THE FACULTY OF GRADUATE STUDIES AND RESEARCH IN PARTIAL FULFILMENT OF THE REQUIREMENTS OF THE DEGREE OF MASTER OF ENGINEERING

The Assessment of Reinforcing Steel Corrosion in the South Section of the Dickson Bridge

by

François Laplante

Department of Civil Engineering and Applied Mechanics
McGill University
Montreal, Canada

July 2000

Abstract

Reinforced concrete structures in aggressive environments can suffer from premature deterioration due to the development of various detrimental physical and chemical mechanisms. Bridges and highway structures designed and constructed without sufficient concern about durability are particularly vulnerable to early deterioration.

To better understand the degradation mechanisms of chloride-induced corrosion, existing corroded structures need to be studied. The decommissioned Dickson bridge, built in 1959 in the eastern part of Montreal in Canada, provided an invaluable opportunity to assess the cause(s) of deterioration of a reinforced concrete bridge structure. The cause of premature deterioration was primarily the development of extensive chloride-induced corrosion of the steel reinforcement.

McGill University, in collaboration with some industrial partners, and the Centre des Études et Recherche en Infrastructure Urbaine (CERIU) undertook a joint research program between 1997 and 1999. Intensive testing of the bridge deck confirmed the causes of deterioration and allowed for the validation and calibration of several testing techniques developed to determine the causes and the extent of the action of various processes related to durability of reinforced concrete structures.

Measuring techniques used on the Dickson bridge can be divided into two distinct categories : techniques measuring the extent of damage to the steel reinforcement and techniques assessing the quality of the protective media (Portland cement concrete). The conclusions of this study can be summarized as follows :

- According to most standard test techniques (half-cell potential, concrete cover, corrosion rate and corrosion potential tests, and the concrete resistivity test), the concrete bridge deck of the south section of the Dickson Bridge showed high risks of developing corrosion of the reinforcing steel : this situation applied for most of the structure. Moreover, the test results indicated that the east and west

sides, along with the north end of the Bridge were in a critical situation with regards to corrosion where the development of the reaction was extensive. By comparing with the results obtained for the central and north section of the bridge, it appeared that the south section of the bridge deck was in a relatively better condition among all three sections;

- The ingress of chloride ions into the concrete was identified as the initiating agent of the corrosion reaction, since no trace of carbonation was found in the vicinity of the deck surface reinforcement where relatively high concentrations of chlorides were observed;
- Based on the complete analysis of the data collected on the Dickson Bridge, it appeared that the half-cell potential test, the chloride concentration test at the rebar level, the electrical resistivity test, the corrosion rate test (LPR) and the compressive strength currently provide the best information concerning the risks of corrosion. They represent valuable standard techniques susceptible to satisfactorily determine the extent of the deterioration of a structure and to characterize the susceptibility of the steel reinforcement embedded in concrete to steel corrosion based on standard criteria;
- The combination of several test techniques appeared to significantly improve and simplify the analysis of results. The comparison of the results obtained from the different tests provided some complementary information leading to the improvement of the individual analyses of testing techniques:
- However, the reliability and accuracy of most in-situ techniques were not clearly established through this research project : the results for the linear polarization resistance test, chloride diffusion migration test, water permeability test and apparent chloride diffusion test showed a high variability and the repeatability of the half-cell potential, linear polarization resistance and concrete cover techniques used were not determined systematically as several readings were obtained for different locations. In addition, the water permeability test, chloride diffusion migration test, and the tests performed on cores were not repeated during this research project. The use of the linear polarization resistance technique was found to be suitable for the in-situ

determination of the corrosion rate and of the corrosion potential, but the results for these tests and for the half-cell potential test were in most cases difficult to correlate. For the newly developed techniques for which no standard procedure exist (Autoclam in-situ water permability test, and the Queen's of Belfast chloride diffusion migration test), the accuracy and the repeatability were neither established properly during the testing phase of this investigation, nor during testing of the north and central sections of the Dickson Bridge. For the three sections of the bridge, the values of the coefficient of variation were indicative of this inadequate situation : for the chloride diffusion migration test on the north, central, and south sections, the coefficients of variation found were 48 %, 55 %, and 136 %, respectively; for the water permeability test on the north and south sections, the coefficients of variation found were 118 %, and 142 %, respectively (an index value was calculated for the central section, and could not be compared). These high coefficients of variation reflect : (1) the inadequacy of the testing technique to perform accurate measurements, and (2) the great variability of the quality of the tested concrete. Consequently, the interpretation of the results obtained using these techniques was found to be limited and the reliability definitely needs to be established before a general and systematic use of these techniques could be recommended. It is important to mention that this situation did not apply to the results for the other techniques.

Further investigation of the various aggressive environments and of the interactions between the various deterioration processes is needed before modification of design codes could be undertaken, however, enough data is available to establish a framework for design of concrete structures for durability against corrosion. Once more results become available, these design methods can be refined further and finally recommended for use by the designer.

Sommaire

Les structures de béton armé construites en milieux agressifs peuvent se détériorer plus rapidement qu'initialement prévu. Ce phénomène est souvent causé par le développement de processus de dégradation physico-chimiques au sein même des différents membres composant la structure. Les ponts et viaducs conçus sans considérer suffisamment certains aspects importants de la durabilité des structures sont particulièrement susceptibles d'exhiber des signes de détérioration prématurée.

Afin de mieux définir les nombreux aspects reliés au phénomène de corrosion des armatures du béton en milieu salin, il est nécessaire de faire l'examen d'ouvrages existants. La désaffectation du viaduc Dickson, construit en 1959 dans la partie Est de l'île de Montréal au Canada, représente une excellente occasion d'étudier et d'identifier les causes de l'abandon prématuré de cette structure en béton armé. La cause première identifiée comme étant responsable de la détérioration rapide du viaduc est le développement du phénomène de corrosion des armatures d'acier, phénomène accéléré par la pénétration d'ions chlore (Cl^-) au sein du béton, ions provenant de l'utilisation d'agents déglaçants.

Entre 1997 et 1999, l'université McGill a mis sur pied un programme de recherche en partenariat avec certaines entreprises et Le Centre des Études et Recherche en Infrastructure Urbaine (CERIU) visant l'examen intensif du tablier du viaduc. À ce jour, les résultats obtenus ont permis de confirmer les causes identifiées de dégradation rapide et ont aussi permis la validation et le calibrage des différentes techniques utilisées durant le programme de recherche afin de mesurer les causes et l'étendue des dommages associés aux différents phénomènes de dégradation susceptibles d'affecter la durabilité des ouvrages en béton armé.

Les techniques de mesure utilisées dans le cadre des essais sur le viaduc Dickson peuvent être divisées en deux catégories : celles mesurant les dommages aux armatures d'acier et

celles mesurant la qualité de l'enveloppe protectrice de béton (béton de ciment Portland). Les conclusions tirées à partir de la présente étude peuvent être résumées ainsi :

- La plupart des tests normalisés (le potentiel de demi-pile, l'épaisseur du couvert de béton sur l'armature, le taux de corrosion, le potentiel de corrosion et la résistance électrique du béton) ont indiqué que la dalle de béton de la section Sud du pont Dickson était fortement susceptible de développer le phénomène de la corrosion des armatures : cette situation s'appliquait à la majeure partie de la section Sud. De plus, les résultats des tests ont indiqué que les côtés Est et Ouest, de même que la bordure Nord du pont ont démontré des signes critiques de développement intensif de la corrosion des armatures. En comparant ces résultats avec ceux des sections Centrale et Nord, il est apparu que l'état de la section Sud du pont était meilleure que celle des deux autres sections;
- L'agent initiateur de la réaction de corrosion a été identifié comme étant la pénétration d'ions chlorures dans la structure : aucun signe de la réaction de carbonatation n'a pu être observé, alors que d'importantes concentrations en chlorures ont été mesurées au niveau des armatures du béton;
- Après analyse des résultats obtenus sur le pont Dickson, il appert que le potentiel de demi-pile, , la concentration en chlorures au niveau de l'armature, la résistance électrique du béton, le taux de corrosion (polarisation linéaire) et la résistance à la compression représentent actuellement les meilleurs indicateurs du risque de développement de la corrosion. Ces techniques de mesure normalisées demeurent intéressantes afin de mesurer l'étendue de la dégradation d'une structure et afin de caractériser la susceptibilité de l'armature et du béton sus-jacent vis-à-vis la corrosion à l'aide de critères normalisés;
- L'utilisation conjointe de plusieurs techniques de mesure a permis d'améliorer et de simplifier de façon significative l'analyse des résultats obtenus : la possibilité de pouvoir comparer les résultats des tests entre eux a permis de vérifier la validité de l'interprétation des résultats faite séparément pour chacune des techniques;

- Cependant, la fiabilité et la précision de la plupart des techniques n'ont pas été clairement démontrées au cours de ce projet de recherche : la variabilité des résultats obtenus pour les tests de polarisation linéaire, de diffusion des chlorures (migration et apparent), ainsi que pour le test de perméabilité du béton a été élevée, alors que la reproductiblité des tests de potentiel de demi-pile, de polarisation linéaire et de la couverture de béton n'a pu être établie de façon systématique malgré l'obtention de plusieurs valeurs par position de test. De plus, les tests de perméabilité du béton, de diffusion des ions chlore (migration), ainsi que les tests effectués sur les carottes de béton n'ont pas été répétés au cours de ce projet de recherche. L'utilisation de la technique de polarisation linéaire s'est avérée satisfaisante afin de mesurer in situ le taux de corrosion et le potentiel de corrosion, mais il s'est avéré difficile de faire la corrélation des résultats de ces tests avec ceux du potentiel de demi-pile. Dans le cas des techniques nouvellement développées et pour lesquelles il n'existe présentement aucune procédure normalisée (test in situ de perméabilité du béton Autoclam et le test de diffusion des ions chlore développé à l'Université Queen's of Belfast), la précision et la reproductibilité n'ont pu être établies au cours de ce projet de recherche, ni même au cours des études portant sur les sections Nord et Centrale du pont Dickson. Pour chacune des trois sections du pont, les coefficients de variation observés pour ces tests ont reflété cette situation : pour le test de diffusion des ions chlore (migration) sur les sections Nord, Centrale, et Sud, les coefficients de variation obtenus sont respectivement 48 %, 55 %, et 136 %; pour le test de perméabilité du béton sur les sections Nord et Sud, les coefficients de variation obtenus sont respectivement 118 % et 142 % (pour la section Centrale, les valeurs obtenues ne peuvent être comparées). Ces valeurs élevées pour le coefficient de variation indiquent : (1) que les techniques sont inadéquates afin d'obtenir des résultats précis, et (2) que la qualité du béton testé varie grandement. Par conséquent, l'interprétation des résultats obtenus à l'aide de ces techniques a été limitée et la fiabilité de ces techniques devra être établie avant de pouvoir.

de façon générale, recommander leur utilisation. Il est important de mentionner que cette situation ne s'appliquait pas aux résultats des autres techniques.

Une étude poussée des différents environnements susceptibles d'accélérer le développement de phénomènes de dégradation et des interactions entre ces dits phénomènes est fortement recommandée avant de considérer la modification des procédures de conception du code de génie civil. Néanmoins, la quantité de données disponible est suffisante afin de permettre la mise sur pied de guides de conception traitant des problèmes de durabilité reliés au phénomène de la corrosion. Ces guides pourront éventuellement servir de fondement pour la modification des codes de génie civil, lorsque l'information disponible permettra de le faire.

Acknowledgements

I would like to sincerely thank all those who contributed in any possible way to the achievement of this research program, from the initial stages of testing to the printing of this thesis. In particular, the following people provided significant help :

I would like to deeply acknowledge my supervisor, Professor M. S. Mirza, for his guidance, patience and support provided throughout the realization of the research program. I would like to simply thank him for the invaluable opportunity to participate in this detailed research program.

The author would like to thank the Natural Sciences and Engineering Research Council (NSERC) for the strategic research grant for the support of this project.

The participation of the Centre des Expertise en Infrastructures Urbaines (CERIU) in assisting the partners in the early stages of project proposal and in procuring the Dickson Bridge from the City of Montreal is greatly acknowledge.

I wish to underline the participation of Professor Luc Chouinard of the Department of Civil Engineering and Applied Mechanics, McGill University. The help provided during the analysis and statistical treatment of data is fully appreciated.

The author is grateful to Professors P.A.M Basheer and A.E. Long from the Queen's University of Belfast for the loan of equipment and overall assistance with the in-situ water permeability and chloride migration tests.

I am also grateful to Ali El-Jachi, Lamya Amleh and Muhammad Amleh for their help and recommendations during these two past years. They contributed to create a stimulating and motivating climate in the Materials Laboratory at McGill University.

I wish to express my gratitude to the following contributors to this research project, their participation made of this project a great success :

MM. Gérard Benchetrit, Nourridine Kadoum, and Yannick Champagne from COREXCO, Montreal.
MM. Robert Cardin and Paul Laberge from the City of Montreal.
MM. M. Przykorski and R. Sheppard from the Concrete Laboratory of the Department of Civil Engineering, McGill University.

I wish to express my deepest appreciation to my family (Maurice, Claudette, and Jean-Pierre) and to my friends (François, Martin, and Sophie) for their support.

Finally, I wish to thank David Nguyen and Craig Harper, colleagues at McGill University, and the staff of the Civil Engineering Department for their support during the past two years.

Table of Content

List of symbols

a	Electrode spacing of the Wenner probe.
a	Tafel's constant.
A_{anode}	Anodic surface area.
AB_astm	Variable representing the absorptivity after immersion values.
$A_{cathode}$	Cathodic surface area.
A°	Angtrom (10^{-10} m).
$a_{oxidation}$	Activity of oxidized species.
$a_{reduction}$	Activity of reduced species.
b	Tafel's constant.
c_b	Bulk concentration of reactants.
CC_rb	Variable representing the chloride ion concentration at rebar values.
CD	Cook's distance.
CD_a	Variable representing the apparent chloride diffusion coefficient values.
CD_m	Variable representing the chloride diffusion migration coefficient values.
cm^2/sec	Square centimeter per second.
COV	Coefficient of variation.
CR	Variable representing the carbonation front depth values.
CR_t	Variable representing the carbonation front depth values for the bridge deck surface.
CS	Variable representing the compressive strength (f'c) values.
CV	Variable representing the concrete cover thickness over rebar values.
CV_bot	Variable representing the concrete cover thickness over rebar values for the bridge deck soffit.
CV_col	Variable representing the concrete cover thickness over rebar values for the bridge columns.

CV_top	Variable representing the concrete cover thickness over rebar values for the bridge deck surface.
D	Diffusion coefficient of the reacting ions.
DOF	Degree of freedom.
e^-	Free electron.
E	Modulus of elasticity.
E	Nearst potential.
e	Residual term.
E_cp	Variable representing the corrosion potential values.
E_cp_top	Variable representing the corrosion potential values for the bridge deck surface.
E_cs	Variable representing the modulus of elasticity (Ec) values.
E_hc	Variable representing the half-cell potential values.
E_hc_bot	Variable representing the half-cell potential values for the bridge deck soffit.
E_hc_col	Variable representing the half-cell potential values for the bridge columns.
E_hc_top	Variable representing the half-cell potential values for the bridge deck surface.
E_pv	Variable representing the apparent modulus of elasticity values.
E_0	Standard Nearst potential.
ER	Variable representing the electrical resistance values.
F	Faraday's constant.
F	F-ratio.
f'_c	Compressive strength of concrete.
g/cm^3	Gram per cubic centimeter.
HC	Variable representing the half-cell potential values.
i	Rate of reaction.
i_0	Rate of reaction at equilibrium for unit activities (Equation 2.13).
i_{ex}	Exchange current density.
i_l	Limiting current density.

K	Kelvin.
km/sec	Kilometer per second.
kW.cm	KiloOhm by centimeter.
ln(CC_rb)	Variable representing the logarithm of the chloride ion concentration at rebar values.
ln(CD_a)	Variable representing the logarithm of the apparent chloride diffusion coefficient values.
ln(CD_m)	Variable representing the logarithm of the chloride diffusion migration coefficient values.
ln(ER)	Variable representing the logarithm of the electrical resistance values.
ln(LP_cr)	Variable representing the logarithm of the corrosion rate values.
LP_cr	Variable representing the corrosion rate values.
LP_cr_top	Variable representing the corrosion rate values for the bridge deck surface.
m/sec	Meter per second.
mm/yr	Millimeter per year.
MV	Millivolt.
n	Number of electrons transferred during a reaction.
N	Number of observations.
°C	Degree Celcius.
$P[O_2]$	Vapour pressure of oxygen at the cathode.
$P'[O_2]$	Vapour pressure of oxygen at the anode.
pH	Hydrogen potential.
PV	Variable representing the pulse velocity values.
R	Gas constant.
R	Pearson correlation coefficient.
R^2	Coefficient of determination or correlation coefficient.
R_e	Internal electrolytic (concrete) resistance.
R_e	Ohmic or uncompensated resistance.
r_{oxid}	Equilibrium oxidation rate.

R_p	Polarized resistance of steel.
r_{red}	Equilibrium reduction rate.
SD_a	Variable representing the saturated density values.
SD_b	Variable representing the dry density values.
SSE	Error sum of squares.
T	Absolute temperature (K).
VAR	Variance.
VV	Variable representing the volume of permeable air voids values.
WP x 10^{-10}	Variable representing the in-situ water permeability coefficient values (multiplied by 10^{-10}).
WP	Variable representing the in-situ water permeability coefficient values.
x	Regressor.
X	Thickness of diffusion layer.
Y	Dependent / response variable.
ΔG	Free energy of a system, of a reaction.
α	Level of significance.
β	Tafel's constant.
β_0	Point of intersection of a line with y = 0.
β_1	Slope of a line.
$\beta_1, \ldots, \beta_n$	Constants referred to as regression coefficients (multipliers).
η	Overpotential; polarization.
η_a	Activation controlled overpotential.
η_c	Concentration controlled overpotential.

List of Figures

List of Tables

1. Introduction

1.1 Durability of structures

1.1.1 General aspects

Since the last century, the most commonly used construction material is concrete, and there are several reasons for that. Unlike other materials (wood, steel, etc.), concrete offers an excellent resistance to water due mainly to its capacity to remain dimensionally stable when immersed or submitted to wetting and drying cycles. Concrete is made from three abundant, inexpensive and locally available resources[1] : water, aggregate, and cement. In addition, concrete can be moulded into different shapes and sizes to form various structural elements. Finally, the use of concrete as a dominant material helps saving energy and allows for recycling of the resources – thus making it environmentally friendly[1].

Since concrete is competing with other materials, costs are often reduced with the modification of the design, construction procedures (placing, compacting, and curing), resulting in a decrease in the expected duration of life of reinforced concrete systems (durability)[2]. Durability can be defined as the continuing performance with minimum (regular) maintenance over the service life of a given system under specific environmental conditions. Today, durability of the concrete is a major issue. Many questions need to be answered. In the first chapter of this thesis, the actual problems and proposed solutions related to durability of concrete structures are reviewed. Here are some of the important topics covered :

- Actions to be taken to increase the durability of concrete;
- Durability concerns in the three distinct phases : materials, design and construction;
- Design for durability based on three major issues : design life, end of life, and reliability;

- Review of the problems related to design for durability of concrete structures;
- Recent developments in supplementary cementitious materials - issues related to durability of structures.

1.1.2 Degradation processes

Durability of concrete is affected by the deterioration mechanisms that can impair the integrity (structural, aesthetical, etc.) of the structure. These mechanisms can be divided into four topics[3] :

- Corrosion of reinforcing steel;
- Alkali-aggregate reaction;
- Acid attack (including sulphate attack);
- Frost action.

Also, for any given deterioration process, it is generally accepted[4] that there are four development stages :

- Design, construction and curing;
- Initiation processes (propagation phase of damage has not begun);
- Propagation of the deterioration;
- Advanced state of propagation with extended damage.

In order to ensure adequate protection to a particular system, there is a need to fully understand the degradation processes and to start designing structures based on the anticipated deterioration processes (action, intensity and duration) relative to a given location[1].

1.1.3 Quantifying the dominant parameters

The first step in order to estimate the service life, and to assess the tolerable deterioration of a structure is to adequately determine the aggressive environments (qualitative process) and their intensities (quantitative process)[1]. At this point in time, it is easier to design concrete structures for strength requirements, since reliable test techniques exist to verify and monitor the evolution of the strength of concrete[2]. On the other hand, it is difficult to quantitatively relate the aggressiveness of the environment to the state-of-health of the structure, and to evaluate the durability of concrete systems at any stage (especially at the design stage).

With regards to durability issues, it is now accepted by the civil engineering industry[4, 5, 6] that compressive strength of concrete is neither a suitable characterising factor of the state-of-health nor an appropriate criterion for the selection of repair materials to ensure long-term efficiency of the repairs. Instead, it is suggested to combine the compressive strength survey with the use of other relevant tests depending on the nature of the studied phenomenon. For example, the half-cell potential, linear polarization resistance, and electrical resistivity tests could be used as additional tests to study the durability problems related to corrosion of the reinforcing steel.

The need to develop and standardize reliable testing techniques is immediate. Testing of material properties in natural exposure conditions using reliable measurement techniques simplify the understanding of the deterioration processes and provide opportunities to quantify the related influencing parameters[3]. Here is a partial list of important topics that need further study :

- Evaluation of the transport mechanisms in the concrete;
- Prediction of the moisture content of a concrete structure in relation with the penetration of the carbonation front (with regards to corrosion of the reinforcing steel);

- Determination of the chloride ion concentration threshold value with regards to corrosion of the reinforcing steel;
- In-situ and laboratory testing of the permeability of concrete.

As a condition to predict the service life of a structure for a given aggressive environment, there is a need[4, 7, 8, 9] to improve the idealization of the different deterioration mechanisms to quantify their effects and also possible interactions between them. Since the quality of the sampling is as decisive for the quality of the estimate as the quality of the model[9], there is also a need to develop standard sampling procedures.

1.1.4 Performance of structures with time : determination of the expected design life

The performance of a structure can be defined as its ability to reach pre-determined levels of satisfaction over a certain period of time based on the initial design goals related to technical, functional and economic aspects. The levels of satisfaction are generally related to the bearing capacity, stability, safety in use, visual appearance, etc. Performance and durability of concrete structures are closely related concepts. For many managers and designers of structures trying to forecast and optimize the performance in time of their systems, the quantification of durability in time is of considerable interest[9]. As the costs of repair works exceed the available funding, there is a need[2, 5, 6, 7, 8, 10, 11] to optimise spending of the available funds, and service life predictions have become a necessary part of the process. Actually, there is no accepted relationship between the minimum acceptable design life of structure and its aggressive environment[6]. In addition, there exists presently a lack of theoretical models for performance and durability predictions of the future state-of-health of structures[8].

Since there is a need to fulfill the minimum accepted technical performance due to the effects caused by the deterioration processes and to be consistent with present

framework of limit state design, it is necessary to develop deterministic design concepts and provisions related jointly to durability and structural performance (shear, torsion and flexure)[7]. Durability issues are not treated in the design codes except for requirements on the cover thickness and the concrete mix of beams and slabs in corrosive environments, and on grade. One major reason for that is the difficulty to provide general criteria to address resistance issues that meet all possible uses of concrete[2]. Similarly, it is difficult to establish individual criteria for all aggressive environments[2] or on the transport mechanisms of concrete (evaluated using standard procedures) along with the intended use of the structural elements, concrete quality, time, etc. It is clear that more developments are needed before any modification to the code could be made possible.

The CSA Standard A23.3 should clarify the definition of end of design life, actually based on the technical design life. Since the only circumstance that comes easily to mind where design life is not defined by economical conditions is that the structure collapses without warning, the end of life of a structure could be the point in life where it is not more economically viable to keep the structure operating[12]. The definition of economically reasonable working life should be based on the following concepts[12] :

- All costs implied in the design, construction, operation, maintenance and repair;
- Risks and consequence of failure of the work during its working life.

The use of life-cycle cost analysis should be used in the planning phase of all reinforced concrete structures[7, 9], because it offers a great potential to minimize the expenses in maintenance, repair and replacement of concrete[2]. The choice of a maintenance strategy (and allowance of the necessary funding) should be made at the design stage. Figure 1.1 clearly shows the different possible outcomes of the performance of a structure in time. Curve 1 shows negligible deterioration (higher initial costs), while curve 3 is associated with a sudden failure due to a possible high

deterioration rate that could result in high consequence costs. Curve 2 exhibits the normal tendency of most structures (minimum initial costs) to moderately deteriorate with time. In that case, monitoring and maintenance allow to increase the service life of the structure at moderate costs.

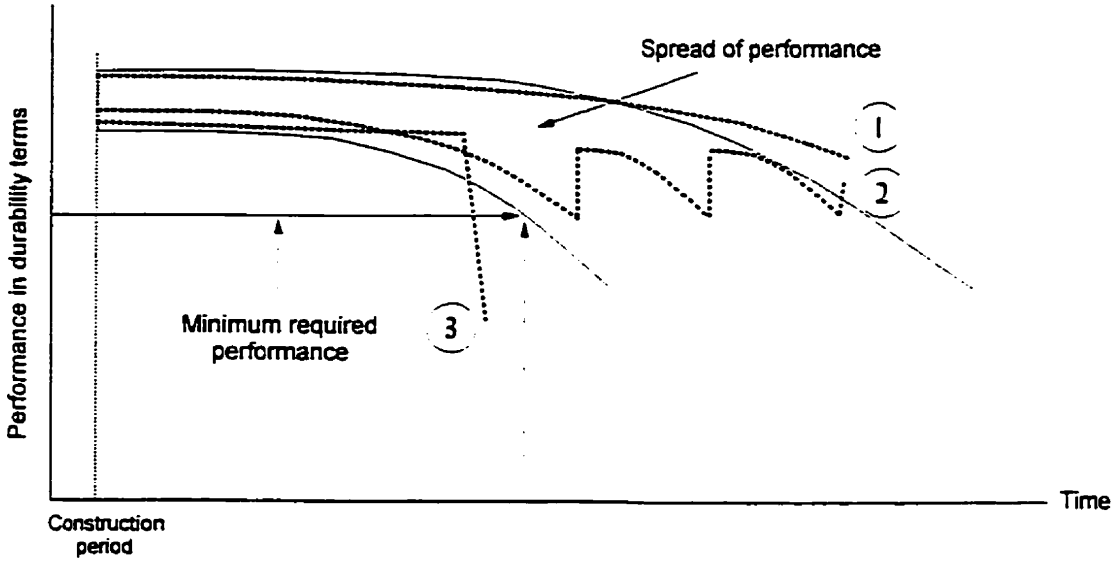

Figure 1.1 Relationship between concrete performance and service life[13].

1.1.5 Costs of premature structural deterioration

Every developed country is now spending about 4 % of its gross national product on metallic corrosion with close to 25 % of this total being preventable by the application of appropriate known technology[14]. Premature deterioration of concrete structures is a major problem whose importance is increasing rapidly. Most countries around the world experience similar problems.

It was reported[15] that in the United States, more than 40 percent of the 572.000 highway bridges built before 1940 are classified as structurally deficient. This is mainly due to premature deterioration. Corrosion of reinforcing steel is thought to be responsible for half of the total damage observed, the magnitude of damage being especially large in structures exposed to marine environments and to de-icing

chemicals. The costs associated with the rehabilitation and the replacement are estimated to be more than $ 50 billion. In the United Kingdom, near 20 percent of all 6,000 highways and trunk routes bridges suffer from premature decay associated with corrosion. Around C$ 300 million are spent annually on bridge maintenance and repair in that country.

In Canada, due to the prevalent use of de-icing chemicals, up to now C$ 200 billion were spent in repair and rehabilitation of concrete structures[13]. The costs associated with corrosion of reinforcing steel approach C$ 30 billion annually[13].

1.1.6 Service life versus reliability

Generally, the design phase is held to be the sole responsible for most durability problems[12]. It appears that the great majority of durability problems arise from the lapses in the quality of the design, construction, and / or maintenance[12], and could instead be classified as reliability-related problems. Since the service life of a structure is a function of different components service lives[7] (generally all different), there is a significant need for[7] :

- Increased quality control on projects;
- Regular inspection and good maintenance of structures;
- Monitoring of structures (especially for old structures).

Reliability problems associated with the determination of the service life of structures need to be considered. The accuracy of the existing models along with uncertainties of all types influence the design decisions. A risk analysis accounting for the following aspects of durability assessment should be made necessary :

- Variability of deterioration models;
- Limitations of testing methods;
- Relatively small quantity of available information;

- Probabilistic treatment of information;
- Consistent treatment of uncertainties;
- Assessment of the effects of influencing parameters;
- Sensitivity analysis to identify critical parameters;
- Evaluation of benefits of monitoring and inspections.

1.1.7 Modifying the design code requirements : the key to success ?

As mentioned before, it would be difficult at this point in time to modify the design code criteria to account for the influence of deterioration mechanisms. On the other hand, some durability-related requirements could be adopted in order to put all competing engineers and contractors on the same level playing field[2]. The introduction of durability requirements in the design code will regularize the acceptance of requirements by designers and contractors[2]. There is also a need to set up codes of good practice to ensure durable repairs and treatments of old structures[8]. Here is a list of concepts that will need to be covered in future versions of the design code[3, 7] :

- Standard procedures for selection of material proportions and construction practices in terms of durability;
- Design consideration of the influence of the environment of the structure in terms of freeze-thaw resistance, corrosion of reinforcing steel, sulphate attack and alkalis-aggregate reaction (including severity of attack and duration);
- Modification of the safety factors as a function of the state-of-health and time for a given structure (for service-life estimation purposes);
- Standard procedures for selection of techniques and materials for repair (considering interactions between repair and substrate materials).

Modifying the requirements of the code can take time and could be made possible only if constant and efficient evaluation of the durability database being developed by

the research community is attempted. However, at this point in time, design for durability is still possible using the limited available data and accounting for the large variability of the results. Consideration of the durability aspects in design can be beneficial in increasing the service life of a structure, even if incomplete information is used.

1.1.8 Immediate problems related to standard design procedures

Actually, the important problems that need to be overcome before adopting standard design procedures are numerous. Here is a list of some problematic aspects concerning design for durability considered to be the most important :

- The identification and quantification of aggressive environments[7];
- The determination and selection of a standard testing procedure for the chloride ions concentration threshold value still need further study[3, 9];
- The determination of procedures for adequate assessment and inspection of concrete structures ensuring that all critical parts have been detected[11];
- The necessity to put up a reliable database for durability issues;
- Most deterioration models use the transport mechanism of diffusion to assess the remaining service life of structures, assuming that the concrete is saturated, which is not always the case[9];
- Most concrete durability problems are related to hidden execution faults difficult to predict[9].

1.1.9 Design of reinforced concrete structures for durability

There are no standard procedures to follow when designing for durability[16]. Different valid defence strategies can be selected depending on the type of structure to be constructed, environment, and available funding. As an example, the multi-barrier approach can be used. This approach is also applicable to the repair procedures of older structures[4], and is described here :

Multi-barrier approach[4] :

1. Identification of the environmental exposure;
2. Initial conceptual design, associated with preliminary sizing of elements and costs :

    - Function and type of structure;
    - Performance requirements;
    - Loads.

3. Identification of the critical structural zones;
4. Identification of transport and degradation mechanisms;
5. Determination of the influencing parameters;
6. Selection of the protective systems (barriers) :

    - Use concrete itself as a protection (cover);
    - Use techniques to reduce variability of the concrete;
    - Use a low water / cement ratio (lowering the permeability);
    - Block the ingress of deleterious substances (membranes, sealers, etc.);
    - Use of materials limiting the development of degradation mechanisms.

7. Detailing of the structural elements :

    - Final shape of cross sections;
    - Integrating the base structure into the final (detailed) design;
    - Numerical methods associated with limit states.

8. Reinforcement arrangements;
9. Selection of future protective means :

- Determine an appropriate maintenance strategy.
- Arrange for planned replacement;

1.1.10 Improved materials to enhance durability

Recent developments in research on materials offer new alternatives to designers for the design and repair of structures[5]. Since most of these discoveries are more expensive to use than the original plain concrete, additional costs related to construction are often repaid by the savings due to the increase of durability of the structure[16].

In selecting one of these new alternatives, it is important to bear in mind that too often excessive reliance is placed on the information and advice provided by the manufacturers[5]. Also, material properties are often obtained using different testing methods and sample sizes (varying from one manufacturer to another)[5]. Some of these new alternatives are described below[5] :

- High performance concrete (HPC) using very low water / cement ratio provides excellent resistance to aggressive agents by considerably reducing the permeability of the concrete;
- The use of pozzalanic materials increases the strength of concrete, decreases its permeability and reduces the risks of initial thermal cracking due to the reduced heat of hydration and increased uniformity of the microstructure : pozzolanic reactions take place sometime after the hydration process has started (one week or even more depending on the type) when the pH value of the pore solution reaches at least 13.2, and results in the reduction the capillary porosity and the refinement of the pore structure of the hydrated cement paste;
- Fiber-reinforced and polymer concretes can be used to enhance ductility, impermeability and shrinkage properties of the concrete, and thus increase the durability of repaired and rehabilitated structures;

- Used mainly for pavements and dams, roller compacted concrete represents alternatives to the designer to lower the water permeability of concrete, while microwave-cured concrete can be used in the same way for precast members (generally beams);
- Shotcrete and self-curing concrete can now be used (mainly for repairs).

1.1.11 Role of maintenance and management

Consideration of the durability aspects in the design of reinforced concrete structures is the key to success in increasing the service life of existing structures[8]. Since this concept is relatively new, there is a need to educate designers and managers about the durability aspects in the design process[2]. Also, there is a need for more interaction between the designers and contractors to eliminate the possible sources of deterioration in relation with durability[2]. Another part of the solution to durability problems is the improvement of the engineering quality : better supervision, better training and education of the staff[12]. Constant and efficient evaluation of the durability database being developed by the research community, and real life experience gained in case-studies represent vital sources of information on which future modifications of the design code could be based[8].

Durability problems are not treated in the code except for requirements on cover and grade of concrete : the durability should be considered as a holistic criterion[5], and modifications to the code should be made in the future. Also, compressive strength should not be the only characterising factor for the concrete quality[4, 5, 6]. In-situ testing of structures is a necessary tool when trying to optimize investments based on service life modelling of concrete repairs and maintenance strategies[9]. Financial and risk analyses should become necessary for all projects[9].

The long-term performance potential of a concrete structure is set at the design stage[17]. Improvements to the design, materials, and workmanship incorporated in a structure at the time of construction can delay or even avoid the need for major

repairs, but these improvements can be costly[17]. Savings due to enhanced durability of structures over a long period of time should be significant and convincing[5, 8].

1.2 Dickson Bridge research program

1.2.1 Introduction

The Dickson Bridge was constructed in 1959 in the heavily industrial eastern end of Montreal, at a cost of less than a million dollars. The role of the bridge was to allow traffic circulation over the Canadian National (CN) rail tracks used frequently at that time. The construction of Notre-Dame Street, a fast access to Downtown Montreal, is responsible for the construction of the bridge which was built to accommodate the traffic coming from Sherbrooke Street.

The Dickson Bridge can be divided (with reference to the St-Laurent river) into three sections : south, central and north. The reinforced concrete structure consists of a concrete slab supported on deep reinforced concrete beams on reinforced concrete columns with the exception of the central section, which is supported on steel girders on steel columns. The dimensions of the bridge are listed in Table 1.1, while the schematic of the structure is presented in Figure 1.2.

1.2.2 Summary of activities

In 1988, the City of Montreal conducted a detailed inspection to evaluate the safety of all its transportation infrastructures. The Dickson Bridge was found to be severely damaged : delaminations, concrete spalling, chloride levels above the maximum allowable content, and insufficient air content to safely resist the freeze-thaw cycles of Montreal's rigorous winter climate. As a consequence of the investigation, the City of Montreal decided to allow only light traffic circulation for

the two interior lanes of the bridge. The bridge rating was reduced to three tons. Also, the remaining two exterior lanes were reinforced by providing a reinforced concrete overlay basically for the trucks.

Table 1.1 Details of geometry of the Dickson Bridge.

Dimensional properties of the Dickson Bridge	
Deck	
Total length	366 m
Total width Thickness of concrete	27 m 150 mm
Beams	
Total thickness	150 mm
Total width	1200 mm
Span	
Typical span dimensions	12 to 18 m

In 1994, the Dickson Bridge was declared unsafe for traffic by the City of Montreal and was decommissioned. A detour road was constructed directly beside the bridge structure. Fortunately, the railway traffic under the bridge decreased significantly over the years and the detour road constructed previously was suitable for both the automotive and railway traffics. Again in 1994, it was decided by the City of Montreal to demolish the bridge as a consequence of the good results of this late alternative. However, demolition is retarded due to the lack of funding.

In 1997, the City of Montreal was approached by McGill University, CERIU (Centre des Expertise et Recherche en Infrastructures Urbaines) and other partners to participate in a joint industry-university multiphase research program to allow the use of the Dickson bridge for investigation of the bridge structure.

To-date, the central and the northern sections of the bridge were studied by El-Jachi[25], Fazio[13] and McCafferty[30], respectively. In addition, Amleh[26] has analyzed several portions of the three sections as part of her Ph. D. thesis.

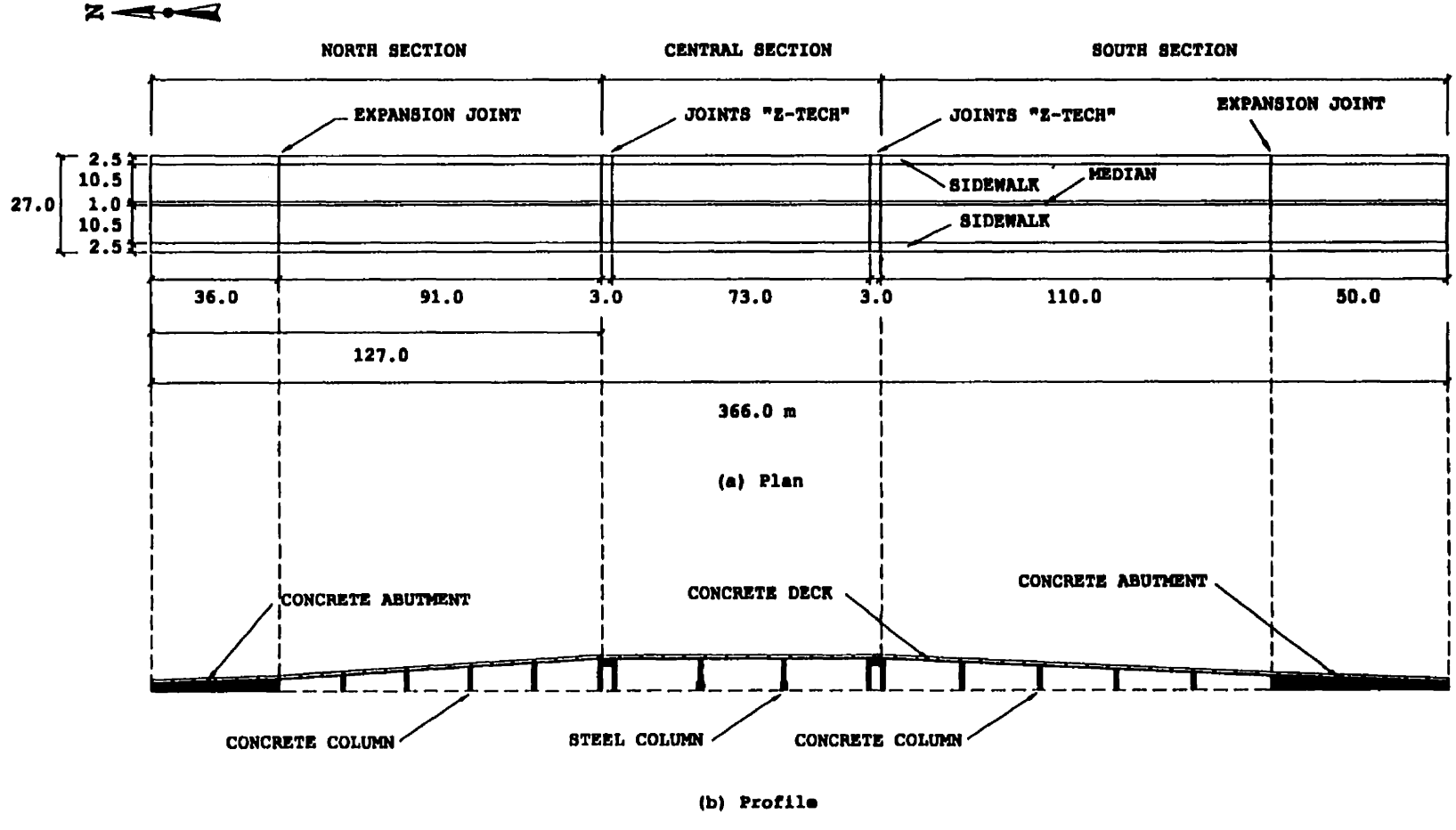

Figure 1.2 Schematic of Dickson Bridge[13].

1.2.3 Objectives and scope of global research project

The proposed program is presented below[13] :

- Use and evaluation of composite materials as reinforcement for deck repairs;
- Evaluation of structural capacity of the deck and the bridge through physical testing and non-linear computer analyses;
- Evaluation of the permeability and carbonation of the deck;
- General condition survey of the bridge utilizing existing and some selected new tests;
- Creation of a detailed databank of the parameters that influence the corrosion process for development of probabilistic models for the various deterioration phenomena and the development of techniques for reliability-based durability design methods to provide protection against corrosion and assessment of service life;
- Evaluation of membranes and other repair techniques (involving polymer concrete) for their ability to bridge cracks;
- Laboratory and field investigations to determine the influence of the rate and the extent of corrosion on bond characteristics between the reinforcing steel and concrete.

1.2.4 Objectives and scope of thesis

The Dickson Bridge structure is relatively large, and its complete analysis using several test techniques requires a significant amount of technical, human, and financial resources. Due to the complexity of the task, it was decided to divide the study of the condition of the Dickson Bridge into three separate parts. As mentioned previously, the north and central sections of the structure were analyzed adequately, and comparisons between the two theses are made possible since the same test techniques and procedures were used. As a continuation of the initial global project,

it was decided to analyze the remaining section (south) of the structure using the same test techniques, modifying only the number of readings and test procedures to account for the recommendations made by the previous researchers. To simplify the analysis process and understanding of this work, the expression 'bridge' will now always refer to the entire south section of the Dickson Bridge.

In the following sections, the role of the concrete surrounding the reinforcing steel in the corrosion process will be investigated. Since concrete protects the reinforcement steel from the aggressive environment, it is expected that the quality of the concrete influences the corrosion of steel in different ways. Therefore, the in-situ test program was aimed at the analysis of the extent and causes of steel reinforcement corrosion and establish the relationship between the electrochemical properties of steel and the physical and chemical properties of the surrounding concrete. The objectives of this thesis are :

- Conduct an examination of the corrosion of the reinforcing steel in the Dickson Bridge deck by measuring the corrosion potential, corrosion rate, and polarization potential;
- Assess the corrosion-induced damage in the concrete deck to determine the state-of-health of the deck and identify the causes of the observed deterioration;
- Identify suitable testing techniques to predict reinforcing steel corrosion by investigating most of the influencing parameters of the concrete, with particular interest on the impact of the environment in the vicinity of the reinforcing steel bar.

1.2.5 Organization of thesis

In Chapter Two, a brief description of the corrosion phenomenon and of the relevant concepts underlying the testing techniques currently used in the field will be made.

The most influencing factors with regards to the corrosion process will also be reviewed.

In Chapter Three, the different testing techniques presently available for the in-situ assessment of deterioration due to corrosion of reinforcement steel will be introduced. The emphasis is put on the actual test techniques that were used on the Dickson Bridge in attempting to evaluate the actual damage to the bridge deck. These techniques also serve to evaluate the interactions between the different important parameters defining the corrosion-related characteristics of both the concrete media and the steel reinforcement.

Chapter Four presents a summary of the results obtained from the test survey. The results of each test are also presented individually. Whenever possible, comparisons with the results from the north and the central sections are made. The assessment of the general condition of the bridge deck is performed based on the test results.

Chapter Five presents the statistical analysis of the data collected from the test survey. General tendencies between measured parameters are verified, and correlations and regressions of the variables are performed in order to analyze the interactions between measured influencing parameters.

In Chapter Six, conclusions of the entire analysis are drawn and recommendations are made to improve future testing of bridge decks. The most influencing parameters are clearly identified. Necessary modifications to the selected test techniques are also underlined.

The organization flowchart of the thesis content is presented below in Figure 1.3.

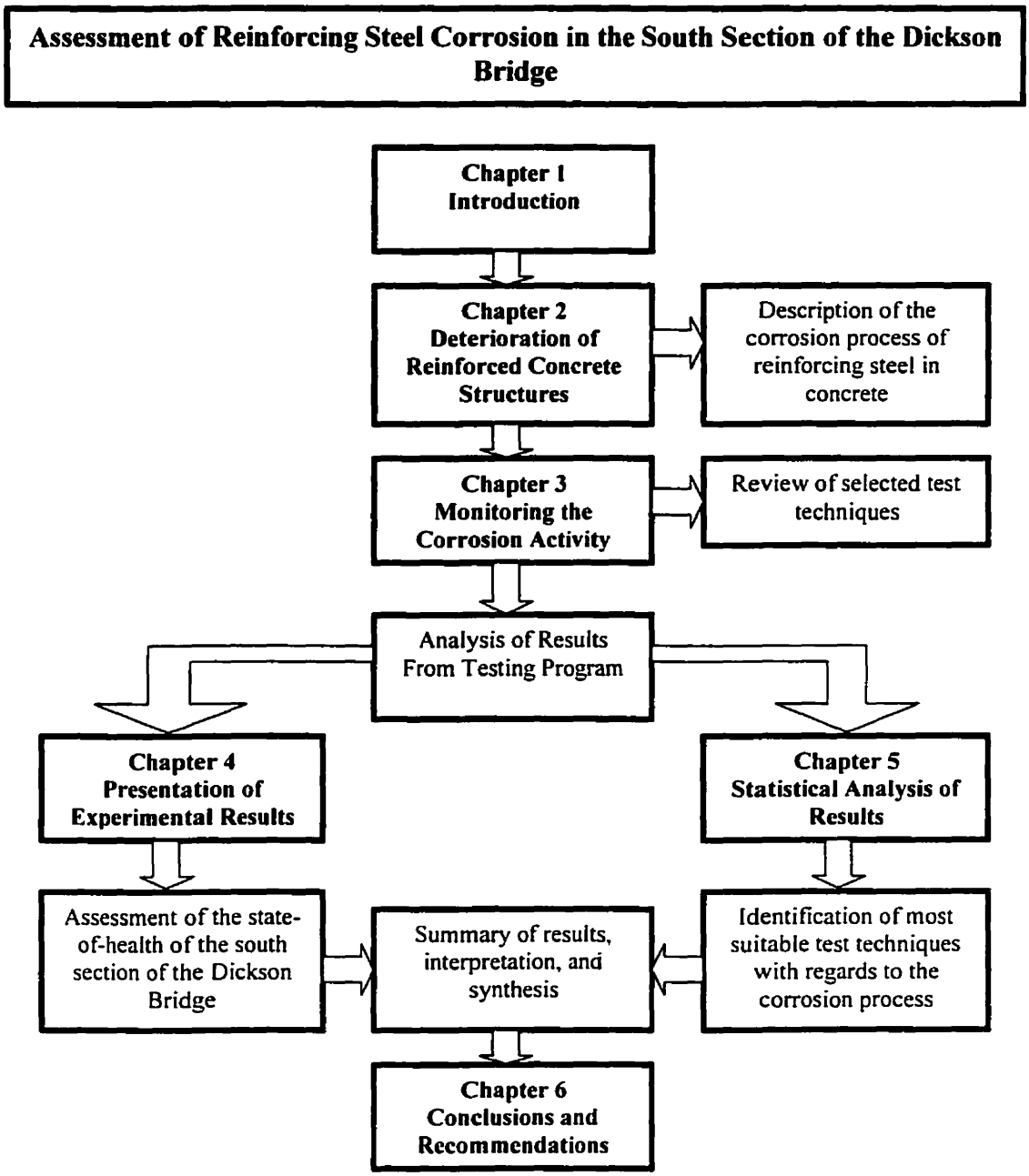

Figure 1.3 Organization flowchart of thesis content.

2. Deterioration of reinforced concrete structures

2.1 Modes of deterioration and causes

The different degradation factors and processes affecting concrete are presented in Table 2.1. It is worth noting that the deterioration of concrete is rarely due to one isolated cause : for this reason it is difficult to assign deterioration to a single factor. It should be observed that the physical and chemical processes of deterioration could act in a synergistic manner, i.e., the action of some processes accelerating the development of others[17].

Table 2.1 Degradation factors and processes[18].

Degradation factor	Process	Degradation
Mechanical		
Static loading	Deformation	Deflection, cracking, failure
Cyclic loading	Fatigue, deformation	Deflection, cracking, failure
Impact loading	Fatigue	Vibration, deflection, cracking, failure
Biological		
Micro-organisms	Acid production	Desintegration of concrete
Chemical		
Soft water	Leaching	Desintegration of concrete
Acid	Leaching	Desintegration of concrete
Acid	Neutralization	Steel depassivation
Acidifying gases	Neutralization	Steel depassivation
Carbon dioxide	Carbonation	
Chlorides	Penetration, destruction of passive film	Steel depassivation
Steel depassivation, oxygen, water	Corrosion	Expansion of steel, loss in diameter of rebars, loss of bond
Stress / chlorides	Stress corrosion	Failure of prestressing tendons
Sulphates	Crystal pressure	Disintegration of concrete
Silicate aggregate, alkalis	Silicate reaction	Expansion, disintegration
Calcium carbonate aggregate	Carbonate reaction	Expansion, disintegration

Table 2.1 Degradation factors and processes (continued)[18].

Degradation factor	Process	Degradation
Physical		
Temperature change	Expansion	Shortening, lengthening, restricted deformation
RH change	Shrinkage, swelling	Shortening, lengthening, restricted deformation
Low temperature, water	Ice formation	Disintegration of concrete
De-icing salt, frost	Heat transfer	Scaling of concrete
Floating ice	Abrasion	Cracking, scaling
Traffic	Abrasion	Rutting, wearing, tearing
Running water	Erosion	Surface damage
Turbulent water	Cavitation	Caves

2.2 Corrosion of reinforcing steel embedded in concrete

2.2.1 Introduction

Corrosion of the reinforcing steel is an electrochemical reaction that can take place only under certain chemical and physical conditions. The corrosion process of reinforcing steel has been well described in the past by several authors. Nevertheless, the mechanism of reaction is complex and varies widely with the environment surrounding the steel. In this section, the corrosion process of steel embedded in concrete is reviewed. Scientifically accepted concepts are introduced using a simplistic approach. The scope of this section is to clearly identify the initiating conditions, the influencing factors and also the measurable governing parameters related to the steel corrosion mechanism.

2.2.2 Description of the corrosion phenomenon

Under normal conditions, steel reinforcement embedded in concrete is protected against corrosion by the formation of a passive layer at the surface of the metal. This phenomenon is called passivation of steel and occurs naturally as a response of the steel material to the chemical attack by the immediate environment[14, 17, 19, 20, 21, 22].

Under normal conditions, metals in concrete are protected by the high alkalinity of the concrete pore solution (pH between 11 and 13). The presence of calcium hydroxide ($Ca(OH)_2$) provides a chemical protection against acids and other aggressive agents by limiting their concentration at the steel interface. As a result, dissolution of steel is impeded[17, 22].

The alkalinity of the pore solution is mainly due to the presence of alkalis (sodium (Na^+) and potassium (K^+) ions), and can be reduced by different processes. Depassivation of steel occurs when the pH of the pore solution drops below 9 in the presence of aggressive agents-most likely the chloride ions[17, 20, 22]. The three most common mechanisms responsible for steel reinforcement depassivation are the following[19, 22] :

- Depassivation of steel due to carbonation of the concrete;
- Depassivation of steel due to the action of the chloride ions;
- Depassivation of steel due to the leaching out of the alkalis by streaming water.

Prior to summarily describing each of these depassivation mechanisms, it is necessary to introduce some fundamental concepts of fluid transport theory. With the exception of the mechanical damage, all adverse influences on durability involve the transport of fluids through the concrete. Since the corrosion process depends highly on the transport mechanism of the fluids through the concrete, it is convenient, at this point, to review the theory of fluid transport.

2.2.2.1 Transport of fluids in concrete

Three important fluids are of interest with respect to concrete : water (pure or containing ions in solution), carbon dioxide, and oxygen. Furthermore, the movement of fluids through concrete can be determined with reference to three distinct

mechanisms, mainly permeability, diffusivity, and sorptivity[17, 19]. These mechanisms are described here :

Permeability : The water permeability of concrete defines its ability to resist the flow of water under a pressure differential. The permeability is controlled by the capillary porosity and thus depends on the size, the distribution, the shape, the tortuosity, and the interconnectivity of the pores[17]. In addition, the degree of hydration, and the properties of the cementitious materials are of great influence[17, 19]. The porosity of concrete defines the void content of the hardened cement paste, while the permeability is a function of the effective porosity (network of interconnected voids). The relationship between permeability and effective porosity of the hardened cement paste is qualitative[17] and refers to :

- The nature of the pore system (bulk of hardened cement paste);
- The nature of the pore system near the interfaces of the concrete paste and the coarse aggregates.

Diffusivity : Property of concrete characterizing a flow under a concentration differential. It is important to note that diffusion of gases through water-saturated voids can be as much as 10^4 to 10^5 times slower than through air voids[17]. It is also important to mention that the diffusivity coefficient of oxygen is 1.17 greater than that for carbon dioxide[17].

Sorptivity : Property of concrete relating the capillary movement in the pores open to the ambient medium (fluid). Capillary suction happens only in partially or completely dry concrete[17, 19]. The hardened cement paste is composed of particles connected over only a small fraction of their total surface. As a result, part of the water is physically bound (or adsorbed) by the solid phase.

In concrete, since flow under pressure differential is not always the principal mechanism of transport, diffusivity and sorptivity tend to replace permeability in

defining the penetrability of concrete, however, permeability is generally accepted to define both characteristics.

2.2.2.2 Depassivation of steel reinforcement

Previously introduced, the three mechanisms of interest with regards to the depassivation of the steel reinforcement are described in this section.

Depassivation due to carbonation of the concrete : Air contains carbon dioxide (CO_2) which, in the presence of moisture, reacts with the hydrated cement paste (the actual reacting agent is the carbonic acid). This action takes place even at small concentrations of CO_2 (such as 0.03 % by volume of air)[17]. The carbon dioxide penetrates from the surface of the concrete to the core via the pore system (entrained air bubbles and interconnected voids) to chemically react with calcium hydroxide molecules ($Ca(OH)_2$) to form lime ($CaCO_3$)[19]. $Ca(OH)_2$ is the hydrate that reacts the most intensively with carbon dioxide[19]. When $Ca(OH)_2$ gets depleted (also by reacting with the pozzolanic silica), the calcium silicate hydrate molecules (C-S-H) start to get carbonized. The equations of the reaction can be formulated as the following[17, 19] :

$$\mathbf{Ca(OH)_2 + CO_2 \Rightarrow CaCO_3 + H_2O} \qquad \mathbf{(2.1)}$$

$$\mathbf{C\text{-}S\text{-}H + CO_2 \Rightarrow CaCO_3 + H_2O} \qquad \mathbf{(2.2)}$$

Carbonation itself does not cause any direct deterioration of the concrete[17]. However, the following effects can indirectly induce other detrimental mechanisms :

- Carbonation shrinkage (inducing cracking of the concrete which accelerates other degradation processes);
- Reduction of the pH below 12;
- Liberation of bound chlorides present in the hardened cement paste (the calcium hydroxide is mainly responsible for binding of chlorides[17]).

Carbonation advances as a front through the concrete. The front is irregular due to the presence of coarse aggregates[17]. The loss of calcium hydroxide molecules is basically responsible for pH drop; totally carbonated concrete would have a pH around 9[17]. The transport mechanism by which the carbon dioxide can penetrate through concrete is diffusion. Since the diffusion process of CO_2 is possible only in air voids, saturated concrete is generally protected against carbonation.

The formation of the carbonation front is relatively slow and depends on the permeability of the concrete. If the relative humidity of the environment media is between 60 % and 95 %, the rate of carbonation of a structure will increase proportionally with an increase of the relative humidity[19]. Otherwise, the carbonation reaction is negligible The depth of the carbonation front varies with time as shown in Figure 2.1.

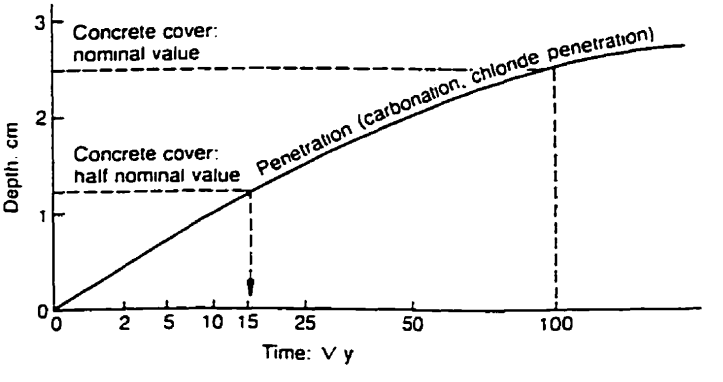

Figure 2.1 Example of the effect of the thickness of the concrete cover on the time necessary to the ingress of aggressive agents[19].

Depassivation due to the action of chloride ions : Chloride ions penetrate the concrete to reach the reinforcing steel and locally destroy the passive layer by chemically reacting with it in a low pH environment (pore solution of concrete)[17, 22]. By osmotic pressure, chlorides also cause the migration of water from the core to the freezing surface which action causes hydraulic pressure at the concrete surface[19].

The action of de-icing agents is similar to ordinary freezing and thawing, but in a more severe way[17].

The two main transport mechanisms in this case are the diffusion through totally or partially water-filled pores and the capillary suction of chloride solutions. Since the concrete has only a certain capacity to chemically bind and physically absorb chloride ions, there exists a dissolution equilibrium between bound chlorides and free chloride ions in the pore solution. In relation with the corrosion process, only the free chloride ions are worthy of interest[17], and their critical concentration in concrete (at which the process is initiated) is still not defined adequately and depends on many parameters, such as the initial concentration at the surface level, cementitious material content, time, ingredient proportions of the concrete mix, and degree of hydration of the hardened cement paste (hcp)[17].

Common sources of chloride ions are the marine water and de-icing chemicals (salts)[19]. Salts commonly used are sodium chloride (NaCl) and the more expensive calcium chloride ($CaCl^2$)[19]. Enrichment of chloride ions with depth occurs when the concrete structure is subjected to repeated wetting and drying cycles by chloride containing solutions. A quantity of chloride ions will be absorbed by capillary suction during the wetting cycles, and as the wetting solution is dried out, the chloride ions will remain in the microstructure[19]. The concentration of absorbed chloride ions is thought to vary with the depth from the surface, as a function of the concrete diffusion and the size of the capillary pores in the hydrated cement paste[17].

Depassivation due to the leaking out of the alkalis by streaming water : The alkalinity of the pore solution is lowered (as the pH) when streaming water leaches the alkalis out of the concrete microstructure[17]. Large cracks, leaky construction joints, and concrete of high permeability are amongst the construction issues associated with this phenomenon.

2.2.2.3 Chloride-induced corrosion process

Corrosion of steel reinforcement in concrete can be simplified to an electrochemical reaction involving two processes : the oxidation and the reduction. With the exceptions of noble metals like silver, gold, and platinum, when metal corrodes, it returns to its natural state (oxides or hydroxides)[22], since the metallic state involves a higher energy level. The thermodynamics of the corrosion reaction are reviewed further in this section.

Corrosion of metals (oxidation) occurs at the anode : it is the conversion of metallic iron into ferrous ions in solution. The process liberates two electrons capable of transferring to the other electrode (cathode) to form rust products (reduction)[22]. At the cathode, oxygen, water and the transferred electrons combine to produce hydroxyl ions. A schematic representation of electrochemical corrosion is presented in Figure 2.2, while the equations of reaction can be formulated as follows :

Anodic reactions :

$$Fe \Rightarrow Fe^{2+} + 2e^{-} \qquad (2.3)$$

$$Fe^{2+} + 2(OH)^{-} \Rightarrow Fe(OH)_2 \quad \textbf{(ferrous hydroxide)} \qquad (2.4)$$

$$4Fe(OH)_2 + 2H_2O + O_2 \Rightarrow 4Fe(OH)_3 \quad \textbf{(ferric hydroxide)} \qquad (2.5)$$

Cathodic reaction :

$$4e^{-} + 2H_2O + O_2 \Rightarrow 4(OH)^{-} \qquad (2.6)$$

Metallic continuity is needed while the ionic conductance is assured by the concrete pore solution[14, 17, 19, 20, 21, 22]. For the case of reinforcing steel corrosion, the anode and the cathode are located on the same bar, or on separate bars. In the later case, the top layer of steel forms the anodic steel where most of the corrosion occurs as a consequence of being closer to the source of chloride ions and water[21]. For

corrosion between different bars to occur, chairs, bent bars, and stirrups are needed to establish electrical continuity. Figure 2.3 presents a schematic representation of the corrosion process inside concrete.

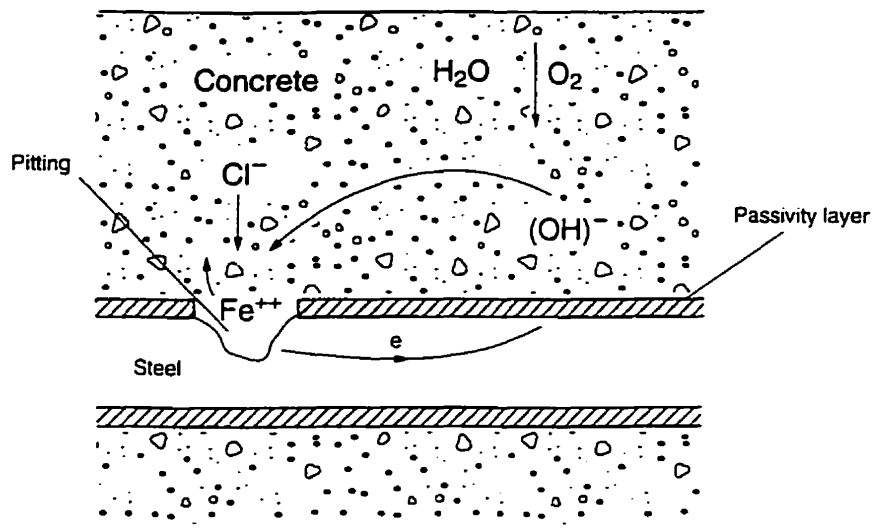

Figure 2.2 Schematic representation of pitting corrosion in the presence of chlorides[17].

In a general manner, these conditions must be achieved for corrosion to develop[17, 22]:

- Presence of oxygen;
- Presence of water (pore solution) acting as an electrolyte;
- Electric contact between half-cells (flow of electrons);
- Presence of chlorides.

The resistance of the concrete media controls the flow of current between the anode and the cathode, and is influenced by the following factors[17, 22] :

- Moisture content;
- Ionic composition of the pore solution;
- Continuity of the pore system in the hardened cement paste.

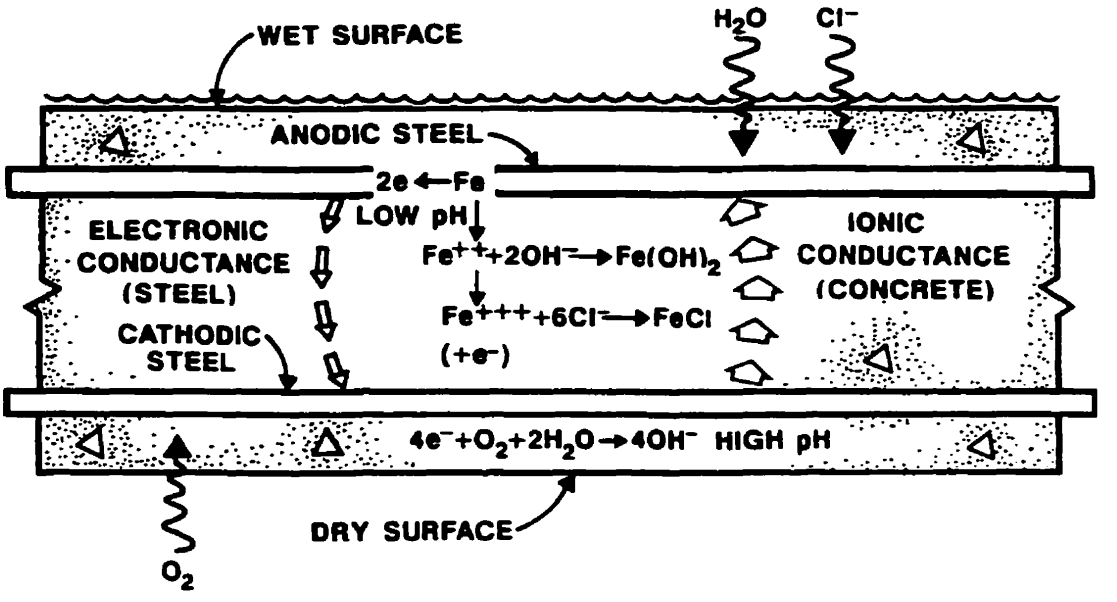

Figure 2.3 Schematic representation of electrolytic corrosion inside concrete[21].

The influence of the various important parameters on the corrosion of reinforcing steel can be summarized as follows[19] :

- The rate of corrosion is slow if induced by carbonation, and fast if induced by the presence of chlorides ions;
- Corrosion does not occur either if the concrete is saturated (no oxygen can diffuse since the voids are saturated), or the concrete material is dry (relative humidity below 60 %). An exception to this is concrete subjected to wave action, where entrainment of air is possible;
- Higher corrosion rates are associated with structures subjected to numerous wetting and drying cycles;
- Chlorides and carbonation : variations in the amount of chloride, moisture or oxygen at different points along the reinforcing bar or between different bars causes potential differentials and can possibly increase the rate of corrosion.

Effect of chlorides

For corrosion to be initiated, the passive layer on the steel reinforcing bar must be penetrated or broken. Chloride ions activate the surface of the steel to form an anode, the passivated surface being the cathode. Carbonation and mechanical surface wear can also accelerate the disruption of the protective film. A possible reaction between chloride ions and iron is given by[17] :

$$Fe^{2+} + 2Cl^- \Rightarrow FeCl_2 \qquad (2.7)$$

$$FeCl_2 + 2H_2O \Rightarrow Fe(OH)_2 + 2HCl \qquad (2.8)$$

In Equation 2.8, the chloride ions (Cl^-) are regenerated and available for reaction in the chloridric acid (HCl). If the polarized electrode is negatively charged, it will attract an excess of positive ions to its vicinity. The converse is also true. Consequently, the chloride ions are attracted to the anode.

Consequences of corrosion

The transformation of metallic iron to rust is accompanied by an increase in volume that can reach 600 percent of the original metal depending on the type of iron oxide produced[14, 17, 19, 20, 21, 22]. This volume increase is believed to be the principal cause of concrete expansion, cracking and spalling. Furthermore, cracking and spalling further ease the ingress of aggressive agents towards steel and accelerate the corrosion reaction[17, 19]. Figure 2.4 illustrates the damage induced by the corrosion of the reinforcement to concrete. Another possible result of the corrosion process is the reduction of the cross-sectional area of the steel reinforcement susceptible to render a structure incapable of safely sustaining its design functions[17].

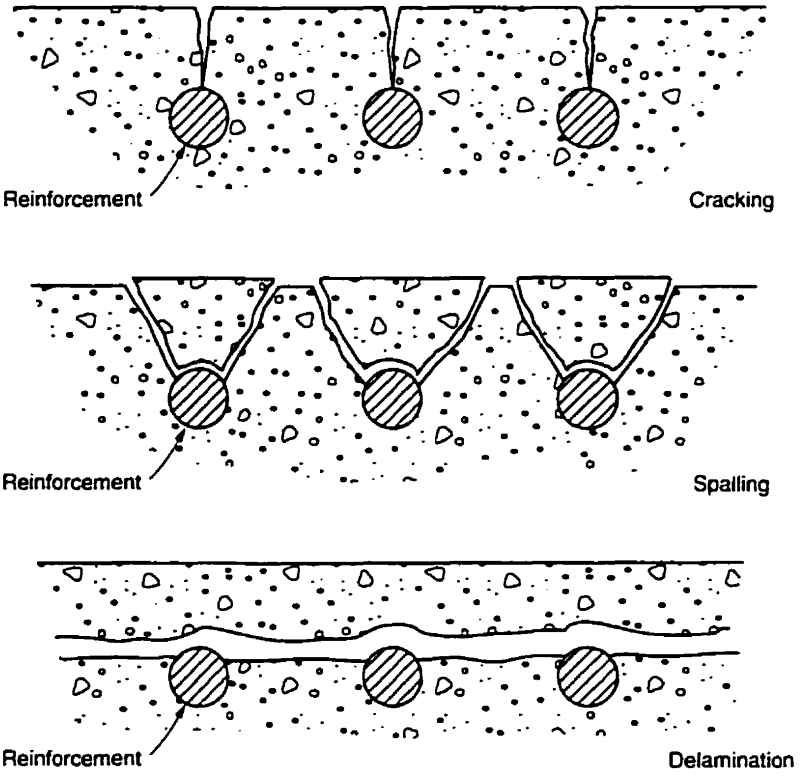

Figure 2.4 Diagrammatic representation of damage induced by corrosion : cracking, spalling, and delamination[17].

2.2.2.4 Different stages of chloride-induced corrosion reaction

Most chemical processes and reactions can be divided into different development stages. In the case of the chloride-induced corrosion process, two distinct development stages are of interest : the initiation stage and the propagation stage. These stages are described below and illustrated in Figure 2.5 :

- Initiation stage : it represents the ingress of deleterious agents in the concrete matrix until the passivity of the steel reinforcement is broken, allowing the corrosion reaction to proceed. Design details, material properties, and environment aggressiveness influence the duration of the initiation stage. These important factors can be subdivided into several categories presented in Section 2.2.4.

- Propagation stage : it starts as the steel reinforcement is depassivated and finishes with the end of the intended purpose of the structure (based on structural, serviceability, or aesthetic requirements). The propagation stage can be subdivided into three steps as shown in Figure 2.5. The first step consists in the development of the corrosion reaction until the formation of corrosion products start to disrupt the concrete matrix (cracking). The second step consists of the accelerating phase where cracking and spalling of the matrix increase both the rate of ingress of deleterious agents and of the corrosion reaction. The third step being the development of the reaction beyond the acceptable limits (at serviceability level) until the failure level is reached (in most cases due to the loss of bond with the concrete and to the critical reduction of the cross-sectional area of the reinforcement). Once the reaction is initiated, the rate of the corrosion reaction controls the propagation stage as a function of the influencing parameters described in Section 2.2.2.3.

2.2.2.5 Modern electrochemical theory of aqueous corrosion

Fontana[22] has presented a clear and concise description of the modern theory of aqueous corrosion, and of the different possible forms of corrosion. Corrosion of reinforcing steel presents characteristics similar to corrosion in aqueous media, the main difference being the surrounding concrete material acting as the transport media. The following section presents a summary of the important concepts supporting the theory of corrosion and an introduction of the influencing parameters summarized from Fontana's work : some being investigated in the scope of the Dickson Bridge research program, conducted at McGill University.

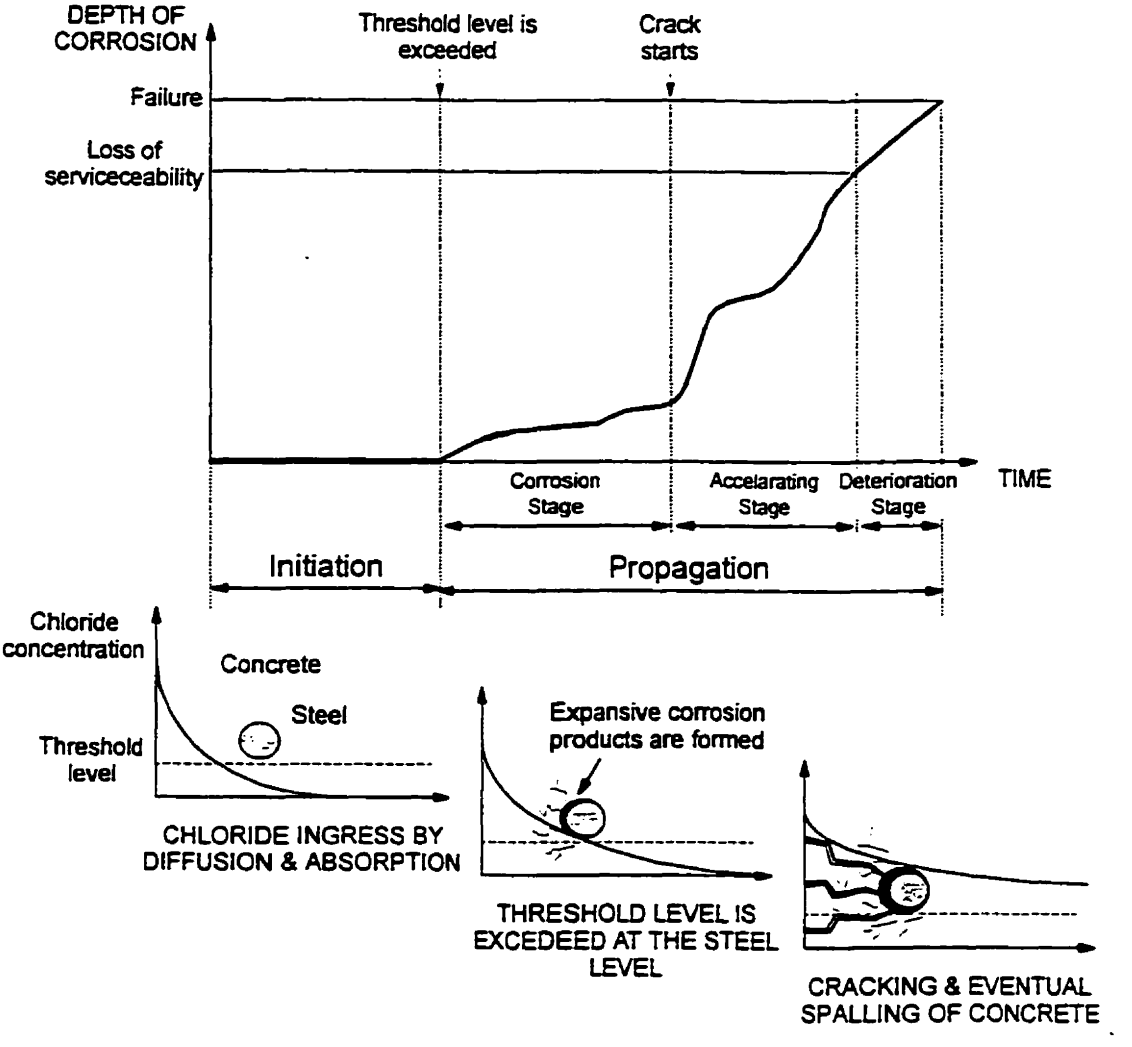

Figure 2.5 Diagrammatic representation of the corrosion stages[13].

Thermodynamics –applied to the corrosion mechanism

Free energy, ΔG

In thermodynamics, the general concept is that if no external forces are applied to a system, the system will tend to return to its lower energy state. As a consequence, chemical reactions more likely to occur are associated with the liberation of the free energy of the system[22]. The change in the free energy is a state function and is independent of the reaction path. Thus, the change in the free energy of a system is

considered to be a measure of the work capacity of the system, or an indication of the spontaneous reaction direction of the system[22]. The change in free energy can be calculated as follows[22] :

$$\Delta G = -n\,F\,E \qquad (2.9)$$

where ΔG represents the change in free energy, n is the number of electrons exchanged in the reaction, F is Faraday's constant, and E is the cell potential.

The potential of corrosion reactions, E, can be calculated using the half-cell reactions of the system. Each half-cell can be defined as an electrode of the overall electrochemical cell lying in a solution of its own dissolution products, and where the reaction of the electrode with its environment (media) is at equilibrium, i.e. the quantity of the metal dissolving in the media at the anode (oxidation) is equal to the quantity of the metal forming at the cathode (reduction)[22]. A standard half-cell potential can be defined if the concentration of the reactants (solution) is maintained at a unit activity (defined as a concentration of one mole per litre). The standard potential is then calculated with respect to the reference potential of the hydrogen reaction (set to zero by convention)[22]. Using the standard half-cell reactions, it is possible to determine the direction of the total reaction and to calculate the electric potential, E, of the system (cell). The electric potential of the system is a measure of the difference of potential between two half-cells. It is convenient to assign positive potentials to metals that are cathodic with respect to hydrogen, and the determination of anodic and cathodic reactions is made by comparing the potentials of the two half-cell reactions (or more if more than two electrodes are present) : the reduction reaction takes place at the cathode and the oxidation takes place at the anode, and both reactions are accompanied by a decrease of the electric potential (natural tendency to reach a minimum energy state)[22]. Standard half-cell reactions are frequently called oxidation-reduction potentials; some examples are presented in Table 2.2 :

Table 2.2 Half-cell potential of different metals with respect to hydrogen[14].

The Electromotive Series

Electrode	Cell Reaction	E° (volts)
Li^+ ½ Li	½ H_2 + Li^+ = Li + H^+	-3.025
K^+ ½ K	½ H_2 + K^+ = K + H^+	-2.925
Ca^{2+} ½ Ca	½ H_2 + ½ Ca^{2+} = ½ Ca + H^+	-2.870
Na^+ ½ Na	½ H_2 + Na^+ = Na + H^+	-2.714
Mg^{2+} ½ Mg	½ H_2 + ½ Mg^{2+} = ½ Mg + H^+	-2.370
Al^{3+} ½ Al	½ H_2 + 1/3 Al^{3+} = 1/3 Al + H^+	-1.660
Zn^{2+} ½ Zn	½ H_2 + ½ Zn^{2+} = ½ Zn + H^+	-0.763
Fe^{2+} ½ Fe	½ H_2 + ½ Fe^{2+} = ½ Fe + H^+	-0.440
Cd^{2+} ½ Cd	½ H_2 + ½ Cd^{2+} = ½ Cd + H^+	-0.402
Ni^{2+} ½ Ni	½ H_2 + ½ Ni^{2+} = ½ Ni + H^+	-0.250
Sn^{2+} ½ Sn	½ H_2 + ½ Sn^{2+} = ½ Sn + H^+	-0.136
Pb^{2+} ½ Pb	½ H_2 + ½ Pb^{2+} = ½ Pb + H^+	-0.126
H^+ ½ H_2, Pt	½ H_2 = H^+ + e	0.000
Cu^{2+} ½ Cu	½ H_2 + ½ Cu^{2+} = ½ Cu + H^+	+0.337
Ag^+ ½ Ag	½ H_2 + Ag^+ = Ag + H^+	+0.799
Au^+ ½ Au	½ H_2 + Au^+ = Au + H^+	+1.680
In general: ½ H_2 + (Oxidized State) = H^+ + (Reduced State).		

The calculation of the electric potential of the global reaction (cell) can be performed using two methods[22] :

1. By calculating the difference of potential between the two half-cells, taken from Table 2.2. This method is valid only if reactants are at unit activity, which is rarely the case;
2. Calculating the electric potential using Nearst's equation and correcting for differences in temperature and activity of the reactants (concentrations) :

$$E = E_0 + 2.3\,(R\,T / n\,F)\,\log([a_{oxidation}] / [a_{reduction}]) \qquad (2.10)$$

where E is the potential of the cell, E_0 is the standard half-cell potential (referring to standard redox potentials), R is the gas constant, T is the

absolute temperature, n is the number of transferred electrons. F is Faraday's constant, $a_{reduction}$ and $a_{oxidation}$ are the activities (concentrations of oxidized and reduced species).

The potential of the oxygen concentration is calculated using Equation 2.11[22]. This quantity influences mainly the pitting and the crevice modes of the corrosion process : the different modes of the corrosion reaction will be described later in this section.

$$E = (R\,T / n\,F)\,\ln(P[O_2] / P'[O_2]) \qquad (2.11)$$

where $P[O_2]$ is the vapour pressure at the cathode (increases at cathode) and $P'[O_2]$ is the vapour pressure at the anode (near zero).

Applications of the thermodynamics to corrosion

Once the electric potential of a reaction is computed, it is possible to determine the change in the free energy or , more importantly, the sign of the change in the free energy to measure the likelihood of the reaction. When studying the corrosion phenomenon, it is useful to predict the most spontaneous reaction that can occur since metals with reversible potentials more negative than hydrogen tend to corrode when put in contact with the acidic solutions. Since most chemical reactions do not proceed at unit activity (concentrations of reactants and products equal to one mole per litre), Nearst's equation must be used in order to determine the tendency of a possible reaction.

Based on the modern thermodynamic theory, a criterion for corrosion can be formulated : corrosion will not occur unless the spontaneous direction of the reaction indicates metal oxidation[17, 19, 20, 22]. The corrosion process is controlled by the likelihood and the rate of the corrosion reaction. It is important to consider that a small rate of corrosion combined with a high likelihood of corrosion results in insignificant damages. The applications of thermodynamics to the prediction of the

corrosion can be visualized using the Pourbaix diagram, which relate the different possible crystalline states of a metal to the potential of the reactions and pH[20, 22]. Pourbaix diagrams can help in (1) predicting the spontaneous direction of reactions. (2) estimating the composition of corrosion products, and (3) predicting environmental changes that will prevent or reduce corrosive attack. Since these diagrams are obtained from deriving the possible reactions under specific conditions, they cannot be used to evaluate the speed of reaction. The Pourbaix diagram for iron ($Fe\text{-}H_2O$) is presented in Figure 2.6. The different chemical forms that can possibly exist for the metal are presented as a function of the electrical potential and pH. It can be observed in Figure 2.6 that the iron is chemically stable below a potential of –600 mV, for pH values below 9. For higher values of the pH (between 9 and 16), the iron will oxide at even the lowest values of the electrical potential : the regions of the formation of the different oxidation products being clearly indicated in the figure.

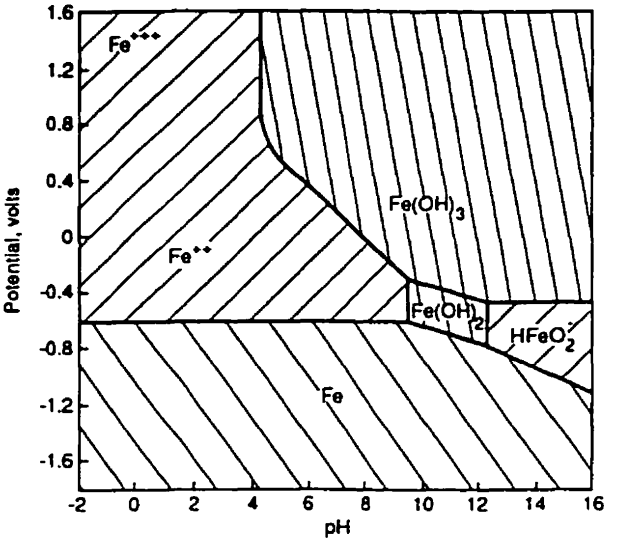

Figure 2.6 Potential-pH diagram for iron[21].

Rate of corrosion

In the prediction of the state-of-health of a structure in relation to corrosion attack of the reinforcing steel, the most important parameter to observe is the rate of corrosion[17, 22]. Before deriving equations to determine the rate of corrosion of a metal (or the speed of the oxidation reaction), some important concepts need to be refreshed :

Anodic reaction : half-cell reaction of oxidation proceeding at the anode (positively charged electrode).

Cathodic reaction : half-cell reaction of reduction proceeding at the cathode (negatively charged electrode).

Polarization : Deviation of an electrode from its equilibrium potential state resulting from a net flow of electrons (current).

Overpotential, η : Intensity or magnitude of the polarization (actual potential) with respect to the equilibrium potential of an electrode (by convention set equal to zero), as illustrated in Figure 2.7. The potential only provides a guide to determine which way a reaction tends to go: the rate of corrosion must also be examined.

Exchange current density

At equilibrium, for a given corrosion reaction, the velocity of half-cell reactions is equal on both sides of the equation : the rate of oxidation equals the rate of reduction[22]. Also, a unique electric potential value is associated with this equilibrium state[22]. The rate of reaction at equilibrium is expressed as the exchange current density, since electrons released during oxidation are consumed during

reduction. The relationship between the reaction rate and the exchange current density is as follows[22] :

$$r_{oxid} = r_{red} = i_0/(n\ F) \qquad (2.12)$$

where r_{oxid} and r_{red} are respectively the equilibrium oxidation and reduction rates. i_0 being the exchange current density, and n and F are as defined previously.

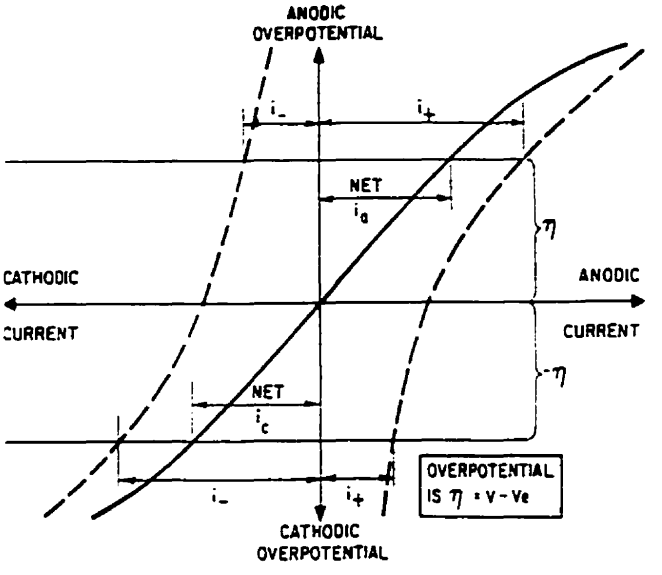

Figure 2.7 Voltage to current diagram for an electrode reaction[14].

If the value of the exchange current is large, a given change in the electric potential will result in a large change in the exchange current. The converse is also valid.

It is important to note that since there is no net current, the exchange current density only represents a convenient expression to define the rate of reaction at equilibrium. The exchange current density must be determined empirically for any given system, and is usually expressed in terms of the geometric surface area[22]. In the case of reinforcing steel corrosion, it is clear that the surface roughness greatly influences the rate of corrosion[17].

Activation polarization versus concentration polarization

Electrochemical polarization of an electrode can be achieved based on two different polarization mechanisms : the activation polarization and the concentration polarization. Table 2.3 summarizes the characteristics of these two basic mechanisms. A third mechanism is also possible as a combination of both mechanisms and referred as combined polarization[22].

Table 2.3 Summary of characteristics for activation and concentration polarization modes.

Activation polarization	**Concentration polarization**
Type of control Controlled by a slow step in the reaction sequence.	**Type of control** Controlled by a limiting rate of the reduction reaction due to a lack of ions in the vicinity of the electrode (cathode).
Formula to determine the overpotential, η $\eta_a = \pm B \log (i / i_0)$ **(2.13)** where B is the Tafel constant (ranging between 0.05 and 0.15 volts), i is the rate of reaction (reduction or oxidation), i_0 is the rate of reaction at equilibrium for unit activities. **Assumptions :** A linear relationship exists between the exchange current density and the rate of reaction The electric potential is greater than ± 50 mV)	**Formula to determine the overpotential, η** First define the limiting diffusion current density, i_l $i_l = D\ n\ F\ c_b / X$ **(2.14)** where D is the diffusion coefficient of the reacting ions, c_b is the concentrations of the reactants in the bulk concentration, X is the thickness of the diffusion layer, and n is the number of electron transferred. $\eta_c = 2.3\ R\ T / (n\ F \log (i_l / i_0))$ **(2.15)** **Assumptions :** The limiting diffusion current density is significant only during the reduction.

Table 2.3 Summary of characteristics for activation and concentration polarization modes (continued).

Activation polarization	**Concentration polarization**
Sensibility : The exchange current density (rate of reaction) is sensitive to a small increase in overpotential (electric potential).	**Sensibility :** Shape and geometry of the cathode influences the limiting diffusion current density. Concentration polarization is only applicable when the limiting diffusion current density is in the vicinity of the net reduction current

Combined polarization

The combined polarization occurs in most cases, and is a mixture of both polarization modes described previously. For small rates of reaction, the activation polarization dominates, as high rates of reaction saturate the cathode and leads to concentration polarization control. Derived from the properties of the polarization modes, the following expressions for the overpotential are valid for almost all oxidation and reduction reactions, with some exceptions applying in the case of metals showing a combined active-passive behaviour.

Oxidation reaction (at the anode)

$$\eta_a = \pm B \log (i / i_0) \qquad (2.16)$$

Reduction reaction (at the cathode)

$$\eta_c = - B \log (i / i_0) + 2.3 R T / (n F \log (i_l / i_0)) \qquad (2.17)$$

Butler-Volmer equation

The Butler-Volmer equation is used to calculate the current density at which the corrosion reaction will proceed based on the overpotential of the system. By using Faraday's equations, it is then possible to relate the exchange current density (i_{ex}) to the quantity of metal corroding per year (i)[22].

$$i = i_{ex} (e^{(1-\beta) F \eta / RT} - e^{-\beta F \eta / R T}) \qquad (2.18)$$

where β is the symmetry factor, η is the overpotential, F, R, and T are as previously defined.

There are two limiting cases to the application of this equation, which are presented below, and illustrated in Figures 2.8 and 2.9[22] :

1) When $|\eta|$ is greater than 50 mV : the second term of Equation 2.18 is ignored and the equation simplifies to $\eta = a + b \ln (i / i_{ex})$ **(2.19),** where a and b are called Tafel's constants : Tafel's equation shows a linear relationship between the overvoltage and the logarithm of current. This case applies only for corrosion reaction controlled by the activation polarization mode.

2) When $|\eta|$ is smaller than 5 mV : Equation 2.18 becomes $\eta = R T i / (i_{ex} F)$ **(2.20)**. Tafel's constants derived from these equations are useful to predict the corrosion behaviour of a given system. Linear polarization techniques used to determine the rate of corrosion (i) are based on these constants.

The techniques used to predict the corrosion behaviour are presented in Chapter Three.

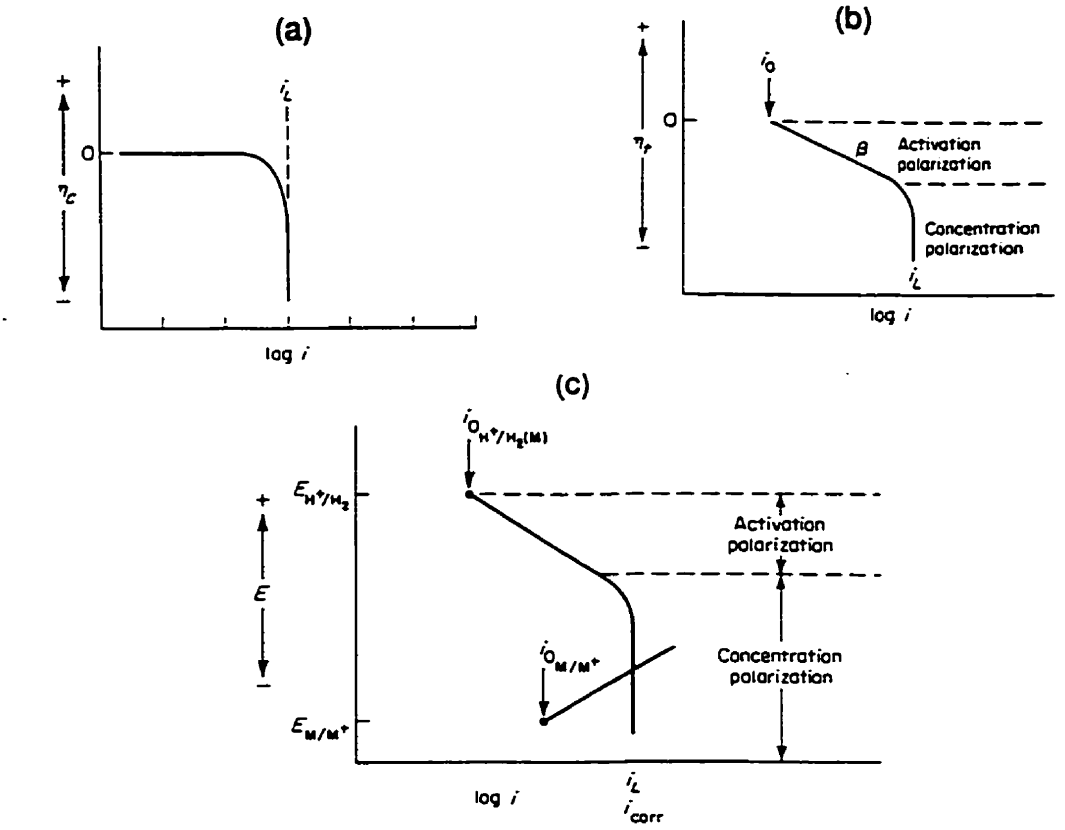

Figure 2.8 (a) Concentration polarization curve, (b) combined polarization curve, (c) corrosion of metal M under reduction-diffusion control[22].

Passivity

Adsorption of negative chloride ions (Cl^-) by the metal (steel reinforcement) is an important phenomenon in corrosion. The small chloride ion can adsorb close to the metal surface and this action leads to irregularities in the adsorbed water dipoles. This is the reason why it is difficult to either develop or maintain protective films when chloride ions are present[17, 22]. The protective film consists of a readily formed insoluble corrosion product that inhibit the anodic reaction. The factors affecting the strength of the protective passive film are[22] :

- Solubility of the corrosion products;
- Cohesion of the corrosion products with the underlying metal;

- Permeability of the concrete to various chemical species:
- Electrical resistivity.

The passivity of certain metals and alloys can be described as their capacity to diminish their chemical reactivity under specific environmental conditions. As a consequence, the corrosion rate of a metal in the passive state is very low (reduction of the order of 10^4 to 10^6 from the active state)[22]. Also, the passive level is considered relatively unstable and subjected to different kinds of damage (scratching, presence of chloride ions, etc.)[17]. According to the literature, the passive characteristics are a result of a thin surface film of about 30 Angstroms (where 1 Angstrom (A°) is equal to 10^{-10} m) forming under equilibrium conditions in the aqueous environment[17, 22]. The complete nature of the film is still undetermined and further research is needed[22] in that domain. However, a possible reaction between chloride ions and metal is presented in Section 2.2.3.

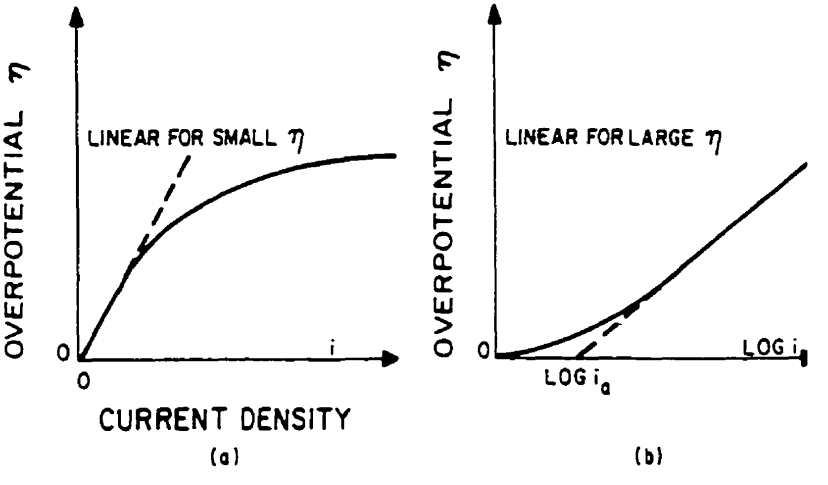

Figure 2.9 Current density to overpotential relationships : (a) for small overpotentials; and (b) for large overpotentials[14].

In relation with the corrosion mechanism of reinforcing steel, the passivity of the rebar is of great importance. Figure 2.10 showing the transition from passive to active state is self-explanatory and typical for iron-steel reinforcement.

The metal initially demonstrates behaviour similar to non-passivating metals. That is, as the oxidation reaction first proceeds, the anode becomes more positive (loss of electrons) and the metal follows typical Tafel behaviour.

Modern theory applications

It is possible to use the mix potential theory to predict complex corrosion behaviour and to develop rapid corrosion rate measurement techniques. The basic concepts underlying these techniques are presented in this section.

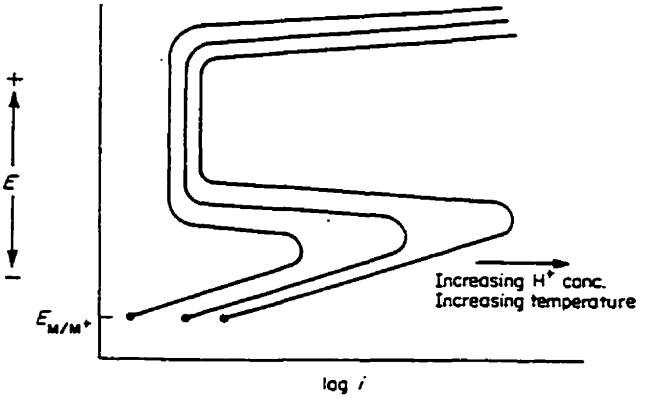

Figure 2.10 Effect of temperature and acid concentration on anodic dissolution behavior of an active-passive metal[22].

Prediction of corrosion behaviour

The prediction of corrosion behaviour is of great engineering interest. When analyzing a corroding system (entire structure, particular member, etc.), several questions need to be answered to determine the remaining service life or to assess the present state-of-health of a structure. For example, the extent of the corrosion-induced deterioration, the rate of corrosion reaction, and the areas showing high risks of developing corrosion in the steel reinforcement can be determined using the

modern theory of electrochemistry. The key factor in this type of analysis remains the accurate evaluation of the rate of reaction. Now that the basic principles of the corrosion mechanism have been described, it is possible to introduce the most influencing factors of the rate of reaction. The three most important ones are presented below :

- Effects of oxidizers : the presence of oxidizers generally increases both the corrosion rate and the corrosion potential (or electric potential)[22]. The magnitude of this augmentation is dependent (1) on the redox potential of the oxidizer, (2) on the exchange current density, and (3) on the value of Tafel's constant (β slope). For metals showing active-passive behaviour, this increase can result in the passivation of the metal (reduction of the rate of corrosion) if the junction potential is lying in the passive area (polarization curves #4 and #5) shown on Figure 2.11. On the same figure, it can be observed that there exists an unstable area (curve #3) where the corrosion potential can take two different values (thus modifying the rate of corrosion);

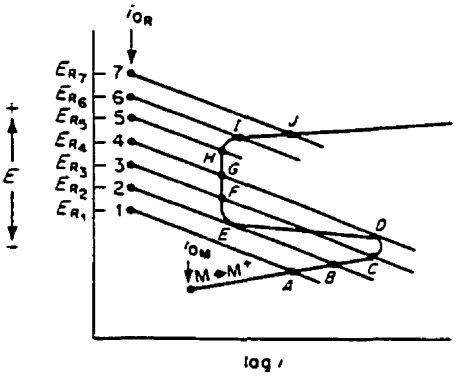

Figure 2.11 Effect of oxidizer concentration on the electrochemical behaviour of an active-passive metal[22].

- Effects of velocity : affect only concentration controlled systems[22]. Both the rate of corrosion and the corrosion potential increase with an

augmentation of the velocity of the solution in the electrolyte (concrete diffusion) near the corroding electrode. When the corrosion rate reaches a maximum value, termed the limiting diffusion current density, the effects becomes negligible[22]. The effects of velocity are illustrated in Figure 2.12;

- Effects of temperature : generally, the rate of reaction of all chemical reactions is accelerated with an increase of the temperature[17, 19, 22]. A simple rule-of-thumb is that an increase in temperature of 10 °C increases the rate of reaction by a factor of two.

Corrosion rate measurements

Corrosion rate measurements can be divided into two parts : the Tafel's extrapolation and the linear polarization techniques. The description of the measurement techniques presently available for laboratory and in-situ testing is beyond the scope of this thesis. However , the techniques selected for the investigation of the south section of the Dickson Bridge with regards to corrosion rate measurement are presented in Chapter Three.

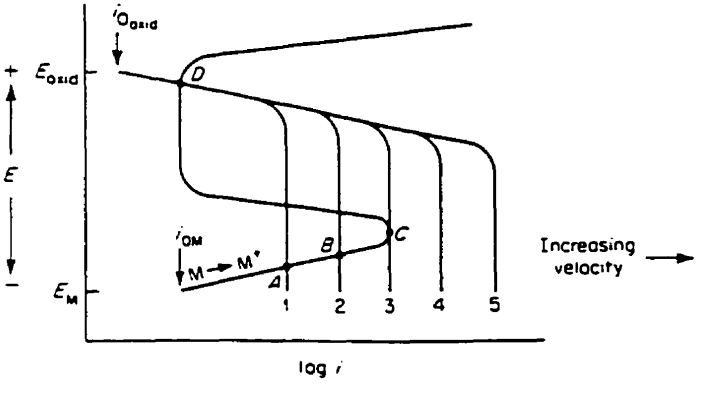

Figure 2.12 Effect of velocity on the electrochemical behaviour of an active-passive metal corroding under diffusion control[22].

2.2.2.6 Different forms of corrosion

There exists several different forms in which corrosion can manifest itself, based on the mechanism of degradation, and on the surface appearance (morphology) of the corroding metal[17, 22]. Each form can be identified by visual inspection. With respect to corrosion of steel reinforcement embedded in concrete, three forms are of high interest : the uniform corrosion, the pitting corrosion and the galvanic corrosion. The most common forms, including the three of common interest, are reviewed and for each of them the particular characteristics are outlined :

- **Uniform corrosion (general attack)** : Most common form of corrosion, the corrosion reaction proceeds uniformly over the whole surface area of steel[22]. It represents the form of corrosion that consumes the largest quantity of metal[17]. Loss of metal over time can be predicted by the use of simple techniques. Loss of bond with concrete is a major concern from a technical standpoint.

- **Galvanic corrosion (two-metal corrosion)** : Two or more metals in electrical contact placed in the same electrolyte produce a galvanic cell where the difference in electric potential (corrosion potential) is sufficient to induce a flow of ions (exchange current), resulting in the oxidation of the less resistant metal (based on redox equilibrium potentials), and the reduction of the other metal. The potential of corrosion of two metals is defined on their relative positions in the galvanic series, the environment aggressiveness, the physical distance between them and the ratio of the cathodic to the anodic area.

- Crevice corrosion : Is also commonly referred as deposit or gasket corrosion. It is the intensive and localized corrosion occurring in crevices and holes of metal surfaces exposed to aggressive environments.

- **Pitting corrosion** : This form of corrosion is considered to be the most destructive and intensive form compared with any others[17, 19, 22]. Failure induced by perforation of metal sections can often be responsible for the premature end of service life of equipment or reinforced concrete members or structures. Pitting corrosion is also very difficult to detect since it is very localized. The presence of chloride ions is thought to increase the rate of reaction but the effects of chlorides on the mechanism are not established. Once the corrosion reaction has started to proceed, the rate of reaction always keeps on accelerating[22]. Most of the time, the subsurface damage is more severe than indicated by surface inspection. In opposition with crevice corrosion, no crevice or hole is needed to induce the pitting corrosion. Stagnant solutions increase the risks of developing this form of corrosion. Figure 2.13 shows the autocatalytic process of pitting corrosion.

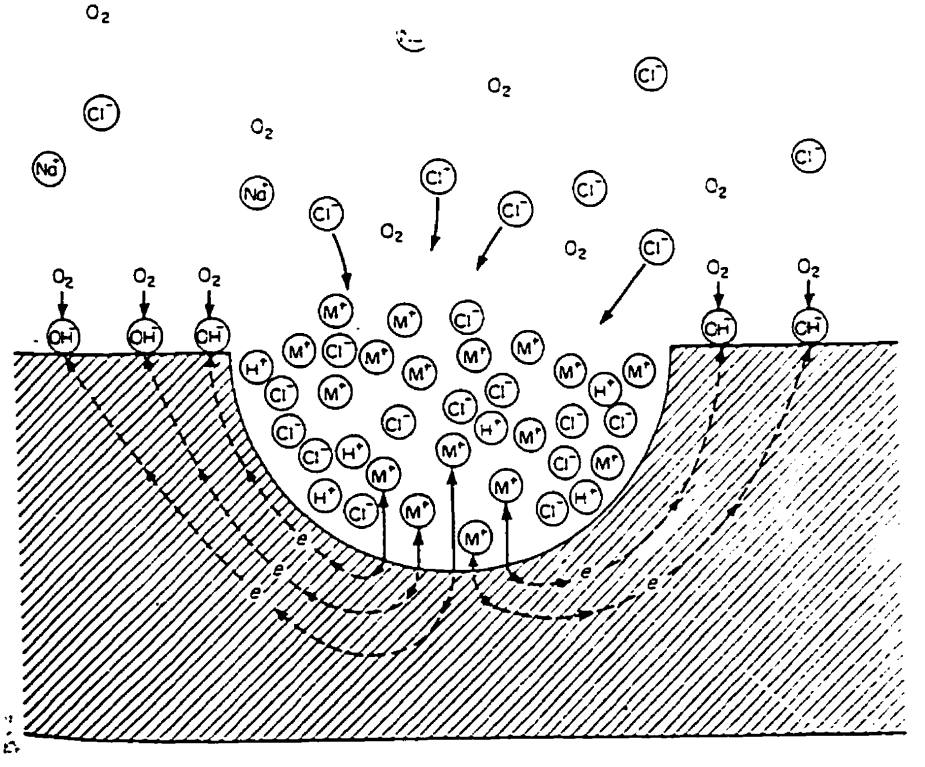

Figure 2.13 Autocatalytic processes occurring in a corrosion pit[22].

- Intergranular corrosion : Form of corrosion due to the difference of corrosion reactivity between the metal grains boundaries and the matrix. Impurities at the grain boundaries and enrichment of alloying elements can be responsible for this form of attack. Intergranular corrosion is of little interest in relation with the corrosion of reinforcing steel.

- Selective leaching : This form of corrosion attack can be defined as the removal of specific elements of the alloy matrix by corrosion processes. The most common case is the dezincification of the zinc in brass alloys[22]. This form of corrosion is also of little interest with respect to reinforcing steel corrosion.

- Erosion-corrosion : Erosion-corrosion results in an increase of the rate of reaction due to the flow of a corrosive solution on a metal surface. Abrasion is often involved, and signs of directional corrosion-induced patterns are representative of this type of attack. The protective film can be destroyed by circulating fluids containing solid particles in suspension. Cavitation damage associated with turbulent flows can increase the intensity of the attack.

- Stress corrosion : This form of corrosion refers to the failure of steel members due to both the presence of an aggressive environment and the tensile loading of a particular steel section. Cracking of steel due to this form of attack implies the progression of fine cracks through the steel while the surface remains uncorroded. From the standpoint of corrosion of steel reinforcement, this type of attack is negligible and of minor significance[17].

2.2.3 Influencing factors

Since the chloride-induced corrosion process necessitates the contribution of external aggressive compounds, the transport mechanisms in the concrete are mainly

responsible for the capacity of the reinforcing steel to preserve its original passivated state[17, 19].

As mentioned in Section 2.2.2.1, the transport mechanisms in concrete are widely influenced by the material properties of the hardened cement paste (hcp), the environment of the concrete structure, decisions made at the design stage (choice of drainage system, selection of materials and dimensioning of members), and the quality of the construction procedures (mixing, placing, and curing of concrete). These factors play an important role in the development of the corrosion process of the steel reinforcement, and are reviewed in this section. The influencing factors can be divided into three main categories :

- Material properties;
- Environmental conditions;
- Structural design.

Interactions between the different influencing factors are deliberately ignored in this review. Nevertheless, it is important to consider these interactions when assessing the aggressiveness of a particular environment, or when determining the resistance of a concrete structure with regards to chloride-induced corrosion or any other mechanism of degradation[19].

2.2.3.1 Material properties

Water / cement ratio of concrete

The water / cement ratio and the degree of hydration determine, under satisfactory placing and compacting conditions, the capillary porosity of the hardened cement paste (hcp)[19]. The quantity of capillary voids in the hcp influences the permeability of the concrete as shown in Figure 2.14. It can be observed in Figure 2.14 that the water permeability of concrete varies exponentially with the water / cement ratio : this

especially true for values of the water / cement ratio above 0.5. Scientifically, it is easy to relate the permeability of concrete to the corrosion process of the reinforcing steel. Meanwhile, it is important to remember that the permeability of concrete varies locally in a structure as a direct consequence of the heterogeneity of the concrete. Also, the choice of the water / cement ratio should be based on other important issues such as the placing procedure, the costs of cement in the overall construction costs, the use of cementitious materials, etc.

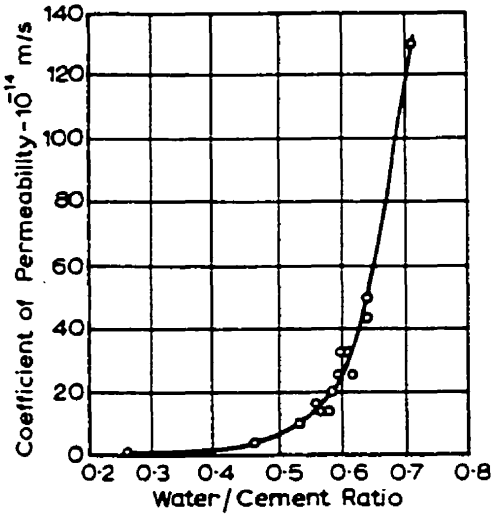

Figure 2.14 Relation between permeability and water / cement ratio for mature cement pastes[17].

Cement content and type

The cement content of the concrete influences the chloride ion content and carbon dioxide binding capacity of the material, as illustrated in Figure 2.15. It can be observed in Figure 2.15 that the water permeability of the concrete increases with the water / cement ratio. The quantity of water that does not participate to the hydration process increases the volume of voids in the hardened cement paste, leading to an increase in the permeability of the concrete. On the other hand, the thermal stability of the structure is decreased with a significant augmentation of the cementitious

content, increasing the risk of shrinkage-induced cracking. For this reason, it is not recommended to use Portland cement alone[17, 19].

The use of pozzolanic cementitious materials in addition to Portland cement can result in a reduction of the permeability of the concrete by decreasing the initial temperature of hydration and retarding the hydration process at a later stage[17, 19]. Meanwhile, special attention should be given to placing and curing requirements.

The supplementary cementing materials of interest are fly ash, ground granulated blast furnace slag and silica fume. All three, when properly proportioned in the mix, significantly reduce the permeability and the electrical resistivity of concrete by the combination of hydration and pozzolanic reactions which have a time lag, further refining the microstructure of the hydrated cement paste and decreasing the water permeability of concrete. Also, the use of these materials offers the possibility to reduce the rate of corrosion in a long term perspective, by limiting the ingress of deleterious agents due to its decreased permeability.

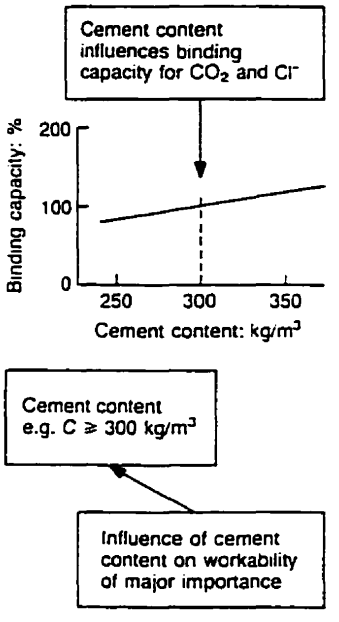

Figure 2.15 Influence of the cement content on binding capacity[19].

Chloride ion binding capacity of the hydrated cement paste is mainly due to the presence of tricalcium aluminate (C_3A) and of tetracalcium aluminoferrite (C_4AF) molecules[17, 19]. For the C_3A, it is thought that chloride ions chemically react with C_3A molecules to form Friedel's salt ($3CaO.Al_2O_3.CaCl_2.10H_2O$). For the C_4AF, since the description C_4AF is a convenient simplification for the solid solution ranging from C_2F to C_6A_2F, the basic reactions are still not perfectly understood and may vary widely.

When deciding on the desirable C_3A content of the cement, it is important to consider the possibility of developing an internal sulphate attack in the concrete if the C_3A content is too high[17]. Nowadays, a good compromise is to use a moderately sulphate resisting cement of Type II (or Type 20) with a C_3A content around 10 % by weight of cement[17].

High C_3A content cements increase the heat of hydration which could be detrimental to large concrete masses by inducing thermal shrinkage cracking. In a different perspective, the type of cement also influences the risk of developing corrosion of the reinforcing steel[17]. The chloride content of the cement should be less than the threshold value given in applicable design codes. The determination of a standard threshold value to be used in the design codes needs further research, but Figure 2.16 presents possible results for the threshold content. The values proposed in Figure 2.16 were derived using models developed to estimate the corrosion process based on Fick's 2nd law of diffusion. The threshold content was defined as the critical chloride concentration necessary to initiate the corrosion reaction. The difficulties to determinate the time of initiation of corrosion reaction and accurately evaluate the chloride concentration at the concrete surface limit the validity of the threshold values obtained here.

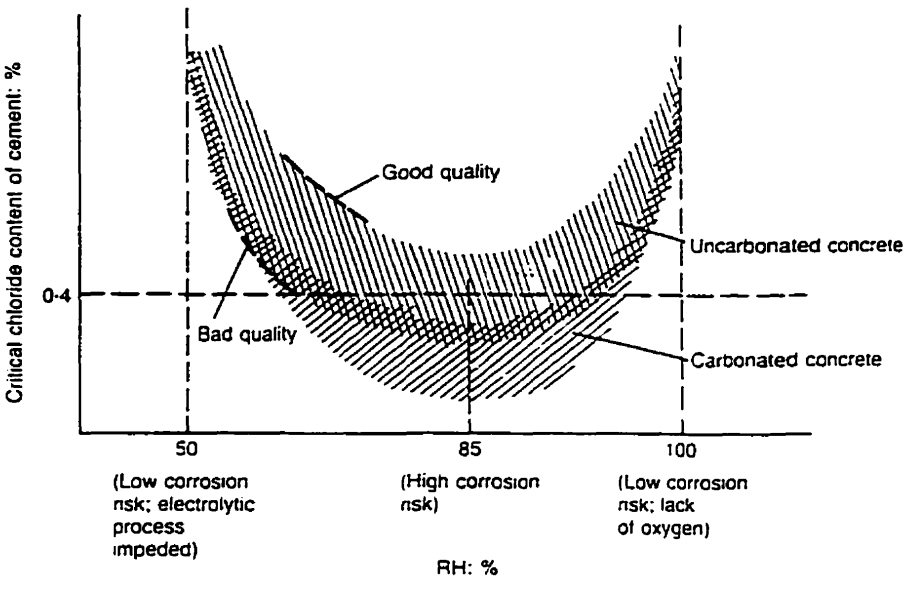

Figure 2.16 Variation of critical chloride content with environment[19].

Curing of concrete

The capillary porosity of the hardened cement paste depends partially on the degree of hydration of the concrete. The hydration process starts instantaneously after all ingredients are mixed together, increasing the temperature of the newly cast concrete, and ceases after either the mix water or the cementitious material has completely reacted to form hydrates or one of these ingredients is not available anymore for hydration (trapped in the hcp matrix). Evaporation of the surface water due to wind and high temperature can stop the hydration process and can lead to partially-hydrated concrete materials with high permeabilities. The curing of concrete prevents premature stopping of the hydration process by protecting the concrete material against the loss of water required for hydration. It should be mentioned that once the hydration process of concrete has stopped, it never starts again[17]. This phenomenon is related to the high entropy energy (activation energy) that would be needed for the hydration process to start again.

Placement and compaction of concrete

Good placement and compaction of concrete ensure its homogeneity, thus reducing significantly the overall coefficient of permeability[19]. The presence of gravel pockets and latence water generally diminishes the protection offered to the steel reinforcement and can impair the durability of the structure on a long term.

2.2.3.2 Environmental conditions

The wide use made of concrete as an engineering material is related to its excellent resistance to water and aggressive environments. In most cases, the interactions between the concrete and its environment contribute to the deterioration processes which can occur. The type and aggressiveness of the environment play a major role in the different possible deleterious mechanisms that can occur in a concrete structure subjected to weathering[19]. The most important environmental issues with regards to corrosion of the reinforcing steel are reviewed here.

The definition and classification of aggressive environmental conditions still represent problematic concepts, despite the fact that many researchers attempted to address the situation by proposing various simplistic models[7]. Presently, there exists no standard method in the North American design codes to clearly define aggressive environments with respect to the potential damage of reinforced concrete structure. On the contrary, European design codes[19] proposed a method to adequately determine the aggressiveness of different possible environments. Nevertheless, the most influencing parameters affecting the aggressiveness of any environment are presented below and summarized in this section[17] :

- Availability of moisture;
- Presence of aggressive substances in moisture;
- Temperature level;
- Freezing and thawing cycles.

Availability of moisture

The presence of water is essential for any deleterious process to take place[17, 19], with the exception of mechanical wear. For that reason, the moisture content of the hardened cement paste is important. Concrete tends to absorb water more rapidly than it loses it, with the consequence of keeping its internal humidity higher than the average ambient relative humidity.

In the hydrated cement paste (hcp), water can exist under different forms : capillary water, absorbed water, interlayer water, and chemically combined water. The free water available for transport mechanisms and chemical reactions in the concrete are the capillary water (not bound) and the adsorbed water (physically adsorbed by the hcp; hydrogen bond can be easily broken)[17].

Presence of aggressive substances in moisture

With regards to the chloride-induced corrosion of steel, the presence of carbon dioxide, chlorides, oxygen and water is necessary to initiate the chemical reaction. As reviewed previously in Section 2.2.2.3, chloride ions and carbon dioxide destroy the passive layer of steel. Oxygen is necessary for the reaction to take place and water acts as a transport agent (electrolytic agent).

Other aggressive substances indirectly related to the corrosion process are the alkalis (with respect to the alkali-aggregate reaction) and the sulphates (sulphate attack). These processes can lead to the formation of an expansive gel that disrupts the concrete structure forming cracks. As a direct consequence, the permeability of the concrete increases and the resistance to the ingress of aggressive agents is reduced. Also, when large amounts of chlorides are present, concrete holds more moisture, decreasing the electrical resistivity of the concrete : once the passive layer is destroyed, the electrical resistivity and the availability of oxygen (O_2) control the corrosion rate[17, 22].

Sources of chlorides

In general, chlorides could either be present in the original mix, or they have ingressed the concrete matrix from several possible sources. It was observed[17] that the corrosion attack is faster if the chloride ions come from the mix than from the external sources. The common possible sources of chlorides are :

Chlorides present in the mix

- use of contaminated aggregates ;
- use of sea or brackish water ;
- use of admixtures containing chlorides (Portland cement contains only a very small amount of chlorides by weight (< 0.01 %), ground granulated blast furnace slag may have significant chloride content if quenched in sea water).

Ingress of chlorides

- Sea water;
- De-icing salts;
- Brackish ground water in contact with concrete;
- Organic materials containing chlorides.

Threshold content of chlorides ions

With the passage of time, a sufficient amount of chloride ions will reach the surface of the reinforcing steel. However, no universally accepted threshold value exists in the literature[7, 17, 19]. However, threshold values for chlorides in the concrete mix were proposed : 0.4 % by mass of cement[17] or 0.6 to 0.9 kg/m^3 of concrete[23]. For chlorides which have penetrated into the concrete, it is difficult to determine a

threshold value because many factors are still imperfectly understood as is the distribution of chloride ions within the hardened cement paste.

Nevertheless, it is now generally accepted that it is not the total chloride content that is relevant to corrosion but only the free chlorides : not chemically bound nor physically adsorbed[17, 19, 23]. In addition, the free chloride content varies in time with the moisture content as a function of the total chloride ions solubility at equilibrium[17, 23]. Finally, it is important to consider the action of the carbonation process of concrete on the free chloride content. Carbonation can lead to the release of chemically bound chlorides held by calcium hydroxides ($Ca(OH)_2$) when the calcium hydroxides react with carbon dioxide molecules from the atmosphere.

Temperature level

As most chemical reactions are accelerated with the increase of temperature, the risk of developing corrosion of the steel reinforcement is enhanced with the increase of the environment temperature. A simple rule-of-thumb is that an increase in temperature of 10 °C causes a doubling of the rate of reaction[19].

Freezing and thawing cycles

The transition from water to ice of the capillary water is accompanied by a change in volume of approximately nine percent (9%). If the concrete pores are saturated, there is no space available to accommodate for this volume augmentation, and the induced tensile stresses could be sufficiently high to disrupt (crack) the concrete matrix.

At the pore surface, the potential energy of the pore solution would be higher compared to that near the centre of the member lowering the freezing point at the pore interface. As a consequence, unfrozen water is still present at very low temperatures (-60 °C). When ice starts to form, this allows for partial diffusion of the unfrozen pore water into the adjacent pores to extend the action of the freezing and thawing process[17].

Deterministic approach to quantify the aggressiveness of the environment – An example

The aggressiveness of different environments can be defined quantitatively based on the electric potential and the pH[20]. An example of approach to identify and quantify aggressive environments is presented here[20].

Definition of aggressive environments

Most reinforced concrete structures (or components) are exposed to multiple environments[20]. For example, the two sides of a supporting wall can show differences in the relative humidity, temperature, concentration in chloride ions, etc. In addition, different modes of corrosion are possible within a particular member, and over a particular reinforcing steel bar[20].

Based on the Pourbaix diagrams, it is possible to define the environments in terms of key parameters such as the electric potential and pH. Also, the roles of environments on the surface can be specified such as the species and their concentrations. As a result, all environments to which a given material or component is exposed can be summarized in a single diagram with potential and pH as coordinates[20].

As a consequence, it becomes possible to compare the range of potential and pH for which a specific environment is specified for a particular (or all) mode(s) of corrosion in a given domain. This is done by superposing the graphics of the domain : the region where the environmental definition and the mode definition intersect is the critical region where corrosion reaction is expected to proceed. In general, components may be exposed to several different environments and modes of corrosion simultaneously[20]. Figure 2.17 developed by Poubaix and later adapted by Staehle[20] summarizes the results obtainable using this approach. Figure 2.17 shows the superposition of environmental definition (in b) on the corrosion mode definition (in a) to obtain a superimposed result (in c). The use of the electrical potential and of

the pH is useful since these quantities are principal variables in kinetic processes. For a particular application. the grade of the metal can be selected based on the expected aggressiveness of the environment with respect to pH and electrical potential in order to design systems with increased durability.

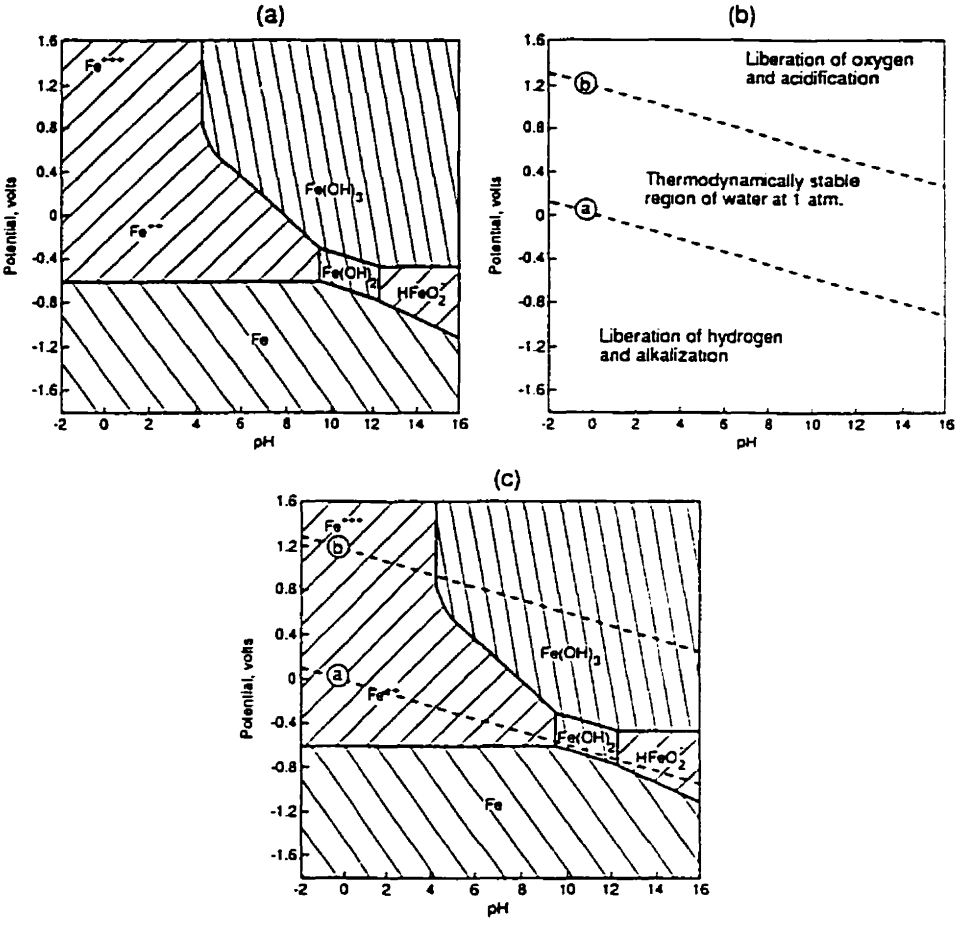

Figure 2.17 Superposition of potential-pH diagrams for iron and water: (a) potential-pH diagram for iron: (b) potential-pH diagram for water: (c) superposition of diagrams to give integrated view of relationship between metal and environment[20].

Environmetal probability

In considering the design life of a component. not all environments are highly probable and some will occur only for a short duration[20]. This can be treated

probabilistically and is beyond the scope of this thesis. However, more work is needed to adequately assess all possible aggressive environments, their probability of occurrence and the extent of damage associated for each[20]. The possible interactions between the different aggressive environments also need to be considered.

2.2.3.3 Structural design

Design aspects

As mentioned previously in Section 1.1, corrosion control must be planned at the design stage in selecting materials on the basis of the most economical solution to the design problem. Selection of materials electrochemically compatible and selection of adequate protection systems from the beginning are important issues to be considered by the designer. Design details should also reflect this philosophy. In this section, a review of some important design details is presented.

Design of details

First of all, design of details should at least conform to the applicable code requirements and regulations. Special attention should be given to the following issues in order to maximize the service life of reinforced concrete structures :

- Provide adequate drainage over the concrete structures : any detail that can trap water must be avoided;
- Provide an impermeable concrete cover of sufficient thickness : unduly large thickness of cover would crack as a result of the presence of a considerable volume of concrete without any reinforcement. For the same reason, the maximum concrete cover should not be more than 50 to 60 mm[17]. If additional protection against penetration of deleterious agents is needed, sealers and membranes can be used;
- Control the presence and width of cracks : chloride ions and carbonation penetrate more rapidly towards the reinforcement when cracks of width

larger than four (4) millimeters are present. Cracks of width smaller than four millimeters represent the cracks self-healing with the deposition of dirt and the formation of rust products[19]. Larger exposed crevices must be neutralized in any possible way, including coating of the cracked surfaces using sealers, membranes, etc.;

- Consider the insulation of dissimilar metals (especially at the mechanical joints)[14, 22];
- Weld head should be relatively cathodic to the rest of the structures.

Figure 2.18 illustrates some of the issues presented previously. It can be observed in Figure 2.18a shows an adequate solution for the design of the supporting beams at the mechanical joints anticipating a leak, while Figure 2.18b illustrates how the drainage path should be designed to avoid the presence of stagnant water on beams.

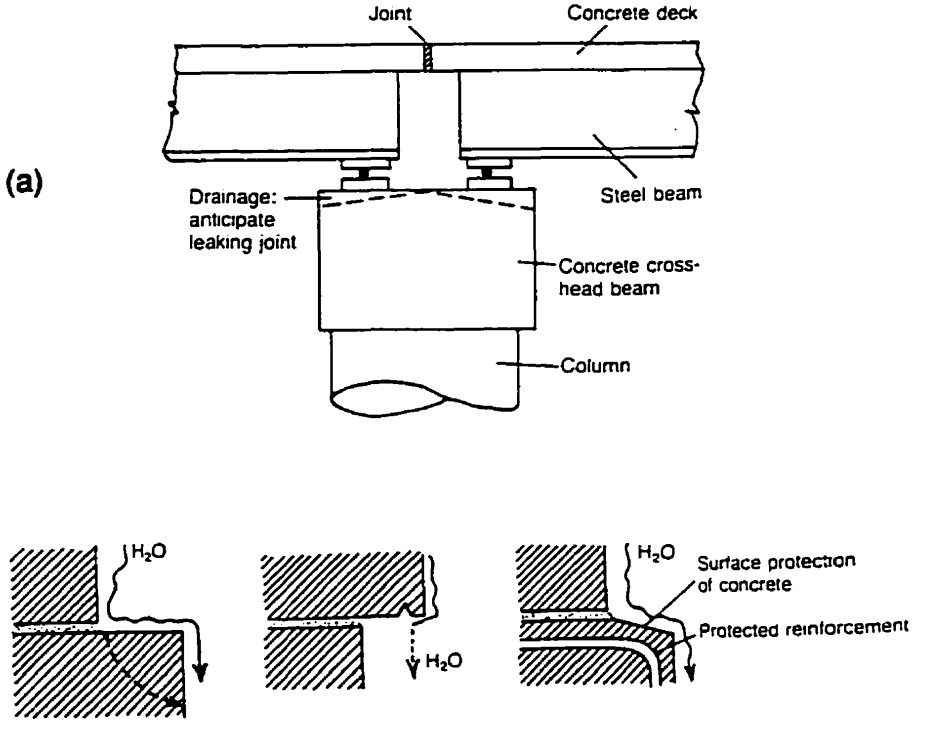

Figure 2.18 Examples of good and not so good designed systems[19].

3. Monitoring corrosion activity

In this section, the different techniques selected for the Dickson Bridge test program are presented. The choice of technique was based on either the capacity to assess the damage of the steel reinforcement, or its ability to quantify the corrosion-related properties of the concrete. The criteria used for the selection of the techniques are also introduced.

3.1 Selection of parameters

The planning phase of a test program is almost as important as the selection of adequate testing techniques itself, because it greatly influences the uncertainty of the results and their interpretation[24]. Satisfactory planning that allows for savings in time, effort and expenses generally involves the following concepts[24] :

- Clear identification at the initial planning stage, of the goals of the investigation;
- Selection of reliable test techniques for which the applicability, limitations, and accuracies have been fully established;
- Interpretation of results made by skilled personnel;
- Testing of different known qualities of concrete (good, moderate, and deteriorated) to observe the variability of a technique through comparison of the test results;
- Consideration of the difficulties to obtain accurate, quantitative estimates of in-situ concrete properties : limitations of testing techniques, relatively small number of measurements performed, human errors using the equipment, etc.;
- Adequate statistical treatment of the collected data to consider and quantify the variability of the test conditions when testing for durability properties.

A full understanding of the variability of the concrete material is essential. For most properties, comparison between laboratory and in-situ testing will result in large differences[24] as standard specimens used for laboratory testing may misrepresent the true quality of the original in-situ concrete[17]. Important causes explaining these differences are :

- Non-uniformity of the concrete within the members of a structure;
- Existence of differences in general workmanship for the mixing, placing, compacting, and curing procedures between concrete areas (especially important for medium and large structures).

The principal reasons for testing concrete structures is to establish if the structure complies with certain requirements and to assess the in-situ quality and integrity of a structure. In-situ testing of damaged and deteriorating structures is often made to determine the causes and extent of the damage and to further develop the understanding of influencing properties of tested materials.

The objectives of the Dickson Bridge test program were discussed in Section 1.2.4 and can be summarized as follows : the assessment of cause(s) and extent of the chloride-induced corrosion deterioration of the bridge deck with regards to both concrete and steel.

Available test methods and standards

Currently available test methods to evaluate the different deterioration-related parameters are presented in Table 3.1, while Table 3.2 presents some available standard procedures for testing of concrete. Available techniques for durability testing of reinforced concrete structures are presented in more details in Table 3.3.

Table 3.1 Principal test methods available[24].

Property under investigation	Test	Equipment type
Corrosion of embedded steel	Half-cell potential	Electrochemical
	Resistivity	Electrical
	Linear polarization resistance	Electrochemical
	A.C. Impedance	Electrochemical
	Cover depth	Electromagnetic
	Carbonation depth	Chemical/microscopic
	Chloride concentration	Chemical/electrical
Concrete quality, durability and deterioration	Surface hardness	Mechanical
	Ultrasonic pulse velocity	Electromechanical
	Radiography	Radioactive
	Radiometry	Radioactive
	Neutron absorption	Radioactive
	Relative humidity	Chemical/electronic
	Permeability	Hydraulic
	Absorption	Hydraulic
	Petrographic	Microscopic
	Sulphate content	Chemical
	Expansion	Mechanical
	Air content	Microscopic
	Cement type and content	Chemical/microscopic
	Abrasion resistance	Mechanical
Concrete strength	Cores	Mechanical
	Pull-out	Mechanical
	Pull-off	Mechanical
	Break-off	Mechanical
	Internal fracture	Mechanical
	Penetration resistance	Mechanical
	Maturity	Chemical/electrical
	Temperature-matched curing	Electrical/electronic
Integrity and performance	Tapping	Mechanical
	Pulse-echo	Mechanical/electronic
	Dynamic response	Mechanical/electronic
	Acoustic emission	Electronic
	Thermoluminescence	Chemical
	Thermography	Infra-red
	Radar	Electromagnetic
	Reinforcement location	Electromagnetic
	Strain or crack measurement	Optical/mechanical/electrical
	Load test	Mechanical/electronic/ electrical

The choice of adequate technique(s) for a given test program should be made based on several factors such as (not in order of importance)[17, 24] :

- Cause of damage;
- Access;
- Cost involved;
- Duration of test;

- Reliability of testing.

The tests selected should optimize the use of human, technical and economical resources and provide results susceptible to meet the objectives of the test survey.

Table 3.2 Relevant available standards[24].

British standards	
BS 1881: Testing concrete	
Part 5	Methods of testing concrete for other than strength
Part 120	Determination of compressive strength of concrete cores
Part 124	Chemical analysis of hardened concrete
Part 201	Guide to the use of NDT for hardened concrete
Part 202	Surface hardness testing by rebound hammer
Part 203	Measurement of the velocity of ultrasonic pulses in concrete
Part 204	The use of electromagnetic covermeters
Part 205	Radiography of concrete
Part 206	Determination of strain in concrete
Part 207	Near to surface test methods for strength
*Part 208	Initial surface absorption test
*In preparation	
BS 812	
Part 1	Sampling and testing mineral aggregates, sands and filters
BS 6089: Assessment of concrete strength in existing structures	
BS 8110: Structural use of concrete	
BS DD92: Temperature matched curing of concrete specimens	
American standards	
ASTM	
C42	Standard method of obtaining and testing drilled cores and sawed beams of concrete
C85	Cement content of hardened Portland cement concrete
C457	Air void content in hardened concrete
C597	Standard test method for pulse velocity through concrete
C779	Abrasion resistance of horizontal concrete surfaces
C803	Penetration resistance of hardened concrete
C805	Rebound number of hardened concrete
C823	Examining and sampling of hardened concrete in constructions
C856	Petrographic examination of hardened concrete
C876	Half-cell potential of uncoated reinforcing steel in concrete
C900	Pull-out strength of hardened concrete
C918	Measurement of early-age compressive strength and projecting later age strength
C944	Abrasion resistance of concrete or mortar surfaces by the rotating cutter method
C1040	Density of unhardened and hardened concrete in place by nuclear methods
C1074	Estimating concrete strength by the maturity method
C1150	Break-off number of concrete
D4580	Measuring delaminations in concrete bridge decks by sounding
D4748	Determining the thickness of bound pavement layers using short-pulse radar
D4788	Detecting delaminations in bridge decks using infrared thermography

Since the test results are applicable only at the specific test locations, i.e., where the readings or samples were obtained, sufficient locations should be tested to assess the

true state of the structure under investigation[24]. It should be kept in mind that for comparative purposes, the truly non-destructive methods are the most efficient, since their speed allows to easily test a large number of locations[24].

Table 3.3 Relevant available techniques for durability testing[24].

Method	Cost	Speed of test	Damage	Applications
Cover measurement	Low	Fast	None	Corrosion risk and cause
Carbonation depth	Low	Fast	Minor	
Chloride content	Moderate/high	Slow	Minor	
Half-cell potential	Low	Fast	Minor	Corrosion risk
Resistivity	Moderate/high	Fast	Minor/none	
LP resistance	Moderate/high	Moderate	Minor	Corrosion rate evaluation
A.C. impedance	Moderate/high	Slow	Minor	
Galvanostatic pulse	Moderate/high	Fast	Minor	
Absorption	Moderate	Slow	Moderate/minor	Cause and Risk of corrosion and concrete deterioration
Permeability	Moderate	Slow	Moderate/minor	
Moisture content	Low	Slow	Minor	
Chemical	High	Slow	Moderate	
Petrographic	High	Slow	Moderate	
Expansion	High	Slow	Moderate	
Radiography	High	Slow	None	

Combination of tests

Most of the test methods available for in-situ testing of concrete show limited reliability when used individually. One way to overcome this problem is to combine the analysis of testing methods[17, 24]. As a result, the process generally improves the calibration accuracy when similar patterns of results can be observed and gives the possibility to correlate combinations of measured values with desired properties. This procedure is also susceptible to increase the accuracy of the results when compared with results obtained from separate analyses of individual test results[24]. Again, this procedure is most appropriate for rapid, non-expensive, and non-destructive techniques. Generally, more than one type of testing is required to determine the nature and cause of deterioration, and to assess future durability.

3.2 Dickson Bridge test program

The scheme of the test program is presented in Figure 3.1. As mentioned previously, the south section of the Dickson Bridge was investigated to assess the cause(s) and the extent of damage due to chloride-induced corrosion of the reinforcing steel. The selection of techniques for durability testing of the Bridge was based on the disruptive character, simplicity of operation, commercial availability, reliability, and cost of operation of corrosion-related in-situ and laboratory techniques. These techniques can be divided into two categories : assessment techniques and prediction techniques. The assessment techniques allow to quantify the extent of damage to the reinforcing steel while the prediction techniques are used to estimate (measure) the influence of the concrete on the chloride-induced corrosion process. Table 3.4 presents the selected techniques by category and in a sequential order.

Investigation methodology

The first step of the analysis was to conduct a half-cell survey over the entire upper surface of the bridge deck, over the asphalt overlay, to determine the locations for further detailed study. The adequacy of this technique (testing concrete over asphalt overlay) was demonstrated[13], and was found adequate to assess the likelihood of corrosion process to develop. Since no visual inspection of the deck surface could be performed to observe the extent of apparent damage, the results of half-cell potential survey was used to select 35 locations of area around two meter square. Areas of different concrete qualities were selected to allow for the technique calibration and to determine the variability of the different tests. It was decided to exclude the two outer lanes of the bridge for this investigation, since they were repaired with a concrete overlay in 1994.

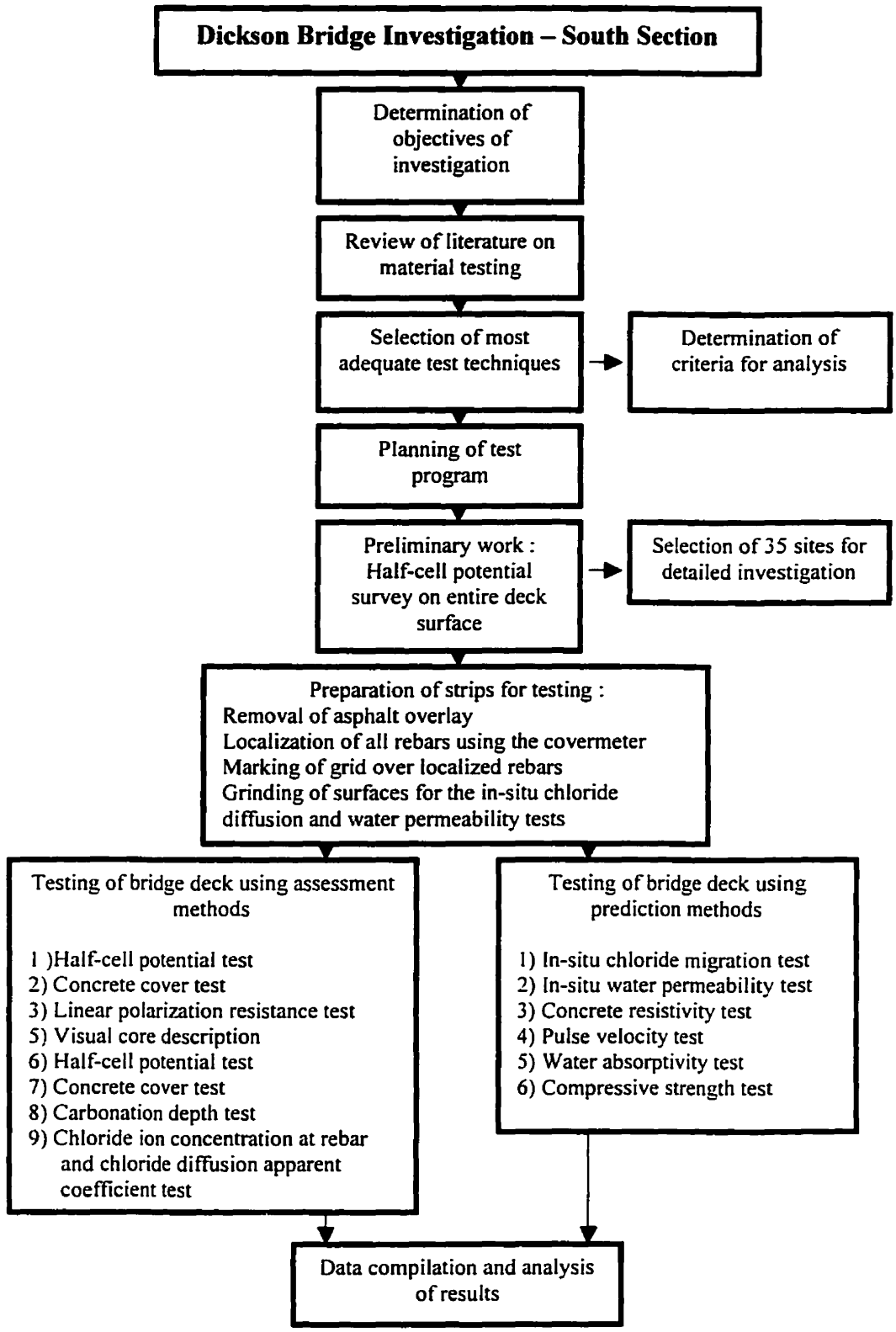

Figure 3.1 Scheme of the test program for the investigation of the south section of the Dickson Bridge.

Table 3.4 Test techniques used for investigation of the south section of the Dickson Bridge.

Test Technique	Technique category	Test specimen
Half-cell potential test	Assessment	Structure (in-situ)
Concrete cover test	Assessment	Structure (in-situ)
In-situ chloride diffusion (migration) test	Prediction	Structure (in-situ)
In-situ water permeability test	Prediction	Structure (in-situ)
Linear polarization resistance test	Assessment	Structure (in-situ)
Concrete resistivity test	Prediction	Structure (in-situ)
Visual core description	Assessment	Core
Pulse velocity test	Prediction	Core
Water absorptivity test	Prediction	Core
Compressive strength test	Prediction	Core
Carbonation depth test	Assessment	Core
Chloride ion concentration at rebar and chloride diffusion (apparent) test	Assessment	Core

Once the selection of the 35 sites was completed, the removal of the asphalt overlay was performed. Due to the nature of the stripping methods used (jackhammer and hydraulic machinery), the concrete cover surface was damaged, but it was decided to continue with the investigation and later consider the damaged concrete cover in the analysis of results. An individual half-cell survey was performed over each of the 35 sites (strips) to identify the areas of interest within each site where other tests could be performed later. Again, the locations of different concrete qualities were identified.

It was decided to perform at least one test per site for all selected test techniques. In the case where it was decided to perform more than one test per site for a given technique, the tests were performed at predetermined locations that would serve for subsequent testing using other techniques. This procedure was used to optimize the analysis of the results, calibration of the techniques, and correlation of the variables[24].

Concrete cores were extracted from the bridge deck at most locations tested using the linear polarization resistance test. The extraction of the cores was performed by the City of Montreal using a water-cooled rotary drill. The diameter of cores collected

was 75 mm, and the drilling was performed downwards and vertically from the surface of the deck. Due to the combined action of intensive deterioration processes over the years and the disruption of the concrete by the coring procedures, only 25 cores out of 63 were found to be in an acceptable condition for further laboratory tests. Most of the cores showed delamination, cracks and signs of corrosion.

3.3 Description of selected techniques

Most of the test techniques selected for the investigation of the south section of the Dickson bridge were previously used on the north and central sections. As a result, for most techniques, a complete description of each technique is available in the theses by Fazio[13] and El Jachi[25]. A brief description of these techniques is presented in this section.

Brief description of selected techniques

Half-cell potential test : The measurement of the half-cell potential is an indicator of the likelihood of the corrosion reaction. A computerized datalogger (potentiostat) measures the relative potential of embedded reinforcing steel bars to a reference half-cell probe (generally copper-copper sulphate). The measurement is made through the concrete cover. The potential difference can be used to empirically estimate the extent of corroded areas of steel reinforcement in the immediate vicinity of the location of the test.

Concrete cover test : The determination of the concrete cover thickness over the steel reinforcing bar can be performed using an electromagnetic device, the CM4 Covermaster by Protovale (Oxford) Ltd. The presence of steel (distance and size of steel reinforcement) modifies the magnetic field generated by the instrument via an electric magnet. The current induced by the response of the steel is first measured, then transformed and displayed either in the form of a voltage intensity used to locate

reinforcing steel bars, or in the form of a distance (thickness of the concrete cover over the steel reinforcement) both directly read on the device.

In-situ chloride diffusion (migration) test : The chloride diffusivity (migration) of the concrete can be measured using a testing device newly developed at Queen's University of Belfast. The apparatus consists of two plexiglass cells (inner and outer) tightly fixed to the concrete surface. A chloride solution is poured into the inner cell and distilled water in the outer. An electrode is placed in each cell, and a difference of potential is applied between the two electrodes, forcing the chloride ions to flow through the concrete in a steady state. The transfer of chloride ions, in the form of a chloride ion concentration, is determined by measuring the change in electric potential. No standard procedure for this test exists at this point in time.

In-situ water permeability test : The in-situ water permeability of the concrete can be determined using the Autoclam, permeability measuring system developed at Queen's University of Belfast. A piston exerts a hydrostatic pressure of 0.5 bar on a given area of concrete. As the water is absorbed by the concrete, the piston moves downwards from its initial position to maintain the water pressure constant . The time and internal position of the piston are recorded by the data acquisition system over a period of 15 minutes. The volume of water absorbed by the concrete is calculated using both the area of the piston and its position in time. The coefficient of water permeability can be determined by calculations (refer to Fazio[13] for details of calculations).

Linear polarization resistance test: This test consists of the application of a series of small electrochemical changes of the electric potential (∓ 20 mV) to the steel reinforcement using an electrode placed on the concrete surface over the embedded steel. The induced change in electric potential modifies the half-cell corrosion potential of steel and from a measurement of the resulting current (ΔI) the polarized resistance R_p is obtained. The corrosion rate can be calculated by making a number

of assumptions on the area of steel polarized and on Tafel's constants introduced in Section 2.2.3.

Concrete electrical resistivity test : The determination of the concrete resistance to ionic current flow can be performed using the Wenner four-probes technique which uses a constant electrode spacing. A low-frequency alternating current is induced in the concrete mass by two the outer electrode while the voltage drop caused by concrete electrical resistivity is measured by the two inner electrodes. Good electrical conductivity is achieved by drilling small holes on the tested surface where wet sponges are later introduced (water acts as a coupling agent).

Visual core description : Cores collected in accordance with standard procedure ASTM C42-90 are inspected visually to determine important properties such as the proportions of air voids, aggregate and cement paste; mineralogy, shape and the size of aggregates; presence of cracks and of possible delaminations. Pictures of as-collected cores are also taken. No standard procedure exists for the description of the cores.

Pulse velocity test : The pulse velocity method allows for the determination of the elastic properties of the tested concrete (Young's modulus, E). A testing device electronically generates repetitive voltage pulses, transmits a pulse to the concrete via a coupling agent in the form of wave bursts of mechanical energy, receives the pulse at the other interface, amplifies it, electronically measures it and displays the travelling time taken on a digital readout. Usually, the results can be compared with those obtain from the compressive strength test.

Water absorptivity test : Concrete cores collected following standard procedure ASTM C42 are cleaned and cut to obtain perfectly cylindrical specimens. The samples are first weighed in ambient temperature and humidity conditions, then submitted to an oven-drying period followed by a water immersion period. The weight of the specimens is recorded after each exposure period when a constant

weight value is obtained (∓ 0.1% of variation between readings). Calculations are made to determine the different absorption properties of the concrete specimens : the absorption after immersion, the dry and saturated densities, and the volume of permeable pore space (voids)[31].

Compressive strength test : To measure the compressive strength (f'_c) and modulus of elasticity (E) of the concrete, concrete cores collected following standard procedure ASTM C42 are cleaned and capped to obtain perfectly level surfaces perpendicular to the core axis. The specimens are then compressed at a constant load rate until the maximum compression force and displacement are obtained and recorded. The mode of failure can also be observed. Corrections for specimens geometry and steel content can be performed.

Carbonation depth test : Freshly broken specimens are sprayed using a phenolphtalein solution, and the depth of carbonation can be measured directly on the tested specimen as the free lime ($Ca(OH)_2$) is coloured pink while the carbonated portion remains uncolored. The phenolphtalein test gives a measure of the pH as a function of the free lime content : the colour being pink above about 9.5.

Chloride ion concentration at rebar and chloride diffusion (apparent) tests : The determination of the chloride ion concentration profile with depth and the determination of the apparent coefficient of chloride diffusion can be obtained for each core using the same specimen tested for the compressive strength. Three grams of representative concrete powder are digested in a solution to extract the chloride ions physically bound by the hardened cement paste. The electric potential between the calibrated probe (Orion ion specific electrode (ISE)) and the solution is measured for each powder sample (depth range) and is later converted into a chloride ion concentration by calculations (refer to Fazio[13] for details of calculations). The results obtained are used to determine the chloride ion profile and the apparent coefficient of chloride diffusion. No standard procedure for this test exists at this point.

3.4 Summary of technical aspects for selected techniques

This section presents a summary of the technical aspects and limitations of all techniques used on the south section of the Dickson Bridge. For each test technique, the following aspects are summarized in a tabular form :

- Purpose of the test;
- Parameter measured;
- Tested area;
- Apparatus;
- Test preparation;
- Analysis of results;
- Limitation of the technique.

3.4.1 Half-cell potential measurements

Table 3.5 Summary of technical aspects for the half-cell potential measurements.

Half-Cell Potential Measurements	
Purpose of test	Determination of the corrosion potential of steel through the concrete media.
Parameter evaluated	Electric potential of steel reinforcement in concrete; termed HC.
Tested area	The entire bridge deck surface and soffit of the south section of Dickson bridge were tested using a grid of 1 meter by 1 meter. The 35 exposed strips were tested using a grid of 15 cm by 30 cm, and 5 selected columns were tested using a grid of 30 cm by 1 m.
Apparatus	MICAPS CDL 200 (COREXCO, Montreal), a computerized data acquisition device using a copper rod and a copper sulphate solution.
Test preparation	Steel reinforcement connectivity over the tested area was verified by exposing the steel at several locations and measuring the difference in electric potential between a reference station : a difference of less than 3 millivolts would indicate adequate connectivity. Electric conductivity with the underlying concrete was obtained by drilling holes through the asphalt overlay every gridpoint where water was poured before each measurement (water assured the electric contact). For measurements taken directly on the concrete, the surface was wet prior to testing for the same reasons.
Procedure	The standard procedure for this test is ASTM C876.
Analysis of results	No calculation is necessary. The risks of corrosion are presented in Section 4.3.
Limitations	The test does not indicate the corrosion rate or the state-of-health of concrete, but only the likelihood of corrosion. The moisture content of concrete greatly affects the results: complete wetting of bridge surface can decrease the electric potential by about 200 mV while complete saturation of structure can decrease the half-cell reading by about 700 mV.
Comments	The adequacy of the technique (testing concrete over asphalt overlay) was demonstrated in the investigation of the north section[13].

3.4.2 Concrete cover measurements

Table 3.6 Summary of technical aspects for the concrete cover measurements.

Concrete Cover Measurements	
Purpose of test	Determination of the concrete cover over the steel reinforcing bar.
Parameter measured	The concrete cover thickness at the steel reinforcement, termed CV.
Tested area	The test survey was performed in combination with the half-cell potential test for all measured locations.
Apparatus	The CM4 Covermaster by Protovale (Oxford) Ltd., an electromagnetic covermeter device, was used.
Test preparation	The concrete surface must be exposed.
Procedure	The standard procedure for this test is BS 1881 : Part 2204.
Analysis of results	No calculation is necessary. Cores extracted from the bridge containing the reinforcing steel can serve as reference to measure the accuracy of the instrument.
Limitations	The presence of other sources of steel in the vicinity of the tested area, such as aggregates rich in magnetic minerals and iron oxide surface coating, affects the accuracy of the testing device. Heavily reinforced concrete members are difficult to investigate for the same reasons. The accuracy of the electromagnetic device (about 15 % for thicknesses less than 100 mm) decreases for deep embedded reinforcing steel bars.
Comments	In the interpretation of the results, it is necessary to consider the loss of concrete cover when removing the asphalt overlay. The use of a jack hammer and other methods caused chipping of concrete in most strips.

3.4.3 In-situ chloride diffusion (migration) measurements

Table 3.7 Summary of technical aspects for the in-situ chloride diffusion (migration) measurements.

In-situ Chloride Diffusion Migration Measurements	
Purpose of test	Determination of the chloride diffusion (migration) coefficient of concrete.
Parameter evaluated	The chloride diffusion (migration) coefficient, termed CD_m.
Tested area	A minimum of one test per strip was performed in all selected locations (strips).
Apparatus	The testing device was developed at Queen's University of Belfast and first tested on the north section of the Dickson Bridge. The appararus consists of a voltmeter, a sodium chloride solution, and two plexiglass cells (outer and inner) securely fixed to the concrete surface by mean of clamps.
Test preparation	The concrete surface was saturated 48 hours prior to testing.
Procedure	No standard procedure for this test exists at this point in time.
Analysis of results	The difference of potential and the current between the two electrodes is used to determine the chloride ion concentration (refer to Fazio[13] for details of calculations). The analysis is made by comparing the results obtained for different test locations.
Limitations	The test is new and further testing should demonstrate its reliability to properly measure the chloride diffusion (migration) coefficient of concrete. The accuracy of the results depends highly on the installation of the cells and is also greatly affected by the change in temperature of the solutions. The weather conditions (especially the wind and the temperature) greatly affect the quality of the results.

3.4.4 In-situ water permeability measurements

Table 3.8 Summary of technical aspects for the in-situ water permeability measurements.

In-situ Water Permeability Measurements	
Purpose of test	Determination of the in-situ water permeability coefficient of concrete.
Parameter evaluated	The water permeability coefficient of concrete, termed WP.
Tested area	A minimum of one test per strip was performed at selected locations arbitrarly determined.
Apparatus	The Autoclam permeability measuring system using a hydrostatic pressure of 0.5 bar. The testing device was newly developed at Queen's University of Belfast and first tested on the north section of the Dickson Bridge.
Test preparation	The concrete surface was saturated 48 hours prior to testing in order to obtain a steady state flow.
Procedure	No standard procedure for this test exists at this time.
Analysis of results	The coefficient of water permeability is calculated (refer to Fazio[13] for details of calculations). The analysis of the results is made by comparing the values obtained for different sites.
Limitations	The test is new and further testing should demonstrate its reliability to assess the chloride migration coefficient. The accuracy of the results depends highly on the ring installation. The applied pressure is close to the surface tension forces in the saturated capillary pores; this affects the accuracy of the technique. Corrections should be made to account for the area of concrete tested (it was not done for this investigation).

3.4.5 Linear polarization resistance measurements

Table 3.9 Summary of technical aspects for the linear polarization resistance measurements.

Linear Polarization Resistance Measurements	
Purpose of test	Determination of the both the corrosion potential and the corrosion rate of the corrosion reaction of reinforcing steel bars.
Parameter measured	The corrosion potential, E_cp, and the corrosion rate, LP_cr.
Tested area	A minimum of two tests per strip were performed at locations of interest selected after examining the results from the half-cell potential survey for each strip.
Apparatus	CMS100 by GAMRY Inc., a potentiostat used with the CMS105 DC corrosion measurement package. The testing device consisted of an internal counter electrode (probe), and an external counter electrode (guard ring) confining the polarized (measurement) area accurately.
Test preparation	The concrete surface was saturated for 48 hours prior to testing. The electrical conductivity with the reinforcing steel bar under test must be ensured.
Procedure	There is no standard procedure for this test
Analysis of results	The results are generated directly by the instrument, which makes all necessary calculations using a software package.
Limitations	The measured corrosion rates are not typical of the mean annual value which is influenced by changes of the temperature, of the moisture level, and of the oxygen concentration at a specific location. Pitting corrosion cannot be detected since the general corrosion type is assumed for calculations. The accuracy of the results is limited to the estimation of important parameters (Tafel's constants, polarized area, type of corrosion). The electrical resistivity of concrete must be compensated by the instrument. The quality of the electric connection greatly affects the quality of the results. The weather conditions (especially the wind and the temperature) greatly affect the quality of the results.

3.4.6 Concrete resistivity measurements

Table 3.10 Summary of technical aspects for the concrete resistivity measurements.

Concrete Resistivity Measurements	
Purpose of test	Determination of the electrical resistance of concrete to ionic current flow.
Parameter measured	Concrete electrical resistance, termed ER.
Tested area	All locations previously tested using the linear polarization resistance technique.
Apparatus	Nilsson Soil Resistance Meter Model 400. The configuration used was Wenner four probes with a constant electrode spacing set to 5.00 cm.
Test preparation	Test locations avoiding the steel reinforcement were identified. To ensure a good electrical contact between electrodes and concrete, small holes were drilled in the exposed concrete surface where wet sponges were introduced (water acting as a coupling agent).
Procedure	The standard procedure for this test is ASTM F43-93.
Analysis of results	The results obtained are used to calculate the electrical resistance of the concrete (refer to Fazio[13] for details of calculations).
Limitations	The investigation depth is about twice the electrode spacing. For calculations, the concrete material needs to be assumed homogeneous at the location of the test. The presence of steel in the vicinity of tested area affects the accuracy of the device in short-circuiting the current flow, and increase the conductivity of the concrete. In addition, the resistivity of concrete greatly decreases with an increase in the moisture content, temperature, and chloride content in the vicinity of the tested area. The presence of aggregates larger than the electrode spacing can affect the readings since the resistance of the aggregate itself would then be measured.

3.4.7 Pulse velocity measurements

Table 3.11 Summary of technical aspects for the pulse velocity measurements.

Pulse Velocity Measurements	
Purpose of test	Determination of the elastic properties of concrete, mainly the mechanical wave (pulse) velocity and the modulus of elasticity (E).
Parameter evaluated	The pulse velocity and the modulus of elasticity, respectively termed PV and E_pv.
Tested area	A total of 25 cores were selected for testing after analyzing the results of the linear polarization resistance test.
Apparatus	The device used, the PUNDIT by CNS Electronics Ltd., conformed to the requirements of the standard procedure ASTM C597-97.
Test preparation	Collected cores were cleaned and cut to obtain perfectly cylindrical specimens. A coupling agent was applied on both plane surfaces of the specimen (core).
Procedure	The standard procedure for this test is ASTM C597-97. Testing was conducted in laboratory, under normal temperature and moisture conditions (21 ° C and relative humidity around 70 %).
Analysis of results	Calculations are performed to determine the pulse velocity, and the modulus of elasticity (assuming a Poisson ratio for concrete of 0.17). The results are corrected to account for the presence of reinforcing steel bars as described in the standard procedure.
Limitations	The presence of steel reinforcement should be avoided for testing (increases the pulse velocity since steel is a stiffer medium than concrete). The temperature and the moisture content have no significant effect on the results of this test. Differences between operators or instruments may affect the accuracy of the instrument by up to 20 %. The minimum length acceptable for testing is a function of the wavelength of the device : 2 cores shorter than the minimum accepted value (6.8 cm corresponding to a wavelength of 54 kHz) were still tested.

3.4.8 Water absorptivity measurements

Table 3.12 Summary of technical aspects for the water absorptivity measurements.

Water Absorptivity Measurements	
Purpose of test	Determination of the water absorption properties of concrete.
Parameter evaluated	The absorptivity after immersion, the dry and saturated densities, and the volume of permeable pore space (voids) of the concrete, respectively termed AB_astm, SD_b, SD_a, and VV.
Tested area	A total of 25 cores were selected for testing after analyzing the results from the linear polarization resistance test.
Apparatus	The apparatus conformed to the requirements of the standard procedure ASTM C642-97.
Test preparation	Collected cores were cleaned and cut to obtain perfectly cylindrical specimens. The first four millimeters of concrete at the core top surface were cut off in order to remove any holes made in preparation for the resistivity test.
Procedure	The standard procedure for this test is ASTM C642-97. It was decided not to perform the saturated mass test after boiling measurement because of the non-availability of the required testing equipment.
Analysis of results	Calculations are performed to determine the absorption properties of the concrete, as described in the standard procedure. The results were corrected for the presence of reinforcing steel bars.
Limitations	It is assumed that the water absorption of steel reinforcement is negligible. The 6 cores found lighter than the minimum accepted value (800 grams) were still tested.

3.4.9 Compressive strength measurements

Table 3.13 Summary of technical aspects for the compressive strength measurements.

Compressive Strength Measurements	
Purpose of test	Determination of the compressive strength (f'_c) and of the modulus of elasticity (E) of concrete.
Parameter measured	The compressive strength and the modulus of elasticity of concrete; respectively termed CS and E_cs.
Tested area	A total of 25 cores selected after analyzing the linear polarization resistance survey.
Apparatus	The apparatus consisted of a MTS Rock Frame from the Civil Engineering Structures Laboratory, McGill University.
Test preparation	Collected cores were cleaned and capped following standard procedure ASTM C42 to obtain perfectly plane concrete cylinders. For each specimen, the height and the mean diameter were measured as prescribed in standard ASTM C39-93.
Procedure	The standard procedures for this test are ASTM C39-93 and C42-90. The specimens were tested in ambient conditions (21 ° C and dry state) at a constant rate of 0.002 millimeter per second.
Analysis of results	The compressive strength of concrete is calculated by dividing the maximum applied force by the mean cross-sectional area of the tested specimen. Corrections are made to account for the presence of reinforcing steel bars and for the specimen geometry.
Limitations	The minimum height for test specimens (ASTM C42-90) was difficult to obtain during the collection of the cores : the presence of steel reinforcement and the deterioration of the concrete affected the length of the cores. However, it was decided to test the short specimens (length to diameter ratio sligthly below 1).

3.4.10 Carbonation depth measurements

Table 3.14 Summary of technical aspects for the carbonation depth measurements.

Carbonation Depth Measurements	
Purpose of test	Determination of the depth of the carbonation front in concrete.
Parameter measured	The depth of the carbonation front at the surface of the bridge deck, termed CR.
Tested area	A total of 25 cores selected after analyzing the linear polarization resistance survey (only the top surface of the bridge deck was tested since the cores did not reach the soffit).
Apparatus	A solution of 1% phenolphtalein in 70% ethyl alcohol contained in a spray bottle.
Test preparation	Collected cores are cleaned and sawed (using a diamond saw) in order to produce a fresh broken surface.
Procedure	The standard procedure for this test is RILEM CPC-18.
Analysis of results	The depth of the carbonation front is measured directly on the specimen. No corrections apply.
Limitations	The pink color only indicates the presence of free lime ($Ca(OH)_2$), but not the true presence of carbonation. For that matter, the method does not distinguish between a low pH caused by carbonation and by other acidic gases.
Comments	The removal of the asphalt overlay over the concrete slab resulted in the chipping of concrete in most slabs. As a result, the cores were collected at chipped locations and led to the measurement of an apparent carbonation depth.

3.4.11 Concrete chloride diffusion (apparent) and chloride ion concentration measurements

Table 3.15 Summary of technical aspects for the concrete chloride diffusion (apparent) and chloride ion concentration measurements.

Chloride Ion Concentration at Rebar and Chloride Diffusion (Apparent) Measurements	
Purpose of test	Determination of the chloride ion concentration at the reinforcing steel level and of the apparent coefficient of chloride diffusion.
Parameter measured	The chloride ion concentration at rebar, termed CC_rb, and the apparent chloride diffusion coefficient of the concrete, termed CD_a.
Tested area	A total of 25 specimens previously tested for linear polarization were selected for this test.
Apparatus	Orion ion specific electrode (ISE); calibration, digestion, and stabilizing solutions; chemical analysis apparatus.
Test preparation	The collection of three grams of representative concrete powder per test was obtained by cutting the cores in 15 mm slices using a diamond saw, and by pulverizing the slices without the coarse aggregates to obtain three grams of powder passing sieve size #50 (ASTM).
Procedure	The standard procedure endorsed by SHRP was followed for this test.
Analysis of results	The chloride ion concentrations at different levels, and the apparent chloride diffusion coefficient are calculated (refer to Fazio[13] for details of calculations). Profile plots are generated and, knowing the thickness of the concrete cover, the chloride ion content at the steel level can be determined.
Limitations	The recovery of three grams of representative powder is time-consuming : cores used for the compressive strength test can be re-used by taking the necessary precautions. The technique provides useful information on the total chloride content of the hardened cement paste, but does not indicate the free chloride content, which is thought to be participating to the corrosion reaction (refer to Section 2.2.2.3).

4. Experimental results

4.1 Introduction

Chapter Four presents the experimental results. The parameters measured using the selected techniques described in Chapter Three are listed in Table 4.1. In the presentation of the results, the symbols representing the different parameters are used for simplicity. In Chapter Four, the results for the half-cell potential and the corrosion potential are treated separately, despite the fact that both parameters estimate the corrosion potential of the steel reinforcement. However, the results for each parameter were obtained differently.

Table 4.1 Identification and designation of measured parameters.

Test Technique	Measured parameter(s)	Symbol
Half-cell potential test	Half-cell potential	**HC**
Concrete cover test	Concrete cover thickness over rebar	**CV**
In-situ chloride diffusion (migration) test	Chloride diffusion (migration) coefficient	**CD_m**
In-situ water permeability test	Water permeability coefficient	**WP**
Linear polarization resistance test	Corrosion potential Corrosion rate	**E_cp** **LP_cr**
Concrete resistivity test	Electrical resistance	**ER**
Visual core description	None used for the statistical analysis	-
Pulse velocity test	Pulse velocity Apparent modulus of elasticity	**PV** **E_pv**
Water absorptivity test	Absorptivity after immersion Dry density Saturated density Volume of permeable pore space (voids)	**AB_astm** **SD_b** **SD_a** **VV**
Compressive strength test	Compressive strength (f'_c) Modulus of elasticity (E_c)	**CS** **E_cs**
Carbonation depth test	Carbonation front depth	**CR**
Chloride ion concentration at rebar and chloride diffusion (apparent) test	Chloride ion concentration at rebar level Chloride diffusion (apparent) coefficient	**CC_rb** **CD_a**

The basic descriptive statistics for all parameters measured during the investigation of the south section of the Dickson Bridge are presented in Table 4.2, while Table 4.3

presents a summary of the results obtained for the common tests on the north, central, and south sections. In Tables 4.2 and 4.3, the east and west sides of the bridge are presented individually to facilitate the assessment of the state-of-health of the structure with regards to chloride-induced corrosion. The condition of the bridge deck can be determined by close examination of the results obtained for each parameter and by comparing with the corrosion risk levels as they exist in the literature and are presented in Table 4.4. Table 4.5 presents the results of the assessment of the corrosion damage on the bridge based on these risk levels.

In addition, Section 4.4 presents the results obtained for each parameter in visual forms (two and three-dimensional surfaces). A short description of the findings and of the graphics generated for each parameter is also presented in Section 4.4, followed by a visual presentation of the results. To ease the visual interpretation of the distribution of the results, Figure 1.2, showing a diagrammatic representation of the Dickson bridge, should be used jointly. The summary of the condition survey is presented in Section 4.5. It is important to consider that the contour lines in Figures 4.1 through 4.46 generally tend to make the results appear as being more uniform than reality. Extrapolations from the least-squares fitting method are observed to dominate the surface fit. Consequently, these graphs should be interpreted carefully.

Appendix A presents a part of the raw data collected on the south section of the bridge for some parameters, while Appendix B presents a summary of experimental results in the form of bar plots.

The analysis of the results and the determination of the extent of the corrosion damage are performed in consideration of the quality of the results obtained, and the interpretations made by the author.

4.2 Corrosion risk levels

The assessment of the state-of-health of the bridge represents a complex task that necessitates the combined analysis of several parameters. For each test technique, the quantitative criteria determining the risks of corrosion development and assessing the durability of the structure were established from the literature[13] for the analysis of the north section of the Dickson Bridge. It was decided to use the risk criteria previously used for the analyses of the north and central sections for the classification of the different parameters considered for the analysis of the south section of the Bridge. This methodology allows for comparison between the two sections of the Bridge, and gives the opportunity to further study the validity of the identified criteria. Table 4.4 summarizes the different criteria selected for the assessment of the condition of the bridge deck. The assessment and prediction techniques are interpreted differently : the risk criteria for the corrosion reaction are used for the assessment techniques, while criteria assessing the quality of the concrete are used for the prediction techniques. In the case where the standard criteria were not available to characterize a certain parameter, the risk criteria would be assessed arbitrarily, especially for the newly developed techniques. The assessment of the condition of the bridge deck is based on the interpretation of the parameters for which standard criteria exist. The remaining parameters provide valuable additional information on which, at this point in time, it would be difficult to put much importance when assessing the condition of the bridge. These parameters are identified in italic characters in Tables 4.4 and 4.5.

Table 4.2 Descriptive statistics of all results obtained on the south section of the Dickson Bridge.

			(a) Entire deck N represent the number of observation						(b) East side of deck N represent the number of observation						(c) West side of deck N represent the number of observation					
Measured parameter(s)	Symbol	Units	N	Min Value	Max Value	Mean Value	VAR	COV	N	Min Value	Max Value	Mean Value	VAR	COV	N	Min Value	Max Value	Mean Value	VAR	COV
Half-cell potential																				
Deck surface	HC top	(mV)	3097	-920	-25	-373	1.5E+04	0.332	1622	-920	-25	-381	2.0E+04	0.365	1475	-780	-70	-362	1.3E+04	0.317
Deck soffit	HC bot	(mV)	1584	-671	-52	-386	1.6E+04	0.329	858	-652	-52	-379	1.6E+04	0.333	726	-671	-52	-393	1.6E+04	0.324
Bridge columns	HC col	(mV)	245	-143	408	71	1.4E+04	1.625	98	-99	384	100	1.4E+04	1.167	147	-143	408	54	1.3E+04	2.128
Concrete cover thickness over rebar (surface)	CV top	(mm)	890	2.0	94.5	39.4	281.1	0.426	465	2.0	94.5	41.2	324.1	0.435	425	3.3	80.3	37.4	230.6	0.406
Concrete cover thickness over rebar (soffit)	CV bot	(mm)	1584	1.3	61.5	25.9	73.0	0.330	858	1.3	57.2	25.9	76.9	0.338	726	2.5	63.5	25.9	68.6	0.319
Concrete cover thickness over rebar (columns)	CV col	(mm)	245	10.2	71.1	41.1	128.7	0.276	98	12.7	55.9	41.1	89.1	0.230	147	10.2	71.1	41.1	155.9	0.304
Chloride diffusion migration coefficient	CD m	(cm^2/sec)	33	8.2E-11	4.4E-07	5.5E-08	5.6E-15	1.361	17	1.5E-08	1.3E-07	4.9E-08	1.0E-15	0.649	16	8.2E-11	4.4E-07	6.1E-08	1.1E-14	1.707
Water permeability coefficient	WP x10^{-10}	(m/sec)	44	2.4E-05	2.0E-03	3.8E-04	2.9E-07	1.419	25	3.5E-05	2.0E-03	3.9E-04	3.3E-07	1.479	19	2.4E-05	1.7E-03	3.6E-04	2.4E-07	1.361
Corrosion potential (surface)	E cp top	(mV)	66	-545.3	-68	-282.579	9.9E+03	0.351	29	-545.3	-68	-290.0	1.5E+04	0.420	37	-483.8	-81.1	-276.765	6.2E+03	0.284
Corrosion rate (surface)	I P cr top	(µm/yr)	66	11	307	66	2.9E+03	0.818	29	11	231	71	2.0E+03	0.632	37	15	307	62	3.6E+03	0.977
Electrical resistance	ER	(kΩ cm)	69	1.88	15.71	4.80	3.58	0.394	32	2.20	15.71	5.03	5.60	0.470	37	1.88	11.00	4.60	3.74	0.420
Pulse velocity	PV	(km/sec)	24	2.90	4.20	3.46	9.3E-01	0.279	9	3.25	3.92	3.48	4.2E-02	0.059	15	2.90	4.20	3.45	8.5E-02	0.084
Apparent modulus of elasticity	E pv	(GPa)	24	10.76	21.44	14.54	4.68	0.149	9	12.98	18.28	14.53	2.90	0.117	15	10.76	21.44	14.54	6.03	0.169
Absorptivity after immersion	AB asim	(%)	24	4.86	7.92	6.21	0.59	0.123	9	5.32	7.55	6.27	0.54	0.117	15	4.86	7.92	6.21	0.66	0.130
Dry density	SD b	(g/cm^3)	24	1.58	1.73	1.63	8.0E-04	0.017	9	1.60	1.66	1.62	4.1E-04	0.012	15	1.58	1.73	1.63	9.6E-04	0.019
Saturated density	SD a	(g/cm^3)	24	1.75	1.95	1.81	2.2E-03	0.026	9	1.75	1.87	1.80	1.7E-03	0.023	15	1.75	1.95	1.82	2.5E-03	0.028
Volume of permeable air voids	VV	(%)	24	7.86	12.87	10.14	1.67	0.127	9	8.51	12.36	10.13	1.55	0.123	15	7.86	12.87	10.15	1.86	0.134
Compressive strength (f'c)	CS	(MPa)	24	27	62	48	58	0.159	9	41	62	50	41	0.130	15	27	58	46	63	0.172
Modulus of elasticity (Ec)	E cs	(MPa)	24	4171	9700	7582	1.5E+06	0.163	9	6040	9601	7709	1.2E+06	0.146	15	4171	9700	7506	1.8E+06	0.177
Carbonation front depth	CR	(mm)	24	0.0	0.0	0.0	0.0	-	9	0.0	0.0	0.0	0.0	-	15	0.0	0.0	0.0	0.0	-
Chloride ion concentration at rebar	CC ib	(%)	21	2.6E-02	6.2E-01	2.2E-01	2.8E-02	0.767	9	3.2E-02	5.9E-01	1.8E-01	1.2E-02	0.957	14	2.6E-02	6.2E-01	2.4E-01	2.6E-02	0.685
Apparent chloride diffusion coefficient	CD a	(cm^2/sec)	24	3.5E-09	2.2E-06	1.7E-07	1.1E-13	3.264	9	7.9E-09	2.7E-06	1.9E-07	7.9E-14	2.265	15	3.5E-09	1.6E-07	1.0E-08	1.8E-15	1.172

Table 4.3 Descriptive statistics of results obtained for the north, central, and south sections of the Dickson Bridge.

			(a) Entire deck (south) N represent the number of observation						(a) Entire deck (central) N represent the number of observation						(a) Entire deck (north) N represent the number of observation					
Measured parameter(s)	Symbol	Units	N	Min Value	Max Value	Mean Value	VAR	COV	N	Min Value	Max Value	Mean Value	VAR	COV	N	Min Value	Max Value	Mean Value	VAR	COV
Half-cell potential																				
Deck surface	HC_top	(mV)	3097	-920	-25	-373	1.5E+04	0.332	37	-550	-256	-395	6.6E+03	0.206	2484	-750	-44	-423	1.1E+04	0.250
Deck soffit	HC_bot	(mV)	1584	-673	-52	-386	1.6E+04	0.329	-	-	-	-	-	-	-	-	-	-	-	-
Bridge columns	HC_col	(mV)	245	-143	408	73	1.4E+04	1.625	-	-	-	-	-	-	-	-	-	-	-	-
Concrete cover thickness over rebar (surface)	CV_top	(mm)	890	2.0	94.5	39.4	281.1	0.426	16	28.0	90.0	43.0	219.6	0.345	137	1.000	90.000	35.000	2.8E+02	0.480
Concrete cover thickness over rebar (soffit)	CV_bot	(mm)	1584	1.3	63.5	25.9	73.0	0.330	-	-	-	-	-	-	-	-	-	-	-	-
Concrete cover thickness over rebar (columns)	CV_col	(mm)	245	10.2	71.1	41.1	128.7	0.276	-	-	-	-	-	-	-	-	-	-	-	-
Chloride diffusion migration coefficient	CD_m	(cm^2/sec)	33	8.2E-11	4.4E-07	5.5E-08	5.6E-15	1.361	16	4.2E-08	2.1E-07	9.8E-08	2.9E-15	0.549	35	1.6E-08	1.4E-07	6.3E-08	9.1E-16	0.480
Water permeability coefficient	WP x 10^{16}	(m/sec)	44	2.4E-05	2.0E-03	3.8E-04	2.9E-07	1.419	-	-	-	-	-	-	34	1.8E-14	8.4E-13	1.6E-13	3.7E-26	1.180
Corrosion potential (surface)	E_cp_top	(mV)	66	-545.3	-68	-282.579	9.9E+03	0.351	16	-433	-249	-324	4.4E+03	0.204	137	-700	-123	-444	2.1E+04	0.330
Corrosion rate (surface)	I.P_cr_top	(μm/yr)	66	11	307	66	2.9E+03	0.818	16	67	242	140	2.8E+03	0.375	137	4	130	52	8.2E+02	0.550
Electrical resistance	ER	(kΩ cm)	69	1.88	15.71	4.80	3.58	0.394	16	3.45	10.29	6.54	3.48	0.285	137	1.00	27.00	6.00	1.9E+01	0.720
Pulse velocity	PV	(km/sec)	24	2.90	4.20	3.46	9.3E-01	0.279	37	3.30	4.19	3.84	5.8E-02	0.063	-	-	-	-	-	-
Apparent modulus of elasticity	E_pv	(GPa)	24	10.76	21.44	14.54	4.68	0.149	-	-	-	-	-	-	-	-	-	-	-	-
Absorptivity after immersion	AB_asim	(%)	24	4.86	7.92	6.23	0.59	0.123	37	4.56	7.85	5.77	0.46	0.118	-	-	-	-	-	-
Dry density	SD_b	(g/cm^3)	24	1.58	1.73	1.63	8.0E-04	0.017	37	2.08	2.33	2.24	3.7E-03	0.027	-	-	-	-	-	-
Saturated density	SD_a	(g/cm^3)	24	1.75	1.95	1.81	2.2E-03	0.026	37	2.45	2.67	2.57	2.4E-03	0.019	-	-	-	-	-	-
Volume of permeable air voids	VV	(%)	24	7.86	12.87	10.14	1.667	0.127	17	10.46	16.32	12.89	1.420	0.092	-	-	-	-	-	-
Compressive strength (f'c)	CS	(MPa)	24	27	62	48	58	0.159	37	22	44	35	39	0.177	34	10	48	27	9.4E+01	0.360
Modulus of elasticity (Ec)	E_cs	(MPa)	24	4171	9700	7582	1.5E+06	0.161	-	-	-	-	-	-	-	-	-	-	-	-
Carbonation front depth	CR	(mm)	24	0.0	0.0	0.0	0.0	-	37	0.0	7.0	1.8	3.0	0.978	-	-	-	-	-	-
Chloride ion concentration at rebar	CC_rb	(%)	23	2.6E-02	6.2E-01	2.2E-01	2.8E-02	0.767	16	2.4E-02	8.2E-01	2.3E-01	4.2E-02	0.891	35	7.0E-02	2.0E-01	7.3E-02	2.8E-03	0.720
Apparent chloride diffusion coefficient	CD_a	(cm^2/sec)	24	5.5E-09	2.7E-06	1.7E-07	1.1E-13	3.264	16	1.1E-09	6.6E-07	1.0E-07	1.3E-14	1.075	32	1.4E-09	5.2E-08	9.3E-09	9.0E-17	1.020

Table 4.4 Criteria for corrosion risk and concrete quality (in italic character).

Measured parameter(s)	Designation	Range of value	Risk criteria
Half-cell potential	**HC**	Below –500 mV -350 to –500 mV -200 to –350 mV Above –200 mV	Critical High Moderate Low
Concrete cover thickness over rebar	**CV**	Below 25 mm 25 to 40 mm 40 to 50 mm Above 50 mm	High Moderate Low Moderate
Chloride diffusion migration coefficient	**CD_m**	*Below $3.0x10^{-8}$ cm^2/sec* *3.0 to $6.0x10^{-8}$ cm^2/sec* *6.0 to $9.0x10^{-8}$ cm^2/sec* *Above $9.0x10^{-8}$ cm^2/sec*	*Adequate* *Acceptable* *Suspect* *Inadequate*
Water permeability coefficient	**WP($x10^{-10}$)**	*Below $10.0x10^{-4}$ cm^2/sec* *10.0 to $20.0x10^{-4}$ cm^2/sec* *20.0 to $30.0x10^{-4}$ cm^2/sec* *Above $30x10^{-4}$ cm^2/sec*	*Adequate* *Acceptable* *Suspect* *Inadequate*
Corrosion potential	**E_cp**	Below –500 mV -350 to –500 mV -200 to –350 mV Above –200 mV	Critical High Moderate Low
Corrosion rate	**LP_cr**	Below 1μm/yr 1 to 10μm/yr 10 to 45μm/yr 45 to 100μm/yr 100 to 1000μm/yr	Low Moderate Medium High Critical
Electrical resistance	**ER**	Below 5000 Ohm.cm 5000 to 10000 Ohm.cm 10000 to 20000 Ohm.cm Above 20000 Ohm.cm	Critical High Moderate Low
Pulse velocity	**PV**	*Below 3.0 km/s* *3.0 to 3.5 km/s* *3.5 to 4.0 km/s* *Above 4.0 km/s*	*Inadequate* *Suspect* *Acceptable* *Adequate*
Apparent modulus of elasticity	**E_pv**	*Below 10 GPa* *10 to 15 GPa* *15 to 20 GPa* *Above 20 GPa*	*Inadequate* *Suspect* *Acceptable* *Adequate*

Table 4.4 Criteria for corrosion risk and concrete quality (in italic character) (continued).

Measured parameter(s)	Designation	Range of value	Risk criteria
Absorptivity after immersion	**AB_astm**	*Below 5.0 %*	*Adequate*
		5.0 to 6.5 %	*Acceptable*
		6.5 to 8.0 %	*Suspect*
		Above 8.0 %	*Inadequate*
Dry density	**SD_b**	*Below 1.60 g/cm³*	*Inadequate*
		1.60 to 1.65 g/cm³	*Suspect*
		1.65 to 1.70 g/cm³	*Acceptable*
		Above 1.70 g/cm³	*Adequate*
Saturated density	**SD_a**	*Below 1.80 g/cm³*	*Inadequate*
		1.80 to 1.85 g/cm³	*Suspect*
		1.85 to 1.90 g/cm³	*Acceptable*
		Above 1.90 g/cm³	*Adequate*
Volume of permeable air voids	**VV**	*Below 8 %*	*Adequate*
		8 to 10 %	*Acceptable*
		10 to 12 %	*Suspect*
		Above 12 %	*Inadequate*
Compressive strength (f'_c)	**CS**	Below 20 MPa	Inadequate
		20 to 30 MPa	Suspect
		30 to 40 MPa	Acceptable
		Above 40 MPa	Adequate
Modulus of elasticity (E_c)	**E_cs**	Below 5000 MPa	Inadequate
		5000 to 7500 MPa	Suspect
		7500 to 10000 MPa	Acceptable
		Above 10000 MPa	Adequate
Carbonation front depth	**CR_t**	Below 5 mm	Adequate
		5 to 15 mm	Acceptable
		15 to 25 mm	Suspect
		Above 25 mm	Inadequate
Chloride ion concentration at rebar	**CC_rb**	*Below 0.2 %*	*Adequate*
		0.2 to 0.4 %	*Acceptable*
		0.4 to 0.6 %	*Suspect*
		Above 0.6 %	*Inadequate*
Apparent chloride diffusion coefficient	**CD_a**	*Below 3.0x10^{-9}cm^2/sec*	*Adequate*
		3.0 to 13.0x10^{-9}cm^2/sec	*Acceptable*
		13.0 to 23.0x10^{-9}cm^2/sec	*Suspect*
		Above 23.0x10^{-9}cm^2/sec	*Inadequate*

Table 4.5 Classification of test results after criteria from Table 4.4.

Designation	Range of value	Risk criteria	Number of values in each range (entire deck) in %
E_hc_top	Below –500 mV	Critical	**9**
	-350 to –500 mV	High	**47**
	-200 to –350 mV	Moderate	**32**
	Above –200 mV	Low	**12**
E_hc_bot	Below –500 mV	Critical	**20**
	-350 to –500 mV	High	**45**
	-200 to –350 mV	Moderate	**24**
	Above –200 mV	Low	**11**
E_hc_col	Below –500 mV	Critical	**100**
	-350 to –500 mV	High	**0**
	-200 to –350 mV	Moderate	**0**
	Above –200 mV	Low	**0**
CV_top	Below 25 mm	High	**19**
	25 to 40 mm	Moderate	**38**
	40 to 50 mm	Low	**19**
	Above 50 mm	Moderate	**24**
CV_bot	Below 25 mm	High	**48**
	25 to 40 mm	Moderate	**44**
	40 to 50 mm	Low	**7**
	Above 50 mm	Moderate	**1**
CV_col	Below 25 mm	High	**10**
	25 to 40 mm	Moderate	**27**
	40 to 50 mm	Low	**42**
	Above 50 mm	Moderate	**20**
CD_m	Below $3.0x10^{-8}cm^2/sec$	Adequate	**36**
	3.0 to $6.0x10^{-8}cm^2/sec$	Acceptable	**42**
	6.0 to $9.0x10^{-8}cm^2/sec$	Suspect	**6**
	Above $9.0x10^{-8}cm^2/sec$	Inadequate	**15**
WP($x10^{-10}$)	Below $10.0x10^{-4}cm^2/sec$	Adequate	**86**
	10.0 to $20.0x10^{-4}cm^2/sec$	Acceptable	**11**
	20.0 to $30.0x10^{-4}cm^2/sec$	Suspect	**2**
	Above $30x10^{-4}cm^2/sec$	Inadequate	**0**
E_cp	Above –500 mV	Critical	**2**
	-350 to –500 mV	High	**22**
	-200 to –350 mV	Moderate	**60**
	Below –200 mV	Low	**16**
LP_cr	Below 1 µm/yr	Low	**0**
	1 to 10µm/yr	Moderate	**0**
	10 to 45µm/yr	Medium	**40**
	45 to 100µm/yr	High	**41**
	100 to 1000µm/yr	Critical	**19**
ER	Below 5000 Ohm.cm	Critical	**100**
	5000 to 10000 Ohm.cm	High	**0**
	10000 to 20000 Ohm.cm	Moderate	**0**
	Above 20000 Ohm.cm	Low	**0**

Table 4.5 Classification of test results after criteria from Table 4.4 (continued).

Designation	Range of value	Risk criteria	Number of values in each range (entire deck) in %
PV	Below 3.0 km/s	Inadequate	**4**
	3.0 to 3.5 km/s	Suspect	**57**
	3.5 to 4.0 km/s	Acceptable	**39**
	Above 4.0 km/s	Adequate	**0**
E_pv	Below 10 MPa	Inadequate	**0**
	10 to 15 MPa	Suspect	**70**
	15 to 20 MPa	Acceptable	**30**
	Above 20 MPa	Adequate	**0**
AB_astm	Below 5.0 %	Adequate	**4**
	5.0 to 6.5 %	Acceptable	**61**
	6.5 to 8.0 %	Suspect	**35**
	Above 8.0 %	Inadequate	**0**
SD_b	Below 1.60 g/cm³	Inadequate	**13**
	1.60 to 1.65 g/cm³	Suspect	**74**
	1.65 to 1.70 g/cm³	Acceptable	**9**
	Above 1.70 g/cm³	Adequate	**4**
SD_a	Below 1.80 g/cm³	Inadequate	**57**
	1.80 to 1.85 g/cm³	Suspect	**22**
	1.85 to 1.90 g/cm³	Acceptable	**17**
	Above 1.90 g/cm³	Adequate	**4**
VV	Below 8 %	Adequate	**4**
	8 to 10 %	Acceptable	**52**
	10 to 12 %	Suspect	**35**
	Above 12 %	Inadequate	**9**
CS	Below 20 MPa	Inadequate	**0**
	20 to 30 MPa	Suspect	**4**
	30 to 40 MPa	Acceptable	**9**
	Above 40 MPa	Adequate	**87**
E_cs	Below 5000 MPa	Inadequate	**4**
	5000 to 7500 MPa	Suspect	**43**
	7500 to 10000 MPa	Acceptable	**52**
	Above 10000 MPa	Adequate	**0**
CR_t	Below 5 mm	Adequate	**100**
	5 to 15 mm	Acceptable	**0**
	15 to 25 mm	Suspect	**0**
	Above 25 mm	Inadequate	**0**

Table 4.5 Classification of test results after criteria from Table 4.4 (continued).

Designation	Range of value	Risk criteria	Number of values in each range (entire deck) in %
CC_rb	Below 0.2 %	Adequate	**48**
	0.2 to 0.4 %	Acceptable	**39**
	0.4 to 0.6 %	Suspect	**9**
	Above 0.6 %	Inadequate	**4**
CD_a	Below $3.0x10^{-9}cm^2/sec$	Adequate	**0**
	3.0 to $13.0x10^{-9}cm^2/sec$	Acceptable	**39**
	13.0 to $23.0x10^{-9}cm^2/sec$	Suspect	**9**
	Above $23.0x10^{-9}cm^2/sec$	Inadequate	**52**

4.4 Individual test results

4.4.1 Half-cell potential tests

The half-cell potential survey was performed :

- on the entire bridge deck surface (using a grid of one meter by one meter) and on the 35 strips selected for additional testing where the asphalt overlay was removed using a grid of 15 cm by 30 cm;
- on part of the bridge deck soffit (using the same grid as used for the bridge deck surface);
- on some structural columns of the bridge (5).

As mentioned in Section 3.4.1, the results obtain from the half-cell potential test are sensitive to the moisture content of the concrete. To ensure the consistency of the results and allow for comparison between the different surveys, the test was always performed in dry conditions, after the occurrence of at least two consecutive days of dry and warm temperature. However, according to the literature[27], the moisture content does not affect the relative intensities of the results (in the form of contour plot), but instead it systematically lowers the potential values obtained.

Half-cell potential of bridge deck surface

The results for the half-cell potential survey of the deck surface vary from a minimum of –920 mV to a maximum of –25 mV with a mean value of –373 mV, and a coefficient of variation of 33.2 %. A total of 3097 locations (gridpoints) were tested. According to Table 4.5, most of the top steel reinforcement (56 %) presents a high risk of corrosion or the corrosion process has reached the propagation stage.

Figure 4.1 shows the three-dimensional surface obtained using the least-squares fitting method with the north direction of the bridge, the level axis representing the length, the line axis representing the width, and the ranges of values used for the

surface plot are also indicated. Figure 4.2 shows the two-dimensional potential curves obtained for the bridge deck as a plan view of Figure 4.1 : again the same information concerning the orientation of the bridge deck and the ranges of values used is presented. In Figures 4.1 and 4.2, it can be observed that the top portion of the bridge deck (north end) presents a high risk of corrosion. The lowest potentials (highest risk) are observed on both west and east sides of the north end, and could be related to the quality of the surface fitting. As a direct consequence, extrapolations made by the surface fitting should be considered with care in the analysis. However, a clear change in the half-cell potential results is visible near the location of the expansion joint (located at level 310 m). It is important to mention that the contour plots indicate only the general tendencies, the local variations not being considered in the interpretation.

Half-cell potential of bridge deck soffit

The results for the half-cell potential survey of the bridge deck soffit vary from a minimum of –693 mV to a maximum of –52 mV, with a mean value of —386 mV and a coefficient of variation of 32.9 %. A total of 1584 locations (gridpoints) were tested. According to Table 4.5, most of the bottom steel reinforcement (65 %) presents a high risk to corrosion or the corrosion has already started.

Figure 4.3 shows the three-dimensional surface obtained using the least-squares fitting method : the north direction of the Bridge, the level axis representing the length, the line axis representing the width, and the ranges of values used for the surface plot are also indicated. Figure 4.4 shows the two-dimensional potential curves obtained for the bridge deck as a plan view of Figure 4.3 : again the same information concerning the orientation of the bridge deck and the ranges of values used is presented. In Figure 4.3 and 4.4, it can be observed that the south end of the bridge deck represents a high risk of corrosion. The lowest potentials (highest risk) are observed at the centre of the south end, and this could be related to the quality of

the estimation of the distribution by surface fitting. Again, extrapolations by surface fitting should be considered with care when interpreting the results.

Half-cell potential of bridge columns

The results for the half-cell potential survey for the bridge columns vary from a minimum of −143 mV to a maximum of 408 mV, with a mean value of 73 mV and a coefficient of variation of 162.5 %. A total of 245 locations (marked points) were tested. According to Table 4.5, the reinforced concrete columns tested present low risks of developing corrosion, but the results of this survey should be interpreted with care as they are abnormally low (positive mean value). Unfortunately, the half-cell and the cover meter tests were performed on the columns only and consequently, there is no possible way to adequately verify the cause of these findings.

Figure 4.5 shows the three-dimensional surface obtained using the least-squares fitting method : the north direction of the Bridge, the level axis representing the length, the line axis representing the width, the locations tested, and the ranges of values used for the surface plot are also indicated. Figure 4.6 shows the two-dimensional potential curves obtained for the bridge deck as a plan view of Figure 4.5 : again the same information concerning the orientation of the bridge deck and the ranges of values used is presented. In Figure 4.5 and 4.6, it can be observed that the results do not follow any significant trend, and that their interpretation is difficult.

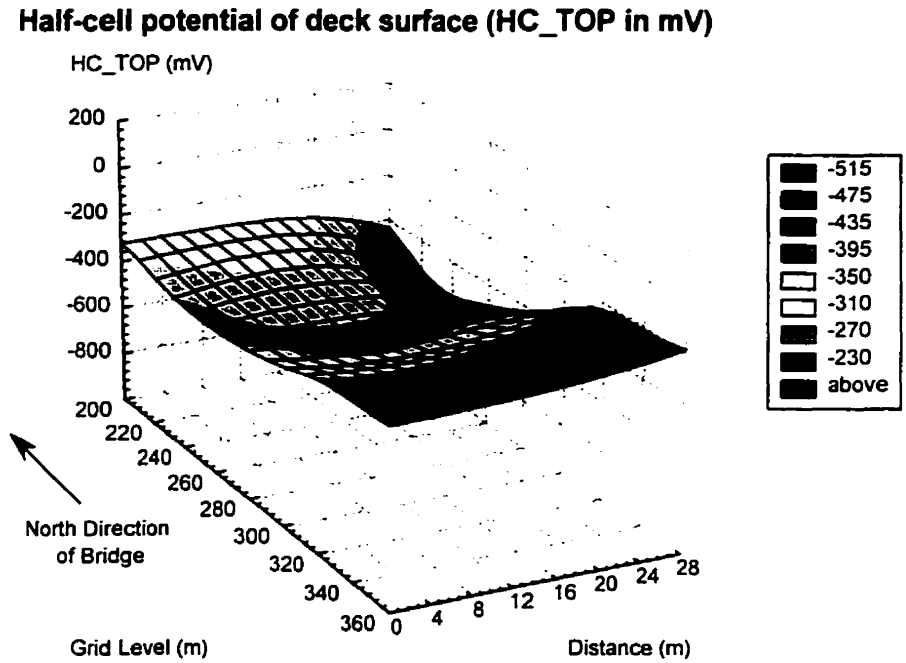

Figure 4.1 Three-dimensional view of half-cell potential tests of the bridge deck surface.

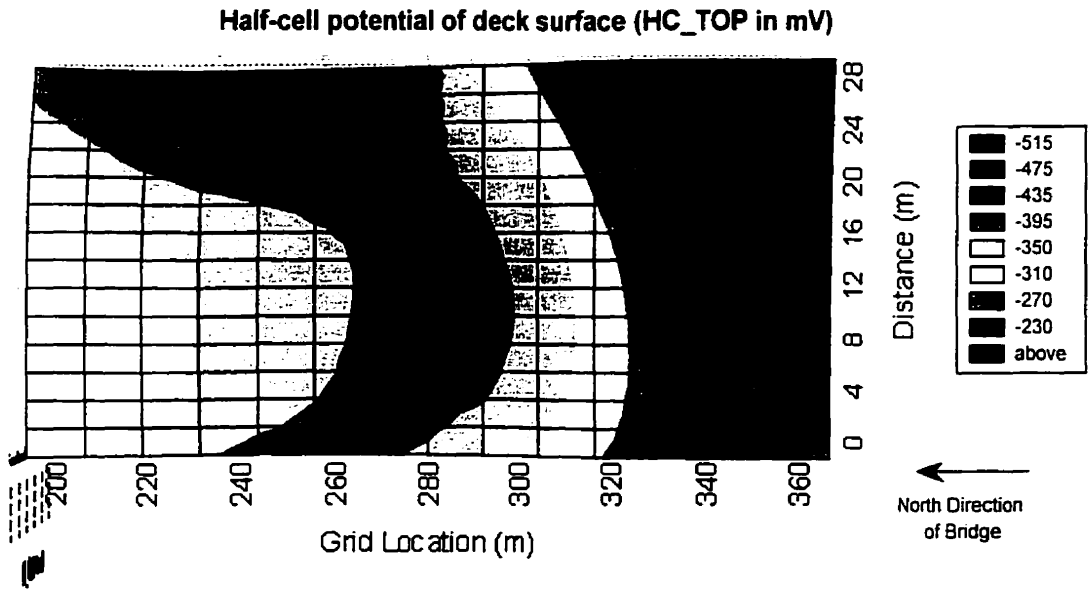

Figure 4.2 Plan view of half-cell potential tests of the bridge deck surface.

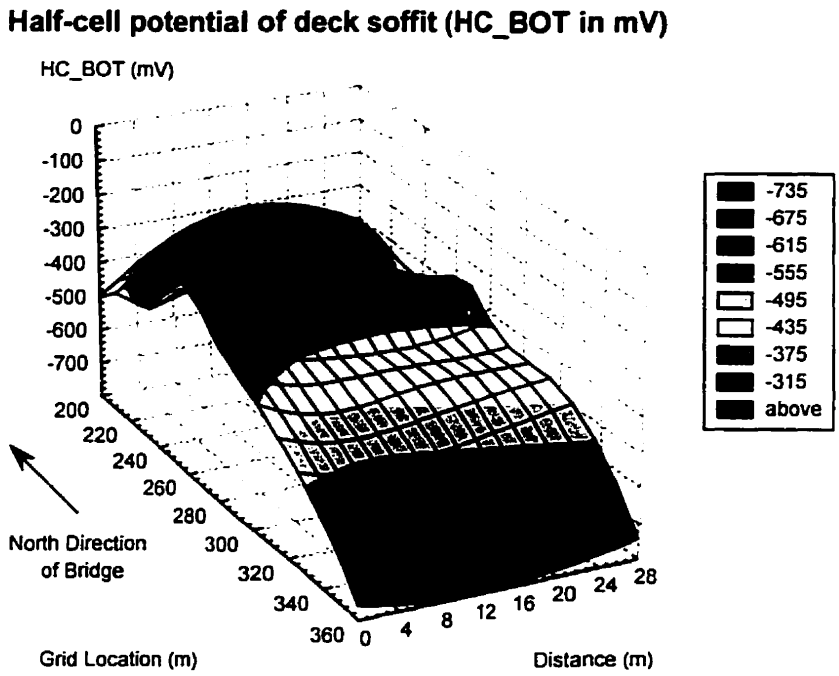

Figure 4.3 Three-dimensional view of half-cell potential tests of the bridge deck soffit.

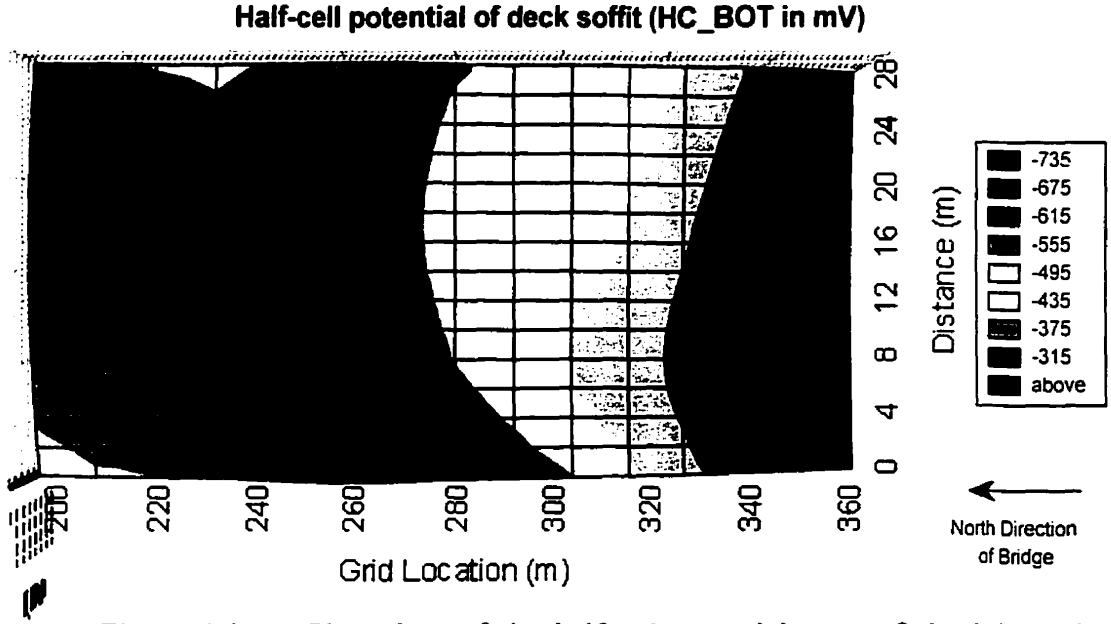

Figure 4.4 Plan view of the half-cell potential tests of the bridge deck soffit.

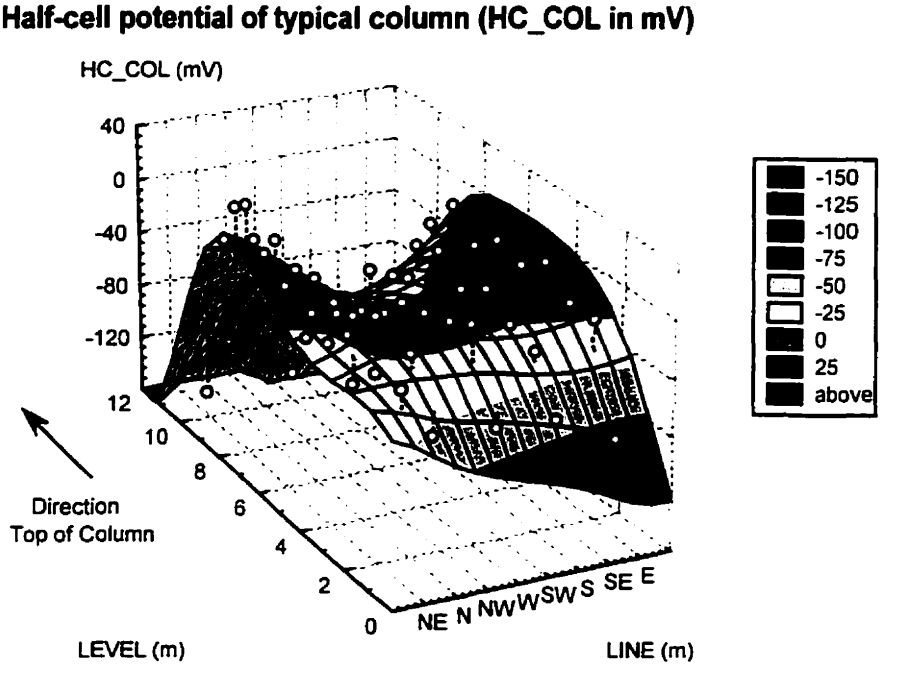

Figure 4.5 Three-dimensional view of half-cell potential tests of a typical column.

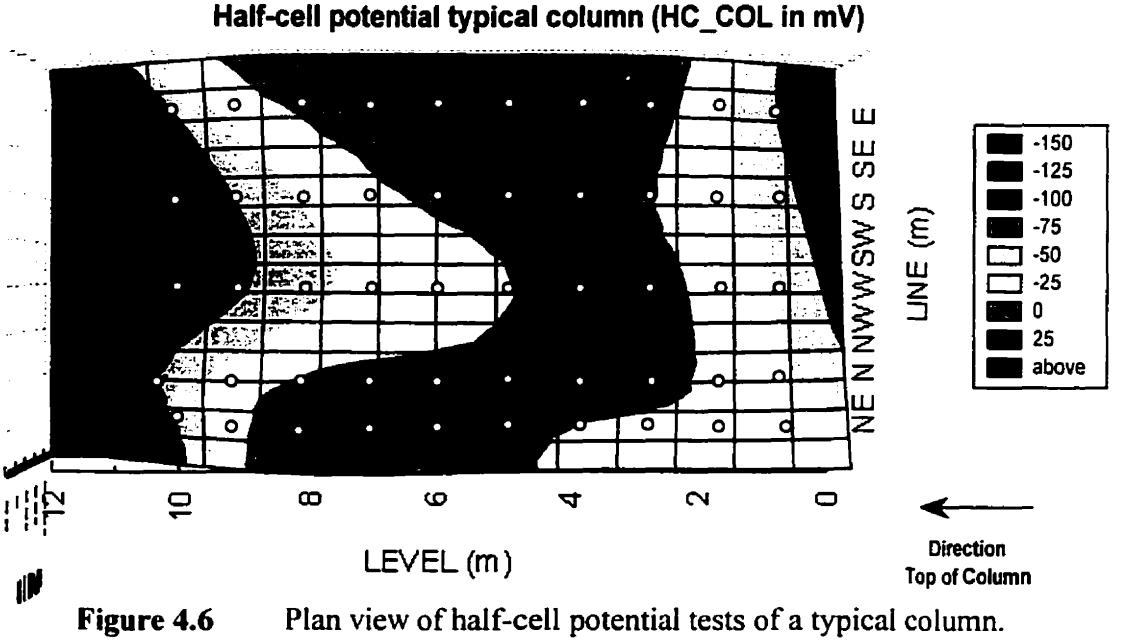

Figure 4.6 Plan view of half-cell potential tests of a typical column.

4.4.2 Concrete cover tests

The concrete cover survey was performed :

- on the 35 strips selected for additional testing where the asphalt overlay was removed using a grid of 15 cm by 30 cm;
- on a part of the bridge deck soffit (using the same grid used for the deck surface);
- on five structural columns using a grid of 30 cm by 1 m.

Concrete cover test of bridge deck surface

The results for the concrete cover survey of the bridge deck surface vary from a minimum cover thickness of 2.0 mm to a maximum of 94.5 mm, with a mean value of 39.4 mm and a coefficient of variation of 42.6 %. A total of 890 locations (gridpoints) were tested. According to Table 4.5, the thickness of the concrete cover of most of the surface deck is considered adequate with 57 % of the readings showing a low to moderate risk of corrosion development. However, according to the design details of the Dickson Bridge, the specified design cover originally proposed was 25 mm. Finally, it is important to mention that the concrete surface tested was damaged due to the asphalt removal process.

Figure 4.7 shows the three-dimensional surface obtained using the least-squares fitting method : the north direction of the Bridge, the level axis representing the length, the line axis representing the width, the locations tested, and the ranges of values used for the surface plot are also indicated. Figure 4.8 shows the two-dimensional curves obtained for the bridge deck as a plan view of Figure 4.7 : again the same information concerning the orientation of the bridge deck and the ranges of values used is presented. In Figure 4.7 and 4.8, it can be observed that the top portion of the bridge deck (north end) presents the lowest concrete covers, but this is based on

only a small number of readings : each value is the average value of concrete cover for each strip since many readings were taken in each strip.

Concrete cover test of bridge deck soffit

The results for the concrete cover survey of the bridge deck soffit vary from a minimum cover thickness of 1.3 mm to a maximum of 63.5 mm, with a mean value of 25.9 mm and a coefficient of variation of 33.0 %. A total of 1584 locations (gridpoints) were tested. According to Table 4.5, the concrete cover thickness of near half (48%) of the surface deck is found to be lower than 25 mm which would explain the development of corrosion on the lower level of the steel reinforcement. However, from the design details of the bridge, the specified cover was 25 mm. Generally, the results obtained are consistent with the original concrete cover thickness (design).

Figure 4.9 shows the three-dimensional surface obtained using the least-squares fitting method : the north direction of the Bridge, the level axis representing the length, the line axis representing the width, the locations tested, and the ranges of values used for the surface plot are also indicated. Figure 4.10 shows the two-dimensional curves obtained for the bridge deck as a plan view of Figure 4.9 : again the same information concerning the orientation of the bridge deck and the ranges of values used is presented. In Figure 4.9 and 4.10, it can be observed that the top portion of the bridge deck (north end) presents higher cover thicknesses. The highest values are observed on both west and east sides of the north end. A clear change in the cover thickness is visible at level 210 m. It can be observed that this region seems to correspond to the region of low concrete cover for the top reinforcement.

Concrete cover test of bridge columns

The values of the concrete cover survey of the bridge columns vary from a minimum of 10.2 mm to a maximum of 71.1 mm, with a mean value of 41.1 mm and a coefficient of variation of 27.6 %. A total of 245 locations (gridpoints) were tested. According to Table 4.5, the thickness of the concrete cover of most of the surface deck is more than adequate with 69 % of the readings being in the range of low to moderate risk of corrosion. However, from the design details of the Dickson Bridge, the cover originally proposed was 25 mm. Since only the half-cell and concrete cover tests were performed on the columns, these results cannot be verified.

Figure 4.11 shows the three-dimensional surface obtained using the least-squares fitting method : the north direction of the Bridge, the level axis representing the length, the line axis representing the width, the locations tested, and the ranges of values used for the surface plot are also indicated. Figure 4.12 shows the two-dimensional curves obtained for the bridge deck as a plan view of Figure 4.11 : again the same information concerning the orientation of the bridge deck and the ranges of values used is presented. The findings are difficult to interpret. The concrete cover along a column is thicker at the middle section than at the top and the bottom sections.

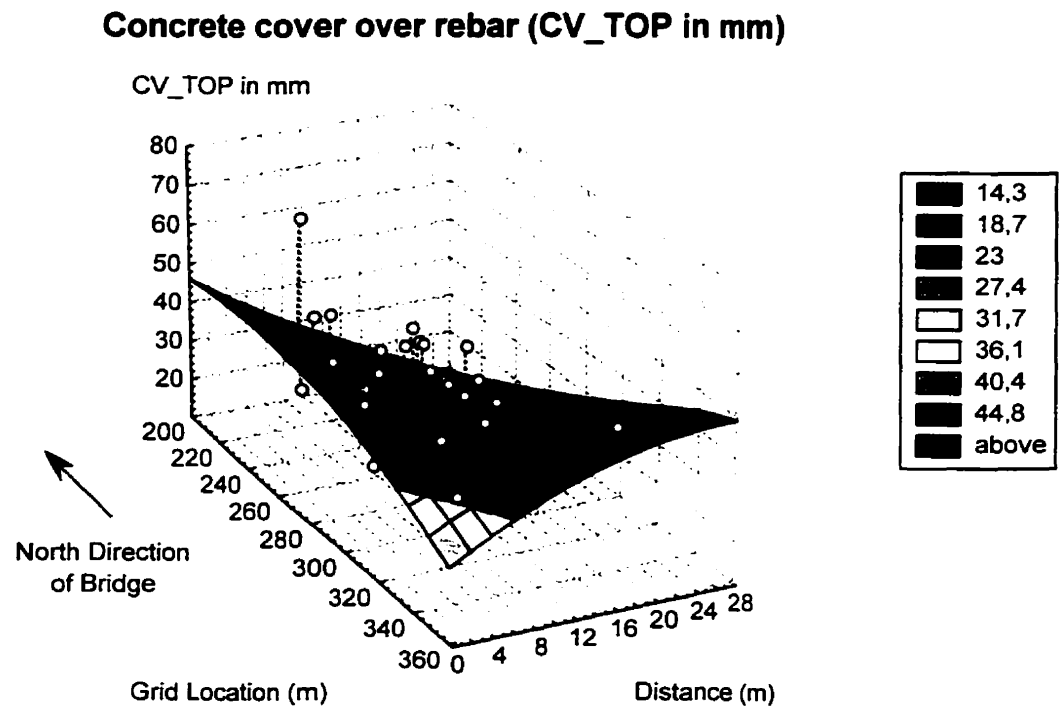

Figure 4.7 Three-dimensional view of concrete cover tests of the bridge deck surface.

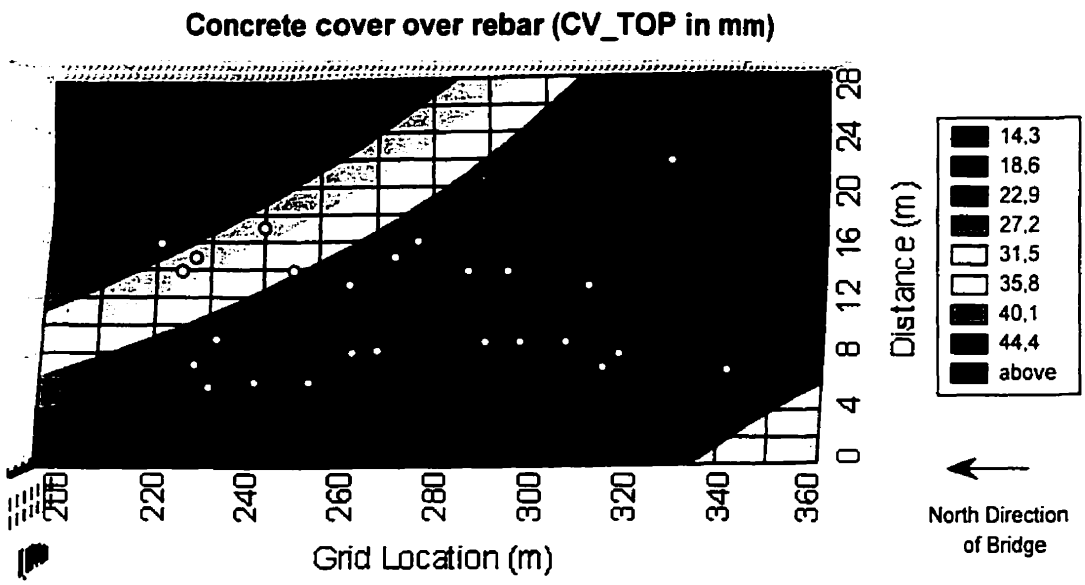

Figure 4.8 Plan view of concrete cover tests of the bridge deck surface.

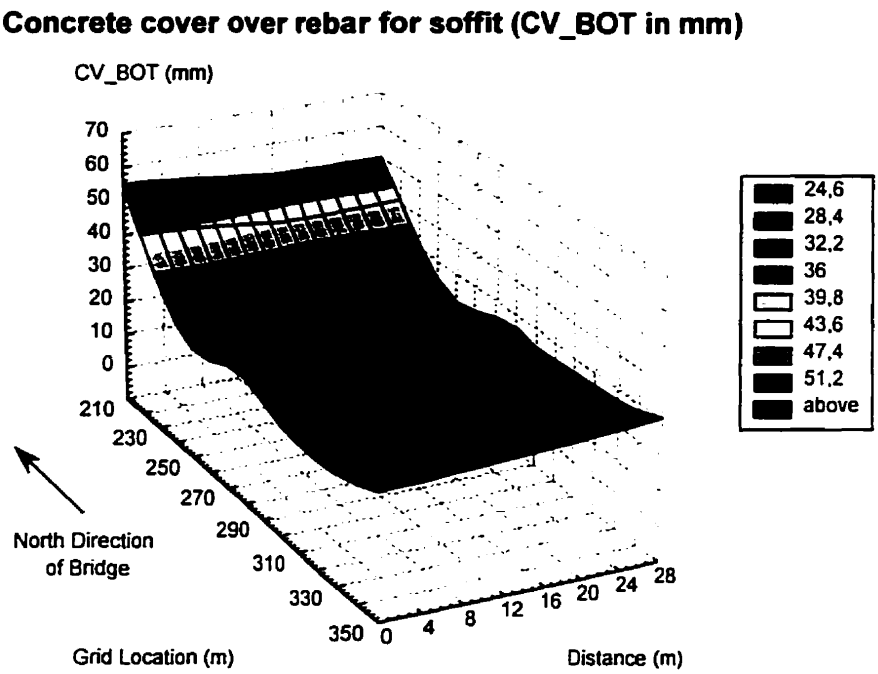

Figure 4.9 Three-dimensional view of concrete cover tests of the bridge deck soffit.

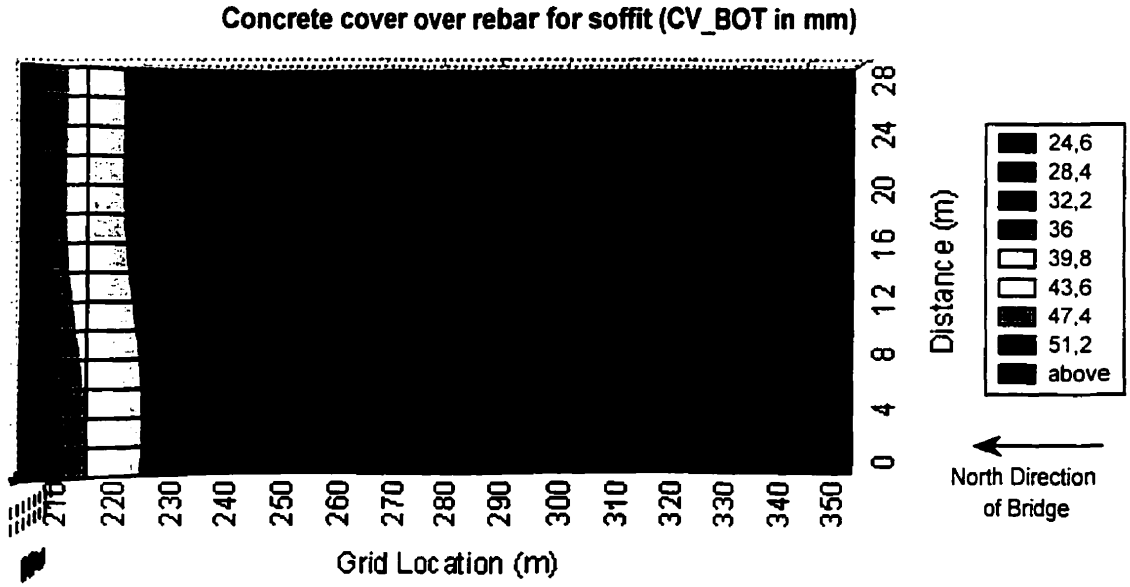

Figure 4.10 Plan view of concrete cover tests of the bridge deck soffit.

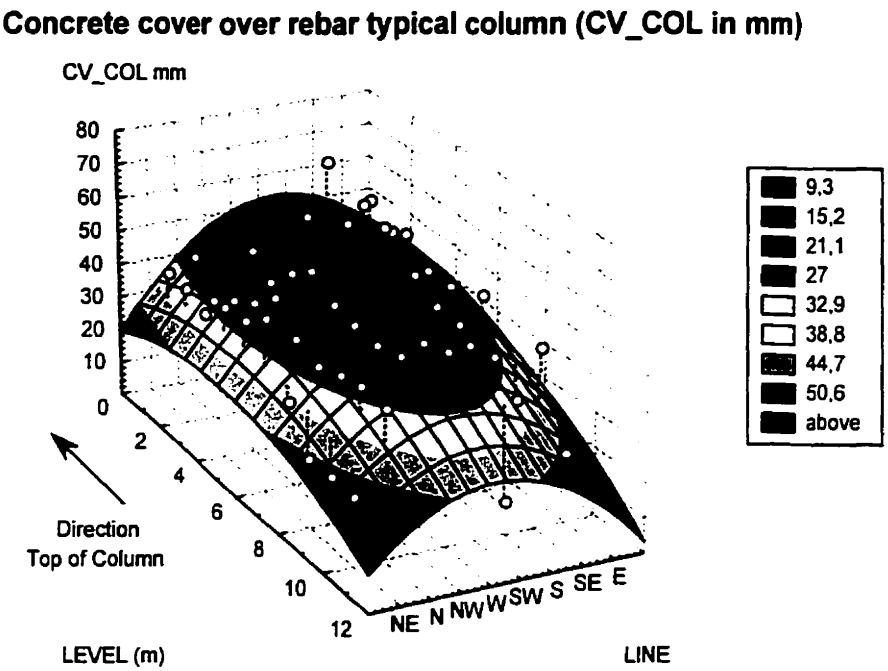

Figure 4.11 Three-dimensional view of concrete cover tests of a typical column.

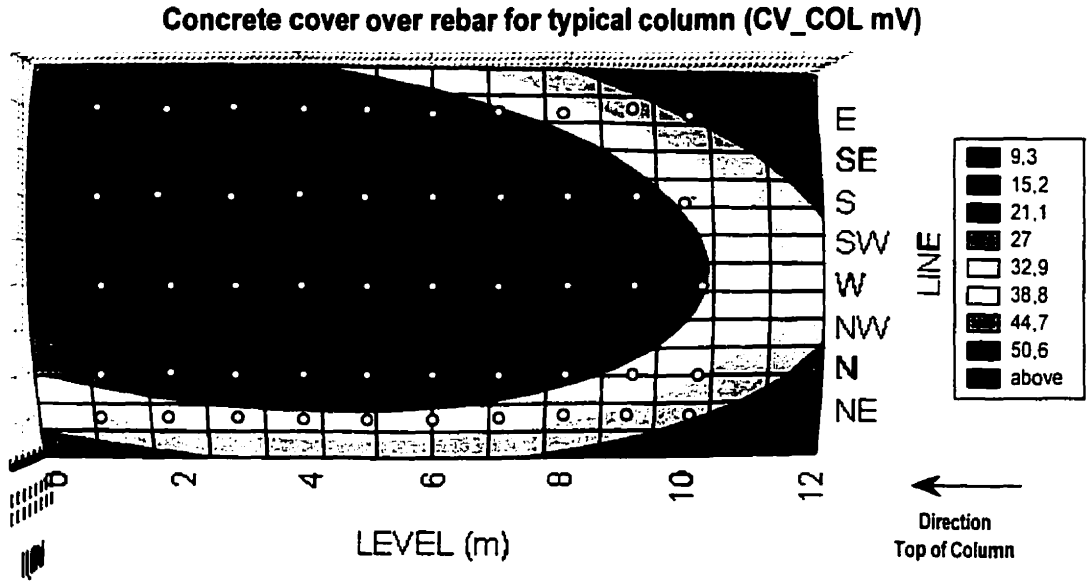

Figure 4.12 Plan view of concrete cover tests of a typical column.

4.4.3 In-situ chloride diffusion (migration) tests

The in-situ chloride diffusion migration survey was performed :

- at specific locations in the 35 areas (strips) selected for additional testing where the asphalt overlay was removed.

In-situ chloride diffusion migration tests of bridge deck surface

The results for the in-situ chloride diffusion migration survey vary from a minimum of 8.16×10^{-11} cm^2/s to a maximum of 4.36×10^{-7} cm^2/s, with a mean value of 5.48×10^{-8} cm^2/s and a coefficient of variation of 136.1 %. A total of 33 locations were tested. According to Table 4.5, 78 % of the readings show that the coefficient of chloride migration is adequate to acceptable for limiting the ingress of chlorides in the concrete matrix. However, only few tests were performed on the south section of the Dickson Bridge, and thus it is difficult to adequately quantify the overall property of the concrete with regards to the diffusion of chlorides. Also, the absence of risk criteria renders the interpretation of the measured chloride diffusion migration coefficients difficult at this point in time. Finally, the repeatability of the testing technique was not established and this needs to be considered in the analysis.

Figure 4.13 shows the three-dimensional surface obtained using the least-squares fitting method : the north direction of the Bridge, the level axis representing the length, the line axis representing the width, the locations tested, and the ranges of values used for the surface plot are also indicated. Figure 4.14 shows the two-dimensional curves obtained for the bridge deck as a plan view of Figure 4.13 : again the same information concerning the orientation of the bridge deck and the ranges of values used is presented. In Figure 4.13 and 4.14, it can generally be observed that the east and west sides of the bridge deck show the highest values while the centre portion presents relatively constant values. The presence of possible outliers, or

inconsistent readings of the results, could be considered to explain these variable findings.

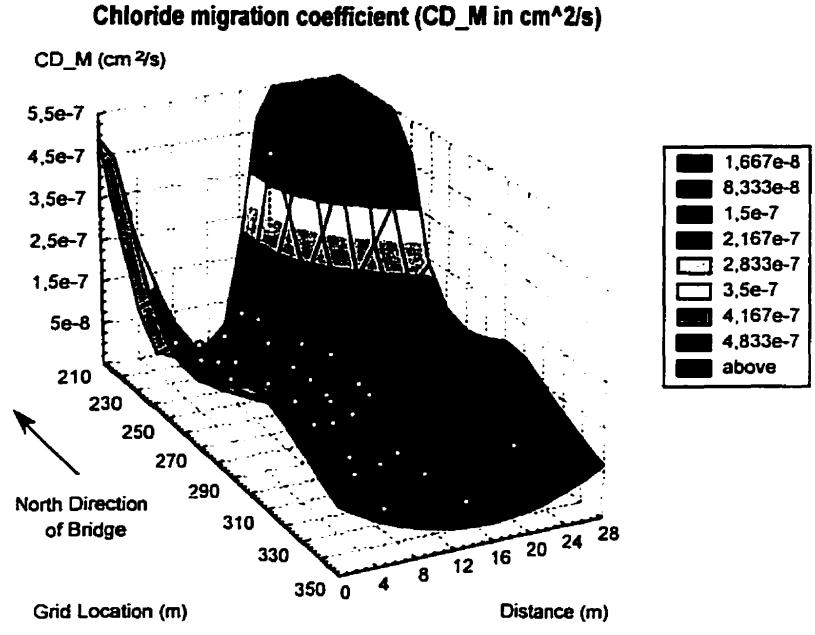

Figure 4.13 Three-dimensional view of in-situ chloride diffusion (migration) tests of bridge deck surface.

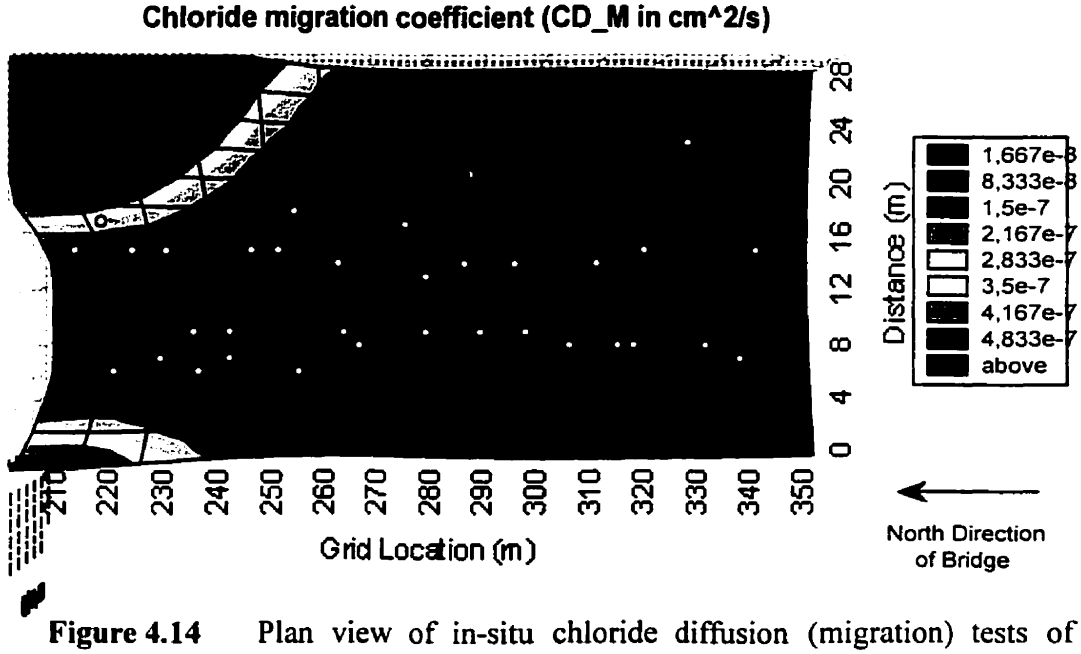

Figure 4.14 Plan view of in-situ chloride diffusion (migration) tests of bridge deck surface.

4.4.4 In-situ water permeability tests

The in-situ water permeability survey was performed :

- at specific locations in the 35 areas (strips) selected for additional testing where the asphalt overlay was removed.

In-situ water permeability tests of bridge deck surface

The results for the in-situ water permeability tests vary from a minimum of 2.42×10^{-15} cm^2/s to a maximum of 2.02×10^{-13} cm^2/s, with a mean value of 3.78×10^{-14} cm^2/s and a coefficient of variation of 141.9 %. A total of 44 locations were tested. According to Table 4.5, 86 % of the readings indicate that the concrete quality with regards to water penetration is adequate. However, only few tests were performed on the south section of the bridge. Also, the absence of risk criteria renders the characterization of the water permeability coefficient difficult at this point in time. Finally, the repeatability of the testing technique was not established and this needs to be considered in the analysis process.

Figure 4.15 shows the three-dimensional surface obtained using the least-squares fitting method : the north direction of the Bridge, the level axis representing the length, the line axis representing the width, the locations tested, and the ranges of values used for the surface plot are also indicated. Figure 4.16 shows the two-dimensional curves obtained for the bridge deck as a plan view of Figure 4.15 : again the same information concerning the orientation of the bridge deck and the ranges of values used is presented. In Figure 4.15 and 4.16, it can be observed that both east and west sides of the north end of the bridge deck present the highest values. In addition, the central portion of the south end shows relatively high results. These areas of high water permeability are indicative of portions of the bridge of low concrete quality.

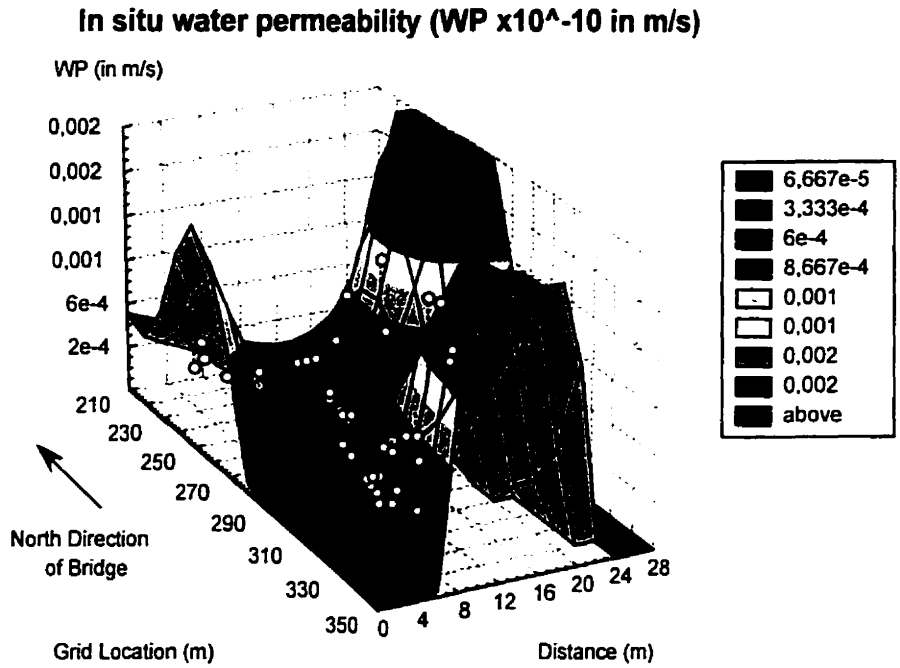

Figure 4.15 Three-dimensional view of in-situ water permeability tests of the bridge deck surface.

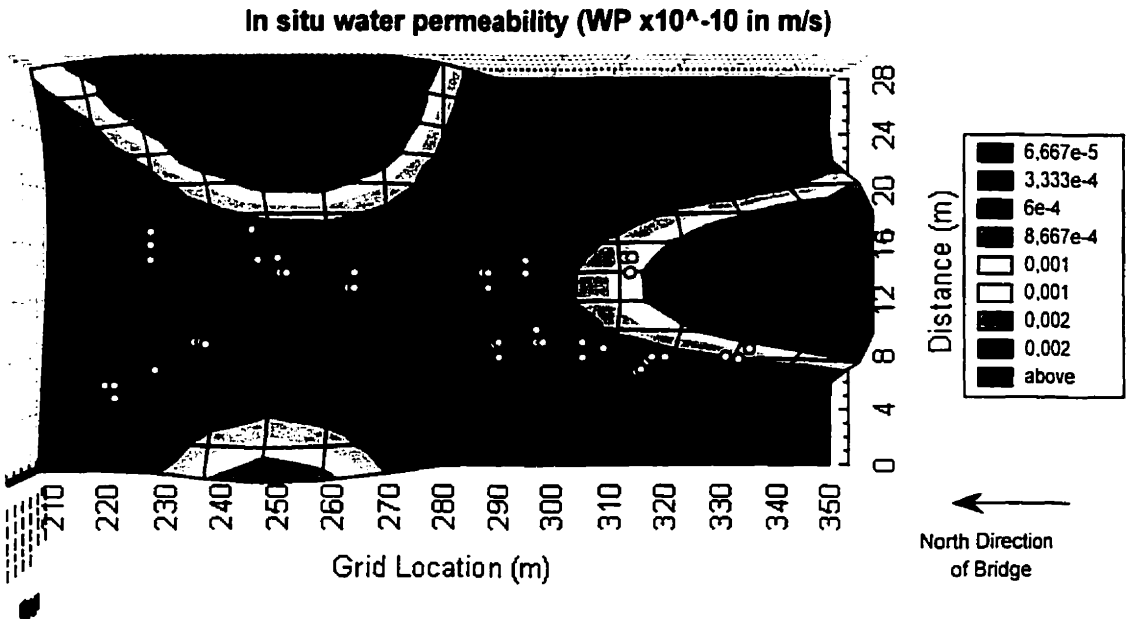

Figure 4.16 Plan view of in-situ water permeability tests of the bridge deck surface.

4.4.5 Linear polarization resistance tests

The linear polarization resistance tests were performed :

- at specific locations in the 35 areas (strips) selected for additional testing where the asphalt overlay was removed.

Corrosion potential test of bridge deck surface

The results for the corrosion potential survey vary from a minimum of -545 mV to a maximum of -68 mV, with a mean value of -283 mV and a coefficient of variation of 35.1 %. A total of 66 locations were tested. According to Table 4.5, 60 % of the results indicate a moderate risk to develop corrosion. The repeatability of the testing technique was not established and this needs to be considered in the analysis process.

Figure 4.17 shows the three-dimensional surface obtained using the least-squares fitting method : the north direction of the Bridge, the level axis representing the length, the line axis representing the width, the locations tested, and the ranges of values used for the surface plot are also indicated. Figure 4.18 shows the two-dimensional curves obtained for the bridge deck as a plan view of Figure 4.17 : again the same information concerning the orientation of the bridge deck and the ranges of values used is presented. In Figure 4.17 and 4.18, it can be observed that the distribution of the results is hard to determine visually, and that the variations observed change locally. However, the areas of low risk of corrosion (high potential readings) seem to correspond to the areas showing the maximum values of the water permeability coefficient.

Corrosion rate of bridge deck surface

The results for the corrosion rate survey vary from a minimum of 11 μm/yr to a maximum of 307 μm/yr, with a mean value of 66 μm/yr and a coefficient of variation

of 81.8 %. A total of 66 locations were tested. According to Table 4.5, 60 % of the readings indicate high to critical values of the corrosion rate leading to intensive loss of metal mass. The repeatability of the testing technique was not established and this needs to be considered in the analysis process.

Figure 4.19 shows the three-dimensional surface obtained using the least-squares fitting method : the north direction of the Bridge, the level axis representing the length, the line axis representing the width, the locations tested, and the ranges of values used for the surface plot are also indicated. Figure 4.20 shows the two-dimensional curves obtained for the bridge deck as a plan view of Figure 4.19 : again the same information concerning the orientation of the bridge deck and the ranges of values used is presented. In Figure 4.19 and 4.20, it can be observed that the highest readings were obtained on both west and east sides of the bridge deck.

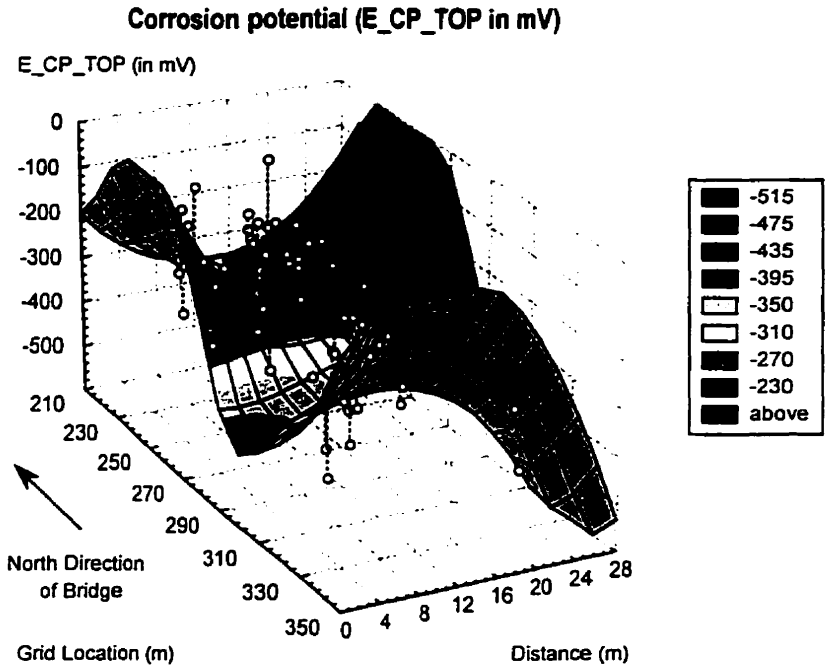

Figure 4.17 Three-dimensional view of corrosion potential tests of the bridge deck surface.

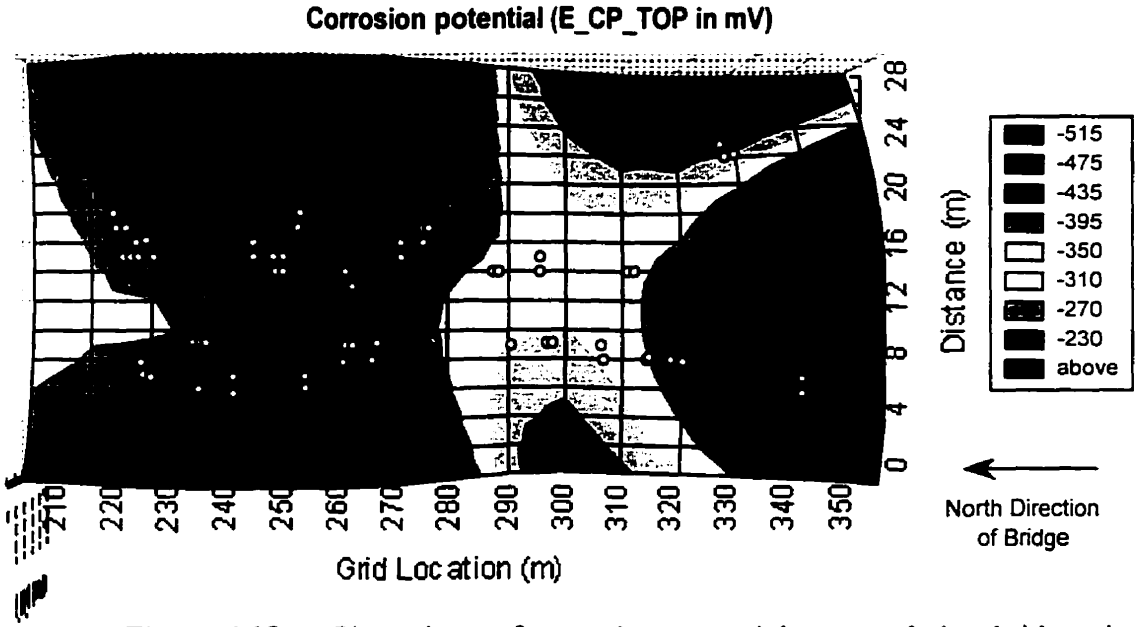

Figure 4.18 Plan view of corrosion potential tests of the bridge deck surface.

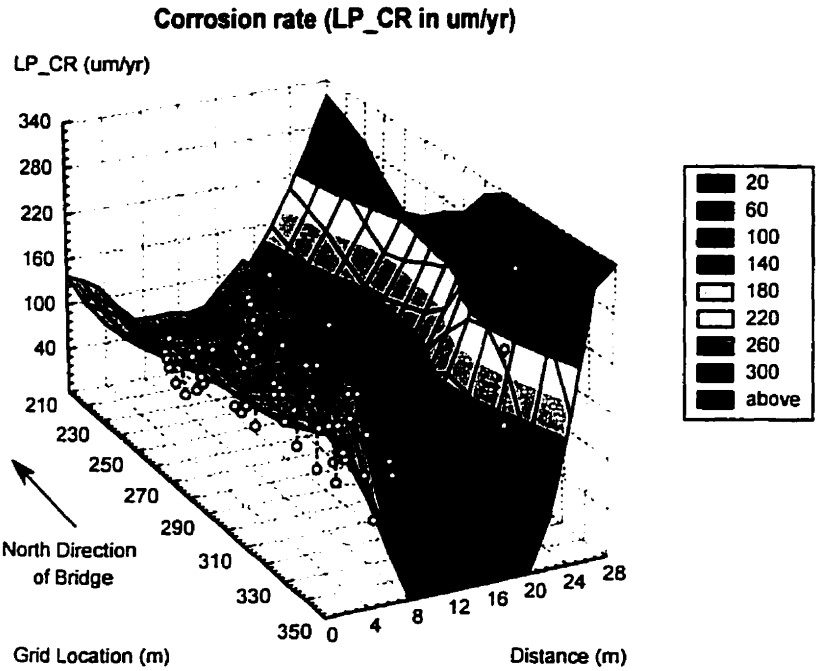

Figure 4.19 Three-dimensional view of corrosion rate tests of the bridge deck surface.

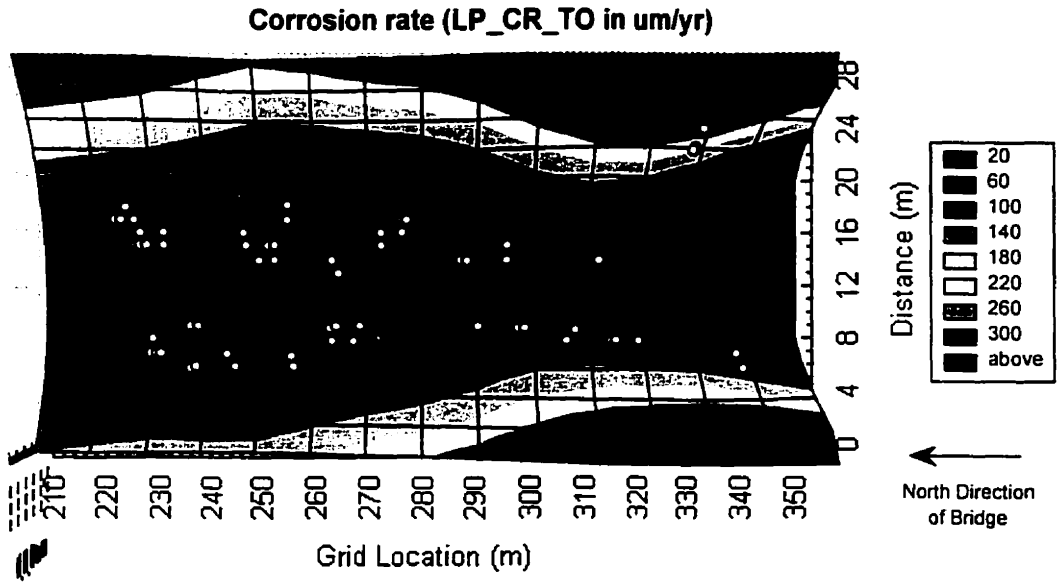

Figure 4.20 Plan view of corrosion rate tests of the bridge deck surface.

4.4.6 Electrical resistivity tests

The electrical resistivity tests were performed :

- at specific locations in the 35 areas (strips) selected for additional testing where the asphalt overlay was removed.

Electrical resistance of bridge deck surface

The results for the electrical resistivity survey vary from a minimum of 1.88 kΩ.cm (kiloOhms.cm) to a maximum of 15.7 kΩ.cm, with a mean value of 4.8 kΩ.cm and a coefficient of variation of 39.4 %. A total of 69 locations were tested. According to Table 4.5, 100 % of the readings are indicative of a critical risk to develop the corrosion process.

Figure 4.21 shows the three-dimensional surface obtained using the least-squares fitting method : the north direction of the Bridge, the level axis representing the length, the line axis representing the width, the locations tested, and the ranges of values used for the surface plot are also indicated. Figure 4.22 shows the two-dimensional curves obtained for the bridge deck as a plan view of Figure 4.21 : again the same information concerning the orientation of the bridge deck and the ranges of values used is presented. In Figure 4.21 and 4.22, it can be observed that the distribution of the results is hard to determine visually, and that the variations observed change locally.

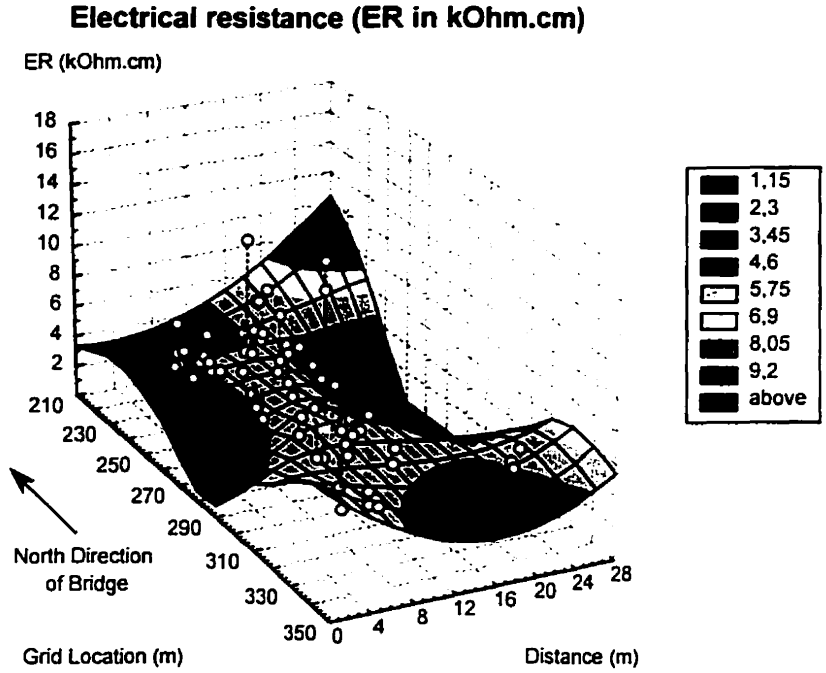

Figure 4.21 Three-dimensional view of electrical resistivity tests of the bridge deck surface.

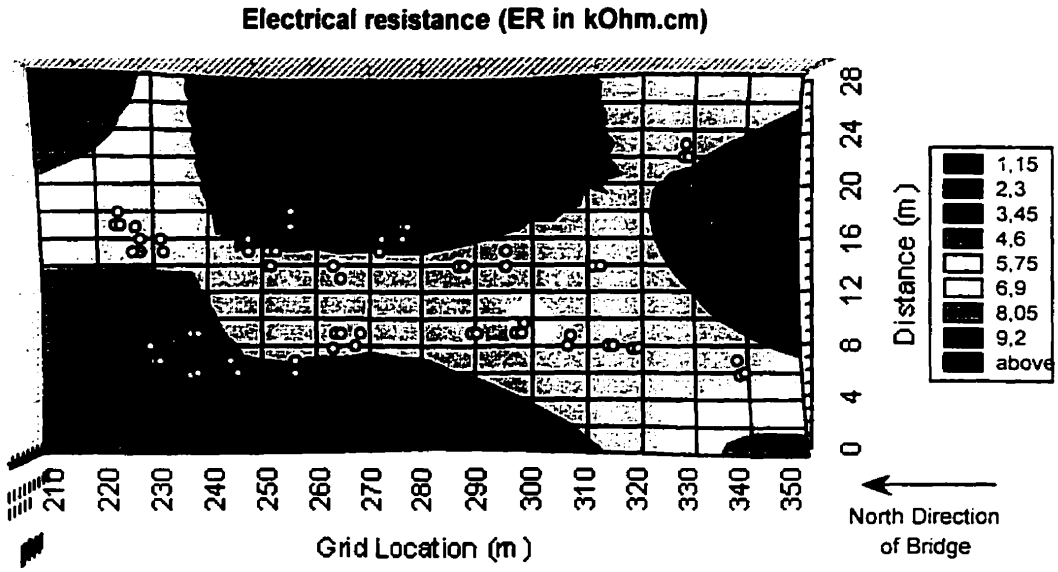

Figure 4.22 Plan view of electrical resistivity tests of the bridge deck surface.

4.4.7 Visual description of cores

Visual core descriptions were performed :

- on the 63 cores collected in specific locations in the 35 areas (strips) selected for additional testing where the asphalt overlay was removed;

Visual core descriptions

An example of the visual core description is presented in Table 4.6, while Figures 4.23 and 4.24 show the as-collected state of a typical core. The visual core description was performed to identify possible important variations in the concrete quality of the bridge deck, and to provide information on the collected cores later used for the laboratory testing phase of the investigation. The results showed that the concrete quality was similar along the bridge deck, some cores showing important signs of corrosion deterioration while others being intact. The percentage of air voids was found to be equal to 7 %. Limestone was used as coarse aggregate with a maximum aggregate size of 40 mm. No particular characteristic likely to influence the development of the corrosion reaction was found by performing the various tests on the cores.

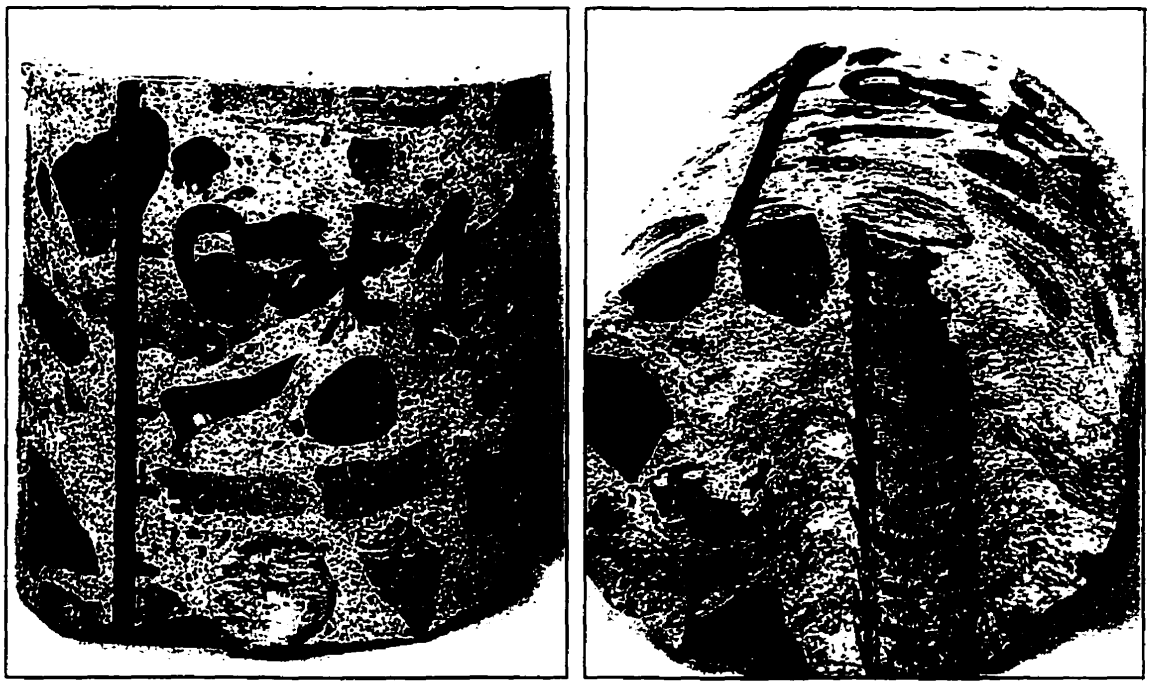

Figures 4.23 (left) and 4.24 (right) Pictures showing different angles of core sample 6SE-1 collected on the Dickson Bridge.

Table 4.6 Description of core sample 6SE-1 collected on the Dickson Bridge.

Identification		**Mineralogy (Agg.)**	
Site number	**6SE**	Aggregate type	**Fine : granitic sand**
Core number	**6SE-1**		**Coarse : limestone**
Date of description	**11/10/99**	Maximum size	**40 mm**
		Surface	**Angular**
Concrete proportions		Shape	**Angular**
Air voids (%)	**5**	Orientation of grains	**None**
Cement paste (%)	**40**		
Fine and coarse agg. (%)	**55**	**Steel reinforcement**	
		Position of bar(s)	**55 mm from top**
Comments :		Degree of corrosion	**Medium**
Cracked during removal		Delamination	**None**
of core			

4.4.8 Pulse velocity tests

The pulse velocity tests were performed :

- on cores collected at specific locations in the 35 areas (strips) selected for additional testing where the asphalt overlay was removed.

Pulse velocity of bridge deck surface

The results for the pulse velocity survey vary from a minimum of 2.9 km/s to a maximum of 4.2 km/s, with a mean value of 3.46 km/s and a coefficient of variation of 27.9 %. A total of 24 locations were tested. According to Table 4.5, 57 % of the readings are indicative of suspect concrete quality susceptible to an increased risk of corrosion development. The repeatability of the testing technique was established, according to the low variance of results for this test.

Figure 4.25 shows the three-dimensional surface obtained using the least-squares fitting method : the north direction of the Bridge, the level axis representing the length, the line axis representing the width, the locations tested, and the ranges of values used for the surface plot are also indicated. Figure 4.26 shows the two-dimensional curves obtained for the bridge deck as a plan view of Figure 4.25 : again the same information concerning the orientation of the bridge deck and the ranges of values used is presented. In Figure 4.25 and 4.26, it can be observed that the distribution of the results is hard to determine visually, and that the variations observed change locally. The highest readings are found on the west and east edges of the central section of the bridge. The results for the pulse velocity survey seem to contradict the results of most of the tests where the lowest concrete qualities and the higher risks of corrosion were found on the east and the west sides of the bridge. Again, these interpretations can be influenced by the surface contours obtained using the fitting method.

Apparent modulus of elasticity of bridge deck surface

The results for the apparent modulus of elasticity survey vary from a minimum of 10.8 GPa to a maximum of 21.4 GPa, with a mean value of 14.5 GPa and a coefficient of variation of 14.9 %. A total of 24 locations were tested. According to Table 4.5, 70 % of the readings are indicative of suspect concrete quality susceptible to increase the risk of corrosion development. The repeatability of the technique was not established and this needs to be considered in the analysis process : the results of this test do not correspond to the results for the modulus of elasticity determined after the compressive strength test.

Figure 4.27 shows the three-dimensional surface obtained using the least-squares fitting method : the north direction of the Bridge, the level axis representing the length, the line axis representing the width, the locations tested, and the ranges of values used for the surface plot are also indicated. Figure 4.28 shows the two-dimensional curves obtained for the bridge deck as a plan view of Figure 4.27 : again the same information concerning the orientation of the bridge deck and the ranges of values used is presented. In Figure 4.27 and 4.28, it can be observed that the distribution of the results is hard to determine visually, and that the variations observed change locally. The highest readings are found on the west and east sides of the central section of the bridge deck.

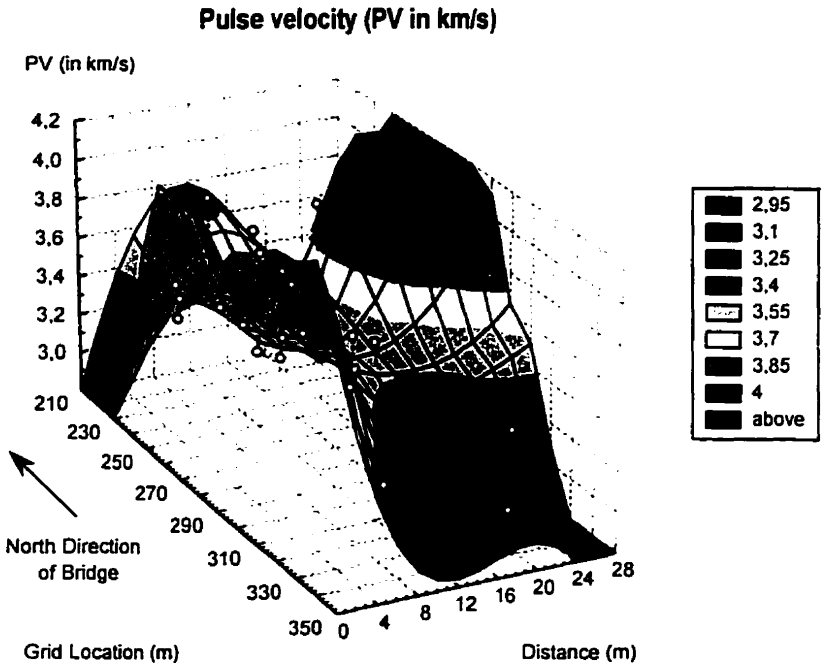

Figure 4.25 Three-dimensional view of pulse velocity tests of the bridge deck surface.

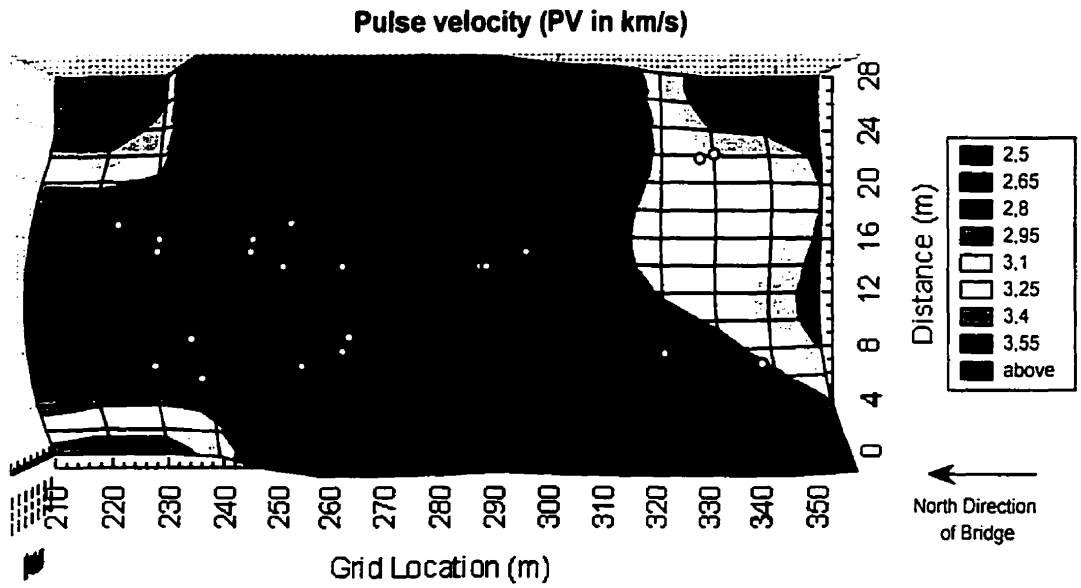

Figure 4.26 Plan view of pulse velocity tests of the bridge deck surface.

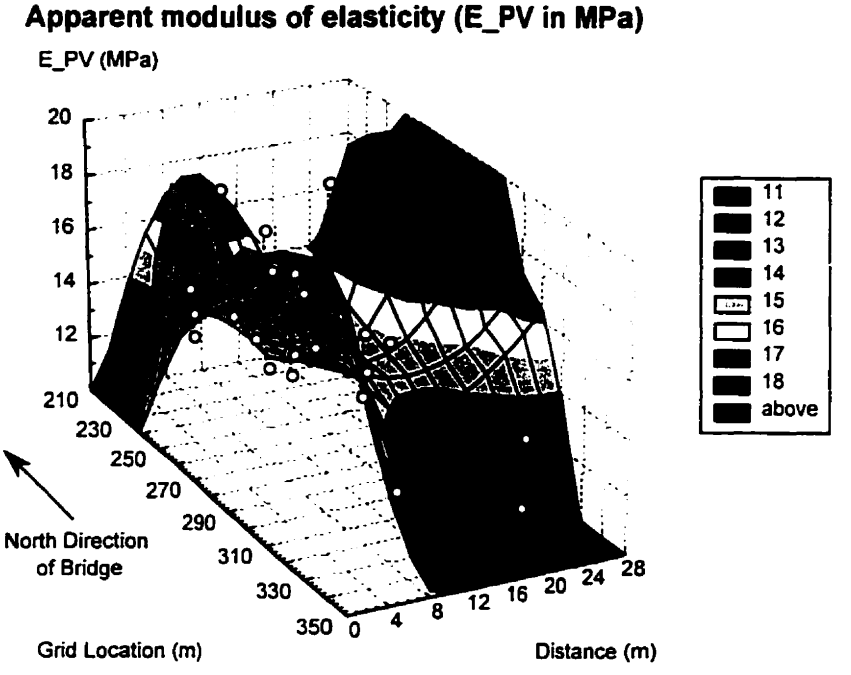

Figure 4.27 Three-dimensional view of apparent modulus of elasticity tests of the bridge deck surface.

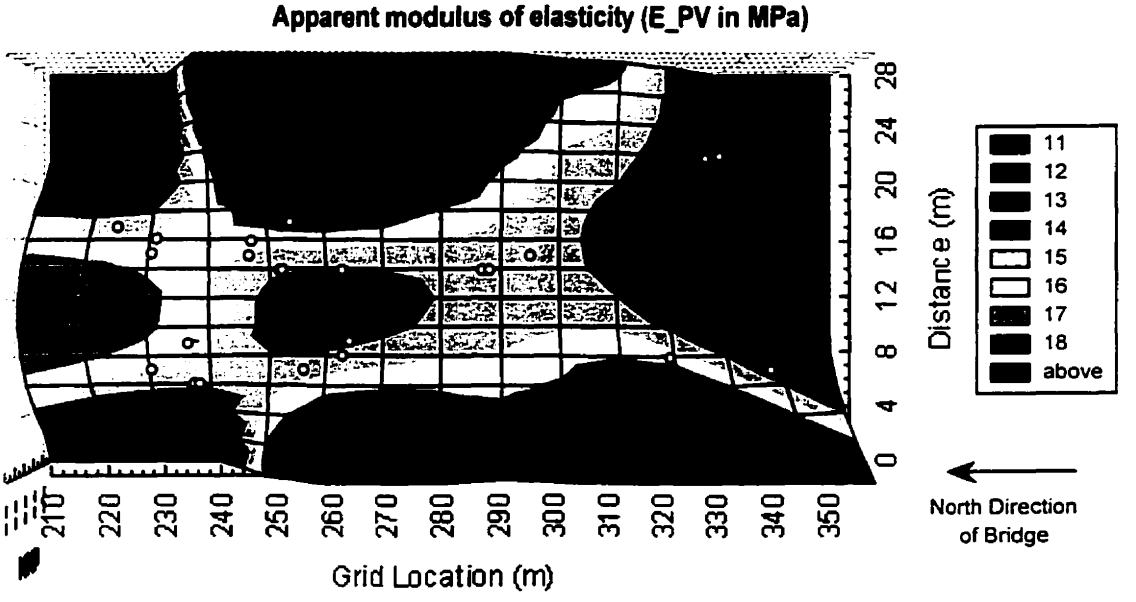

Figure 4.28 Plan view of apparent modulus of elasticity tests of the bridge deck surface.

4.4.9 Water absorptivity tests

The water absorptivity tests were performed :

- on cores collected at specific locations in the 35 areas (strips) selected for additional testing where the asphalt overlay was removed.

Absorptivity after immersion tests of bridge deck surface

The results for the absorptivity after immersion survey vary from a minimum of 4.86 % to a maximum of 7.92 %, with a mean value of 6.23 % and a coefficient of variation of 12.3 %. A total of 24 locations were tested. According to Table 4.5, 61% of the readings are indicative of adequate concrete quality susceptible to limit the risk of corrosion development.

Figure 4.29 shows the three-dimensional surface obtained using the least-squares fitting method : the north direction of the Bridge, the level axis representing the length, the line axis representing the width, the locations tested, and the ranges of values used for the surface plot are also indicated. Figure 4.30 shows the two-dimensional curves obtained for the bridge deck as a plan view of Figure 4.29 : again the same information concerning the orientation of the bridge deck and the ranges of values used is presented.

Dry density tests of bridge deck surface

The results for the dry density survey vary from a minimum of 1.58 g/cm^3 to a maximum of 1.73 g/cm^3, with a mean value of 1.63 g/cm^3 and a coefficient of variation of 1.7 %. A total of 24 locations were tested. According to Table 4.5, 87 % of the readings are indicative of suspect concrete quality susceptible to increase the risk of corrosion development.

Figure 4.31 shows the three-dimensional surface obtained using the least-squares fitting method : the north direction of the Bridge, the level axis representing the length, the line axis representing the width, the locations tested, and the ranges of values used for the surface plot are also indicated. Figure 4.32 shows the two-dimensional curves obtained for the bridge deck as a plan view of Figure 4.31 : again the same information concerning the orientation of the bridge deck and the ranges of values used is presented.

Saturated density tests of bridge deck surface

The results for the saturated density survey vary from a minimum of 1.75 g/cm^3 to a maximum of 1.95 g/cm^3, with a mean value of 1.81g/cm^3 and a coefficient of variation of 2.6 %. A total of 24 locations were tested. According to Table 4.5, 61 % of the readings are indicative of inadequate concrete quality susceptible to increase the risk of corrosion development.

Figure 4.33 shows the three-dimensional surface obtained using the least-squares fitting method : the north direction of the Bridge, the level axis representing the length, the line axis representing the width, the locations tested, and the ranges of values used for the surface plot are also indicated. Figure 4.34 shows the two-dimensional curves obtained for the bridge deck as a plan view of Figure 4.33 : again the same information concerning the orientation of the bridge deck and the ranges of values used is presented.

Volume of permeable voids tests of bridge deck surface

The results for the volume of permeable voids vary from a minimum of 7.86 % to a maximum of 12.87 %, with a mean value of 10.14 % and a coefficient of variation of 12.7 %. A total of 24 locations were tested. According to Table 4.5, 52 % of the readings are indicative of acceptable concrete quality susceptible to limit the risk of corrosion development.

Figure 4.35 shows the three-dimensional surface obtained using the least-squares fitting method : the north direction of the Bridge, the level axis representing the length, the line axis representing the width, the locations tested, and the ranges of values used for the surface plot are also indicated. Figure 4.36 shows the two-dimensional curves obtained for the bridge deck as a plan view of Figure 4.35 : again the same information concerning the orientation of the bridge deck and the ranges of values used is presented.

In Figures 4.29 to 4.36, it can be observed that the distribution of the results for all of the parameters described above is similar : the highest readings are found in both north and south sections, while the central section presents relatively constant values. Furthermore, the distribution of the results for the dry and saturated density tests are identical showing that these parameters are closely correlated or dependent.

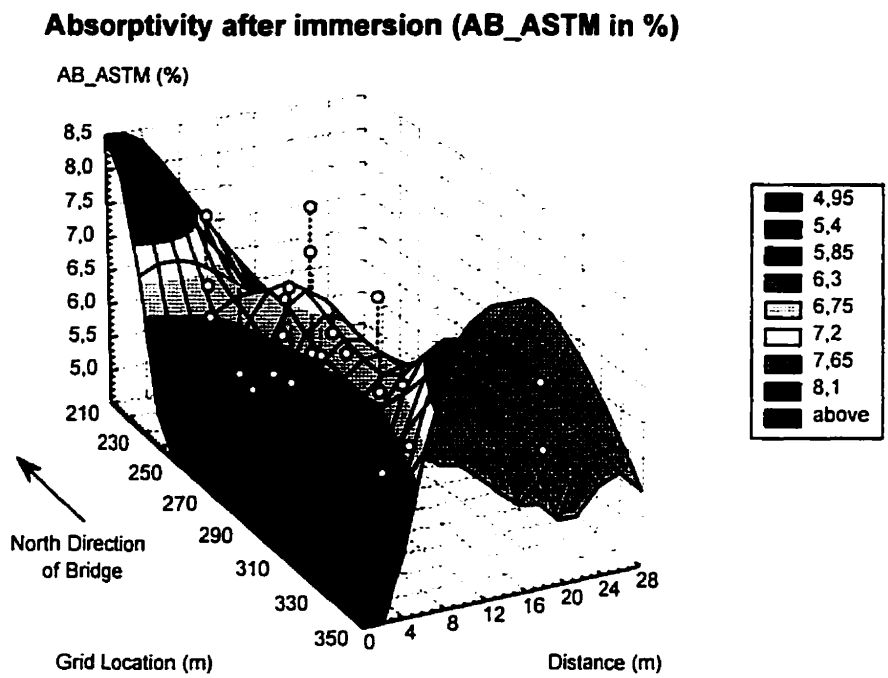

Figure 4.29 Three-dimensional view of absorptivity after immersion tests of the bridge deck surface.

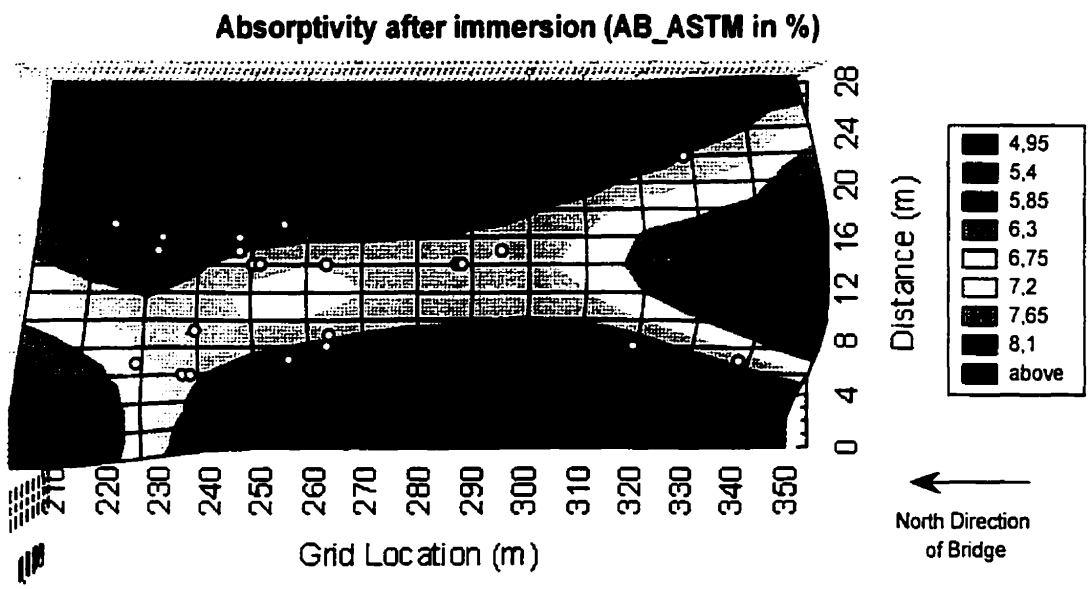

Figure 4.30 Plan view of absorptivity after immersion tests of the bridge deck surface.

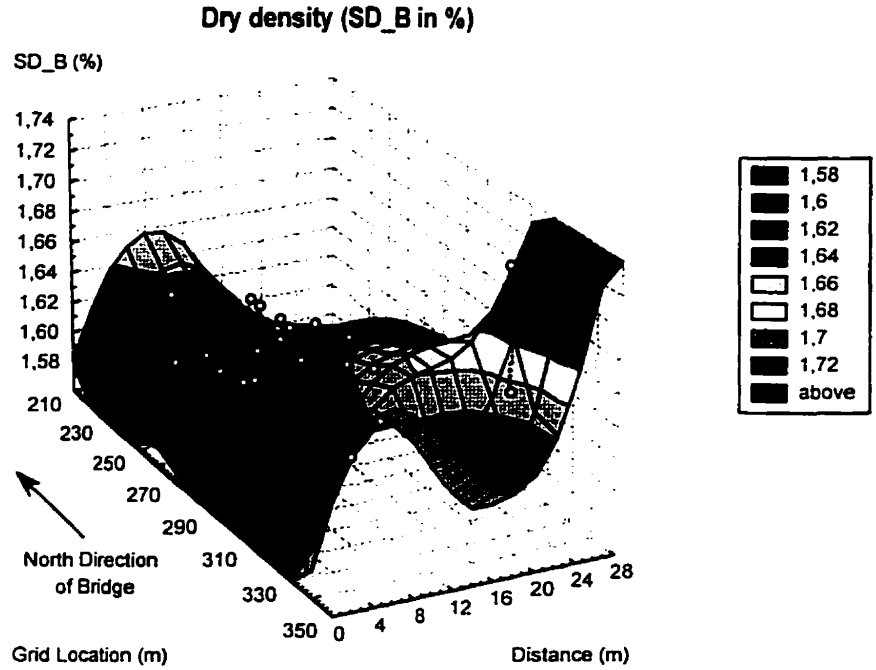

Figure 4.31 Three-dimensional view of dry density tests of the bridge deck surface.

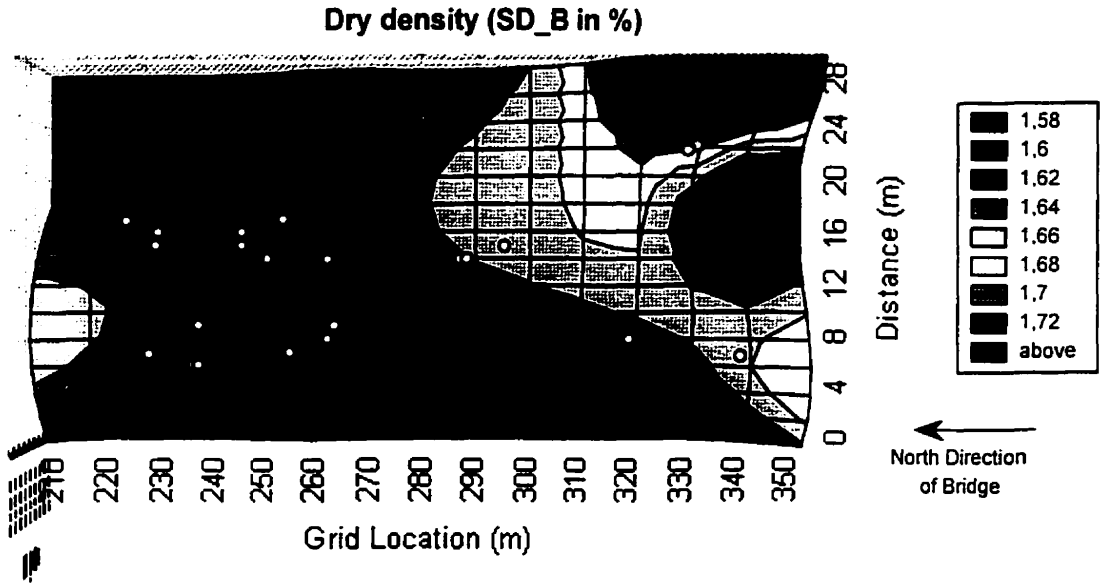

Figure 4.32 Plan view of dry density tests of the bridge deck surface.

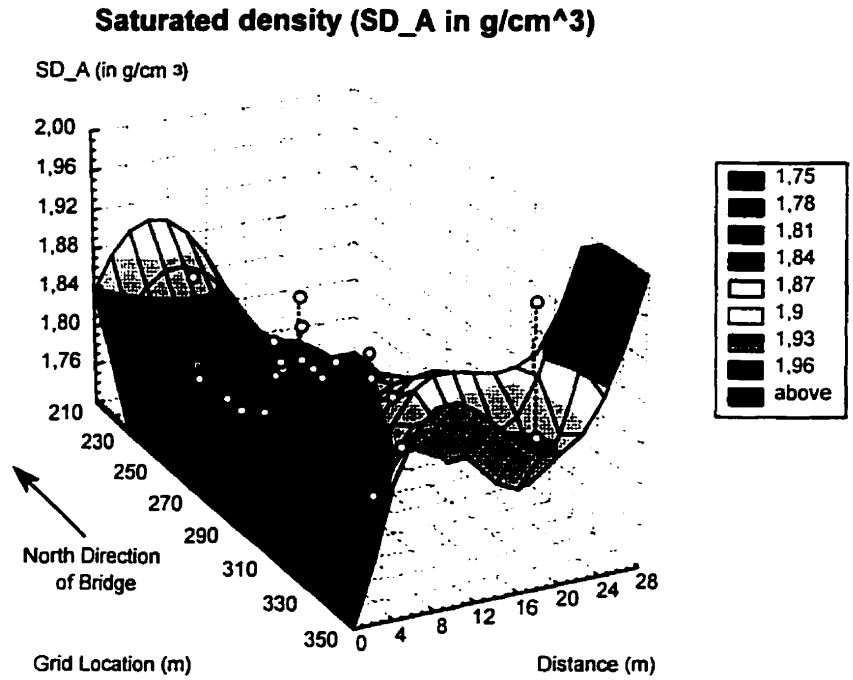

Figure 4.33 Three-dimensional view of saturated density tests of the bridge deck surface.

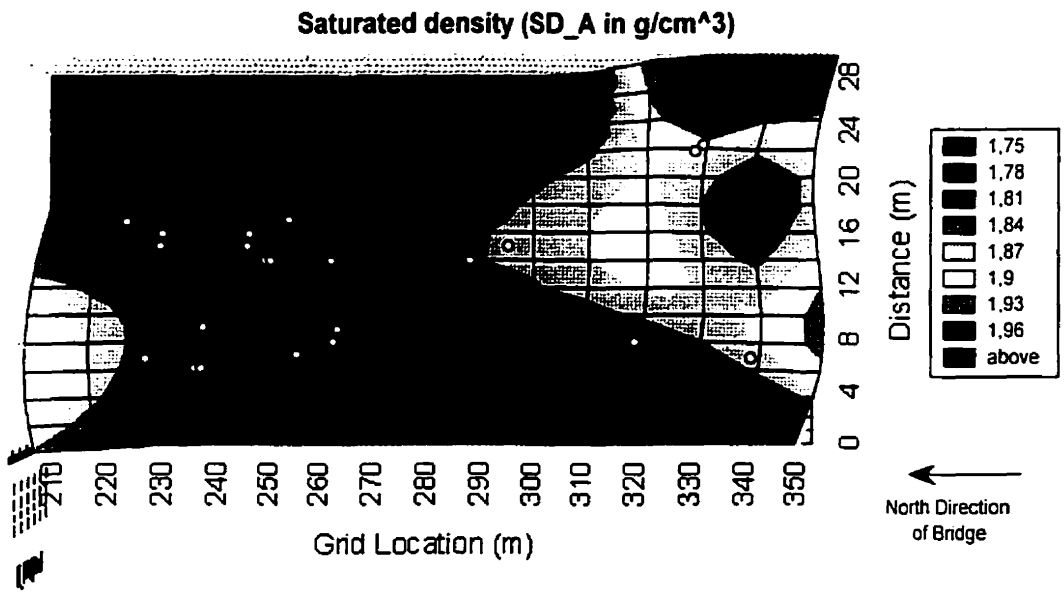

Figure 4.34 Plan view of saturated density tests of the bridge deck surface.

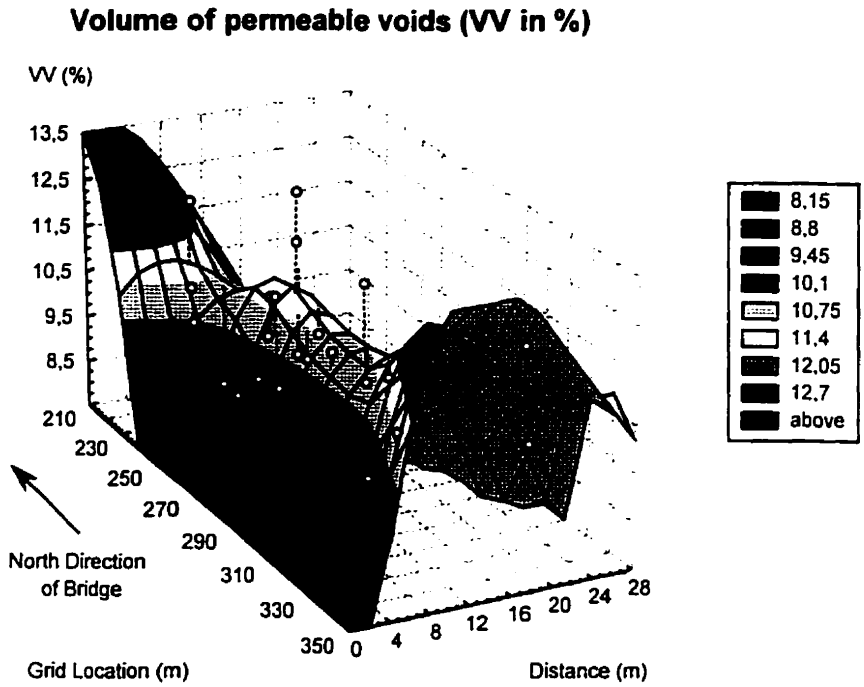

Figure 4.35 Three-dimensional view of volume of permeable voids tests of the bridge deck surface.

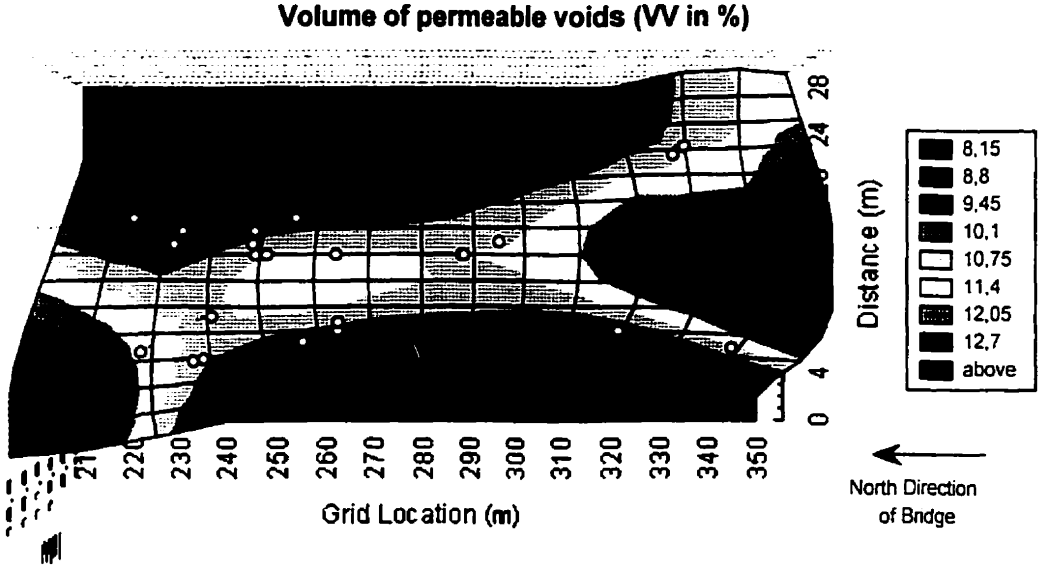

Figure 4.36 Plan view of volume of permeable voids tests of the bridge deck surface.

4.4.10 Compressive strength tests

The compressive strength tests were performed :

- on cores collected at specific locations in the 35 areas (strips) selected for additional testing where the asphalt overlay was removed.

Compressive strength tests of bridge deck surface

The results for the compressive strength survey vary from a minimum of 27 MPa to a maximum of 62 MPa, with a mean value of 48 MPa and a coefficient of variation of 15.9 %. A total of 24 locations were tested. According to Table 4.5, 87 % of the readings of the compressive strength are indicative of acceptable concrete quality susceptible to limit the risk of corrosion development.

Figure 4.37 shows the three-dimensional surface obtained using the least-squares fitting method : the north direction of the Bridge, the level axis representing the length, the line axis representing the width, the locations tested, and the ranges of values used for the surface plot are also indicated. Figure 4.38 shows the two-dimensional curves obtained for the bridge deck as a plan view of Figure 4.37 : again the same information concerning the orientation of the bridge deck and the ranges of values used is presented.

Modulus of elasticity tests of bridge deck surface

The results for the modulus of elasticity survey vary from a minimum of 4 GPa to a maximum of 9.7 GPa, with a mean value of 7.6 GPa and a coefficient of variation of 16.3 %. A total of 24 locations were tested. According to Table 4.5, 52 % of the readings are indicative of acceptable concrete quality susceptible to limit the risk of development of the corrosion reaction.

Figure 4.39 shows the three-dimensional surface obtained using the least-squares fitting method : the north direction of the Bridge, the level axis representing the length, the line axis representing the width, the locations tested, and the ranges of values used for the surface plot are also indicated. Figure 4.40 shows the two-dimensional curves obtained for the bridge deck as a plan view of Figure 4.39 : again the same information concerning the orientation of the bridge deck and the ranges of values used is presented.

In Figures 4.37 to 4.40, it can be observed that the distribution of the results for the compressive strength and the modulus of elasticity are identical but difficult to interpret visually, with the variations being randomly distributed. The average compressive strength is found to be relatively high for a deteriorated bridge.

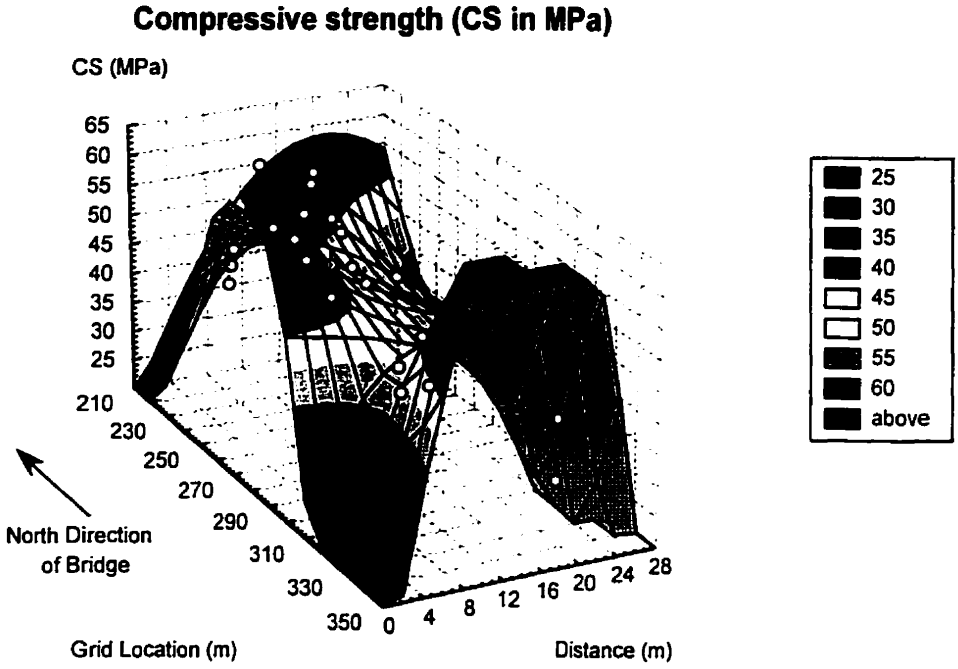

Figure 4.37 Three-dimensional view of compressive strength tests of the bridge deck surface.

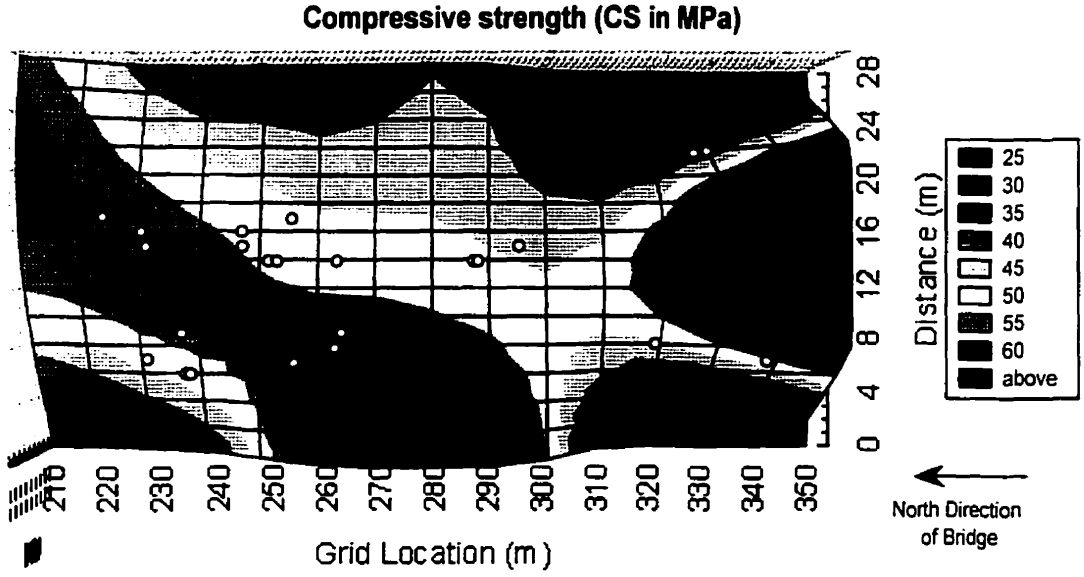

Figure 4.38 Plan view of compressive strength tests of the bridge deck surface.

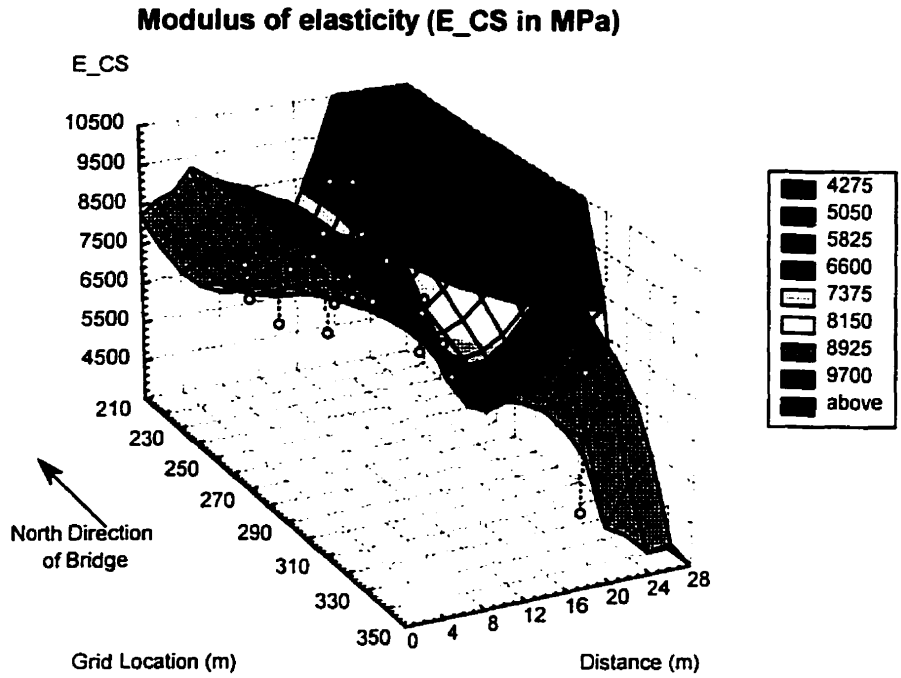

Figure 4.39 Three-dimensional view modulus of elasticity tests of the bridge deck surface.

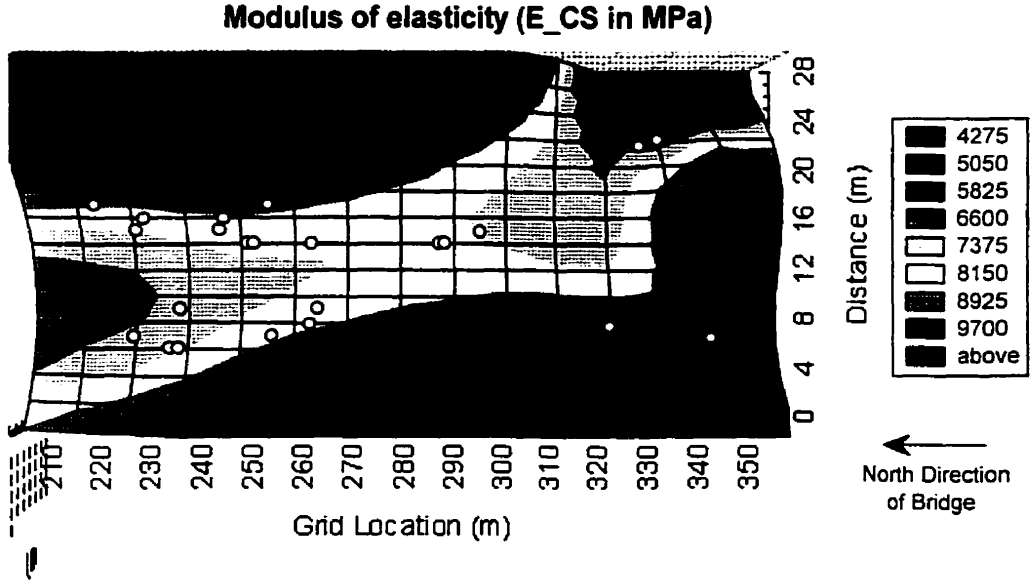

Figure 4.40 Plan view of modulus of elasticity tests of the bridge deck surface.

4.4.11 Carbonation depth tests

The carbonation depth tests were performed :

- on cores collected at specific locations in the 35 areas (strips) selected for additional testing where the asphalt overlay was removed.

Carbonation depth tests of bridge deck surface

The results for the carbonation depth survey indicate that the presence of carbonation was not detected on any of the specimens tested. A total of 24 locations were tested, and the depths of the carbonation front were all equal to zero. According to Table 4.5, 100 % of the readings are indicative of adequate concrete quality (with regards to carbonation) susceptible to limit the risk of corrosion development. The descriptive statistics are presented in Table 4.2.

Figure 4.41 shows the three-dimensional surface obtained using the least-squares fitting method : the north direction of the Bridge, the level axis representing the length, the line axis representing the width, the locations tested, and the ranges of values used for the surface plot are also indicated. Figure 4.42 shows the two-dimensional curves obtained for the bridge deck as a plan view of Figure 4.41 : again the same information concerning the orientation of the bridge deck and the ranges of values used is presented. In Figure 4.41 and 4.42, the distribution of the results can be observed. The findings indicate that the carbonation process is not responsible for the depassivation of the steel reinforcement which led to the development of corrosion of the reinforcing steel.

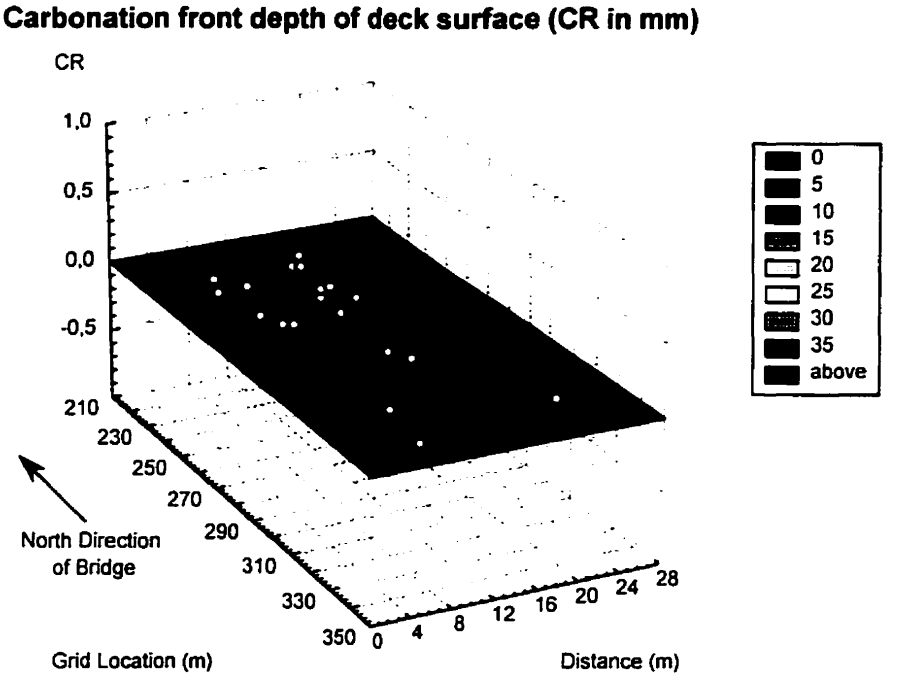

Figure 4.41 Three-dimensional view of carbonation depth tests of the bridge deck surface.

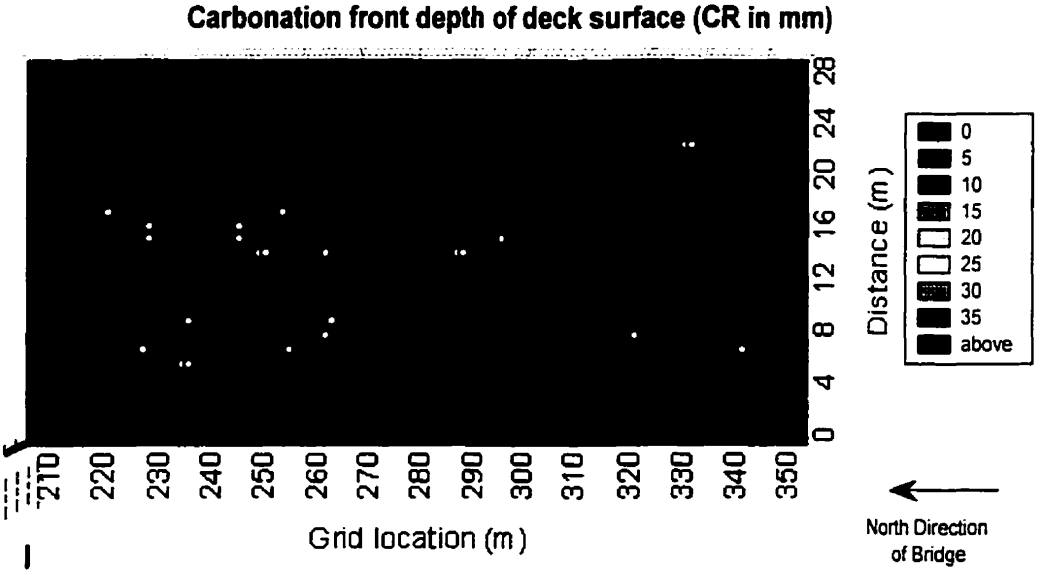

Figure 4.42 Plan view of carbonation depth tests of the bridge deck surface.

4.4.12 Chloride ion concentration at rebar and chloride diffusion apparent coefficient tests

The chloride ion concentration at rebar and chloride diffusion apparent coefficient tests were performed :

- on cores collected at specific locations in the 35 areas (strips) selected for additional testing where the asphalt overlay was removed.

Chloride ion concentration at rebar tests of bridge deck surface

The results for the chloride ion concentration at rebar survey vary from a minimum of 0.026 % concrete weight to a maximum of 0.62 %, with a mean value of 0.22 % concrete weight and a coefficient of variation of 76.7 %. A total of 24 locations were tested. According to Table 4.5, 87 % of the readings are indicative of adequate or acceptable concrete quality susceptible to limit the risk of corrosion development.

Figure 4.43 shows the three-dimensional surface obtained using the least-squares fitting method : the north direction of the Bridge, the level axis representing the length, the line axis representing the width, the locations tested, and the ranges of values used for the surface plot are also indicated. Figure 4.44 shows the two-dimensional curves obtained for the bridge deck as a plan view of Figure 4.43 : again the same information concerning the orientation of the bridge deck and the ranges of values used is presented. In Figure 4.43 and 4.44, it can be observed that the highest readings were obtained at or near the south and north edges of the bridge deck.

Apparent chloride diffusion tests of bridge deck surface

The results for the chloride diffusion apparent coefficient survey vary from a minimum of 5.53×10^{-9} cm²/s to a maximum of 2.74×10^{-6} cm²/s, with a mean value of 1.70×10^{-7} cm²/s and a very large coefficient of variation of 326.4 %. A total of 24

locations were tested. According to Table 4.5, 52 % of the readings indicate that the concrete quality is inadequate to limit the risk of corrosion development. The large variability observed for the results of the apparent chloride diffusion tests can be related to the variability of the in-situ technique that needs to be further develop, and to the variation in the quality of the tested concrete on the bridge.

Figure 4.45 shows the three-dimensional surface obtained using the least-squares fitting method : the north direction of the Bridge, the level axis representing the length, the line axis representing the width, the locations tested, and the ranges of values used for the surface plot are also indicated. Figure 4.46 shows the two-dimensional curves obtained for the bridge deck as a plan view of Figure 4.45 : again the same information concerning the orientation of the bridge deck and the ranges of values used is presented. In Figure 4.45 and 4.46, it can be observed that the highest readings were obtained at or near the north edge of the bridge deck.

Chloride ion concentration profiles of the bridge deck surface

The chloride ion profiles are presented in Figure 4.47 and 4.48 for the cores collected on the west and east portions of the bridge deck. It can be seen in these figures that the chloride ion concentrations decrease from the surface of the deck to the core for almost all 24 tested cores. These results are indicative of the presence of large quantities of chlorides in the south section of the bridge. The profiles also indicate that the chlorides have penetrated the concrete matrix from the surface, thus proving that the source of chlorides is external. The use of large quantities of de-icing chemicals during the winter is thought to be principal source of chlorides. A threshold value of 0.1 % of concrete weight was plot on the graphs to show that most cores exhibit higher chloride concentrations at rebar level than the threshold value. The risk criteria indicated a low risk of corrosion while the chlorides are found to be responsible for the depassivation of the steel reinforcement leading to the development of corrosion. They are found to be inadequate.

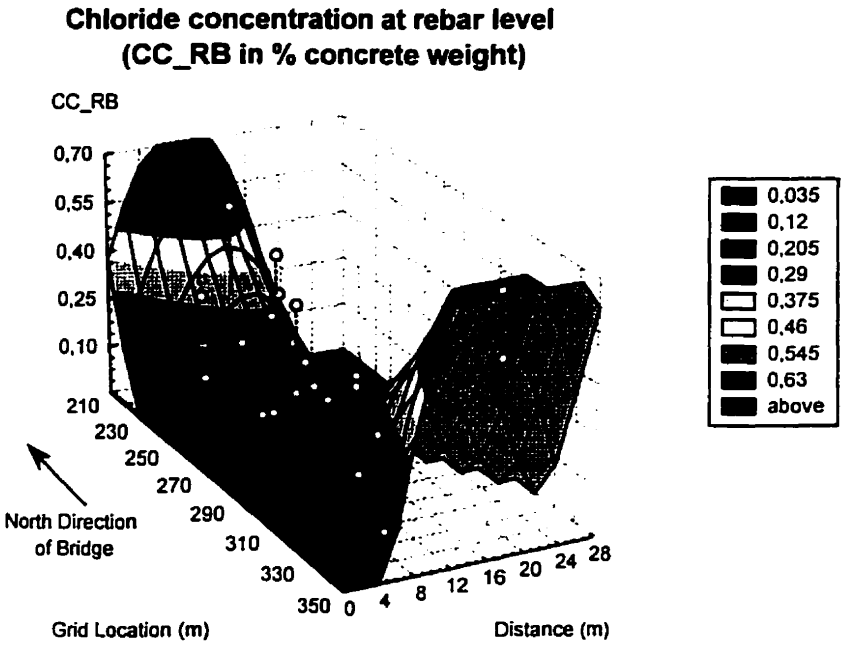

Figure 4.43 Three-dimensional view of chloride ion concentration at rebar tests of the bridge deck surface.

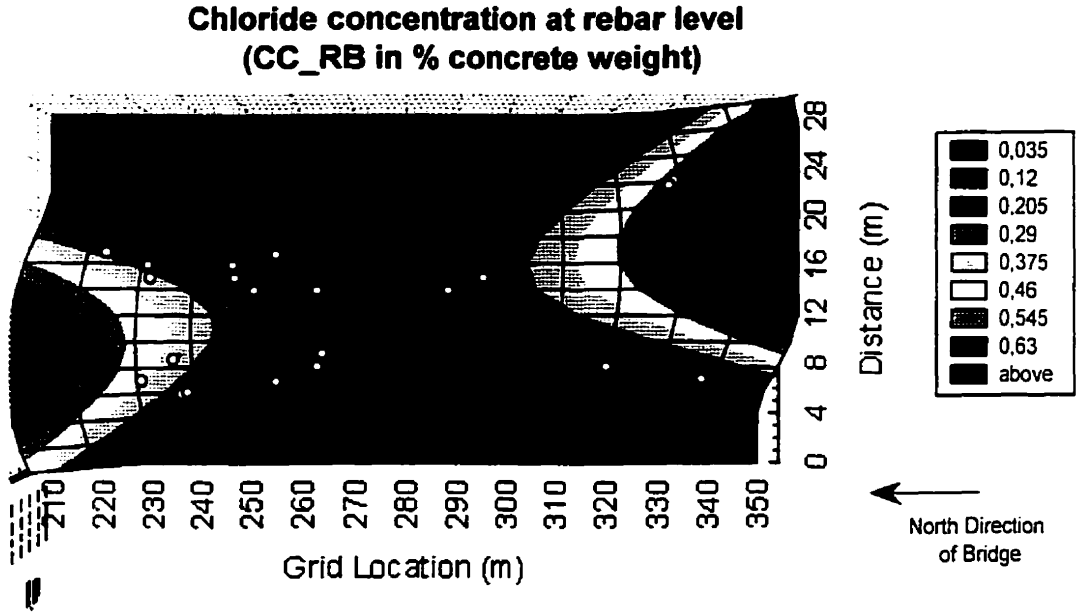

Figure 4.44 Plan view of chloride ion concentration at rebar tests of the bridge deck surface.

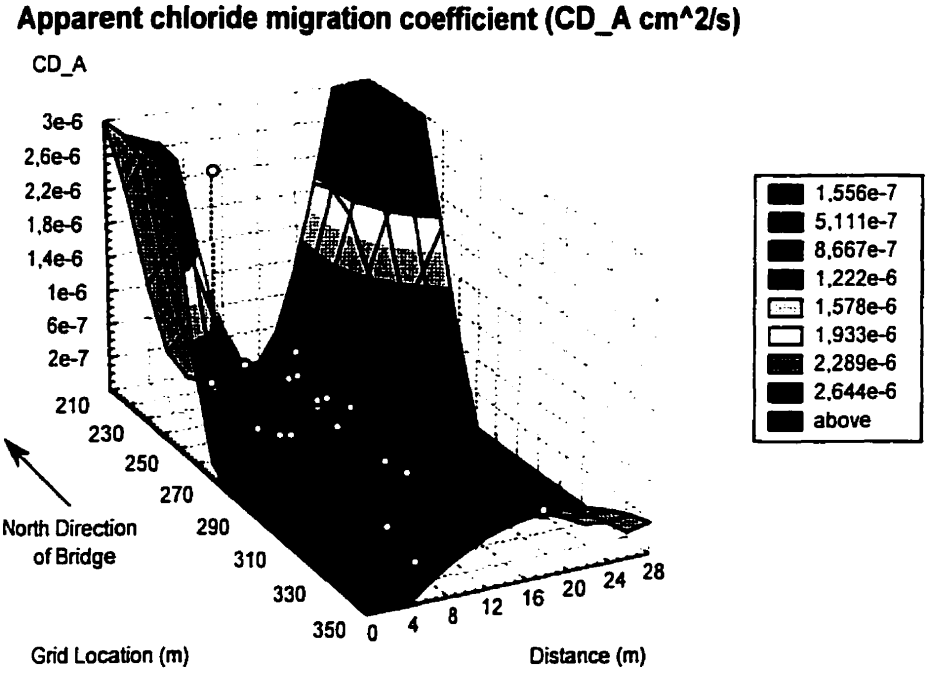

Figure 4.45 Three-dimensional view of apparent chloride diffusion coefficient tests of the bridge deck surface.

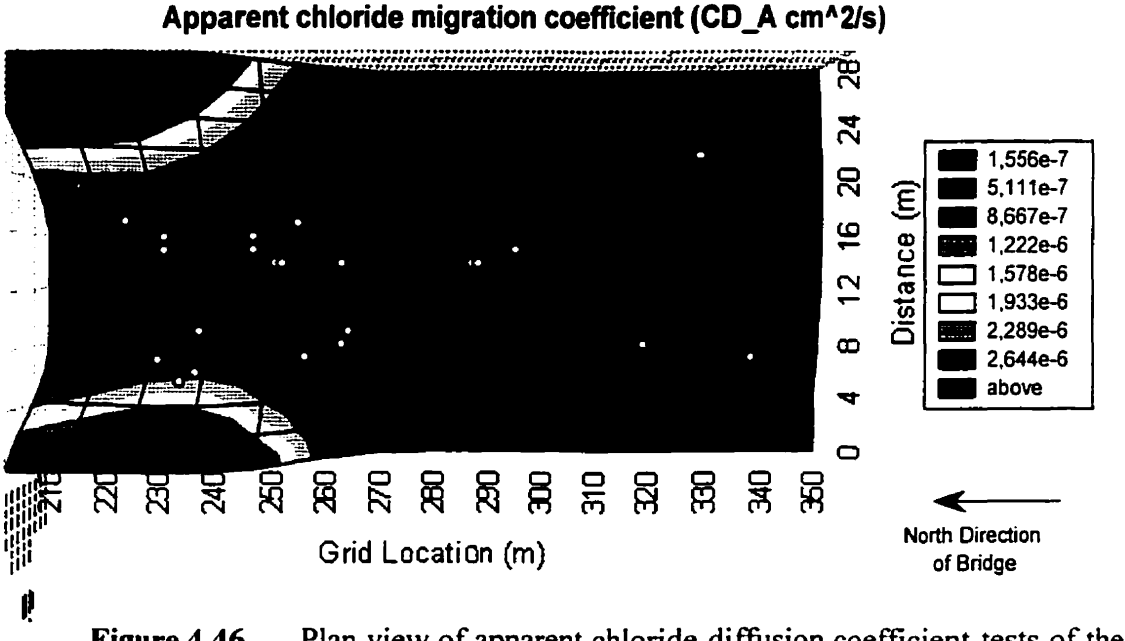

Figure 4.46 Plan view of apparent chloride diffusion coefficient tests of the bridge deck surface.

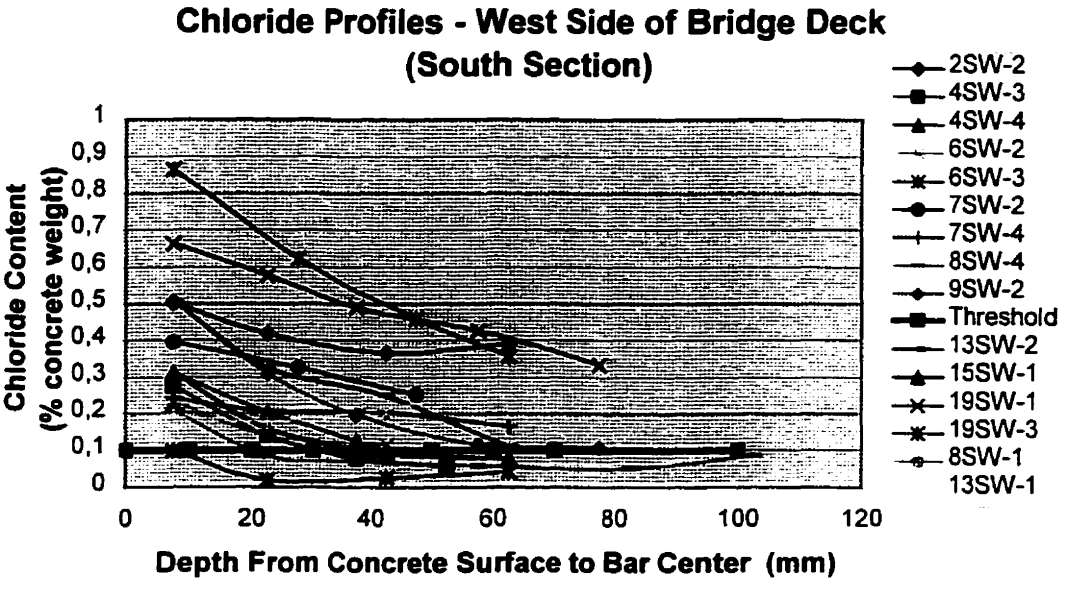

Figure 4.47 Chloride ion concentration profiles for the west side of the south section of the Dickson Bridge.

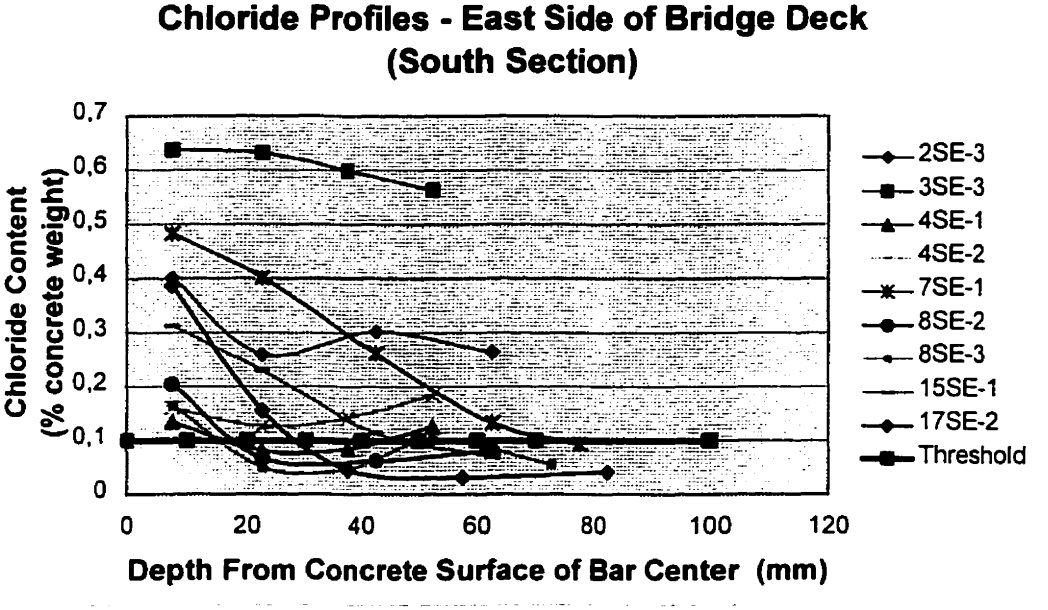

Figure 4.48 Chloride ion concentration profiles for the west side of the south section of the Dickson Bridge.

4.5 Assessment of the state-of-health of bridge

It is important to mention that the assessment of the condition of the bridge deck is performed by considering uniquely the results obtained from the selected testing techniques. Since no verification of the real damage to the steel reinforcement was performed, the assessment of the state-of-health of the bridge is entirely based on the findings from the interpretation of the different test results. Now, with regards to the condition of the deck of the south section of the bridge, the following comments can be formulated :

- From the interpretation of all parameters measured during testing of the south section of the Dickson Bridge, it can be stated that the bridge deck is showing a critical risk of corrosion development of the reinforcing steel : the half-cell potential and the corrosion potential measurements indicate a high likelihood of corrosion development for most of the surface of the bridge upper and lower reinforcement meshes. In addition, the corrosion rate measurements are indicative of high corrosion activity for most of the bridge deck area.
- The results from the carbonation depth and the chloride concentration at rebar measurements show that the depassivation of the top layer of the reinforcing steel would have been caused by the ingress of chloride ions from external source(s). The areas of high chloride content generally coincide with the location of significant corrosion damage.
- It is found that the north and south ends of the bridge deck are in the most critical conditions. It is possible that the largest quantities of de-icing chemicals were used on the top portion of the bridge (north end) and on the steepest portions of the bridge. The lack of drainage can also have influenced the distribution of chlorides along the bridge : as the snow would melt and percolate downwards to the bottom end, a large quantity of chlorides would accumulate at that point and penetrate the concrete. The use of an asphalt overlay over the concrete slab is also susceptible to have

trapped chloride containing solutions and facilitated the ingress of chlorides in the concrete.

- However, the results for the compressive strength test seem to contradict the results obtained from most tests : the average compressive strength is found to be relatively high, while the north and south end present the highest values. This can be explained by the bias of the core collection : fractured and delaminated cores extracted from the bridge deck could not be tested and would probably have indicated a lower concrete quality. Also, it can be seen that the results from the compressive strength test should be analyzed with care when estimating the durability of concrete structures.
- After analysis of the results for the concrete cover survey, it appears that there has been a general short fall in the compliance with the design specifications. The alignment of the top reinforcement mesh was found to be neither straight or regular (repetitive). For large portions of the bridge deck, the concrete cover was found thicker than the original specified value of 25 mm. Considering that most of the concrete cover was damaged during the asphalt removal, it can be seen that the design specifications were either changed or not respected. The results from the concrete cover survey contradict other tests : thick concrete covers correspond with highly corroding areas. This can be explained by the influence of the concrete quality on the other parameters instead of the overall thickness. Once the concrete cover has cracked, the ingress of the aggressive elements and the risk of corrosion development are increased, independently of the thickness of the cover.
- The results for the water permeability and the chloride diffusion coefficients give the impression that the quality of the concrete is adequate to prevent the ingress of deleterious agents. However, since it was observed that the results for these tests correlated with those of the half-cell potential and corrosion rate tests, which indicated that most of the bridge deck is in a critical condition with regards to corrosion. Therefore, the

criteria used to interpret the results of the water permeability and chloride diffusion migration tests seem inadequate, and should be verified further.

- Finally, the results for the pulse velocity and water absorptivity tests do not correspond to the results obtained for the half-cell and the corrosion rate. These results provide additional information on different properties of concrete not necessarily of high importance with regards to the corrosion reaction.
- After comparison of the results for the north, central and south sections of the bridge in Table 4.3, it appears that the results obtained are similar, with variabilities of the different parameters measured in the same ranges.
- The number of readings obtained for some tests is relatively low compared to the dimensions of the bridge. Also, the repeatability of some methods was not established and could influence the results obtained and their interpretation.
- With the exception of the apparent modulus of elasticity measurement, for which the results cannot be compared with the modulus of elasticity, all tests provide valuable information on the state-of-health of the structure. The general trends were previously identified in this chapter and the interrelations between the measured parameters need to be confirmed in the statistical analysis are presented in Chapter Five.

5. Statistical analysis of results

5.1 Introduction

The results of the statistical analysis of the different parameters for the south section of the Dickson Bridge are presented in Chapter Five. Since the quantity of information collected on the bridge is limited, a statistical analysis is performed to verify the assumptions made during the analysis of the south section of the bridge and to validate the interpretations made in Chapter Four. The statistical analysis of variables needs to be performed rigorously and carefully. The desired outcomes of the analysis of the south section of the Dickson Bridge are :

- Identification of the most influencing variables (parameters) measured on the bridge with regards to the corrosion process of steel reinforcement;
- Identification of the theoretical relationships existing between the most influencing parameters on the chloride-induced corrosion of the reinforcing steel;
- Determination of existing correlations between all variables investigated during the test program on the south section of the bridge;
- Verification of the hypotheses formulated concerning the theoretical relationships between parameters using statistical relationships;
- Development of a statistical model estimating the corrosion process of the reinforcing steel using the rate of corrosion as the dependent variable and some of the most influencing variables (parameters) as independent variables;
- Comparison of the statistical model obtained for the south section of the Dickson Bridge to similar models obtained from the analysis of the north and central sections.

The scheme of the overall multivariate analysis is presented in Figure 5.1. The different parameters measured are described in the Chapter Four, and can be divided

into two categories : (1) prediction methods assessing the quality of the concrete and (2) assessment methods measuring the extent of the corrosion-induced damage to the steel reinforcement.

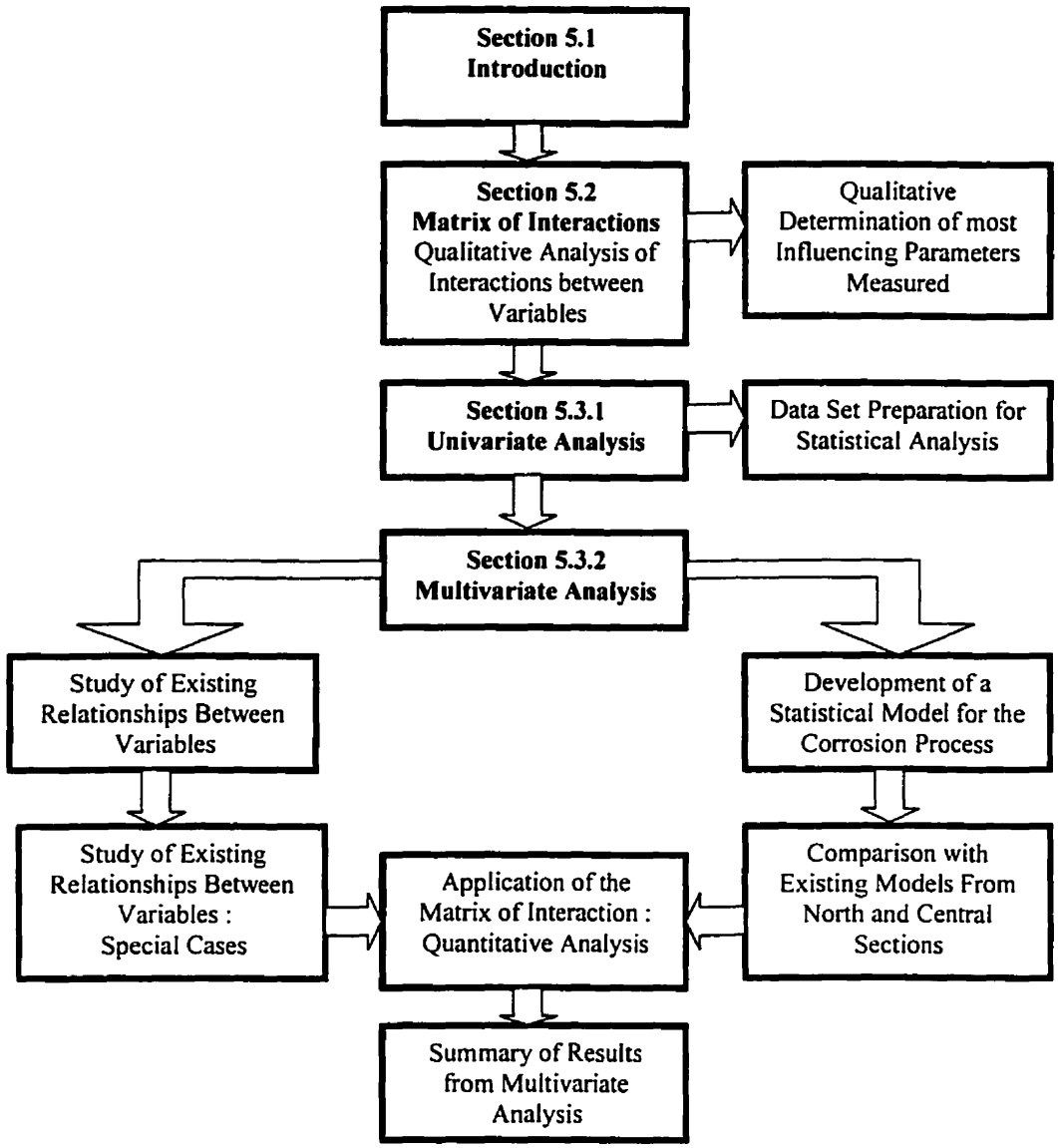

Figure 5.1 Scheme for multivariate analysis of south section of Dickson Bridge.

5.2 Identification of theoretical relationships between parameters

In Chapter Three, various techniques used to define the quality of the concrete and the extent of damage to the steel reinforcement were introduced. Chapter Four presented the descriptive statistics of the results obtained from the different tests. In Chapter Five, a statistical analysis of the data collected is performed based on two approaches: (1) the typical statistical analysis using computer packages; and (2) the matrix of interaction method. The latter method was found appropriate to identify and evaluate the most influencing parameters of the system under investigation and is presented in this chapter.

5.2.1 Matrix of interaction

First developed for mining and geological engineering applications, the matrix of interaction method can be use to characterize relationships between components defining a system. In addition, the method offers the possibility to assess, for a system that can be divided into a series of influencing components, both the effect of a given component on the global system and the effect of the system on a particular component. The application of this method to the analysis of deteriorated reinforced concrete systems is considered to be of valuable interest. In the following sections, some concepts relative to the matrix of interaction method are reviewed. The application of the method to the analysis of the corroded deck of the Dickson Bridge follows in the next section.

General theory

The matrix of interaction method offers the possibility to represent the different possible interactions between components of a particular system. The matrix format offers the possibility to use the same presentation and analytical procedures for any

circumstances, or project[28]. The universality of such a method offers great potential for the investigation of deteriorating reinforced concrete structures by allowing for the assessment of interactions between the expected influencing parameters.

The basic method consists of : (1) identification of parameters susceptible to influence the deterioration of a particular structure, (2) placing these parameters along the leading diagonal of a square matrix (from top left to bottom right), and (3) determination of the interactions between the items of the leading diagonal as follows : the influence of Parameter 1 on Parameter 2 corresponds to the off-diagonal entry of the matrix of coordinate (1,2).

The resolution of the matrix, or the number of leading diagonal items, can be adjusted by subdividing (or by grouping) the initial parameters under study into a number of various characteristics, resulting in a deeper (or coarser) analysis of the mechanisms involved[28]. As a result, by linking two parameters at a time, the multivariate analysis of a system is made possible. Figure 5.2 illustrates the possible application of the interaction matrix for the investigation of deteriorating reinforced concrete structures. It is worth mentioning that the matrix of interaction is in most cases assymetric, as a consequence of the following principle : the way in which Parameter A influences Parameter B is not necessarily the same as the way in which Parameter B influences Parameter A. For example, with reference to Figure 5.2, the influence of the concrete quality (A) on the damage of the reinforcing steel (B) can be seen as the ability of the concrete to facilitate the ingress of gases, water and chlorides susceptible to break the passivity of the steel reinforcement and thus provoke the formation of rust products, whereas the influence of the damage of the reinforcing steel (B) on the concrete quality (A) can be expressed as the augmentation of the water permeability due to cracking of the concrete by the formation of rusts products (damage).

A Concrete Quality	Influence of A on B	Influence of A on C	Influence of A on D	Influence of A on E
Influence of B on A	B Damage to Steel Reinforcement	Influence of B on C	Influence of B on D	Influence of B on E
Influence of C on A	Influence of C on B	C Environmental Exposure	Influence of C on D	Influence of C on E
Influence of D on A	Influence of D on B	Influence of D on C	D Structural Design	Influence of D on E
Influence of E on A	Influence of E on B	Influence of E on C	Influence of E on D	E Construction and Maintenance

Figure 5.2 Application of the interaction matrix for deteriorating reinforced concrete structures.

A possible limitation of this method is when a large number of leading diagonal terms are considered in the analysis, increasing significantly the number of interaction terms produced and the complexity of interpretation. As a requirement of this method, it must be ensured that the interaction matrix will be able to deal comprehensively with any circumstances[28]. Therefore, the level of complexity considered in the application of the method must be considered with care : for a matrix with N leading diagonal terms, there will be N × (N-1) interaction terms. Also, the matrix resolution (or number of leading diagonal entries) should include the inner field, the outer field and the far field items related to a particular system or project[28]. In other words, the analysis of a particular system (project) should consider the contribution of different aspects, some significant and others less significant (far field) in order to adequately represent the complete system (or project). Figure 5.3 illustrates the concept of matrix resolution.

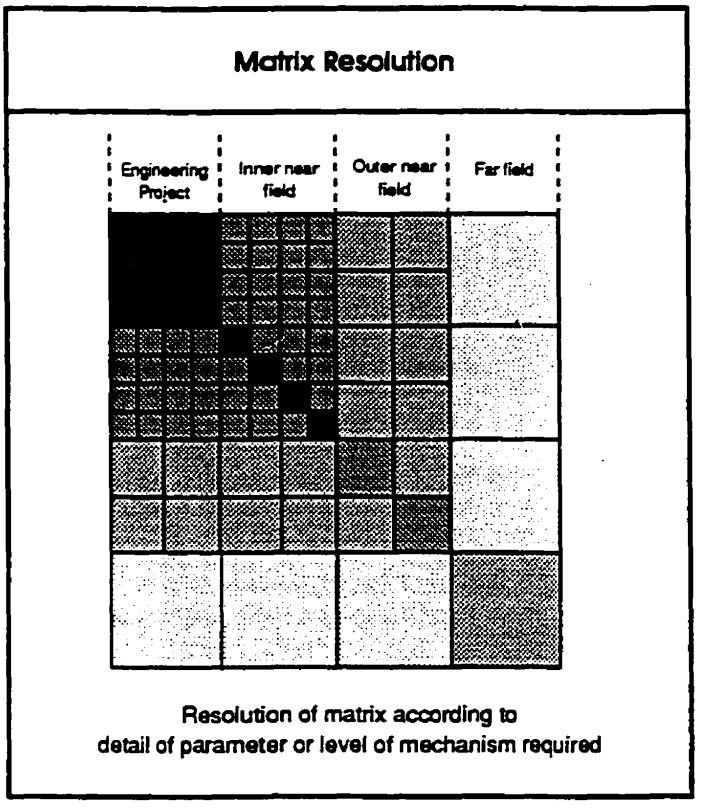

Figure 5.3 The matrix resolution can be matched to the level of the analysis, being finest for the project and coarser farther away[28].

One of the advantages of this method is that the leading diagonal terms do not need to be quantitative values, even if the use of quantitative values allows for the introduction of standard evaluation procedures[28]. Another advantage of the method is that it offers the possibility to determine the interactions between the input parameters in a qualitative way, thus improving the comprehension of a particular system through the analysis of its components. Since some properties or characteristics can be difficult to measure, their influence could still be assessed qualitatively, or based on knowledge or experience[28].

At a later stage, a quantitative evaluation can also be performed by assigning numerical values to the interaction terms of the matrix, a process called matrix

coding. Different matrix coding methods can be used, the most important being listed below[28] :

- Binary method: the interaction terms are switched on or off, taking the corresponding values of 0 or 1;
- Expert semi-quantitative method (ESQ) : an extension of the binary method that offers more sensibility with the consideration of five levels of interaction instead of two; the value of the interaction terms vary from 0 (no interaction) to 5 (critical interaction);
- Correlation method : the interaction terms are determined based on the coefficient of correlation calculated between two variables (valid only if the relationships between the variables are linear);
- Partial differential equations method : numerical models are used to obtain numerical solutions for the assessment of the interaction terms;
- Complete numerical analysis method : the complete numerical analysis of parameters lead to the assessment of the interaction terms.

For the investigation of the south section of the Dickson Bridge, the general interaction matrix presented in Figure 5.2 can be refined by subdividing the different main factors into a series of different parameters measured during the testing phase of the project. As a result, the prediction methods can be used to evaluate the concrete quality, while the assessment methods can similarly serve to evaluate the damage to the steel reinforcement. Furthermore, some characteristics defining the environmental exposure, structural design, and construction can be included in the matrix. Since no tests were performed to measure these properties, their influence can only be evaluated qualitatively. However, the consideration of these external factors into the statistical analysis is beyond the scope of this thesis. Nevertheless, further testing in that domain could eventually lead to the quantification of these parameters.

The matrix of interaction will be used in this chapter to define the various mechanisms affecting the premature deterioration of reinforced concrete structures with regards to chloride-induced corrosion. The use of the matrix format to represent the different influencing factors affecting the durability of structures is at an early stage and could eventually be developed further when additional statistical information and testing techniques become available.

5.2.2 Elements of matrix of interaction

The parameters considered in the matrix of interaction are grouped into categories (fields) and placed along the leading diagonal. The selection of relevant parameters to form the interaction matrix should consider the scope of the analysis, degree of resolution wanted (completeness of analysis), and availability of testing techniques. The initial choice of parameter could later be modified based on the results of the analysis.

Once the leading diagonal parameters are selected, a review of expected theoretical interactions between all parameters is performed. The existence of particular relationships between parameters helps in further describing the mechanism of action of the system under study. It is possible that a parameter influences a number of parameters (or all) in the same way, as in most cases there exists no distinct relationships between inner field and far field parameters. For example, the water permeability and the chloride diffusion of concrete (inner field parameters) are influenced identically by the drainage system selected (far field parameter) for a particular system.

Description of elements of the matrix of interaction

The elements of the matrix of interaction for the analysis of the south section of the Dickson Bridge are presented in this section. Since the number of parameters considered for the analysis is large, it would be too long to review all of the

interaction terms. However, the main parameters are listed, and as an example, the expected theoretical relationships relative to the first parameter (chloride diffusion [migration] of concrete) are reviewed in Table 5.1.

Leading diagonal terms (P_i)

A) Concrete quality (P_1 to P_9)

- [P_1] In-situ chloride diffusion (migration) coefficient;
- [P_2] In-situ water permeability coefficient;
- [P_3] Electrical resistivity;
- [P_4] Pulse velocity;
- [P_5] Absorption after immersion;
- [P_6] Dry density;
- [P_7] Volume of permeable voids;
- [P_8] Compressive strength;
- [P_9] Modulus of elasticity.

B) Damage to the steel reinforcement (P_{10} to P_{15})

- [P_{10}] Half-cell potential;
- [P_{11}] Concrete cover thickness;
- [P_{12}] Corrosion rate;
- [P_{13}] Depth of carbonation front;
- [P_{14}] Concentration of chloride ions at rebar;
- [P_{15}] Chloride diffusion (apparent) coefficient.

C) Environmental exposure (P_{16} to P_{20})

- [P_{16}] Mean annual quantity of de-icing agent used;

- $[P_{17}]$ Average concentration of carbon dioxide (CO_2) in atmosphere;
- $[P_{18}]$ Mean annual amount of precipitation;
- $[P_{19}]$ Mean annual temperature;
- $[P_{20}]$ Annual number of freeze-thaw cycles.

D) Structural design (P_{21} to P_{25})

- $[P_{21}]$ Adequacy of the drainage system;
- $[P_{22}]$ Adequacy of the concrete cover thickness.

E) Construction and maintenance (P_{23})

- $[P_{23}]$ Quality of the placement, compaction and curing of concrete.

Parameter interaction terms ($I_{i,i}$) for the in-situ chloride diffusion (migration) coefficient

Table 5.1 Influence of the in-situ chloride diffusion (migration) coefficient and other parameters.

Influence of $[P_1]$in-situ chloride diffusion (migration) coefficient on others :
A) Concrete quality
$[P_2] \rightarrow [I_{1,2}]$ In-situ water permeability coefficient of concrete : since the ingress of chloride ions weakly affects the concrete permeability to water, a small interaction between the two coefficients should be observed. $[P_3] \rightarrow [I_{1,3}]$ Electrical resistivity of concrete : as more chloride ions penetrate the concrete, the total ion content of the material increases thus increasing the electrical conductivity, and reducing the resistivity significantly. $[P_4] \rightarrow [I_{1,4}]$ Pulse velocity of concrete : the quantity of chloride ions present in the concrete do not significantly affect the pulse velocity measurements, unless a large quantity of ions deposit at the pore surfaces to decrease the air void content. $[P_5] \rightarrow [I_{1,5}]$ Absorption after immersion : the chloride ions present can limit the access to water molecules, generally at the micropore level, affecting the water absorption of concrete. However, the relatively small quantity of chloride ions present in the concrete is found to be insignificant.

Table 5.1 (Continued) Influence of the in-situ chloride diffusion (migration) coefficient and other parameters.

$[P_6] \rightarrow [I_{1,6}]$ Dry density : the relatively small quantity of chloride ions present in the concrete (up to 0.6 % by weight) is found to be insignificant in affecting the total mass of concrete.
$[P_7] \rightarrow [I_{1,7}]$ Volume of permeable pore space (voids) : insignificant, unless a large quantity of ions deposit at the pore surfaces to decrease their volume.
$[P_8] \rightarrow [I_{1,8}]$ Compressive strength : insignificant relationship, the quantity of ions present being insufficient to modify the quality of the concrete by itself.
$[P_9] \rightarrow [I_{1,9}]$ Modulus of elasticity : same as $[I_{1,8}]$

B) Damage to steel reinforcement (P_{10} to P_{15})

$[P_{10}] \rightarrow [I_{1,10}]$ Half-cell potential : since the presence of a greater quantity of chloride ions intensifies the corrosion reaction by depassivating the steel. the corrosion potential should also increase significantly.
$[P_{11}] \rightarrow [I_{1,11}]$ Concrete cover thickness : no direct effect on the concrete cover should be observed.
$[P_{12}] \rightarrow [I_{1,12}]$ Corrosion rate : a strong influence should be observed as the presence of chloride ions initiates and accelerates most modes of the corrosion process.
$[P_{13}] \rightarrow [I_{1,13}]$ Depth of the carbonation front : a small influence should be observed since the quantity of ions present can limit the ingress of carbon dioxide in the concrete by blocking the pore channels.
$[P_{14}] \rightarrow [I_{1,14}]$ Concentration in chloride ions at rebar : this parameter should be strongly influenced, as the diffusion process is the transport mechanism of importance for chlorides in concrete.
$[P_{15}] \rightarrow [I_{1,15}]$ Apparent chloride diffusion coefficient : a strong influence should be observed, as the apparent coefficient is a measure of the same quantity in the laboratory.

C) Environmental exposure (P_{16} to P_{20})

$[P_{16}] \rightarrow [I_{1,16}]$ Overall quantity of de-icing agent used : insignificant.
$[P_{17}] \rightarrow [I_{1,17}]$ Concentration of carbon dioxide CO_2 in atmosphere : insignificant.
$[P_{18}] \rightarrow [I_{1,18}]$ Annual amount of precipitation : insignificant.
$[P_{19}] \rightarrow [I_{1,19}]$ Mean annual temperature : insignificant.
$[P_{20}] \rightarrow [I_{1,20}]$ Number of freeze-thaw cycle : insignificant.

D) Structural design (P_{21} to P_{25})

$[P_{21}] \rightarrow [I_{1,21}]$ Adequacy of the drainage system : insignificant.
$[P_{22}] \rightarrow [I_{1,22}]$ Adequacy of the concrete cover thickness : insignificant.

Table 5.1 (Continued) Influence of the in-situ chloride diffusion (migration) coefficient and other parameters.

E) Construction and maintenance (P_{23})
$[P_{23}] \rightarrow [I_{1,23}]$ Quality of the construction : insignificant.

It can be seen from Table 5.1 that the review of all parameter interactions is a long and tedious operation, especially when many parameters are included in the analysis. The complete review of parameter interactions is beyond the scope of this thesis and will not be performed. However, the matrix of interaction including all of the 23 parameters described previously is presented in Figure 5.4 (using a simplified terminology). Figure 5.5 shows the same matrix after the matrix coding was performed using the expert semi-quantitative method (ESQ) with four degrees of influence : a strong interaction between the parameters would be assigned a value of 3; a moderate interaction would be assigned a value of 2, while low and no interaction would be assigned values of 1 and 0, respectively. It can be seen that the matrix is not symmetric, and that the entries of the leading diagonal have been set to zero : the off-diagonal terms representing the different interactions existing between parameters.

This first attempt to perform the matrix coding is based purely on the expected theoretical relationships. At a later stage, numerical relationships (correlations) between variables determined through statistical analysis of the results from the south section of the Dickson Bridge will be used to verify the findings of this first analysis.

5.2.3 Interpretation of matrix of interaction

Once the matrix coding has been performed, it is possible to quantify the significance of a parameter by using two measures of the parameter interaction : the intensity and the dominance. This method allows for the determination of the parameters that exert

a greater influence on the system, and similarly, the identification of components of the system having the most effect on a particular parameter[28].

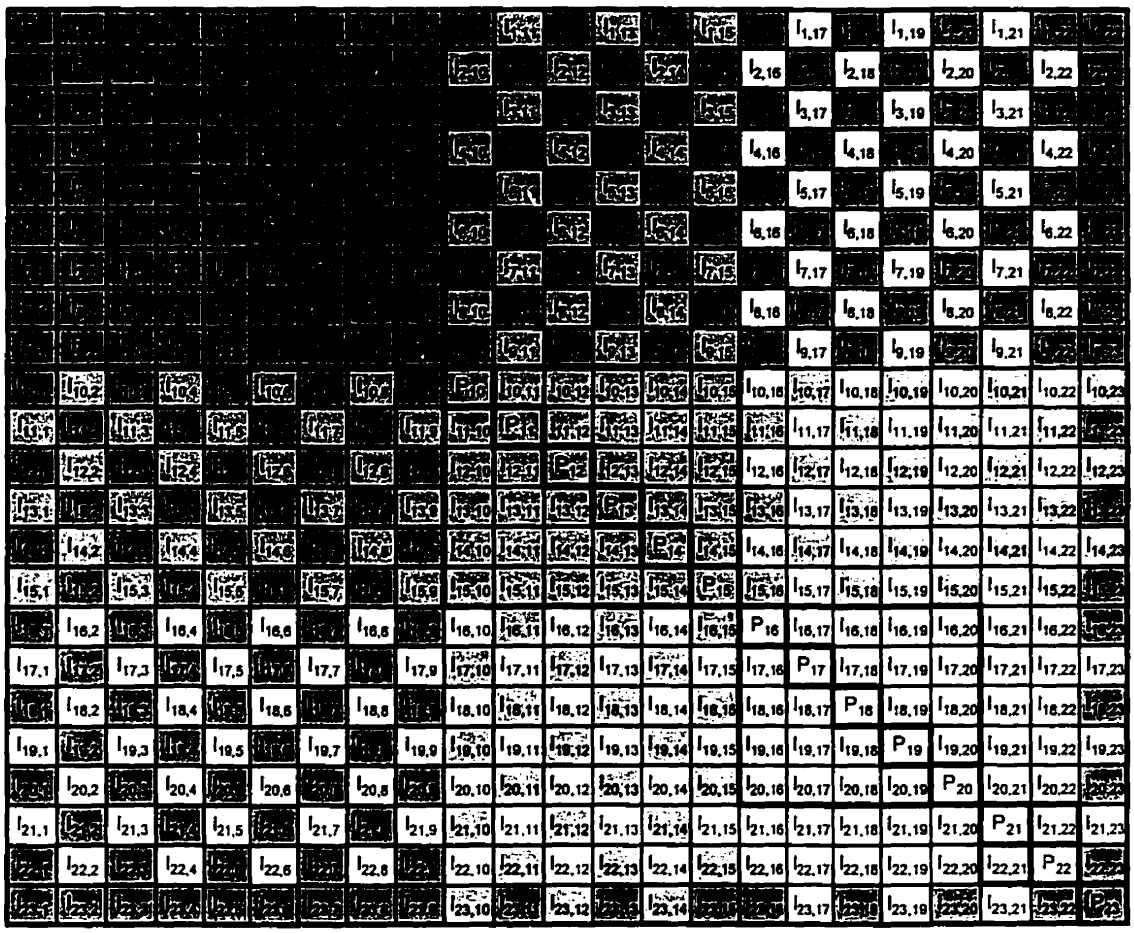

Figure 5.4 Proposed matrix of interaction for the south section of the Dickson Bridge.

The interaction matrix can be interpreted in terms of causes and effects for the different main parameters (P_i) listed along the leading diagonal. It can be seen that the row passing through any one main parameter P_i represents the influence of that parameter on all other parameters of the system[28]. In the same way, the column passing through P_i represents the influence of the remaining parameters describing the influence of the system on P_i.

The influence of a given parameter P_i on the system is termed the cause, C, and is determined by performing the summation of all the influence factors of the row corresponding to that parameter[28]. The influence of the rest of the system on P_i is termed the effect, E, and is again determined by performing the summation of all the influence factors within the corresponding column[28]. Using these two coefficients, each parameter can be assigned a coordinate (C, E)[28].

For the Dickson Bridge interaction matrix, the matrix coding was performed using the expert semi-qualitative method for four degrees of influence, with influence factors varying between 0 and 3. As mentioned previously, it can be observed in Figure 5.5 that the entries of the leading diagonal were set to zero : this is based on the assumption that a parameter is not influencing itself. As a result, the maximum value that C or E can take is equal to the value associated with the highest degree of influence multiplied by the number of parameters of the matrix ignoring the parameter under study, or (I max) × (N-1). The minimum value that can take C or E is zero, and would correspond to a parameter neither exerting any influence on the system (all other parameters) nor it is influenced by the system.

Using the coordinates (C,E) obtained for all parameters, the different components of the system can be plotted in the cause vs. effect space. Figure 5.6 presents the cause vs. effect plot of the parameters of the interaction matrix for the Dickson Bridge.

The position of the points in the cause vs. effect space indicates the mode of interaction of each parameter[28]. The most interactive parameters will have high (C+E) values, while the most dominant parameters will have high (C-E) values. Conversely, low (C+E) values will be associated to the less interactive parameters, while low (C-E) values will be associated with the subordinate parameters. The comparison of the parameters together using (C-E) and (C+E) coefficients is made possible by normalizing the (C+E) and (C-E) values with respect to the maximum value possible. This is achieved by dividing the values by the square root of two.

Table 5.2 shows the coefficients obtained for the parameters considered for the Dickson Bridge.

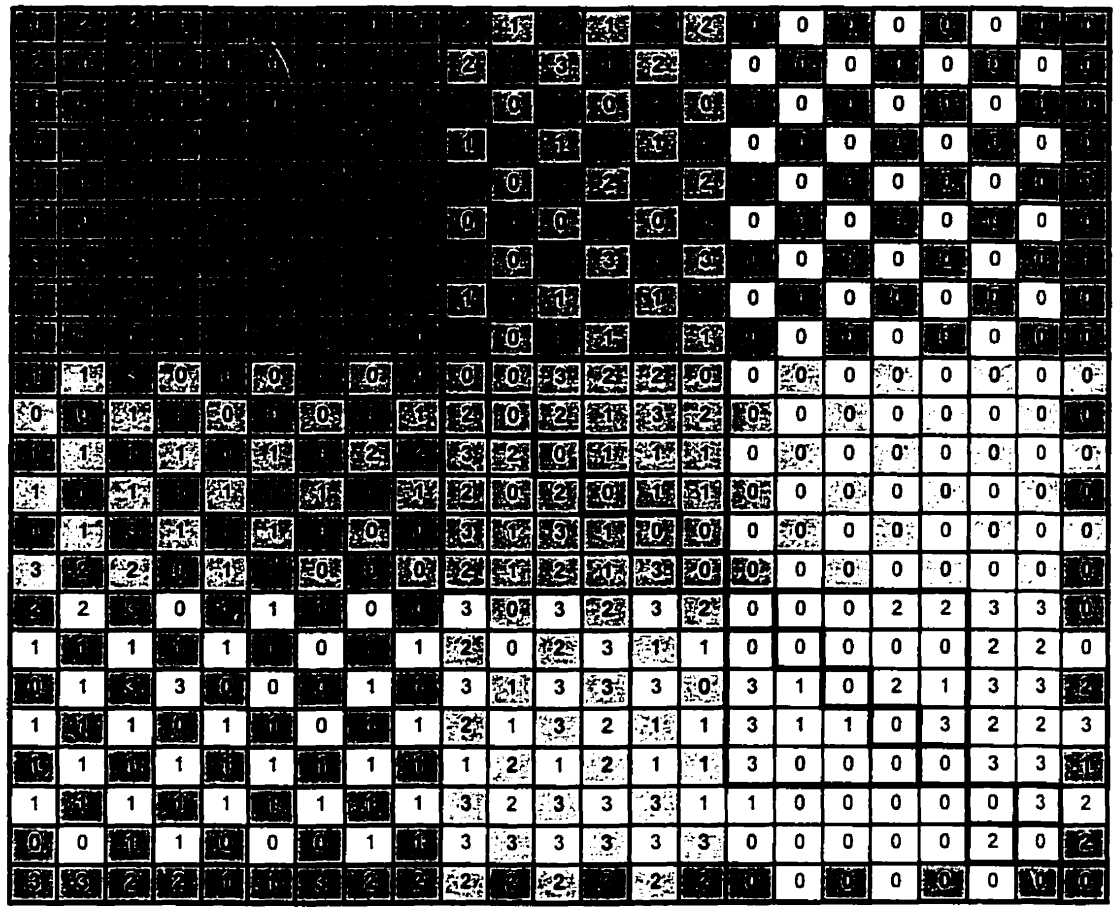

Figure 5.5 Coding of matrix of interaction for the Dickson Bridge using the expert semi-quantitative method with four degrees of influence (between 0 and 3).

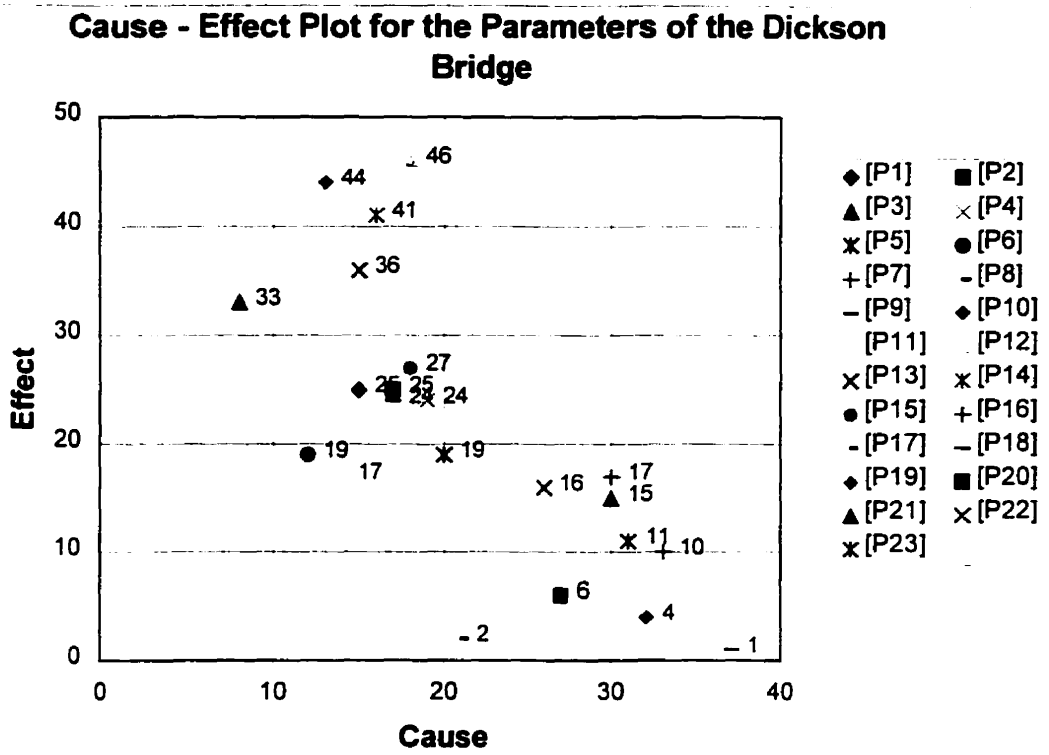

Figure 5.6 Cause vs. effect of the main parameters of the matrix of interaction of the Dickson Bridge.

Table 5.2 Coefficients of interaction and dominance obtained for the parameters considered in the Dickson Bridge.

Parameter	C Value	E Value	C+E Value	C-E Value	$(C+E)/\sqrt{(2)}$ Value	$(C-E)/\sqrt{(2)}$ Value
$[P_1]$: CD_m	15	25	40	-10	28	-7
$[P_2]$: WP	17	25	42	-8	30	-6
$[P_3]$: ER	8	33	41	-25	29	-18
$[P_4]$: PV	19	24	43	-5	30	-4
$[P_5]$: AB_astm	20	19	39	1	28	1
$[P_6]$: SD_b	12	19	31	-7	22	-5
$[P_7]$: VV	30	17	47	13	33	9
$[P_8]$: CS	17	24	41	-7	29	-5
$[P_9]$: E_cs	17	24	41	-7	29	-5
$[P_{10}]$: HC	13	44	57	-31	40	-22
$[P_{11}]$: CV	14	17	31	-3	22	-2

Table 5.2 Coefficients of interaction and dominance obtained for the parameters considered in the Dickson Bridge (continued).

Parameter	C Value	E Value	C+E Value	C-E Value	(C+E)/√(2) Value	(C-E)/√(2) Value
[P_{12}] : LP_cr	18	46	64	-28	45	-20
[P_{13}] : CR	15	36	51	-21	36	-15
[P_{14}] : CC_rebar	16	41	57	-25	40	-18
[P_{15}] : CD_m	18	27	45	-9	32	-6
[P_{16}]	33	10	43	23	30	16
[P_{17}]	21	2	23	19	16	13
[P_{18}]	37	1	38	36	27	25
[P_{19}]	32	4	36	28	25	20
[P_{20}]	27	6	33	21	23	15
[P_{21}]	30	15	45	15	32	11
[P_{22}]	26	16	42	10	30	7
[P_{23}]	31	11	42	20	30	14

5.2.4 Qualitative analysis using the matrix of interaction

The mathematics of the generation of cause vs. effect plots are straightforward, and it can be seen that the procedure allows for the selection of the most adequate parameters (or testing techniques) for a particular analysis[28]. Also, the same procedure will be later used to verify the results obtain at this point, when sufficient information becomes available to numerically quantify the parameter interactions using the statistical correlations between variables. This will be done in Section 5.3, from the results of the investigation of the south section of the bridge. However, at this point, it is possible to interpret the results obtained using the expert semi-quantitative coding method presented in Table 5.3.

The most interactive parameters were identified as :

1) Corrosion rate (LP_cr);
2) Half-cell potential (HC) and chloride concentration at rebar level (CC_rb);

3) Carbonation depth (CR);
4) Volume of permeable voids (VV);
5) Chloride diffusion (migration) coefficient (CD_m) and the adequacy of the drainage system ($P_{[21]}$).

Since the corrosion rate is the only direct measurement of the corrosion activity from all parameters, it is normal that it is the most interactive component of a system describing the deterioration due to corrosion. It is also observed that the influences of the half-cell potential and chloride concentration at rebar are important. Finally, it is found that the volume of permeable pore space (voids), chloride diffusion (migration) coefficient, and adequacy of the drainage influence greatly the corrosion process of reinforcing steel. From this qualitative analysis, it can be observed that the compressive strength does not influence the system significantly.

Also, the most dominant parameters are found to be :

1) Quantity of precipitation : $P_{[18]}$;
2) Temperature : $P_{[19]}$;
3) Quantity of de-icing chemicals : $P_{[16]}$;
4) Number of freeze-thaw cycles : $P_{[20]}$;
5) Quality of the construction : $P_{[23]}$.

It can be seen that none of the parameters describing either the concrete quality or the damage to the reinforcing steel figure as the most dominant parameters. On the other hand, the outer and far field parameters cannot be influenced by the inner field parameters and account for all of the dominant parameters. Again, the results from the qualitative analysis are consistent. The validity of these interpretations is limited to the quality of the assessment of the influence factors. As mentioned previously, the verification of these interpretations is made possible by quantitatively assessing the influence factors statistically. This is performed in the next section using the data collected through testing of the south section of the Dickson Bridge.

Table 5.3 Most important coefficients of interaction and dominance.

Most interactive parameters	**Most dominant parameters**
1) LP_cr	1) $P_{[18]}$ Quantity of precipitation
2) HC and CC_rb	2) $P_{[19]}$ Temperature
3) CR	3) $P_{[16]}$ Quantity of De-icing chemicals
4) VV	4) $P_{[20]}$ Number of freeze-thaw cycles
5) CD_M and $P_{[21]}$ (Drainage system)	5) $P_{[23]}$ Quality of the construction
Less interactive parameters	**Most subordinate parameters**
1) $P_{[17]}$ Concentration in CO_2	1) HC
2) CV	2) LP_cr
3) SD_b	3) CC_rb
4) $P_{[20]}$ Number of freeze-thaw cycles	4) ER
5) $P_{[19]}$ Mean annual temperature	5) CR

5.3 Statistical analysis of results

The results for all parameters were examined individually in Chapter Four : the descriptive statistics were presented and the collected results were plotted in the three-dimensional space to allow for rapid interpretation.

The testing survey of the Dickson Bridge produced a large quantity of information that could lead to the formulation of valuable interpretations if the information is adequately treated. This section presents the statistical analysis of the data set generated by the investigation of the south section of the bridge. Some desired outcomes of the statistical analysis can be formulated as follows :

- The quantification of relationships between measured parameters (variables);
- The identification of highly correlated test techniques allowing for the calibration of different techniques together; this is especially important for new techniques for which no standards exist;
- The identification of the most appropriate techniques (most contributive) to quantify the corrosion process;

However, before undertaking the statistical analysis, a number of numerical verifications need to be performed on the initial data set (as-collected). These essential verifications are made to determine (1) the type of statistical distribution estimating the actual variable distributions and (2) some important quantities quantifying these statistical distributions. The preparation of the data set for the multivariate statistical analysis is made by performing an univariate analysis, which can be summarized as follows :

1. Perform graphical representations of the results obtained in scatter plots to identify visually the possible relationships between variables ;
2. Determine the statistical models best estimating the actual distribution of a variable; this needs to be performed individually for all variables;
3. Identify and eliminate possible outliers present in the data set;
4. Perform a variable transformation when the distribution of residuals of the univariate regression (using a constant independent variable) is non-normally distributed : as a condition to undertake statistical tests on multivariate regressions.

Both the data set preparation and the statistical analysis can be performed efficiently using an appropriate statistical software. In most cases, due to the large quantity of information (data) considered for the statistical analysis, a single example of the different computations will be presented in the text for simplicity, the remainder being presented in the different appendices (as referred in text).

Assumptions and hypotheses for the statistical analysis

It can be observed in Chapter Five that some variables (parameters) were neglected when performing the multivariate analysis using the matrix of interaction. For example, all of the parameters measured on the bridge except two were selected to appear in the matrix. It was decided that the apparent modulus of elasticity, termed E_pv, and the saturated density, termed SD_a, would be neglected for different

reasons : the results obtained for the apparent modulus of elasticity were found to be inconsistent with those from the modulus of elasticity (E_cs), while the saturated density is considered as a redundant variable closely related to the dry density (SD_b) and to the volume of permeable pore space (voids) termed VV. Therefore, these variables will not be considered for the statistical analysis.

In addition, is was decided to group the analysis of variables of the same nature together, based on the assumption that the relationship between any two variables is the same for any member of the structure. For example, all observations (readings) relative the half-cell potential (deck surface and soffit) were grouped together for the statistical analysis. All data relative to the bridge columns were neglected since the results were found to be inconsistent with those of the bridge deck (mean positive value for the half-cell survey of the columns). Finally, the variable representing the corrosion potential and the half-cell potential were grouped together for the statistical analysis, since they represent two measures of the same quantity (potential of corrosion).

Also, it was decided that no estimation of missing data would be performed : the statistical analysis of variables is performed to quantify (1) the statistical distribution of each variable and (2) the existence of trends between variables. The estimation of the missing variables can jeopardize the validity of the analyzing process in increasing the propagation of uncertainty. In certain cases, only a few observations are available to characterize the statistical distribution of some variables and their relationships with others. As a result, only observations (readings) obtained at the same test locations are considered in the multivariate analysis.

5.3.1 Univariate analysis

5.3.1.1 Graphical representation of variable interaction

The graphical representation of results in the form of scatter plots is commonly used to first visualize relationships (dependencies) between variables (parameters). This

type of representation provides useful information about the collinearity of the different variables studied. The property of collinearity is indicative of the degree of linear dependence of the two variables, normally distributed or not, also called correlation. Also, the scatter plot representation provides insight into the presence of outliers in the data test, defined as inconsistent observations of the data set.

Scatter plots of all variables are presented in a matrix format. The matrix format allows for rapid examination of the trends between variables and the identification of the most important relationships. The leading diagonal entries are histograms representing the distribution of the variable. They also provide valuable information about the type of distribution representing the variables (normal or not). Since 15 variables are considered in the statistical analysis, a scatter plot matrix of dimensions 15 by 15 is produced. To simplify the presentation, the scatter plot matrix is divided into three 10 by 10 sub-matrices presented in Figures 5.7 to 5.9.

The scatter plots presented in Figures 5.7 to 5.9 were obtained using the data collected at the location where the 24 cores used for laboratory testing were collected. Additional data on the surface and soffit of the deck were also collected for different variables (parameters). Scatter plots of these variables are presented in Figure 5.10 to 5.11. The number of observations and descriptive statistics for all variables are presented in Table 4.2.

Figure 5.7 Scatter plot sub-matrix for results of all variables (first ten parameters considered).

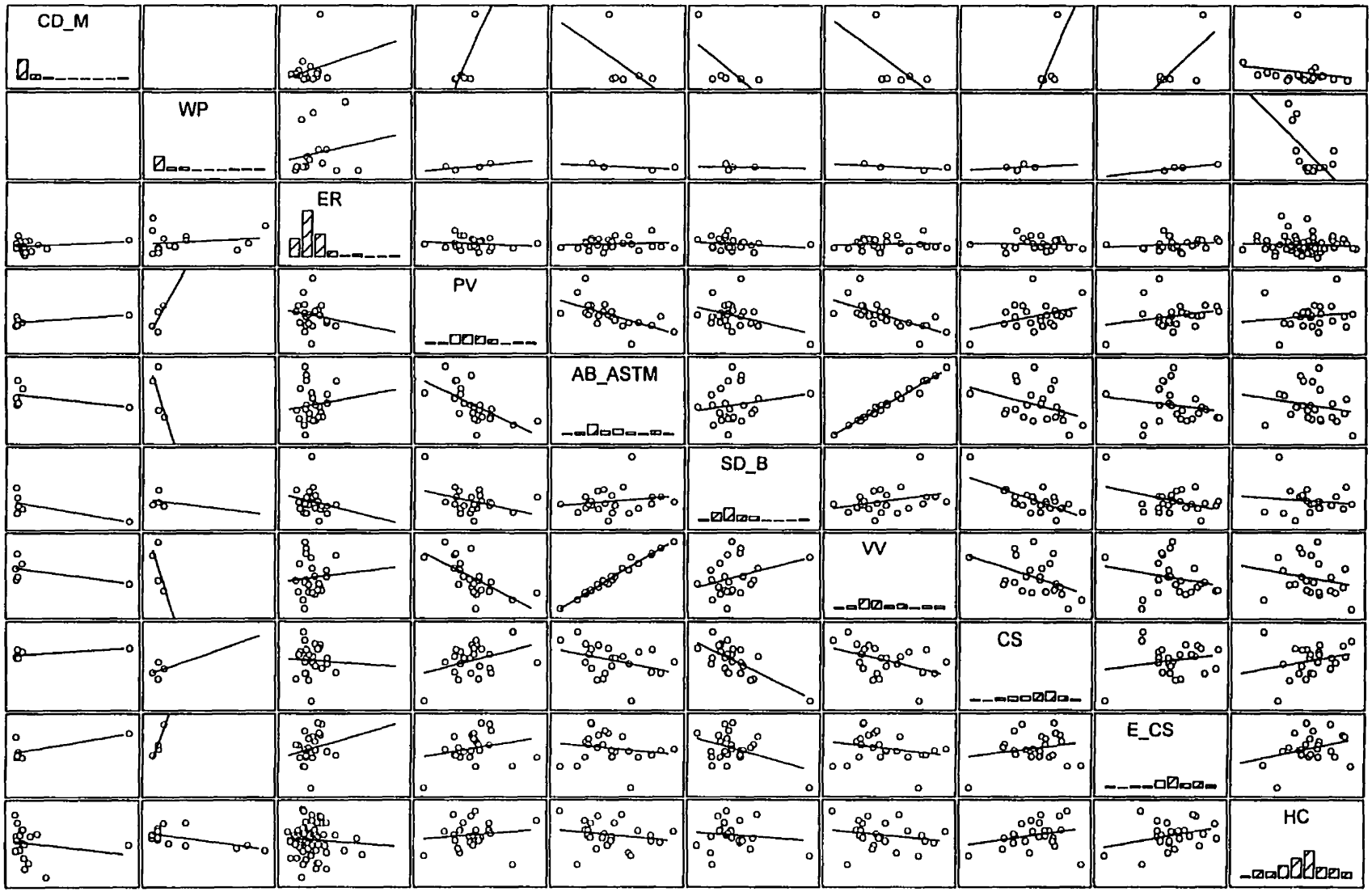

Figure 5.8 Scatter plot sub-matrix for results of all variables (last ten parameters considered).

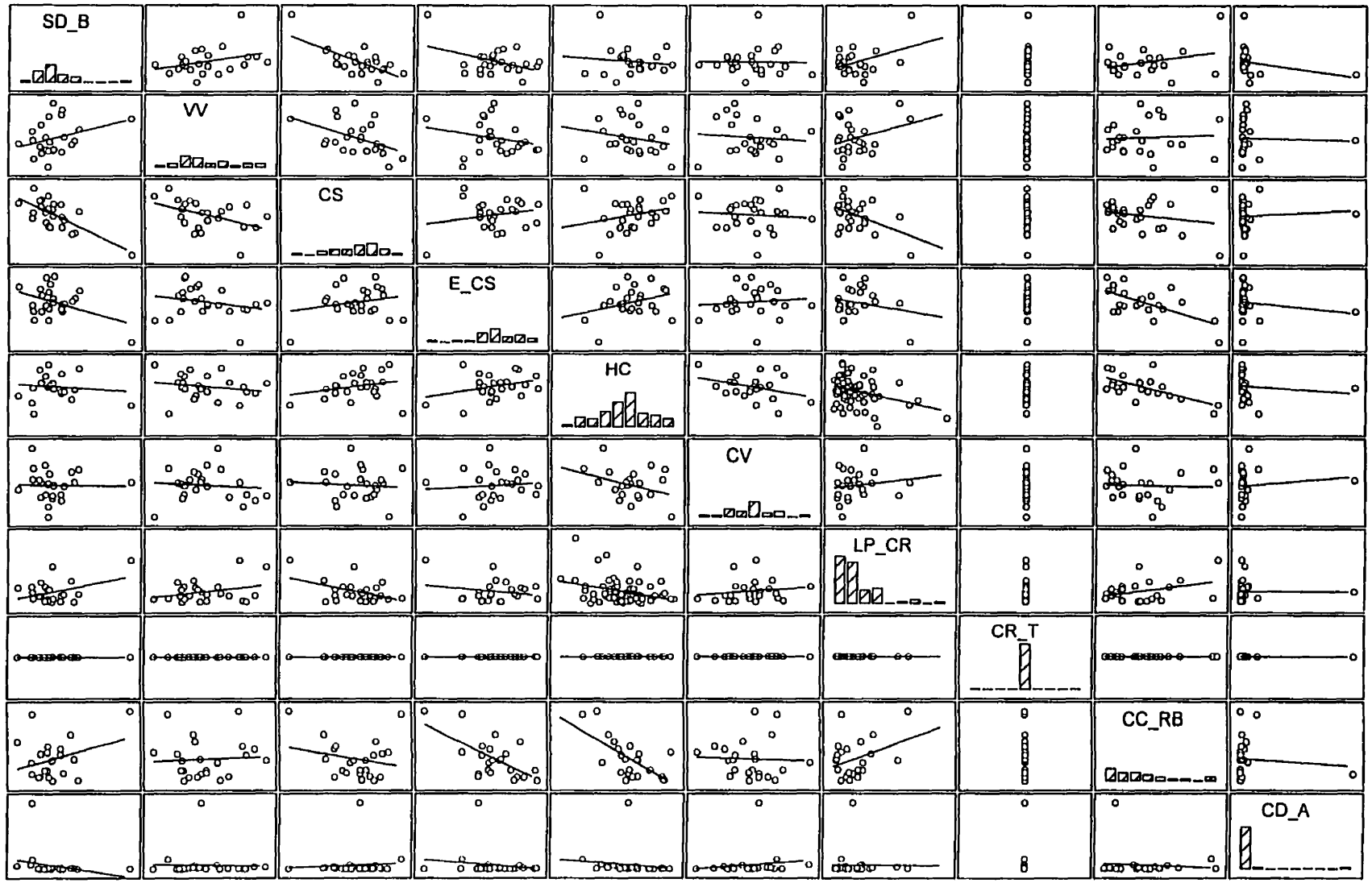

Figure 5.9 Scatter plot sub-matrix for results of all variables (first five and last five parameters considered).

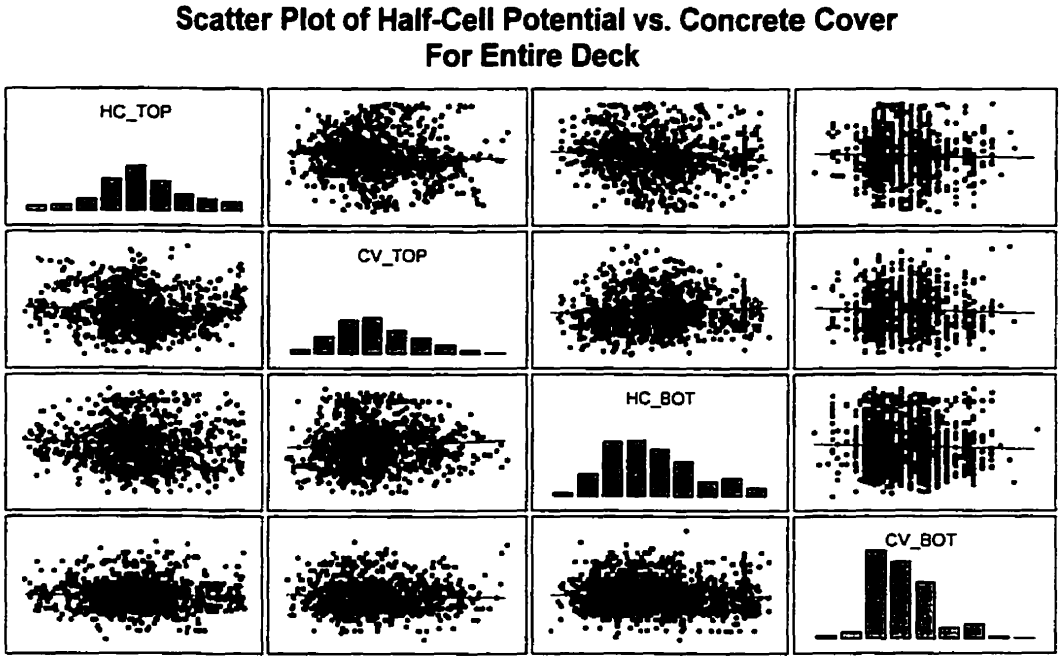

Figure 5.10 Scatter plot matrix including additional results for particular variables.

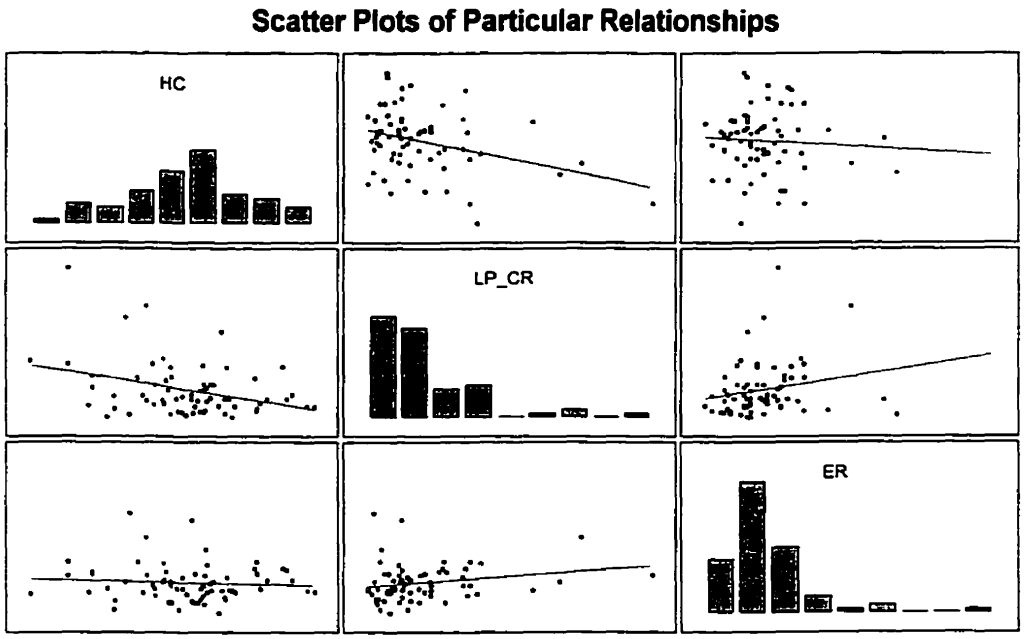

Figure 5.11 Scatter plot matrix including additional results for particular variables.

From close examination of Figure 5.7 to 5.11, trends can be identified. The trend of the graphical distribution can be defined as the slope of the regression curve. Positive trends consist in ascending regression curves, while negative trends are associated to descending regression curves. A horizontal line represents the absence of trend, of interaction. It is important that the identification of trends be considered carefully done since many factors can influence the trends observed such as the environmental conditions (at the time of testing), the presence of outliers, and the accuracy of instrument used. However, according to the scatter plots obtained for the 15 variables of interest, the following observations can be made :

- The absorptivity after immersion (AB_astm) is highly and positively correlated with the volume of permeable pore space (VV), and both quantities are negatively correlated with the pulse velocity measurement (PV) and the compressive strength (CS). It is expected that an increase of the volume of air voids increases the water absorption and decreases the pulse velocity and the resistance of the concrete to compression;
- The half-cell potential (HC) is highly and negatively correlated with the compressive strength (CS), modulus of elasticity (E_cs), chloride concentration at the rebar level (CC_rb), and water permeability (WP). Theoretically, it is assumed that as the risks of corrosion increase (measured by the HC), the overall rigidity of the concrete decreases, and the water permeability increases;
- The chloride concentration at rebar (CC_rb) is negatively correlated with the compressive strength (CS), but positively correlated with the corrosion rate (LP_cr). The presence of chloride ions should first induce, and later accelerate the corrosion rate of steel, while the development of corrosion should decrease the;
- The corrosion rate (LP_cr) is positively correlated with the volume of permeable pore space (VV), dry density (SD_b), and water permeability (WP), while it shows negative correlations with the compressive strength (CS), half-cell potential (HC), and pulse velocity (PV). The number and

volume of interconnected air voids positively influence the ingress of water in concrete to accelerate the corrosion reaction (measured by the corrosion rate);

- It appears that the modulus of elasticity (E_cs) and the compressive strength (CS) are not well correlated. These quantities measure the mechanical properties of concrete;
- Also, the concrete cover (CV) is not significantly correlated to any parameter : thin concrete covers should facilitate the ingress of water and deleterious agents in concrete, resulting in an increase of the rate of the corrosion reaction;
- The carbonation depth should be neglected for the statistical analysis : the results obtained are of no statistical value;
- Finally, the results from the water permeability (WP) and the chloride diffusion migration (CD_m) need to be interpreted with care : the trends observed indicate the influence of extreme values of the variables distributions (outliers).

5.3.1.2 Variable distribution and outliers

The identification and elimination of outliers from the data set is an important operation which must be performed with care. The elimination of outliers greatly affects the accuracy of the statistical analysis, especially when performed on a small sample size (small number of observations). Outliers can be defined as inconsistent observations of the data set, or extreme values of the variable distribution. There are several ways to identify the presence of outliers in the variable distribution, the most common being presented here :

- Normality tests : Normality tests of statistical softwares can be used to determine if the variable is normally distributed. However, for small numbers of observations (below 100), these standard tests are found of little significance;

- Stem-leaf plots of the random variable : Stem-and-leaf plots of a variable take the form of a histogram which is used to identify the outliers;
- Box plots of the random variable : In this method, the variable distribution is assumed to be normal and different quantities (25th, 50th, and 75th percentiles) are used to characterize the normal distribution;
- Normal probability plots of the variable : The method consists in the plot of the inverse of the standard normal cumulative probability (expected normal deviate) versus the ordered observations. Straight lines are indicative of perfectly normal distribution, while deviations of the straight line can be interpreted as being not normal.

By close examination of the results obtained from the Dickson Bridge, it can be seen that less than 35 observations (readings) were obtained for most variables. The identification of outliers for such small statistical samples (numbers of observations) is hazardous, and, if not performed with extreme care, can result in the loss of important information. However, for each test, the number of observation is found sufficient (above 5) to perform a reliable statistical analysis.

It was decided to first use normal probability plots to determine the normality character of the distributions (a good indication was given by the histogram diagrams of the scatter plot matrix presented in Section 5.3.1.1). In the case where a variable was not normally distributed, the log-normal distribution was also tested either by transforming the observations obtained for a particular variable to the log-normal format and again plotting normality curves, or by performing directly the log-normality tests using the statistical software. The last verification performed to determine the variable distributions was to graph the normality plots of residuals after regressing all variables individually with the variable representing the corrosion rate (LP_cr). The regression and residual analyses are described further in Section 5.3. The normality distribution of the residuals of a regression is a condition to perform statistical tests on multiple regressions of the variables. The multiple regression is useful when constructing statistical models using the best variables. The statistical

distribution of the variables was modified to obtain normal probability plots for all variables, considering the normality character of the residuals as the most important criteria to satisfy. Table 5.4 shows the effect of the variable transformations on all variables.

It is important to mention that no outliers were sucessfully identified during the univariate analysis. Due to the small number of observations, the elimination of outliers was found to affect negatively the correlations obtained between variables. It was concluded that the important information was deleted by the elimination of outliers, and no attempt was made to modify the content of the data set. It is important to consider that the deletion of a single observation of a variable actually result in the deletion of the corresponding values for all other variables of the data set when performing multivariate analysis.

The univariate analysis of the apparent chloride diffusion coefficient is presented in Figure 5.12, while the complete analysis of other variables is presented in Appendix C.

A review of the results for the north and central sections revealed that most variables were found to be either normally or log-normally distributed, as shown in Table 5.5. Since all variables need to present a normal distribution of the residuals in order to perform statistical tests on multivariate regressions, the statistical distribution of each variable was modified whenever necessary to obtain that property and the parameter designation was changed accordingly. Only the normal and log-normal formats were used. It was always verified that the normal distribution of the residuals was obtained for all transformed variables (regressed individually with the ln(LP_cr)). This procedure is consistent with the procedures used for the statistical analysis of the north and central sections, and allows for the comparison of statistical models developed for all three sections of the Dickson Bridge.

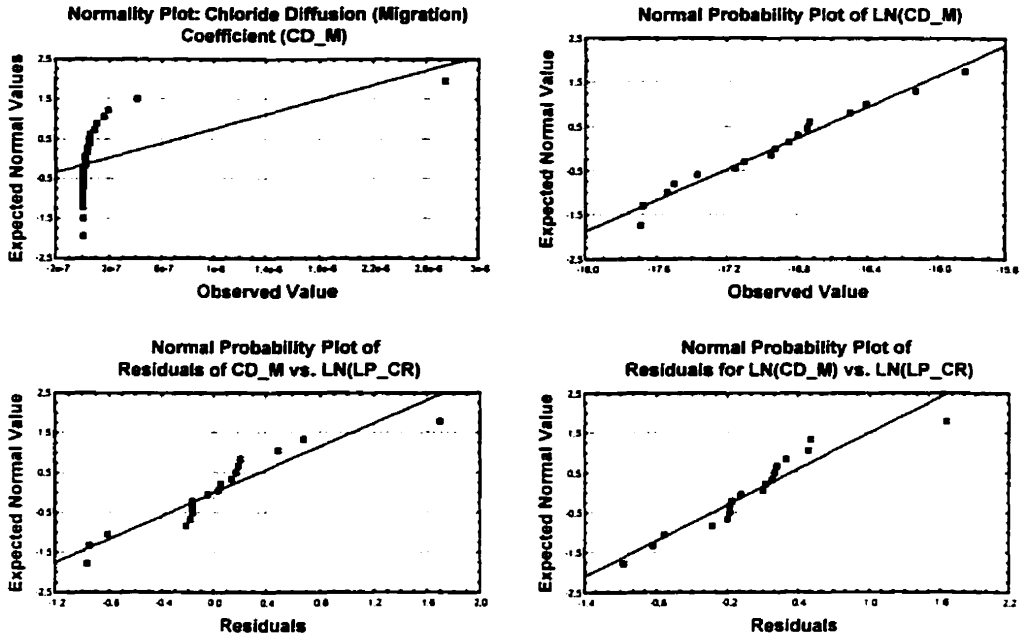

Figure 5.12 Normal probability plots of variable (top) and residuals (bottom) before (left) and after (right) variable transformation for the chloride diffusion migration CD_m.

Table 5.4 Results of univariate analysis for the Entire Bridge Deck.

Parameter Symbol	No. of Readings	VAR	New Symbol	No. of Readings	VAR
CD_m	18	9.06E-15	ln(CD_m)	18	5.57E-01
WP	16	4.27E-27	WP	16	4.27E-27
ER	69	4.58E+00	ln(ER)	69	1.36E-01
PV	24	6.66E-02	PV	24	6.66E-02
AB_astm	24	5.86E-01	AB_astm	24	5.86E-01
SD_b	24	8.01E-04	SD_b	24	8.01E-04
VV	24	1.67E+00	VV	24	1.67E+00
CS	24	5.81E+01	CS	24	5.81E+01
E_cs	24	1.52E+06	ln(E_cs)	24	3.20E-02
HC	66	9.85E+03	ln(HC)	66	1.66E-01
CV	23	1.80E+02	ln(CV)	23	1.63E-01
LP_cr	66	2.90E+03	ln(LP_cr)	66	5.19E-01

Table 5.4 Results of univariate analysis (continued).

Parameter Symbol	No. of Readings	VAR	New Symbol	No. of Readings	VAR
CR	24	0.00E+00	CR	24	0.00E+00
CC_rb	23	2.78E-02	CC_rb	23	2.78E-02
CD_a	24	3.08E-13	ln(CD_a)	24	2.33E+00

Table 5.5 Statistical distributions of variables for the north, central, and south sections of the Dickson Bridge.

Variables (parameters)	Type of statistical distribution (north)	Type of statistical distribution (central)	Type of statistical distribution (south)	New variable name (south)
CD_m	Log-normal	Log-normal	Log-normal	**ln(CD_m)**
WP	Log-normal	Log-normal	Normal	**WP**
ER	Log-normal	Normal	Log-normal	**ln(ER)**
PV	-	Normal	Normal	**PV**
AB_astm	-	Normal	Normal	**AB_astm**
SD_b	-	Normal	Normal	**SD_b**
VV	-	Normal	Normal	**VV**
CS	Normal	Normal	Normal	**CS**
E_cs	-	-	Log-normal	**ln(E_cs)**
HC	Normal	Normal	Log-normal	**ln(HC)**
CV	Normal	Log-normal	Log-normal	**ln(CV)**
LP_cr	Log-normal	Normal	Log-normal	**ln(LP_cr)**
CR	-	Normal	Normal	**CR**
CC_rb	Log-normal	Log-normal	Normal	**CC_rb**
CD_a	Log-normal	Log-normal	Log-normal	**ln(CD_a)**

It can be noted from Table 5.5 that for some variables, the type of statistical distributions used for the investigation of the Dickson Bridge differed for the central, north, and south sections. This is due to the method used to determine the normality character of the variable distribution : for the analysis of the south section, some variables normally distributed were transformed to the log-normal format to obtain a normal distribution of the residuals (obtained by performing an univariate regression using the corrosion rate as the dependent variable). This procedure was not necessarily used by the other authors for the investigation of the north and central sections.

5.3.2 Multivariate analysis

The multivariate analysis consists in performing individual and combined statistical regressions of the modified variables. The multivariate analysis is an important part of the overall investigation procedure as it provides a numerical quantification of the existing relationships between the measured variables (parameters). The results of the multivariate analysis presented in this section will be used later to verify the qualitative interpretations made using the matrix of interaction in Section 5.2.5. Also, a model estimating the corrosion process will be developed after the most influencing techniques will be outlined. Finally, the model obtained for the south section of the Dickson Bridge will be compared with those obtained from separate analyses of the north and central sections. The underlying concepts about statistical regressions are quickly reviewed here.

Univariate regression

For the individual regression, the independent variables (regressors) are related to the dependent one separately, using the following equation :

$$y_{(i)} = (B_{(0)} + B_{(1)}x_{(i)}) + e_{(i)} \qquad (5.1)$$

where $y_{(i)}$ is the dependent variable, $B_{(0)}$ and $B_{(1)}$ are respectively the intercept and the slope of the regression curve of the scatter plot of y vs. x, x is the regressor, and $e_{(i)}$ is the error of the regression process, also called residual.

The goal is to obtain the best estimate of the dependent variable by using the independent variables separately. The process implies the minimization of the sum of the squared errors of prediction. Individual regressions are performed by computer processing considering all observations of both the dependent and independent variables. A residual distribution analysis is usually performed to determine the level

of performance of the regression process. The residual analysis is reviewed further in this section.

Multivariate regression

The multivariate regression is an extension of the individual variable regression for several regressing variables. The independent variables (regressors) are related to the dependent one using the general form of the regression equation :

$$y_{(i)} = (B_{(0)} + B_{(1)}x_{(i1)} + B_{(2)}x_{(i2)} + \ldots + B_{(n)}x_{(in)}) + e_{(i)} \qquad (5.2)$$

where $y_{(i)}$ is the dependent variable, $B_{(0)}$ and $B_{(ii)}$ are respectively the intercept and the slopes of the n-dimension regression surface with reference to the i^{th} regressor (axis) of the surface plot of y vs. all x (1 to n); the x terms are the regressors, and $e_{(i)}$ is the residual term (vector).

The goal, this time, is to obtain the best estimate of the dependent variable by using selected independent variables jointly. Again, the process implies the minimization of the sum of the errors of prediction. However, a restricted number of independent variables must be selected in order to obtain a consistent solution. As the number of regressors increases, the capacity of the equation (model) to fit the random distribution of the dependent variable decreases. A measure of this capacity is the degree of freedom of a model defined as the number of observations minus the number of regressors used in the regression. The multiple regression is performed by computer processing for all observations of both the dependent and the independent variables. A residual distribution analysis is also usually performed to determine the level of performance of the regression process.

Residual distribution analysis

The analysis of the distribution of errors, or residual terms, is important to establish the performance of both the univariate and multivariate regressions. In most statistical softwares, a number of tools can be used to perform this type of analysis, and most of them assume (1) the residual terms are independently distributed, (2) a standard normal distribution of the residual terms, (3) no bias in the residuals, (4) constant variance of the residuals. Based on these assumptions, the quantities of interest for the analysis of residuals are presented in Table 5.6.

5.3.2.1 Univariate regression

A univariate regression of all variables of interest was performed to identify the most contributive parameters quantifying the corrosion process. As mentioned previously, the test techniques used on the Dickson Bridge were divided into two categories, assessment and prediction techniques. The choice of the corrosion rate as the dependent variable was found to be the most appropriate, since the corrosion rate is the only direct measurement of the intensity of the corrosion reaction. A total of 14 independent variables (regressors) was considered in the analysis, and the results are presented in Table 5.7. Some quantities of Table 5.6 were used to determine the quality of the regression process. It can be observed that no single variable provided a satisfactory estimate of the corrosion rate (ln(LP_cr)). From the results obtained, the water permeability (WP), compressive strength (CS), pulse velocity (PV), and chloride diffusion (migration) (ln(CD_m)) provide the best individual estimates of the corrosion rate, while the half-cell potential (LN(HC)), electrical resistance (ln(ER)) and concrete cover (LN(CV)) are also closely related to the dependent variable, at a lower level.

Table 5.6 Description of quantities of interest in the analysis of residual terms of statistical regressions.

Quantities of interest	Description	Formula
N or n	Number of observations used for the regression.	
m	Total number of variables used for the regression.	
SSE	Error summation of squares : calculated as the summation of all the residual terms squared about the regression.	$\Sigma(Y-Yreg)^2$ **(5.3)**
SSY	Error summation of squares : calculated as the summation of all the residual terms squared about the mean.	$\Sigma(Y-Ymean)^2$ **(5.4)**
R^2	Coefficient of determination : ranging between 0 and 1, it represents the influence of the SSE on the model of the mean value of y. A value close to one is indicative of good performance of the model.	1-(SSE/SSY) **(5.5)**
R^2adj.	Shrinkage coefficient : indicates the ability of the model to estimate observations taken outside of the sample and used to determine R^2 (generally reducing its value). R^2adj. can take negative values when : (1) m is greater than two with SSE close to SSY or when SSE is greater than SSY.	1-(SSE/(n-m))/ (SSY/(n-1)) **(5.6)**
F-ratio	F-ratio : measures the improvement of a model after its modification. The significance of a model is confirmed if the F-value is greater than the critical value obtained either from the literature (tables of F) or calculated by the software. The F-ratio allows for comparison of the different models together : the highest value is associated with the best model estimate.	Refer to statistical hanbooks[29]
Cook's distance	Cook's distance : measures the effect of an outlier both on the dependent variable and on the independent one(s). According to the literature[29], values above one are indicative of probable outliers.	Refer to statistical hanbooks[29]
Normality plot of residuals	Used to verify the normality assumption : a straight line (horizontal) is indicative of a satisfactory result.	
Plot of residual vs. predicted value of y	Used to verify the constant variation assumption : a horizontal band is indicative of a satisfactory performance of the model.	

Another possible way to quantify the interactions between variables, is to compute the Pearson correlation matrix where the correlation coefficients between all variables are

determined as follows : first, the R square coefficients are calculated for all pairs of variables, and secondly, the coefficients of the matrix are determined as being the positive or the negative values of the square root of R square. As mentioned previously, a positive sign is associated with an ascending linear trend between two variables. This method is based on the assumption that all variables are normally distributed.

Table 5.7 Residual information from regression of the independent variables with the dependent variables.

Regressors	N	R^2 (%)	R^2adj (%)	Decrease in R^2	F-ratio	F critical
ln(CD_m)	18	9.9	4.2	57,6 %	1.75	0.47
WP	15	17.6	11.2	36,4 %	2.77	-11.53
ln(ER)	66	4.9	3.4	30,6 %	3.30	-9.44
PV	24	11.3	7.2	36,3 %	2.80	0.058
AB_astm	24	2.4	-2.01	183,8 %	0.55	-3.25
SD_b	24	4.2	-0.13	103,1 %	0.97	-1.35
VV	24	3.2	-1.12	135,0 %	0.74	-3.48
CS	24	11.6	8.6	25,9 %	3.16	-1.68
ln(E_cs)	24	1.2	-3.3	375,0 %	0.26	0.10
ln(HC)	66	4.5	3.0	33,3 %	3.03	-4.20
ln(CV)	23	7.3	2.9	60,3 %	1.66	-3.53
CR	-	-	-	-	-	-
CC_rb	23	4.3	-0.2	104,7 %	0.95	-13
ln(CD_a)	24	4.7	0.4	91,5 %	1.09	-.80

The matrix obtained is symmetric : the R coefficient obtained for the regression of variable A using B is equal to the R coefficient obtained for the regression of B using A as the regressing variable. R coefficients near unity are indicative of high dependency between variables. The converse is also valid : low coefficient values either indicate the absence of linear relationship or the incapacity of the data set analyzed to satisfactorily assess that particular relationship. The leading diagonal terms are all equal to unity since the correlation of any particular variable with itself is at a maximum (R value of 1). It is interesting to observe the difference with the interaction matrix in which the leading diagonal terms were set equal to zero based on the assumption that a particular variable was not influencing itself. Figure 5.13

presents the Pearson correlation matrix obtained by the analysis of the 15 variables of interest for the south section of the Dickson Bridge. It can be observed in Figure 5.13 that the chloride diffusion migration (ln(CD_m) and the water permeability (WP) could not be considered in the derivation of the correlation matrix, due to the lack of the corresponding observations. They are considered in the analysis of particular relationships between variables.

Particular cases of the univariate regression

The Pearson correlation matrix presented in Figure 5.13 considered only the data set associated to the tests performed both in the laboratory (on extracted cores) and in-situ (at bored locations), as a consequence of the decision to perform both the univariate and the multivariate regression analyses using only corresponding observations, i. e., observations obtained at identical locations, where the cores were extracted.

On the other hand, the test program of the south section of the Dickson Bridge produced a large quantity of data, obtained from the testing of the bridge deck surface, soffit, and columns. It was decided, in order to consider all of the collected data in the statistical analysis, to perform univariate regressions on variables for which observations were obtained at identical locations, both not necessarily at cored locations. As a result, a series of specific correlations can be obtained to improve the content of the general matrix of correlation obtained for the 15 variables of interest. The contributions of these additional correlation terms to the general correlation matrix should be significant, since a greater number of observations (including the observations considered in the first univariate regression) can be considered in the analysis by regressing some variables separately. These particular correlations are investigated here.

Relationship between half-cell potential and concrete cover thickness

A total of 2468 corresponding observations were obtained from testing jointly for the concrete cover thickness and the half-cell potential. An univariate regression was performed using variables representing the combination of all observations taken from the bridge deck (surface and soffit). The data from the columns and the observations taken at delaminated locations (concrete cover thickness equal to zero) were rejected for this analysis. The Pearson correlation matrix obtained is presented in Figure 5.14. It can be observed that the correlation coefficient obtained is quite low (-0.07) with a large number of observations, indicating that the two variables are weakly correlated.

	Ln CD	WP	Ln ER	PV	AB Ast.	SD _b	VV	CS	Ln Ecs	Ln HC	Ln CV	Ln LP	CC rb	Ln CD
lnCD_m	-	-	-	-	-	-	-	-	-	-	-	-	-	-
WP	-	-	-	-	-	-	-	-	-	-	-	-	-	-
lnER	-	-	1.00	-0.21	0.09	-0.18	0.06	-0.03	0.18	-0.08	0.17	0.16	-0.08	-0.06
PV	-	-	-0.21	1.00	-0.65	-0.55	-0.71	0.51	0.45	-0.01	0.02	-0.39	-0.15	0.10
AB_astm	-	-	0.09	-0.65	1.00	0.21	0.99	-0.39	-0.19	0.25	-0.02	0.15	0.01	0.18
SD_b	-	-	-0.18	-0.55	0.21	1.00	0.35	-0.71	-0.49	0.11	0.03	0.21	0.32	-0.35
VV	-	-	0.06	-0.71	0.99	0.35	1.00	-0.48	-0.25	0.26	-0.01	0.18	0.06	0.12
CS	-	-	-0.03	0.51	-0.39	-0.71	-0.48	1.00	0.27	-0.33	-0.13	-0.36	-0.22	0.00
lnE_cs	-	-	0.18	0.45	-0.19	-0.49	-0.25	0.27	1.00	-0.25	0.17	-0.11	-0.67	-0.10
lnHC	-	-	-0.08	-0.01	0.25	0.11	0.26	-0.33	-0.25	1.00	0.41	0.21	0.52	0.49
lnCV	-	-	0.17	0.02	-0.02	0.03	-0.01	-0.13	0.17	0.41	1.00	0.27	-0.07	0.34
lnLP_cr	-	-	0.16	-0.39	0.15	0.21	0.18	-0.36	-0.11	0.21	0.27	1.00	0.21	0.21
CC_rb	-	-	-0.08	-0.15	0.01	0.32	0.06	-0.22	-0.67	0.52	-0.07	0.21	1.00	0.21
lnCD_a	-	-	-0.06	0.10	0.18	-0.35	0.12	0.00	-0.10	0.49	0.34	0.21	0.21	1.00

Figure 5.13 Pearson's correlation matrix for the variables of interest of the south section of the Dickson Bridge.

Relationships between half-cell potential, corrosion rate, electrical resistance, and chloride diffusion (migration)

A total of 18 corresponding observations were obtained by testing jointly for the corrosion rate, the electrical resistivity, the half-cell potential, and the chloride diffusion (migration). A univariate regression was performed using all of the data from the deck surface. The Pearson correlation matrix obtained is presented in Figure 5.15. However, 63 corresponding observations were obtained for the half-cell test, the corrosion rate test, and the electrical resistivity test. Since corresponding observations are values of tests obtained at identical locations on the bridge, this means that from the 63 locations tested for these tests only 18 values were obtained for the chloride diffusion (migration) test. In the same manner, from those 63 locations only 15 observations (values) were obtained for the in-situ water permeability test (Figure 5.16). It appears that only 6 locations were tested jointly for the in-situ water permeability and the chloride diffusion (migration) test : these 6 locations were also tested for the HC, CR and ER tests. This is the reason why two separate analyses were needed (leading to Figures 5.15 and 5.16) and why some coefficients of correlation presented in Figure 5.17 could not be obtained.

	ln(HC)	ln(CV)
ln(HC)	1,00	-0,07
ln(CV)	-0,07	1,00

Figure 5.14 Pearson correlation matrix for the half-cell potential (ln(HC)) and concrete cover (ln(CV)).

	ln(HC)	ln(LP_cr)	ln(ER)	ln(CD_m)
ln(HC)	1,00	-0,58	0,14	-0,18
ln(LP_cr)	-0,58	1,00	0,15	0,12
ln(ER)	0,14	0,15	1,00	0,22
ln(CD_m)	-0,18	0,12	0,22	1,00

Figure 5.15 Partial Pearson correlation matrix for the half-cell potential (ln(HC)), corrosion rate (ln(LP_cr)), electrical resistance (ln(ER)), and chloride diffusion migration (ln(CD_m)).

Specific relationships between the half-cell potential, corrosion rate, electrical resistance, and in-situ water permeability

A total of 15 valid observations were obtained from testing jointly for the corrosion rate, the electrical resistance, the in-situ water permeability, and the half-cell potential. Since the in-situ water permeability and chloride diffusion (migration) tests were performed jointly at only 6 locations, from the 15 observations considered here the remaining (9) were obtained at different locations and were not considered in Figure 5.15. Again, a univariate regression was performed using the data from the deck surface. The partial Pearson correlation matrix obtained is presented in Figure 5.16. It is observed by comparison of Figures 5.15 and 5.16 that the correlation coefficients of the half-cell potential, of the electrical resistance, and of the corrosion rate are significantly changed by the use of a certain number of new observations (9). This demonstrates that the number of observations obtained is too small to significantly estimate the interrelationships between the variables.

Modified version of the Pearson correlation matrix

The modified and final version of the matrix of interaction can be obtained by updating the coefficients of correlation obtained for the specific cases of the univariate regression analysis. The modified version is presented in Figure 5.17.

	ln(HC)	ln(LP_cr)	ln(ER)	WP
ln(HC)	1,00	-0,36	-0,14	-0,61
ln(LP_cr)	-0,36	1,00	0,31	0,45
ln(ER)	-0,14	0,31	1,00	0,18
WP	-0,61	0,45	0,18	1,00

Figure 5.16 Partial Pearson correlation matrix for the half-cell potential (ln(HC)), corrosion rate (ln(LP_cr)), electrical resistance (ln(ER)), and water permeability (WP).

According to the findings of this analysis, it can be observed that correlations of importance are :

- The absorption after immersion, the dry density and the volume of permeable pore space (voids) are highly and positively correlated together and negatively correlated with the compressive strength, modulus of elasticity and pulse velocity;
- The pulse velocity is positively correlated with the compressive strength and modulus of elasticity;
- The water permeability is negatively correlated with half-cell potential, but positively correlated with corrosion rate and chloride diffusion migration;
- The corrosion rate shows significant correlations with the water permeability, pulse velocity, half-cell potential, compressive strength, electrical resistance and concrete cover.

The calibration of the new techniques for which no standards exist (at this point in time) can be performed by identifying significant correlations between the measured parameters and parameters obtained using standard measurement techniques. For example, the pulse velocity correlates well with the compressive strength test, water permeability and the two chloride diffusion measurements correlate significantly with the half-cell potential measurement. The use of non-destructive techniques to calibrate destructive techniques is desired, and the half-cell potential and pulse velocity tests represent, from the results of the Pearson correlation matrix, potential techniques to play such roles.

	Ln CD	WP	Ln ER	PV	AB Ast.	SD _b	VV	CS	Ln Ecs	Ln HC	Ln CV	Ln LP	CC rb	Ln CD
lnCD_m	-	-	*0.22*	-	-	-	-	-	-	*-0.18*	-	*0.12*	-	-
WP	-	-	*0.18*	-	-	-	-	-	-	*-0.61*	-	*0.45*	-	-
lnER	*0.22*	*0.18*	1.00	-0.21	0.09	-0.18	0.06	-0.03	0.18	*-0.14*	0.17	*0.31*	-0.08	-0.06
PV	-	-	-0.21	1.00	-0.65	-0.55	-0.71	0.51	0.45	-0.01	0.02	-0.39	-0.15	0.10
AB_astm	-	-	0.09	-0.65	1.00	0.21	0.99	-0.39	-0.19	0.25	-0.02	0.15	0.01	0.18
SD_b	-	-	-0.18	-0.55	0.21	1.00	0.35	-0.71	-0.49	0.11	0.03	0.21	0.32	-0.35
VV	-	-	0.06	-0.71	0.99	0.35	1.00	-0.48	-0.25	0.26	-0.01	0.18	0.06	0.12
CS	-	-	-0.03	0.51	-0.39	-0.71	-0.48	1.00	0.27	-0.33	-0.13	-0.36	-0.22	0.00
lnE_cs	-	-	0.18	0.45	-0.19	-0.49	-0.25	0.27	1.00	-0.25	0.17	-0.11	-0.67	-0.10
lnHC	*-0.18*	*-0.61*	*-0.14*	-0.01	0.25	0.11	0.26	-0.33	-0.25	1.00	*-0.07*	*-0.36*	0.52	0.49
lnCV	-	-	0.17	0.02	-0.02	0.03	-0.01	-0.13	0.17	*-0.07*	1.00	0.27	-0.07	0.34
lnLP_cr	*0.12*	*0.45*	*0.31*	-0.39	0.15	0.21	0.18	-0.36	-0.11	*-0.36*	0.27	1.00	0.21	0.21
CC_rb	-	-	-0.08	-0.15	0.01	0.32	0.06	-0.22	-0.67	0.52	-0.07	0.21	1.00	0.21
lnCD_a	-	-	-0.06	0.10	0.18	-0.35	0.12	0.00	-0.10	0.49	0.34	0.21	0.21	1.00

Figure 5.17 Final Pearson correlation matrix for the 15 variables of interest obtained from the investigation of the south section of the Dickson Bridge.

5.3.2.2 Quantitative analysis using the matrix of interaction

In Section 5.2.5, a qualitative analysis of the relationships between the influencing parameters of the chloride-induced corrosion process was performed. Assessed semi-quantitatively, the interaction terms were used to identify the most dominant and influencing parameters. In Section 5.2, it was mentioned that the matrix coding of the matrix of interaction was possible using the correlations between parameters of the matrix.

The quantitative analysis of the variables of interest is performed using the matrix of interaction. Since only the first 15 parameters were tested, no correlation coefficients were determined for the other parameters considered in Section 5.2. Consequently, the matrix of interaction reduces to a size 15 by 15. The Pearson matrix of correlation for the 15 first variables obtained in Figure 5.17 can be used as the coded matrix of interaction after some modifications are made. The leading diagonal terms have to be set equal to zero, based on the assumption that the parameters are not influencing themselves. Also, when performing the calculations leading to the determination of the most influencing and dominant parameters, the absolute value of the correlation coefficients are used. It is finally important to observe that since the Pearson correlation matrix is symmetric so will be the matrix of interaction. This leads to a situation where no dominant parameters can be identified, since the (C-E) value will be zero for all parameters. However, the matrix of interaction is presented in Figure 5.18, while the corresponding cause vs effect graphic relationship is presented in Figure 5.19. Table 5.8 shows the coefficients obtained for the classification of parameters measured on the Dickson Bridge.

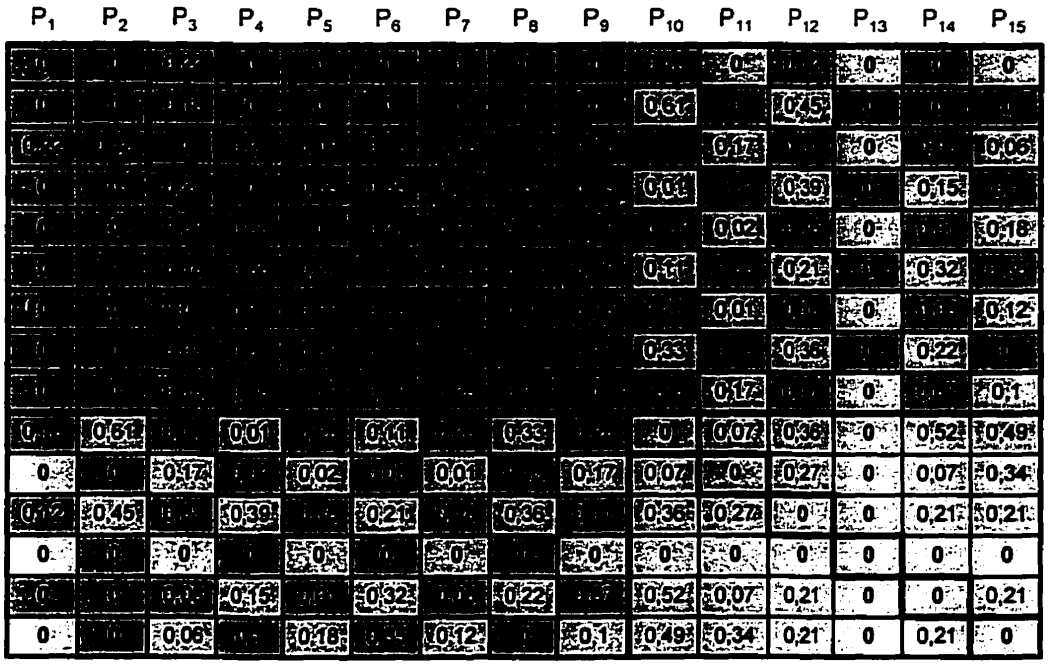

Figure 5.18 Modified form of the matrix of interaction based on the Pearson correlation coefficients.

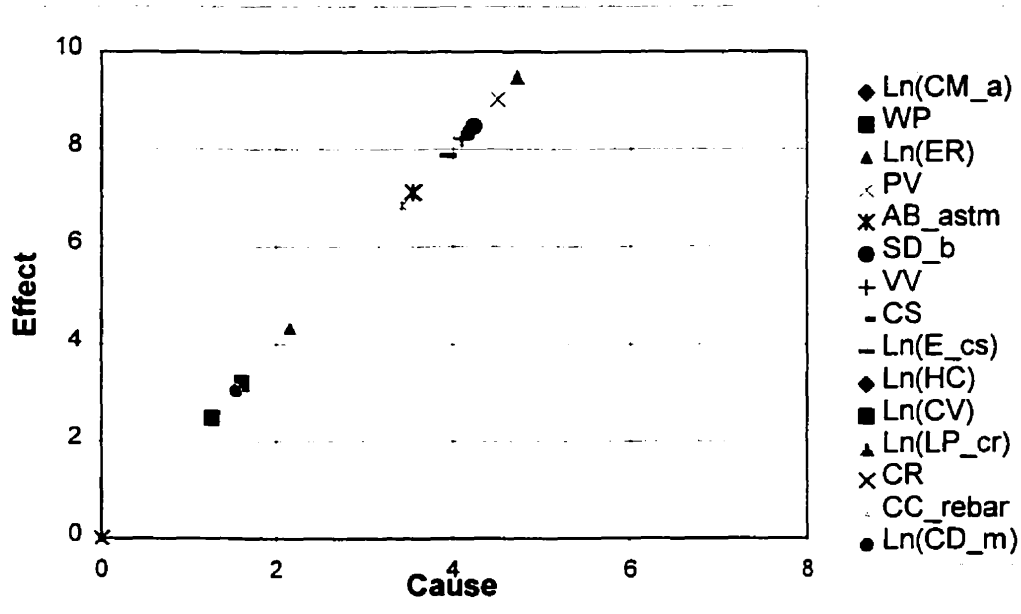

Figure 5.19 Cause vs. effect plot of the 15 first parameters of the matrix of interaction tested on the Dickson Bridge.

Table 5.8 Comparison of the 15 parameters of interest tested on the Dickson Bridge.

Parameter	C Value	E Value	C+E Value	C-E Value	(C+E)/√(2) Value	(C-E)/√(2) Value
ln(CD_m)	0.52	0.52	1.04	0	0.74	0
WP	1.24	1.24	2.48	0	1.75	0
ln(ER)	1.91	1.91	3.82	0	2.70	0
PV	3.75	3.75	7.5	0	5.30	0
AB_astm	3.13	3.13	6.26	0	4.43	0
SD_b	3.51	3.51	7.02	0	4.96	0
VV	3.47	3.47	6.94	0	4.91	0
CS	3.43	3.43	6.86	0	4.85	0
ln(E_cs)	3.13	3.13	6.26	0	4.43	0
ln(HC)	3.58	3.58	7.16	0	5.06	0
ln(CV)	1.3	1.3	2.6	0	1.84	0
ln(LP_cr)	3.33	3.33	6.66	0	4.71	0
CR	0	0	0	0	0.00	0
CC_rebar	2.52	2.52	5.04	0	3.56	0
ln(CD_a)	2.16	2.16	4.32	0	3.05	0

Results of the quantitative analysis

Based on the results presented in Table 5.8, the most interactive parameters (highest [C+E] values) have been identified. On the contrary, it was impossible to determine the most dominant parameters (highest [C-E] values) since the matrix of interaction used for the calculations was symmetric. That is, the cumulative influence of a parameter on the other components of the system equaled the cumulative influence of all other components of the system on that parameter.

The most influencing parameters for the corrosion process can be identified as :

1) The pulse velocity measurement (PV);
2) The half-cell potential (ln(HC));
3) The dry density (SD_b);
4) The volume of permeable pore space (VV);

5) The compressive stength (CS) and the corrosion rate (ln(LP_cr)).

On the other hand, the less influencing parameters were also identified. It is important to consider that correlation coefficients were missing in the matrix of interaction. The influence of the water permeability and chloride diffusion migration on the other parameters was not determined satisfactorily, as is reflected in the calculations. However, the less influencing factors are :

1) The carbonation depth (CR);
2) The chloride diffusion migration (ln(CD_m));
3) The water permeability (WP);
4) The concrete cover (ln(CV));
5) The electrical resistance (ln(ER)).

5.3.2.3 Multivariate regression

The ideal situation when performing a statistical regression is when the regressing variables are independent from one another and highly correlated with the dependent one[29]. As a result, the estimation of the dependent variable using the others is at a maximum and the contributions of the independent variables provide an important quantity of information obtained from different (independent) sources.

The choice of the dependent and independent variables for the multivariate regression is very important. The selection of the corrosion rate as the dependent variable was found to be appropriate, while the five parameters influencing the most the corrosion rate were selected as independent variables (regressors). The choice of regressors was based on the results of the univariate regressions and the interpretations made after both the qualitative and quantitative analysis were performed using the matrix of interaction. These results are summarized in Table 5.9. The choice of the parameters (independent variables) identified as most influencing in all three analyses would

have been the ideal situation. However, this situation was not observed and the following parameters were finally selected as regressors :

1) Compressive strength (CS);
2) Pulse velocity (PV);
3) Half-cell potential (ln(HC));
4) Volume of permeable voids (VV);
5) Chloride diffusion migration (ln(CD_m)).

Table 5.9 Comparison of most important parameters for the corrosion process.

Choice of regressors to estimate the corrosion process using the corrosion rate as dependent variable based on the different analyses made		
Qualitative analysis	Univariate Regression	Quantitative analysis
1 – HC	1 – WP	1 – PV
2 – CC_rb	2 – CS	2 – HC
3 – CR	3 – PV	3 – SD_b
4 – VV	4 – CD_m	4 – VV
5 – CD_m	5 - HC	5 – CS

The development of a model describing the corrosion rate using multivariate regressions of the independent variables can be performed using the multiple regression package of a statistical software. Different combinations of independent variables should be tried and a residual analysis performed using most of the quantities of interest described in Table 5.6.

Based on the results from the univariate regression analysis, the quantity of data collected on the south section of the Dickson Bridge is insufficient to obtain an adequate estimation of the corrosion process. The correlations obtained between the variables change significantly depending on the number of observations considered in the analysis. Also, the number of observations is too small to quantify the complex

process of corrosion of the steel reinforcement. For these reasons, it was decided to perform a multivariate regression on the corrosion rate (LP_cr) using all of the most influencing parameters identified in this investigation. The chloride concentration at the rebar level was used instead of the chloride diffusion (migration) since the data on chloride diffusion (migration) did not correspond with the data obtained for the other variables (not the same locations were tested).

It is not intended to continue further with the statistical analysis, since it is found that the information available does not allow to do so. The model obtained for the south section of the bridge is presented in Table 5.10 with the models obtained from the statistical analyses of the north and central sections[13, 25]. It is important to mention that the models presented for the north and central sections use only the parameters either describing the concrete quality, or the parameters assessing the damage to the steel. For the analyses of the north and central sections of the bridge, the assessment and the prediction techniques were analyzed separately. However, since it is assumed that the use of both types of techniques is necessary in order to quantify the corrosion process, it was decided for the south section of the bridge to analyze jointly both types of techniques to identify the overall most important parameters. The missing parameters for the statistical model of the north section could not be obtained.

In the model obtained for the south section of the bridge, it can be observed that it was not possible to explain more then 27 % of the variability. This is very low, and reflects that the correlations between variables were not sufficiently assessed. The number and locations of the readings taken on the bridge combined with the variability of the instruments or techniques used can probably account for a large part of the unexplained variability. The parameters of importance were however outlined. The quantification of the corrosion process is not a simple task and should be performed in a very rigorous way. The analysis performed in this thesis did not allow to construct a satisfactory statistical model to quantify the corrosion process, but allowed to identify and quantify further the relationships of importance between the

Table 5.10 Results of the multiple linear regression analysis for all sections of the Dickson Bridge[13, 25]

Analysis	Response variable (Y)	Regressor variable (X)	Intercept (b_0)	Multiplier ($b_0 \ldots b_n$)	Variability			R^2
					Explained (%)	Total (%)	Non-explained (%)	
North section of bridge[13]	log(LP_cr)	log(CC_rb)	1.597	0.54	31.5			
		CS		-0.012	17.5			
		log(ER)		0.022	2.8			
		log(WP)		-0.061	1.2	53	47	0.53
Central section of bridge[25]	log(LP_cr)	log(CC_rb)	Not provided	Not provided	Not provided			
		HC		"	"			
		ER		"	"			
		ln(WP)		"	"			
		ln(CD_a)		"	"	47	53	0.47
South section of bridge	ln(LP_cr)	ln(CC_rb)	3.87	-0.02	4.3			
		PV		-0.57	13.4			
		VV		-0.37	1.7			
		CS		0.16	3.6			
		ln(HC)		0.26	3.7	26.7	73.3	0.27

measured parameters. However, more testing is necessary to further develop the research on corrosion of the reinforcing steel in concrete.

5.4 Summary of statistical analyses

As mentioned previously, the scope of the statistical analysis was not to predict the remaining service life of the Dickson Bridge, but to quantitatively determine the relationships between the parameters of interest measured during the testing program. The matrix of interaction proved to be a valuable tool for the analysis of deteriorating reinforced concrete structures. The quantification of interrelationships between the parameters should be based on a good understanding of the expected relations that can be determined theoretically using this method. The method also allows for the consideration of non-measured parameters in the analysis of relationships and to qualitatively identify the most influencing and influenced parameters. Finally, the results of the qualitative analysis can serve as a guideline for the statistical analysis.

The identification of the most influencing parameters was performed using three different approaches : qualitative and quantitative analyses using the matrix of interaction and univariate regression analysis of all variables. It was observed that no individual variable was able to explain adequately the parameter of interest (with regards to the corrosion reaction) : the corrosion rate. The results obtained from the three analyses corresponded well : the most important variables identified being mostly identical : the half-cell potential, compressive strength, volume of permeable pore space (voids), pulse velocity, and chloride diffusion (migration) were identified as the most contributive parameters to the corrosion process.

The water permeability was not considered properly in the analysis since the locations tested for water permeability did not correspond with the locations tested for other tests. It was decided not to average the results obtained based on the observed variability of the test technique and of the concrete on the Dickson Bridge.

Significant relationships were outlined between newly developed techniques and standard techniques, and it was found that the half-cell potential and the pulse

velocity measurements could be used in the future to calibrate the results obtained for the in-situ chloride diffusion migration and the compressive strength, respectively.

The transport mechanisms of water in concrete are of considerable importance since they control the type and velocity of the corrosion reaction. It was found that the quantity of permeable voids greatly influences the absorptivity after immersion, the dry density, the pulse velocity and the half-cell potential. The absorptivity tests all correlate well together, the measurement of the pulse velocity provided valuable information about the permeability of the concrete matrix (highest correlations). The ingress of water and deleterious agents is certainly related to the quantity of interconnected air voids, and is reflected in the results of the analysis. The risks and the rate of corrosion increase with the quantity of air voids present in the vicinity of the steel reinforcement.

Surprisingly, the electrical resistance of concrete, concrete cover and chloride concentration at the rebar level did not correlate well with the other parameters. The electrical resistance measurement is highly influenced by the moisture content of the concrete and the changes locally. Simple to measure, this quantity is not always representative of the concrete quality near the steel reinforcement. The chloride content at the rebar level was found to be correlated with the corrosion rate, but its influence was found to be weaker than expected. The concrete cover and the half-cell potential were not correlated significantly, indicating that the depth of the concrete cover is as important as the quality of the concrete. The ability of the material to resist the ingress of water and deleterious agents is found to be related to the condition of concrete in the vicinity of the steel instead of the actual thickness of the cover.

However, the presence of chlorides and the absence of signs of carbonation were indicative of the mechanism of depassivation of the steel reinforcement. Consequently, the determination of the chloride concentration at the rebar level and of

the carbonation depth are important and contribute to the definition of the mode of attack and of rate of corrosion process.

The determination of the mechanical properties of the concrete using the compressive strength and the pulse velocity measurements proved to contribute significantly to the assessment of the state-of-health of the structure. These quantities estimate the damage to the concrete as a consequence of the expansion of the steel and other detrimental mechanisms (for example the frost action). The mechanical properties of the concrete should therefore be determined in combination with other quantities of interest related to the corrosion process. Also, the extent of concrete deterioration due to steel reinforcement corrosion can only be detected at a late stage of the process, after the expansion of steel leads to the cracking of the surrounding concrete.

The use of several test techniques of different nature is found to be, at this point in time, the best solution to assess the condition of a structure. The number of locations tested should be sufficient to assess the condition of the structure and allow to perform a valid and representative statistical analysis. The locations of the different tests performed should be coincident in order to be considered in the analysis. Because the corrosion process is complex and varies locally with the immediate environment of a member, it is difficult to construct a statistical model that accurately estimate the corrosion reaction at any location. At present, the emphasis should be placed on the development of existing test techniques of interest. Once the condition of a structure can be assessed satisfactorily on a local basis, the collection of data using standard test techniques can eventually lead to the construction of a statistical model for the corrosion process.

6. Conclusions and recommendations

Based on the detailed tests and the results reported in this thesis, the following conclusions and recommendations are formulated.

6.1 Conclusions

Based on the analysis of the data obtained from the testing of the south section of the Dickson Bridge, the following conclusions can be drawn :

- The state-of-health of the south section of the Dickson Bridge was established using all of the results obtained from the different testing techniques. Prediction and assessment techniques, respectively describing the quality of the concrete and the extent of damage to the steel reinforcement, were used. They were found to be the most appropriate techniques available for in-situ and laboratory testing. According to most standard test techniques (half-cell potential, concrete cover, corrosion rate and corrosion potential tests), the concrete bridge deck of the south section of the Bridge showed high risks of developing corrosion of the reinforcing steel for most of the structure. Moreover, the tests results indicated that the east and west sides, along with the north end of the Bridge were in a critical situation with regards to corrosion where the development of the reaction was extensive. However, some portions of the Bridge were found to present moderate to low risks of corrosion and this situation is reflected in the laboratory test results : the cores successfully extracted from the bridge deck (showing no delamination and suitable for laboratory testing) consisted of good and sound concrete with no signs of corrosion in the vicinity the reinforcing steel. This can explain why the results from the laboratory tests contradicted the results of the half-cell potential and other standard tests : the selection of cores suitable for testing was biased since only the specimens of good concrete quality offered the possibility to undertake the laboratory tests. The ingress of chloride ions in the concrete can be identified

as the initiating agent of the corrosion reaction, since no trace of carbonation was found in the vicinity of the deck surface reinforcement where relatively high concentrations of chlorides were observed. In addition, the environmental exposure, especially wetting and drying and freezing and thawing cycles, played an important role in the disruption of the concrete leading to the increase of the general permeability of the media;

- The in-situ measurement of the parameter of interest, the corrosion rate of the reinforcing steel, was performed using the linear polarization resistance technique. Some precautions had to be taken to accurately measure the polarized area of steel, and this was attempted by using a controlling 'guard ring'. According to the risk criteria used, the results obtained by using this LPR method indicated that most of the bridge deck surface reinforcement was in a critical state. The use of this technique is suitable for the in-situ determination of the corrosion rate and of the corrosion potential. However, there is a need to establish the repeatability of the results using this technique : it was observed that the preparation of the test, quality of the electrical connection, and the weather conditions influence greatly the quality of the results obtained;

- The testing program of the south section of the Dickson Bridge was undertaken over two consecutive summers, and necessitated the exposition of some concrete areas (strips) beneath the asphalt overlay sites. The removal of the asphalt overlay started in the summer of 1997. As a consequence, the combined action of the frost and of the mechanical removal of the asphalt cover was found to influence the quality of the results obtained for most tests. In a different perspective, the number of readings, for most tests, was found to be relatively small to allow for the appropriate assessment of the condition of the structure and to undertake a rigorous statistical analysis of the results. However, this situation did not apply to the half-cell potential, linear polarization resistance (which provided the corrosion potential and the corrosion rate measurements), electrical resistivity, and concrete cover tests;

- For the newly developed techniques for which no standard procedure exist (Autoclam in-situ water permability test, and the Queen's of Belfast chloride diffusion migration test, the accuracy and the repeatability were neither established properly during the testing phase of this investigation, nor during testing of the north and central sections of the Dickson Bridge. For the three sections of the bridge, the large values of the coefficient of variation were indicative of this inadequate situation. For the Autoclam water permeability test, the coefficients of variation for the south, and north sections were 142 % and 118 %, respectively. For the central section, a permeability index value was calculated instead of the coefficient of permeability, and cannot be compared directly. Also the results of Table 4.3 show that the situation is similar for the chloride diffusion migration test, even if lower values of the coefficient of variation were obtained for the north and central sections. As a result, the reliability of these techniques remains indeterminate and the interpretation of the results obtained using these techniques was found to be limited. It is important to mention that this situation did not apply to the results for the other techniques;

- The concrete cover survey contradicts all other tests confirming that the quality of the concrete over the steel reinforcement is as important as the thickness with regards to the ingress of water and deleterious agents. It was also observed that the placement of the steel reinforcement mesh was not implemented accurately according to the drawings on the south section of the Dickson Bridge. Both top and bottom steel reinforcement meshes were neither straight nor uniformly spaced with excessively large concrete cover at many locations. Finally, it is important to mention that the real thickness of the concrete cover was not accurately measured due to asphalt removal methodology and / or due to the action of the frost on the exposed strips since in some cases the asphalt removal was performed up to three years prior to the testing. However, it was difficult to determine the average concrete thickness lost while stripping, but it is estimated that a minimum of 10 millimeters of concrete were removed during this operation. The exposure of the strips to weathering is considered to have influenced (accelerated) the

deterioration process of the concrete and the steel reinforcement in the strips, and this is also considered to have contributed to the large variability observed in the results;

- The estimation of the important transport properties in concrete (diffusivity, permeability, and absorptivity) tend to characterize the quality of the hardened cement paste (microstructure). These properties are of invaluable interest for the investigation of deteriorating structure due to durability problems. It is found in this study that the results for chloride diffusion and electrical resistance correlated well with the results from the corrosion rate. On the contrary, the water permeability of the concrete shows a low correlation with the electrical resistance, but correlates well with the half-cell potential and the corrosion rate. As mentioned previously, the large variability observed for the results of the in-situ water permeability is indicative either that the Autoclam method necessitates to be improved, or that the number of observations (readings) considered in the statistical analysis (since most water permeability tests were performed at locations not tested for other tests) was insufficient. This situation would probably be corrected by the establishment of the reliability of the in-situ water permeability test through additional laboratory testing of members of known permeabilities. For this investigation, the results obtained for the water permeability test using the Autoclam should be interpreted with care;

- Considerable effort has been directed into the development of in-situ test techniques to measure the corrosion rate of the steel reinforcement, and water and chloride ion permeabilities. However, these techniques necessitate the formulation of several assumptions which can be partially responsible for the observed variability of the results. For example, the corrosion rate measurement using the linear polarization resistance (LPR) method provide instantaneous results of the general mode of corrosion and neglect to consider the effect of the moisture level and the temperature in the vicinity of the reinforcing bar. Consequently, the results obtained for this investigation using the LPR method are

only representative of the electrochemical situation at the time of testing. It is important to consider that the mean annual rate of corrosion was not measured : the temperature changes within a year, the changes in the moisture content, and the quantity of chlorides in the vicinity of the steel reinforcement are amongst the factors influencing the rate of corrosion at different times of the year. In addition, the pitting corrosion mode cannot be detected by the use of this technique, even if it is one of the most destructive form of corrosion observed. To overcome the limitations of this technique, a combination of several assessment and prediction techniques was used, to obtain the complete picture of the degradation process:

- The multivariate statistical analysis represent an essential aspect of the investigation of deteriorating structures. The correlation of the different tests together is not a simple task and necessitates the preparation of the data set. The matrix of interaction, first developed for mining and geological engineering purposes, can be applied for the analysis of deteriorating structures related to durability aspects. This method provides a valuable tool susceptible to improve the understanding of the expected relationships between the numerous components of an engineering system (structure). In addition, the technique allows for the identification of the most influencing (and influenced) parameters based either on qualitative or quantitative assessment of the influence factors between components (parameters);

- Based on the complete analysis of the data collected on the Dickson Bridge, it appears that the measurement of the corrosion potential is quite important in assessing the corrosion damage. This test should also be performed in combination with the tests for chloride concentration evaluation at the rebar level, the electrical resistivity test, the corrosion rate measurement and the compressive strength;

- The scope of this thesis was not to develop a model susceptible to determine or evaluate the remaining service life of the Dickson Bridge deck, but instead to

identify the most suitable techniques to quantify and assess the state of the corrosion process. It is found that the combined use of several different assessment and prediction techniques is most suitable to explain the corrosion process (represented by the corrosion rate) and to limit the level of the uncertainty. It was decided not to analyze the results of the east and west portions of the bridge separately in this investigation. The main reason for that is that the development of an applicable statistical model for the corrosion process should be independent of the testing area. However, the analysis of the results of all tests performed, the east and west sides of the south section present the same high risks of corrosion. It was not possible to note any significant differences between the results of the two sides. By comparing the results for the three sections of the Dickson Bridge, the following comments can be formulated :

- Based on the results for the half-cell potential, the concrete cover and the corrosion potential tests the north section showed the highest risks of corrosion (critical condition);
- The corrosion rate measurements indicated that the highest readings were observed in the central section, with similar results for the south and north sections;
- The highest chloride concentrations at the rebar level were observed in the south and central sections;
- Finally, the quality of the concrete in the south section was found to be superior to that of the central and north section, with an average compressive strength around 40 MPa;
- It is difficult to determine the section of the Bridge in the most critical situation, but by consideration of all test results, the north section can be identified as the most deteriorated section from all three.

- More work is needed in order to develop reliable models estimating the extent of the damage due to chloride-induced corrosion. The assessment (damage of the steel reinforcement) and prediction (concrete quality) techniques used for the

investigation of the south section of the Dickson Bridge are capable of detecting and quantifying the extent of advanced state of corrosion in the structure. Additional testing should permit quantification of the state and extent of the corrosion process at an earlier stage.

6.2 Recommendations

The investigation of the south section of the Dickson Bridge initially aimed at proposing further development of the in-situ measurement of important relevant parameters with regards to chloride-induced corrosion of the reinforcing steel. According to the analysis of the results, the future of in-situ and laboratory testing of reinforced concrete structures is promising. However, presently, several drawbacks of the methods used in the realization of the testing program of the south section of the Dickson Bridge were identified. It is required that these techniques be studied further before they could lead to an accurate quantification of the corrosion process. In that sense, the following recommendations can be formulated :

- Since the corrosion rate measurement of the steel reinforcement using the linear polarization resistance technique does not account for the moisture level, temperature, and mode of the corrosion reaction, the development of a testing method addressing these concerns should be undertaken in order to possibly consider the possibility of detecting the extent of the pitting corrosion mode, considered as the most destructive form of all. From the three influencing factors mentioned above, the moisture level is the most significant one, followed by the temperature and finally the mode of corrosion. The chloride concentration at the rebar level and the electrical resistance also influence the corrosion reaction significantly, but they should be measured individually. Because it remains economically and technically difficult to collect data on a continuous basis for the different seasons, a viable alternative to estimate the corrosion rate could be to measure the highest rate of corrosion associated with the mean moisture and temperature conditions. In addition, laboratory measurement of the most corroded bars identified using the half-cell potential test could be used to obtain good estimates of the relationships between these two techniques. Furthermore, the half-cell test could be calibrated and used to estimate the extent of the corrosion reaction. The solutions proposed here would allow limiting the costs of

testing at a minimum, since the economical implications represent a major issue in the investigation of reinforced concrete structures;

- The considerations of external influencing factors affecting the corrosion process such as the environmental exposure, and the design, and workmanship quality should be included in any durability analysis. The use of matrix of interactions revealed to be a valuable tool in considering the relationships of a series of factors. The quantification of these external factors remains difficult presently, and further research is needed;

- The scope of the project was to perform a post-mortem analysis of the Dickson Bridge deck and to identify the strengths and weaknesses of available testing methods of interest for testing of the corrosion reaction of the reinforcing steel. This was done and, as a result, the most suitable techniques were identified and selected to develop a model for the corrosion process. However, the reliability and the accuracy of most techniques were not determined appropriately. Again, further work is needed in this direction;

- Intensive testing of bridge decks is costly, and, before undertaking expensive in-situ test programs on deteriorating structures, it is recommended to perform additional laboratory development of the techniques involved;

- Testing of concrete remains a complex task. The variable character of the concrete microstructure is basically responsible for the difficulties in obtaining representative measurement of some properties. In addition, the formation of the corrosion micro-cells within the reinforcement mesh is difficult to detect or predict. As a consequence, the estimation of the extent of damage due to the corrosion reaction can only be achieved by the consideration of several properties of both the concrete and the steel reinforcement. Adequate planning of the testing program combined with the complete statistical analysis of the results, and the use of documented reliable testing techniques appear to be the best solution to obtain

a satisfying estimate of the existing deterioration in a structure. In the present investigation, the in-situ water permeability test using the Autoclam method, the in-situ chloride diffusion (migration) test developed at Queen's University of Belfast, the linear polarization resistance technique were identified as the testing techniques requiring further development.

7. References

[1] Mather, B., "Realizing the Potential of Concrete As A Construction Material", Design, Materials, Construction, Proceedings of the International Congress 'Creating with Concrete', Thomas Telford Ltd., University of Dundee, Scotland, 1999, pp. 1-10.

[2] Hoff, G. C., "Integrating Durability Into the Design Process", Opening and Leader Papers, Proceedings of the International Congress 'Creating with Concrete', Thomas Telford Ltd., University of Dundee, Scotland, 1999, pp.101-114.

[3] Tuutti, K., "Repair Philosophy for Concrete Structures", Concrete Durability and Repair Technology, Proceedings of the International Congress 'Creating with Concrete', Thomas Telford Ltd., University of Dundee, Scotland, 1999, pp. 159-169.

[4] Geiker, M., "Durability Design of Concrete Structures Minimising Total Life-Cycle Costs – Considerations and Examples", Concrete Durability and Repair Technology, Proceedings of the International Congress 'Creating with Concrete', Thomas Telford Ltd., University of Dundee, Scotland, 1999, pp.319-333.

[5] Brandt, A. M., Kucharska, L., "Developments in Cement-Based Composites", Extending Performance of Concrete Structures, Proceedings of the International Congress 'Creating with Concrete', Thomas Telford Ltd., University of Dundee, Scotland, 1999, pp. 17-32.

[6] Tajalli, S. M. A. , Rigden, S.R., "Non and Partially Destructive Testing of Forty Concrete Bridges", Concrete Durability and Repair Technology,

Proceedings of the International Congress 'Creating with Concrete', Thomas Telford Ltd., University of Dundee, Scotland, 1999, pp. 219-228.

[7] Sommerville, G., "Whole Life Design for Durability, Where Are We Going, And How Do We Get There ?", Opening and Leader Papers, Proceedings of the International Congress 'Creating with Concrete', Thomas Telford Ltd., University of Dundee, Scotland, 1999, pp. 221-239.

[8] Van Gemert, D., "Extending Structural Performance of Concrete Constructions", Extending Performance of Concrete Structures, Proceedings of the International Congress 'Creating with Concrete', Thomas Telford Ltd., University of Dundee, Scotland, 1999, pp. 1-16.

[9] Henriksen, C., Michaux, C., "Prediction of Service Life and Choice of Repair Strategy", Concrete Durability and Repair Technology, Proceedings of the International Congress 'Creating with Concrete', Thomas Telford Ltd., University of Dundee, Scotland, 1999, pp. 611-619.

[10] Mangat, P. S., O'Flaherty, F., "Long Term Performance Criteria for Concrete Repair Materials", Concrete Durability and Repair Technology, Proceedings of the International Congress 'Creating with Concrete', Thomas Telford Ltd., University of Dundee, Scotland, 1999, pp. 381-393.

[11] Vogel, T., "Operation Suceccessful, Patient Died - The Assigment of Structures As An Engineering (Or Medical) Problem", Concrete Durability and Repair Technology, Proceedings of the International Congress 'Creating with Concrete', Thomas Telford Ltd., University of Dundee, Scotland, 1999, pp. 549-562.

[12] Beeby, A. W., "Design for Life", Design, Materials, Construction, Proceedings of the International Congress 'Concrete 2000 - Economic and

Durable Construction Through Excellence', Vol. 1, E and FN Spon Ltd., University of Dundee, Scotland, 1993, pp. 37-50.

[13] Fazio, R., "The Assessment and Prediction of Reinforcing Steel Corrosion on the Dickson Bridge", M.Eng. Thesis, McGill University, Montreal, Canada, 1999.

[14] Atkinson, J. T. N., Van Droffelaar, H., "Corrosion and Its Control", Second Edition, NACE International Book Publications, Houston, USA, 1995.

[15] Tullu, K.S., "Rehabilitation of Concrete Bridges", M.Eng. Thesis, McGill University, Montreal, Canada, 1992.

[16] Etebar, K., "Alternative forms of reinforcement for beams subjected to high shear", Extending Performance of Concrete Structures, Proceedings of the International Congress 'Creating with Concrete', Thomas Telford Ltd., University of Dundee, Scotland, 1999, pp. 63-73.

[17] Neville, A. M., "Properties of Concrete", Fourth Edition, Longman Group Ltd, London, UK, 1995.

[18] Sarja A.,. Vesikari E., "Durability Design of Concrete Structures", Report of RILEM Technical Committee 130-CSL, E and FN Spon Ltd., Espoo, Finland, 1996.

[19] Comité Euro-International du Béton (CEB), "Durable Concrete Structures", Thomas Telford Ltd., London, UK, 1992.

[20] Staehle, R. W., "Relationship Among Statistical Distributions, Accelerated Testing, and Future Environments", Application of Accelerated Corrosion Tests To Service Life Prediction of Materials, ASTM STP1194, Gustavo

Cragnolino and Narasi Sridhar, Eds., American Society of Testing Materials, Philadelphia, USA, 1994.

[21] Perenchio, W. F., "Corrosion of Reinforcing Steel", Significance of Tests and Properties of Concrete and Concrete-Making Materials, ASTM STP 169C, P. Klieger and J.F. Lamond, Eds, Fredericksburg, USA, 1994.

[22] Fontana, M. G., "Corrosion Engineering", McGraw-Hill Ltd., Toronto, Canada, 1986.

[23] Mehta, P. K., "Durability of Concrete Structures", McGraw-Hill Ltd., Toronto, Canada, 1986.

[24] Bungey, H. H., Millard S. G., "Testing of Concrete in Structures", Blackie Academic and Professional Ltd., London, UK, 1995.

[25] El-Jachi, A., "Corrosion Deterioration of Central Section of Dickson Bridge", M.Eng. Project Report, McGill University, Montreal, Canada, 1999.

[26] Amleh, L., "Corrosion of Reinforcing Steel on the Dickson Bridge", Ph. D. Thesis, McGill University, Montreal, Canada, Fall 2000.

[27] Vassie, P. R., "The Half-Cell Potential Method of Locating Corroding Reinforcement in Concrete Structures", Transport Research Laboratory Application Guide AG9, Crowthorne Ltd., Berkshire, UK, 1991.

[28] Hudson, J. A., "Rock Engineering Systems", Ellis Horwood Ltd., Chichester, UK, 1992.

[29] Schiff, D., D'Agostino R.B., "Practical Engineering Statistics", John Wiley and Sons Ltd., New York, USA, 1996.

[30] McCafferty, E., "Relationship Between Permeation Properties and Concrete Deterioration on the Dickson Bridge", M. Sc. Dissertation, The Queen's University of Belfast, Belfast, UK, 1998.

[31] ASTM C642. "Standard Test Method for Density, Absorption, and Voids in Hardened Concrete", American Society for Testing and Materials, Philadelphia, USA, 1997.

Appendix A : Experimental results

Appendix A presents some experimental results for the different parameters of interest measured on the south section of the Dickson Bridge. Since it would be too exhaustive to present all of the experimental data collected during the investigation of the bridge deck, the results for the half-cell potential, the cover meter are not presented here. Also, for the chloride diffusion migration test, the apparent chloride diffusion test, the in-situ water permeability test, the electrical resistivity test, the corrosion rate test, and the chloride concentration at rebar test only an example of collected data is presented. Figures A.1 to A.10 follow :

A.1 In-situ chloride diffusion migration test (CD_m)

Chloride Ion Migration Test

Bridge Span	South
Bridge Side	East
Strip Number	1 SE
Strip Coordinate	222F
Date of testing	9/24/98
Operator	Ali

Calibration :

Voltmeter Reading V (mV)	Cl- Concentration CCl (ppm)
180.70	100.00
125.60	1000.00

Site data

Sample	Time	Temperature			Current
		Ambient (*)	Anode (out)	Cathode (in)	
	(24 hrs)	t_m (°C)	t_a (°C)	t_c (°C)	I (A)
Initial	16:10	16	16	16	0.06
# 1	18:10	15	16.5	17	0.07
# 2	19:10	15.5	17	17.5	0.09
# 3	20:10	15	17	18	0.1
# 4	21:10	15	17	19	0.11
# 5	22:10	14	17	19	0.11

Laboratory analysis

Voltmeter Reading V (mV)	Cl^- Concentration C_{Cl} (ppm)	Steady State Cl^- Migration dc/dt ($mol.cm^{-3}.s^{-1}$)	Volume of Anodic Cell V (cm^3)	Temp. of Anodic Cell T (K)	Flux of Chloride Ions J ($mol.cm^{-2}.s^{-1}$)	CD Coefficient Migration CD_m ($cm^2.s^{-1}$)
213.3	25.6	1.003228E-10	725.00	289.65	6.22E-10	5.76E-09
198.9	46.7	1.656002E-10	705.00	290.15	9.98E-10	9.26E-09
188.2	73.1	2.065041E-10	685.00	290.15	1.21E-09	1.12E-08
177.0	116.7	3.418515E-10	665.00	290.15	1.94E-09	1.80E-08
165.5	188.7	5.643139E-10	645.00	290.15	3.11E-09	2.89E-08
						1.46E-08

Remarks : (*) Ambient temperature : in sun shade and wind shield

Figure A.1 Experimental results for the in-situ chloride diffusion migration tests.

A.2 In-situ water permeability test (WP)

Water Permeability Test

Bridge Span : South
Bridge Side : East
Strip Number 3SE
Strip Coordinate : 234-237/I-J
Date of testing : 09/09/98
Operator : A.M.

Time	Spot #1		Spot #2		Spot #3		Spot #4	
	Piston	Volume	Piston	Volume	Piston	Volume	Piston	Volume
(minute)	(mm)	(m^3)	(mm)	(m^3)	(mm)	(m^3)	(mm)	(m^3)
0	0.000	0.000E+00	0.000	0.000E+00	Chloride		0.000	0.000E+00
1	0.034	6.008E-09	0.136	2.403E-08	Migration		0.089	1.573E-08
2	0.067	1.184E-08	0.229	4.047E-08	Test		0.145	2.562E-08
3	0.094	1.661E-08	0.297	5.248E-08			0.191	3.375E-08
4	0.112	1.979E-08	0.354	6.256E-08			0.226	3.994E-08
5	0.128	2.262E-08	0.402	7.104E-08			0.254	4.489E-08
6	0.140	2.474E-08	0.447	7.899E-08			0.280	4.948E-08
7	0.148	2.615E-08	0.481	8.500E-08			0.305	5.390E-08
8	0.160	2.827E-08	0.519	9.171E-08			0.325	5.743E-08
9	0.171	3.022E-08	0.552	9.755E-08			0.344	6.079E-08
10	0.179	3.163E-08	0.580	1.025E-07			0.364	6.432E-08
11	0.188	3.322E-08	0.612	1.081E-07			0.384	6.786E-08
12	0.198	3.499E-08	0.638	1.127E-07			0.400	7.069E-08
13	0.206	3.640E-08	0.664	1.173E-07			0.409	7.228E-08
14	0.214	3.782E-08	0.686	1.212E-07			0.414	7.316E-08
15	0.221	3.905E-08	0.711	1.256E-07			0.420	7.422E-08
WP (m/s)		5.698E-15		1.856E-14				1.035E-14

Remarks : Calibration factor = 0.207 x 10^{-3} WP Results : 1.154E-14 m/s (average value from all tests)

Figure A.2 Experimental results for the in-situ water permeability tests.

A.3 Electrical resistivity test (ER)

Standard Test of Concrete Resistivity

Spacing between probes (Weiner configuration) : 5.00 cm

Strip #	Location #	Resistance ρ (ohm)	Resistivity ER (ohm x cm)	Resistivity ER (ohm x cm)
2 South West	2SW-1	125	3926.99	3926.99
	2SW-2	95	2984.51	2984.51
	2SW-4	130	4084.07	4084.07
3 South West	3SW-1	130	4084.07	4084.07
	3SW-2	130	4084.07	4084.07
	3SW-3	175	5497.79	5497.79
	3SW-4	120	3769.91	3769.91
	3SW-5	130	4084.07	4084.07
4 South West	4SW-3	210	6597.34	6597.34
	4SW-4	120	3769.91	3769.91
6 South West	6SW-2	150	4712.39	4712.39
	6SW-3	165	5183.63	5183.63
	6SW-4	170	5340.71	5340.71
7 South West	7SW-1	110	3455.75	3455.75
	7SW-2	105	3298.67	3298.67
	7SW-3	185	5811.95	5811.95
	7SW-4	95	2984.51	2984.51
8 South West	8SW-1	150	4712.39	4712.39
	8SW-2	170	5340.71	5340.71
	8SW-3	130	4084.07	4084.07
	8SW-4	115	3612.83	3612.83
9 South West	9SW-1	210	6597.34	6597.34
	9SW-2	500	15707.96	15707.96

Figure A.3 Experimental results for the electrical resistivity tests.

A.4 Pulse velocity test (PV and E_pv)

Standard Test Method for Pulse Velocity through Concrete
ASTM C 597-97

Masses	A2	A3	A	B	C	=A*B/C
Sample Ident. Number	Length of steel (mm)	Location of steel E = Edge C = Center T = Transversal	Correction factor for steel	Length (measured) (mm)	Transit Time (10^{-6}s)	Pulse Velocity (km/s)
2SE-3	15.88	T - C	0.947	98.04	27.0	3.44
3SE-3	0.00	-	1.000	61.18	15.6	3.92
4SE-1	0.00	-	1.000	84.36	24.6	3.43
4SE-2	0.00	-	1.000	105.12	31.7	3.32
7SE-1	15.88	T - E	0.945	93.48	25.2	3.50
8SE-2	15.88	T - C	0.940	85.46	24.2	3.32
8SE-3	15.88	T - E	0.950	102.88	28.3	3.45
12SE-?	0.00	-	1.000	79.76	20.1	3.97
15SE-1	15.88	T - C+E	0.953	109.66	28.6	3.65
17SE-2	31.76	T - C+E	0.914	119.38	33.6	3.25
2SW-2	15.88	T - E	0.943	90.92	24.7	3.47
4SW-3	0.00	-	1.000	60.90	17.4	3.50
4SW-4	0.00	-	1.000	91.66	25.1	3.65
6SW-2	15.88	T - E	0.947	96.50	26.3	3.47
6SW-3	15.88	T - E	0.950	103.74	27.7	3.56
7SW-2	15.88	T - C	0.948	99.42	29.0	3.25
7SW-4	15.88	T - C	0.949	101.20	30.6	3.14
8SW-1	0.00	-	1.000	68.46	16.3	4.20
8SW-4	15.88	T - E	0.951	104.68	27.1	3.67
9SW-2	15.88	T - C	0.943	90.76	25.5	3.36
13SW-1	15.88	T - C	0.945	93.78	25.1	3.53
13SW-2	15.88	T - C	0.929	72.42	20.6	3.27
15SW-1	15.88	T - C	0.946	95.76	25.6	3.54
19SW-1	15.88	T - C	0.953	109.00	31.5	3.30
19SW-3	15.88	T - E	0.932	75.56	24.3	2.90

Calibration = Using steel bar t=25.7micro sec, f = 54 kHz
Apparatus = Length Mitotoyo accuracy = 0.02mm
Location of test = Material Lab T = 24 C
Date of testing = 11/11/99
Operator = Francois Laplante

$k = 1 - .325 \times L_S / L$ (pundit manual, fig. 7)
$V = k \times L / T$
Bar diameter = 5/8" = 15.88 mm
X : core not suitable for testing.

Figure A.4 Experimental results for the pulse velocity tests.

A.5 Absorptivity tests (AB_astm, SD_b, SD_a, and VV)

Standard Test Method for Density, Absorption, and Voids in Hardened Concrete
ASTM C 642-97

Masses

#	A-1	A	Corr. A	A Corr.	B	Corr. B	B Corr.	C	D	Corr. D	D Corr.
Sample Ident. Number	Ambient (g)	Oven Dry (g)	Steel Dry (g)	Oven Dry Corrected (g)	Saturated Immersion (g)	Steel Immersion (g)	Corr. Sat. Immersion (g)	Saturated After Boil. (g)	Immersed Apparent (g)	Steel Immersed (g)	Corrected Imm. App. (g)
2SE-3	1031.45	1030.3	112.08	918.2	1099.67	112.08	987.59	Use B	441	14.60	426.4
3SE-3	660.09	659.7	0.00	659.7	694.80	0.00	694.80	Use B	282.5	0.00	282.5
4SE-1	891.18	890.4	0.00	890.4	946.02	0.00	946.02	Use B	389.2	0.00	389.2
4SE-2	1105.57	1104.3	0.00	1104.3	1178.22	0.00	1178.22	Use B	487.2	0.00	487.2
7SE-1	1034.62	1033.7	54.27	979.4	1087.95	54.27	1033.68	Use B	432.6	7.20	425.4
8SE-2	959.72	959.1	108.49	850.6	1018.26	108.49	909.77	Use B	395.2	13.90	381.3
8SE-3	1078.90	1077.8	17.50	1060.3	1140.12	17.50	1122.62	Use B	465.3	2.20	463.1
12SE-7	773.63	772.2	0.00	772.2	823.63	0.00	823.63	Use B	355	0.00	355
15SE-1	1251.88	1251.1	170.04	1081.1	1312.62	170.04	1142.58	Use B	495.6	22.10	473.5
17SE-2	1319.64	1318.4	198.33	1120.1	1391.52	198.33	1193.19	Use B	528.7	10.70	518
2SW-2	964.55	963.6	61.66	901.9	1019.00	61.66	957.34	Use B	409.6	23.00	386.6
4SW-3	712.95	712.5	0.00	712.5	747.11	0.00	747.11	Use B	307	0.00	307
4SW-4	968.00	967.2	0.00	967.2	1021.50	0.00	1021.50	Use B	426.1	0.00	426.1
6SW-2	1089.52	1088.5	96.85	991.7	1144.16	96.85	1047.31	Use B	448.1	13.40	434.7
6SW-3	1151.50	1150.4	86.66	1063.7	1210.78	86.66	1124.12	Use B	481.2	11.40	469.8
7SW-2	1084.51	1083.1	99.17	983.9	1155.00	99.17	1055.83	Use B	461.3	13.20	448.1
7SW-4	1067.12	1066.0	89.36	976.6	1143.35	89.36	1053.99	Use B	465.2	12.30	452.9
8SW-1	707.53	706.8	0.00	706.8	745.82	0.00	745.82	Use B	313.8	0.00	313.8
8SW-4	1127.43	1126.6	69.20	1057.4	1190.64	69.20	1121.44	Use B	479.5	10.50	469
9SW-2	1015.22	1014.0	115.31	898.7	1070.79	115.31	955.48	Use B	414.2	15.00	399.2
13SW-1	1015.39	1014.7	110.17	904.5	1069.04	110.17	958.87	Use B	426.7	15.00	411.7
13SW-2	785.45	784.7	109.70	675.0	834.12	109.70	724.42	Use B	327.3	15.60	311.7
15SW-1	1045.81	1045.0	114.08	930.9	1103.00	114.08	988.92	Use B	436.5	15.40	421.1
19SW-1	1182.59	1181.3	114.60	1066.7	1243.68	114.60	1129.08	Use B	497.6	15.20	482.4
19SW-3	777.43	776.0	97.36	678.6	821.87	97.36	724.51	Use B	344.6	13.20	331.4
Date :	4/11/99 12:30	3/11/99 13:30			8/11/99 17:30				8/11/99 17:30		

Monday @ 12.00 Put in oven (100degC +-5) for at least 48 hrs
Wednesday @ 13:30 Weighed in grad lab using balance near the oven Reading A taken
Thursday @ 13:30 End of 24 hrs period for cooling to ambient temperature Reading A-1 taken
Thursday @ 13.30 Start of immersion in water @ 21 C for at least 48 hrs
Monday @ 17:30 Readings B (samples surface dryed using a towel) and D (just after C using elastics) taken

Assuming no water is absorbed by the steel reinforcement

Figure A.5 Experimental results for the absorptivity tests.

A.6 Compressive strength test (CS and E_cs)

Standard Test Method for Compressive Strength
ASTM C 42-90

Masses	A	B	C	D	E	F	G	H
Sample Ident. Number	Length (capped) (mm)	Length (uncapped) (mm)	Specimen Diameter (mm)	A / C Ratio	Correction factor for steel	Specimen Area (mm^2)	Force Peak (kN)	f'c (kPa)
2SE-3	106.0	98.04	74.0	1.4	0.9519	4300.8	185.604	41.1
3SE-3	69.0	61.18	74.0	0.9	0.8700	4300.8	306.184	61.9
4SE-1	97.0	84.36	74.0	1.3	0.9373	4300.8	224.681	49.0
4SE-2	116.0	105.12	74.0	1.6	0.9654	4300.8	204.612	45.9
7SE-1	104.0	93.48	73.5	1.4	0.9498	4242.9	249.491	55.8
8SE-2	100.0	85.46	74.0	1.4	0.9422	4300.8	237.706	52.1
8SE-3	109.0	102.88	74.0	1.5	0.9568	4300.8	248.716	55.3
12SE-?	88.0	79.76	74.0	1.2	0.9154	4300.8	194.908	41.5
15SE-1	119.0	109.66	73.5	1.6	0.9695	4242.9	190.566	43.5
17SE-2	125.0	119.38	73.5	1.7	0.9761	4242.9	215.680	49.6
2SW-2	96.0	90.92	74.5	1.3	0.9346	4359.2	251.352	53.9
4SW-3	76.0	60.90	74.5	1.0	0.8748	4359.2	287.638	57.7
4SW-4	100.0	91.66	74.5	1.3	0.9411	4359.2	235.146	50.8
6SW-2	103.0	96.50	74.0	1.4	0.9470	4300.8	231.193	50.9
6SW-3	117.5	103.74	74.5	1.6	0.9662	4359.2	240.963	53.4
7SW-2	108.0	99.42	74.0	1.5	0.9551	4300.8	187.310	41.6
7SW-4	108.0	101.20	74.5	1.4	0.9540	4359.2	214.601	47.0
8SW-1	75.0	68.46	74.0	1.0	0.8732	4300.8	229.023	46.5
8SW-4	116.0	104.68	73.5	1.6	0.9663	4242.9	180.642	41.1
9SW-2	99.0	90.76	74.0	1.3	0.9405	4300.8	224.215	49.0
13SW-1	104.0	93.78	73.0	1.4	0.9510	4185.4	168.392	38.3
13SW-2	82.0	72.42	73.5	1.1	0.8978	4242.9	251.042	53.1
15SW-1	110.0	95.76	73.5	1.5	0.9596	4242.9	197.854	44.7
19SW-1	118.0	109.00	74.0	1.6	0.9676	4300.8	167.926	37.8
19SW-3	92.0	75.56	74.0	1.2	0.9284	4300.8	125.948	27.2

Loading rate = 0.001 mm/s for 1st 4 tests then 0.002 mm/s
Apparatus = MTS Press
Levelling technique = Capping compound
Date of testing = 21/12/1999
Operator = F. Laplante

Figure A.6 Experimental results for the compressive strength tests.

A.7 Linear polarization resistance test (LP_cr and E_cp)

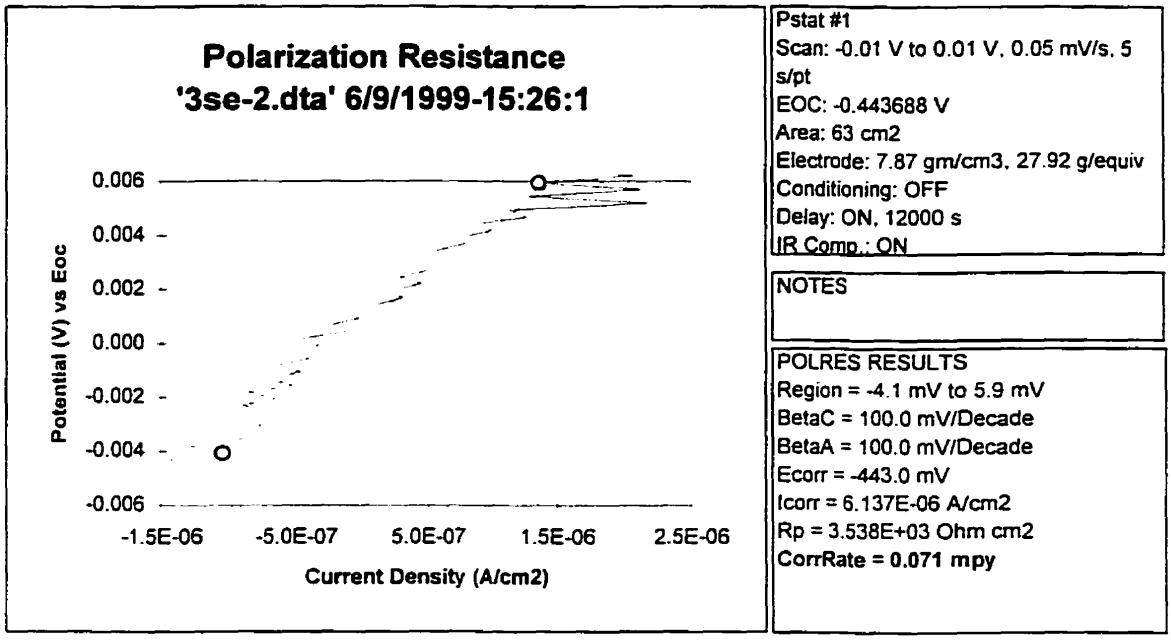

Figure A.7 Experimental results for the linear polarization resistance tests (site 3SE, location 2).

A.8 Carbonation depth test (CR)

Carbonation Depth test (taken directly on the samples)

Sample Identification Number	Thickness of concrete cut from assumed surface (mm)	Carbonation Depth Core Top (mm)	Carbonation Depth Core Bottom (mm)
2SE-3	2	0.0	Not tested
3SE-3	1	0.0	Not tested
4SE-1	2	0.0	Not tested
4SE-2	1	0.0	Not tested
7SE-1	2	0.0	Not tested
8SE-2	1	0.0	Not tested
8SE-3	1	0.0	Not tested
12SE-?	1	0.0	Not tested
15SE-1	1	0.0	Not tested
17SE-2	2	0.0	Not tested
2SW-2	1	0.0	Not tested
4SW-3	1	0.0	Not tested
4SW-4	5	0.0	Not tested
6SW-2	1	0.0	Not tested
6SW-3	1	0.0	Not tested
7SW-2	5	0.0	Not tested
7SW-4	5	0.0	Not tested
8SW-1	1	0.0	Not tested
8SW-4	5	0.0	Not tested
9SW-2	1	0.0	Not tested
13SW-1	3	0.0	Not tested
13SW-2	2	0.0	Not tested
15SW-1	1	0.0	Not tested
19SW-1	1	0.0	Not tested
19SW-3	1	0.0	Not tested

12/1/2000 17:00:00 P12/1/2000 17:00:00 PM

Apparatus = Phenolphtalein solution in a spray bottle
Location of test = Material Lab T = 24 C
Date of testing = 12th of January 2000
Operator = Francois Laplante

Figure A.8 Experimental results for the carbonation depth tests.

A.9 Chloride ion concentration at rebar test (CC_rb and CD_a)

Sample Ident. Number	Depth of bottom (mm)	Depth of center (mm)	Chloride potential Test Value (mV)	Chloride Content (% weigth)	Chloride Diffusion Intercept	Chloride Diffusion Slope	Chloride Diffusion Coefficient (cm2/s)	Presence of Steel
2SE-3	15	7.5	190.6	0.401	6.058E-01	-1.613E-03	1.065E-07	-
	30	22.5	200.1	0.259				-
	55	42.5	196.8	0.302				Steel
	70	62.5	199.7	0.264				-
3SE-3	15	7.5	180.4	0.638	8.123E-01	-1.090E-03	4.192E-07	-
	30	22.5	180.6	0.632				-
	45	37.5	181.8	0.598				CM Steel
	60	52.5	183.1	0.564				-
4SE-1	15	7.5	208.8	0.134	3.295E-01	-1.730E-04	2.739E-06	-
	30	22.5	218.8	0.081				-
	45	37.5	218.0	0.085				CM Steel
	60	52.5	210.0	0.126				-
4SE-2	15	7.5	205.1	0.160	3.688E-01	7.436E-04	1.857E-07	-
	30	22.5	209.9	0.127				-
	45	37.5	207.5	0.143				-
	60	52.5	202.1	0.185				CM Steel
7SE-1	15	7.5	186.5	0.483	7.505E-01	-5.845E-03	1.245E-08	-
	30	22.5	190.6	0.401				-
	55	42.5	199.9	0.262				Steel
	70	62.5	214.3	0.133				-
	85	77.5	221.5	0.094				-

Figure A.9 Experimental results for the chloride ion concentration at rebar tests.

Chloride Diffusion Coefficient (Apparent)
Chloride profiles

	Probe Check	Date	1 millimeter	10 millimeters	Difference
		19/01/2000	240.8	186.9	53.9
	Calibration	19/01/2000			
	Solution 5	**Solution 4**	**Solution 3**	**Solution 2**	**Solution 1**
[Cl], %	**1.25%**	**0.60%**	**0.30%**	**0.03%**	**0.01%**
[Cl], ppm	**374**	**180**	**90**	**9**	**3**
Value 1, mV	159.8	176.2	196.9	247.5	258.7
Value 2, mV	156.5	175.6	198.8	249	260.3
Value 3, mV	157.8	178.9	200.8	249.7	262.8
Mean, m	**158.03**	**176.90**	**198.83**	**248.73**	**260.60**
Variance, VAR	2.76	3.09	3.80	1.26	4.27
Max. variance	4.5	4.5	4.5	4.5	4.5
Acceptance	**Accepted**	**Accepted**	**Accepted**	**Accepted**	**Accepted**
	Probe Check	**Date**	**1 millimeter**	**10 millimeters**	**Difference**
		20/01/2000	242.4	189.2	53.2

Calibration Equation

Intercept	Slope
b	a
5.770614998	-0.019786525

Figure A.10 Experimental results for the apparent chloride diffusion tests.

Appendix B : Summary of individual results

The following are supplementary graphs for Chapter Four. The results for each parameter are plotted showing the corresponding values obtained for each linear polarization location test locations where the cores were taken. It is important to note that only the variables (parameters) used for the statistical analyses of Chapter Five are presented here : as a result, the saturated density and the apparent modulus of elasticity were omitted (for more details refer to Section 5.2).

B.1 In-situ chloride diffusion migration (CD_m)

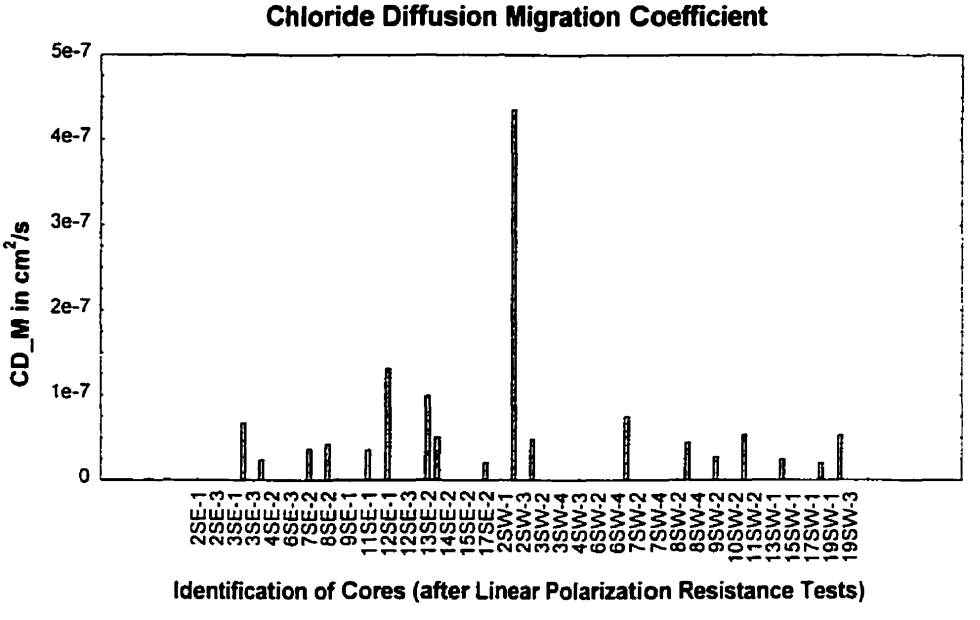

Figure B.1 Bar plot for the in-situ chloride diffusion migration (CD_m).

B.2 In-situ water permeability (WP)

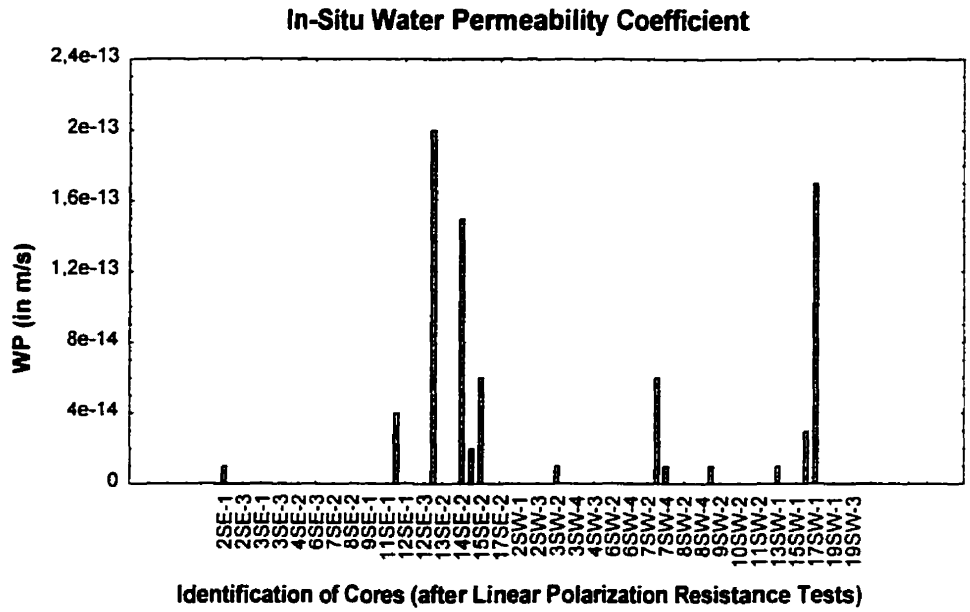

Figure B.2 Bar plot for the in-situ water permeability (WP).

B.3 Electrical resistance (ER)

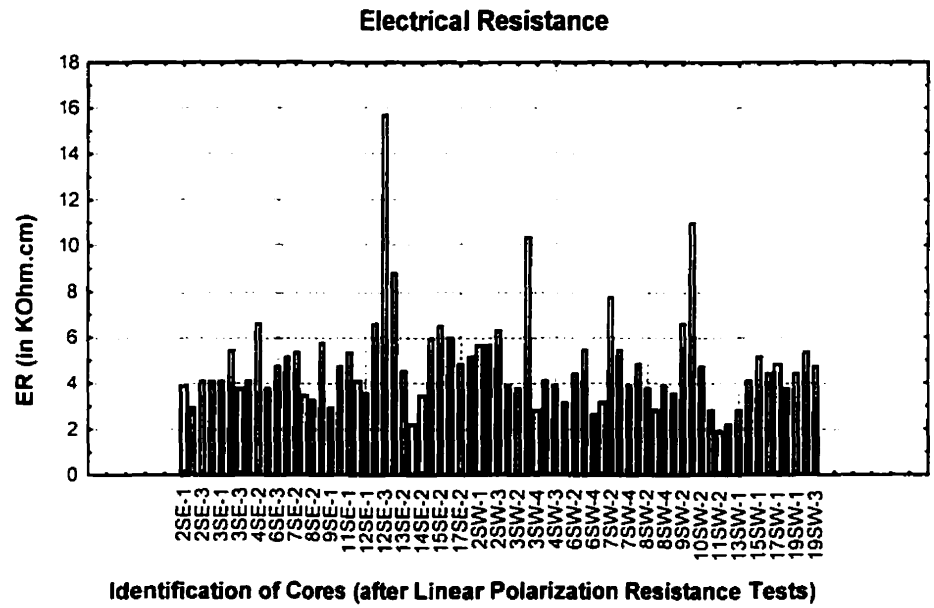

Figure B.3 Bar plot for the electrical resistance (ER).

B.4 Pulse velocity (PV)

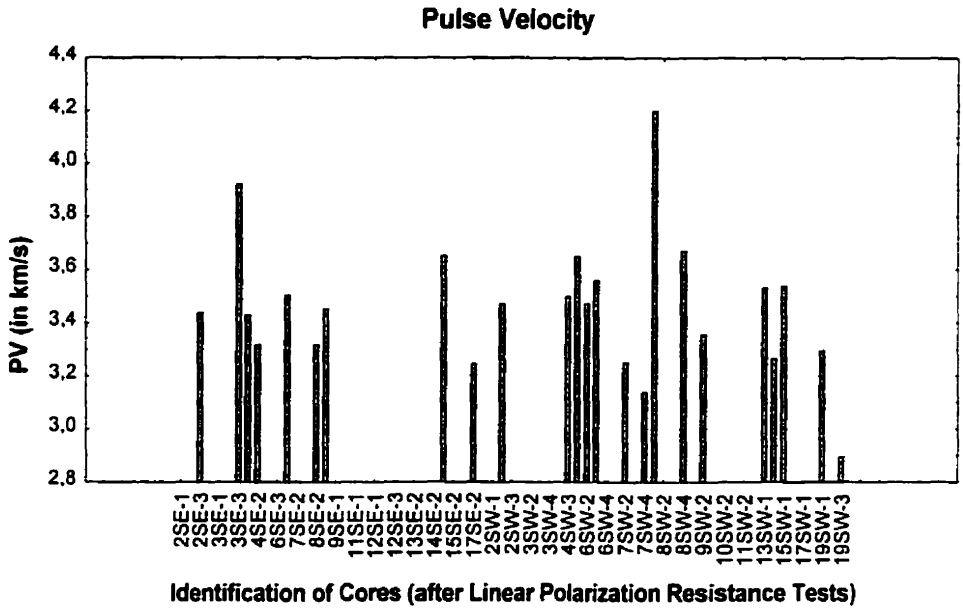

Figure B.4 Bar plot for the pulse velocity (PV).

B.5 Absorptivity after immersion (AB_astm)

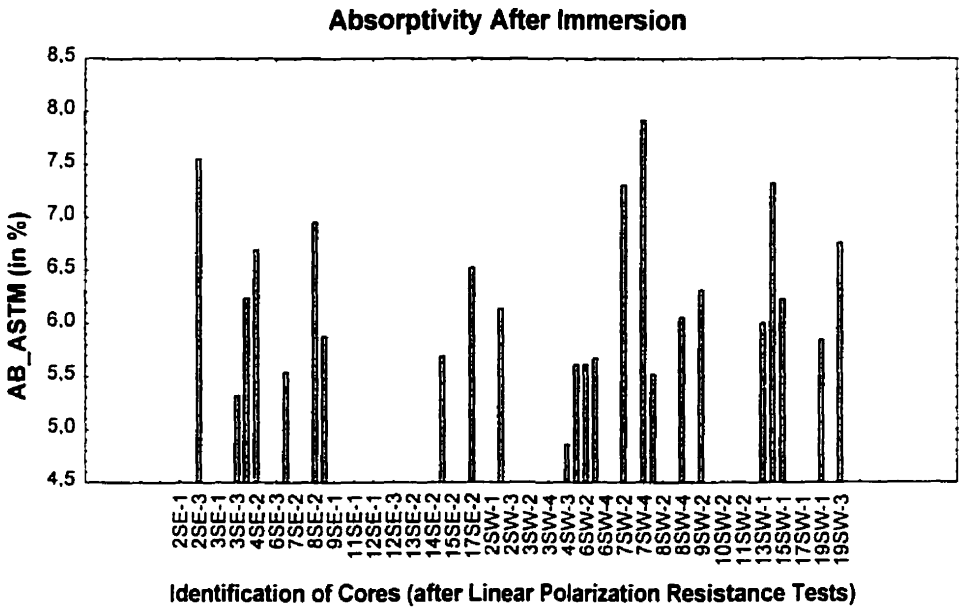

Figure B.5 Bar plot for the absorptivity after immersion (AB_astm).

B.6 Dry density (SD_b)

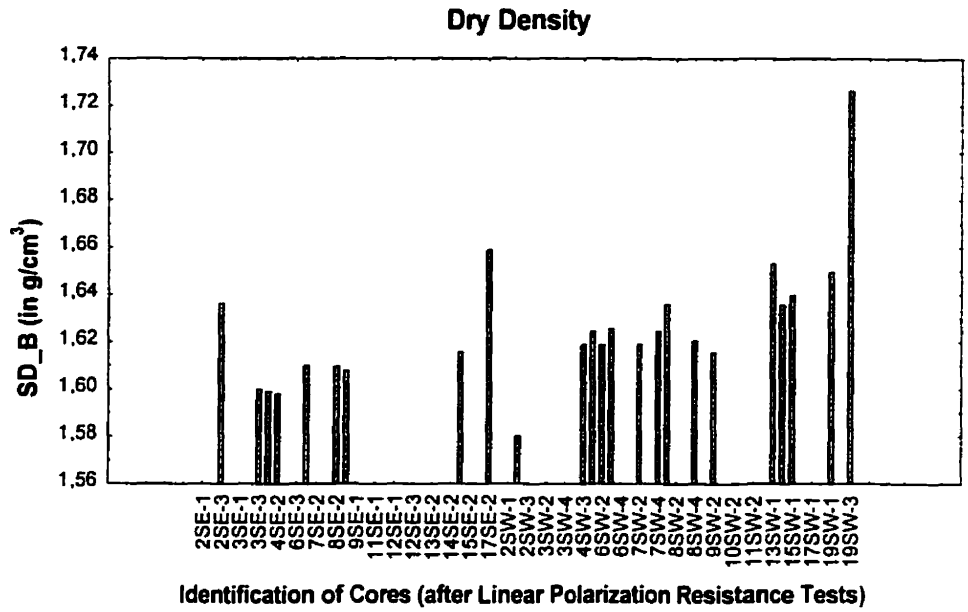

Figure B.6 Bar plot for the dry density (SD_b).

B.7 Volume of permeable voids (VV)

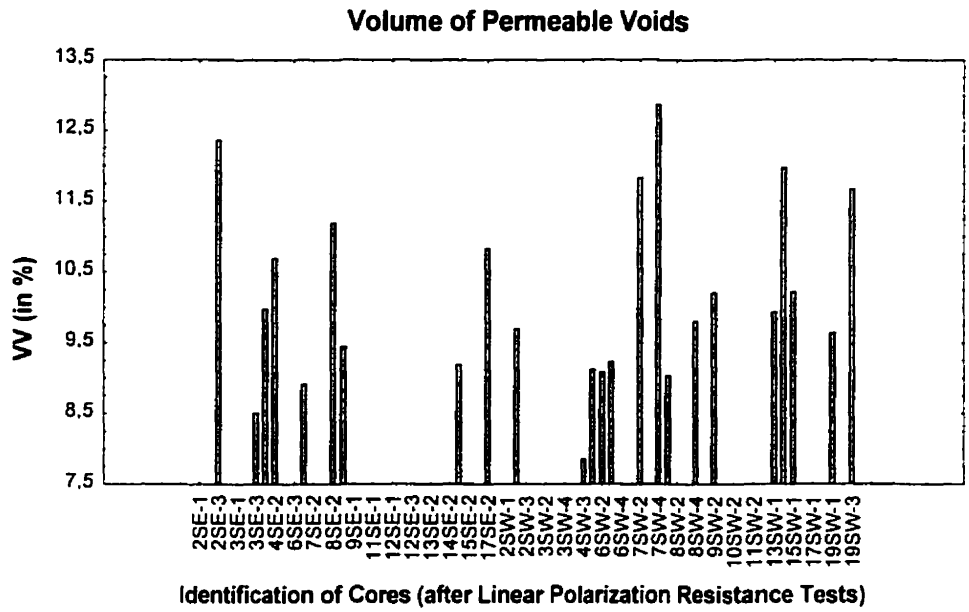

Figure B.7 Bar plot for the volume of permeable voids (VV).

B.8 Compressive strength (CS)

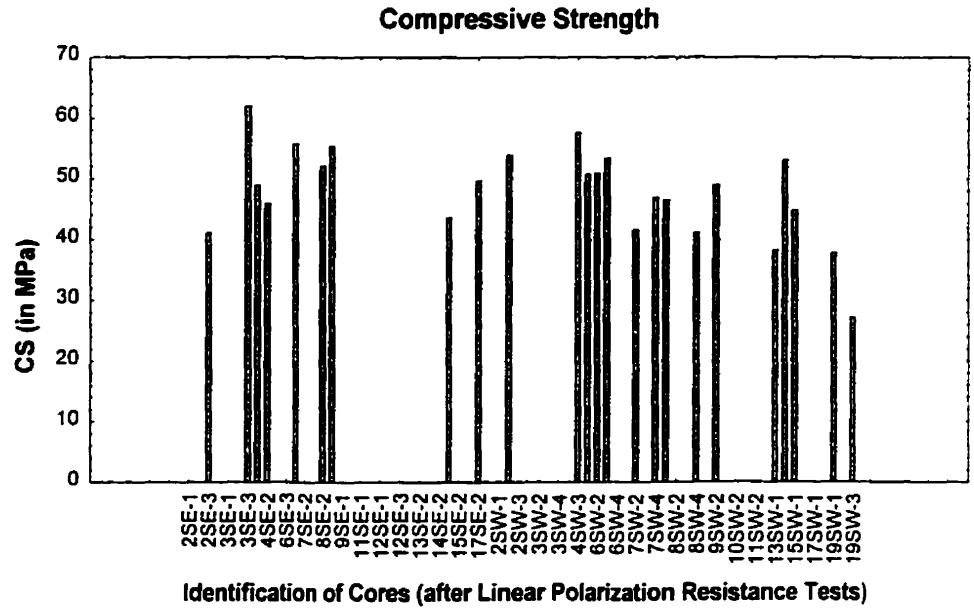

Figure B.8 Bar plot for the compressive strength (CS).

B.9 Modulus of elasticity (E_cs)

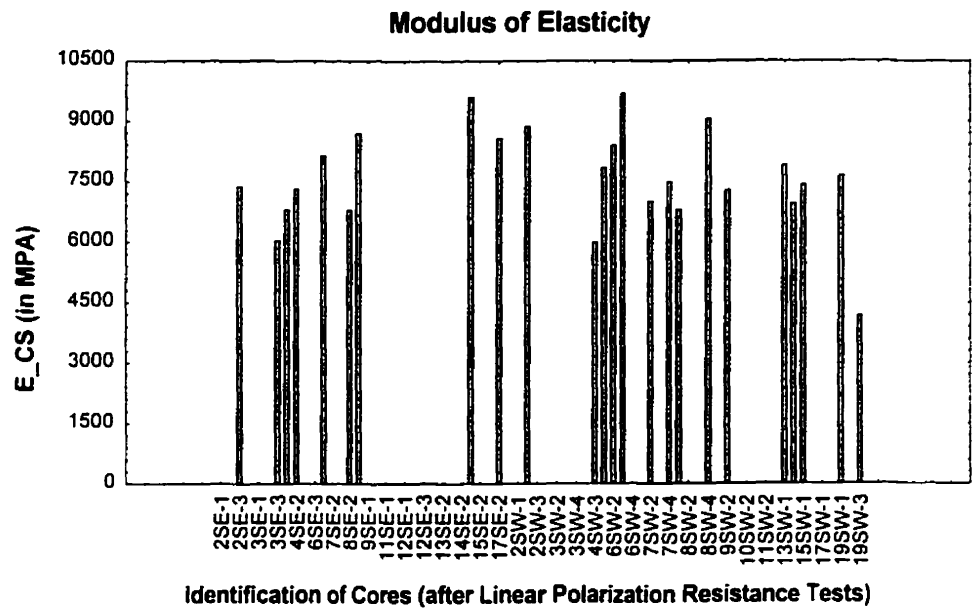

Figure B.9 Bar plot for the modulus of elasticity (E_cs).

B.10 Half-cell potential (HC)

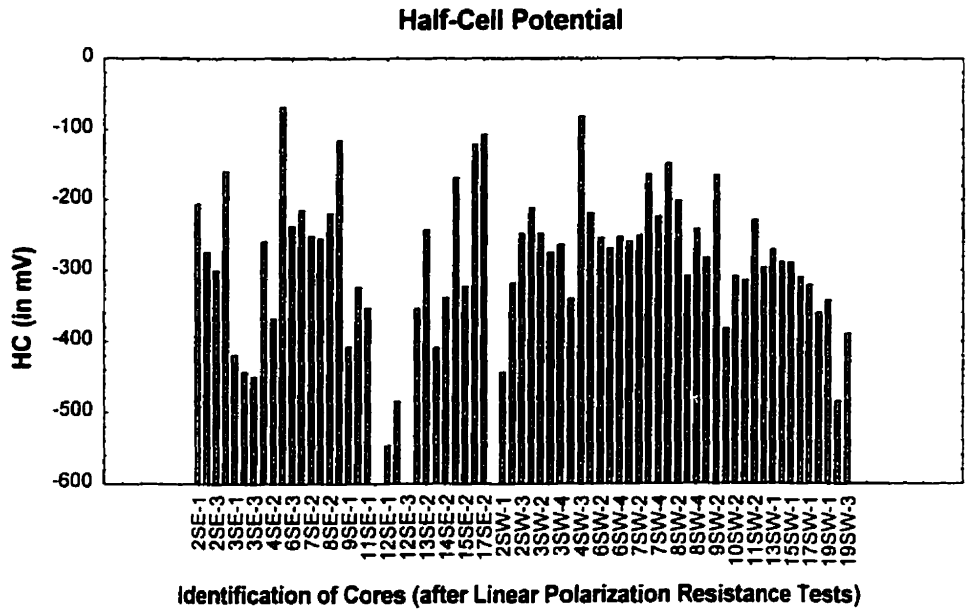

Figure B.10 Bar plot for the half-cell potential (HC).

B.11 Concrete cover (CV)

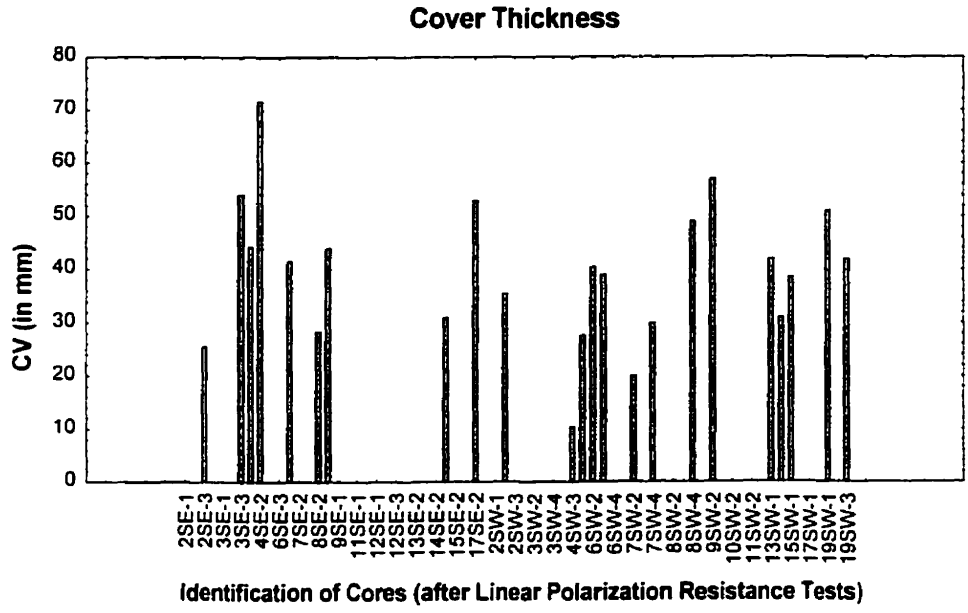

Figure B.11 Bar plot for the concrete cover (CV).

B.12 Corrosion rate (LP_cr)

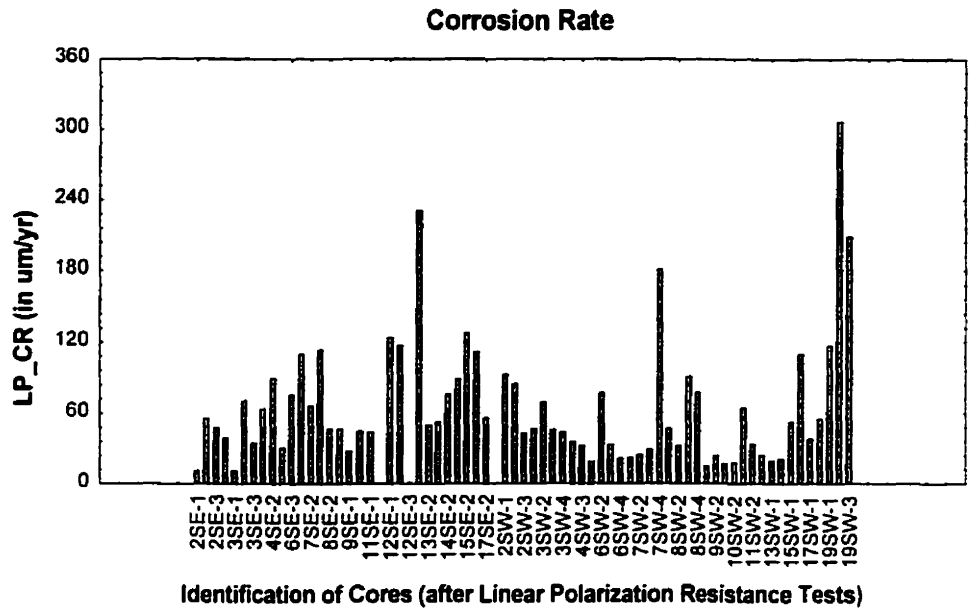

Figure B.12 Bar plot for the corrosion rate (LP_cr).

B.13 Carbonation depth (CR)

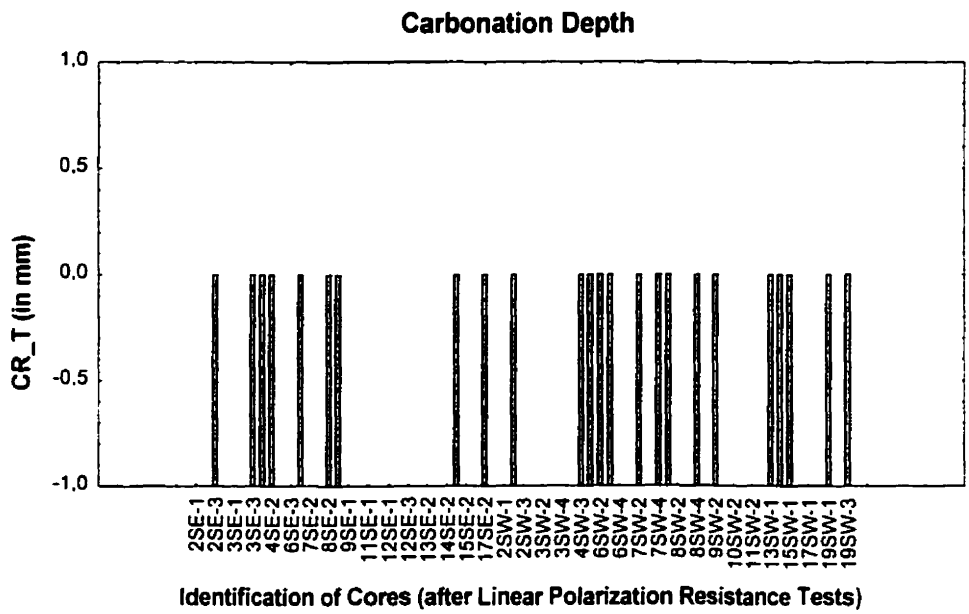

Figure B.13 Bar plot for the carbonation depth (CR).

B.14 Chloride ion concentration at rebar (CC_rb)

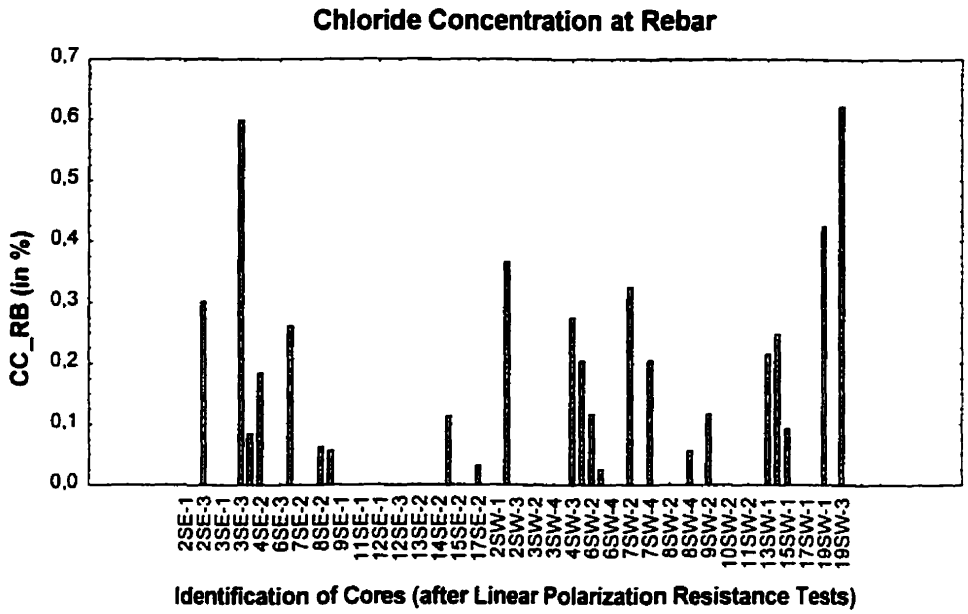

Figure B.14 Bar plot for the chloride ion concentration at rebar (CC_rb).

B.15 Apparent chloride diffusion (CD_a)

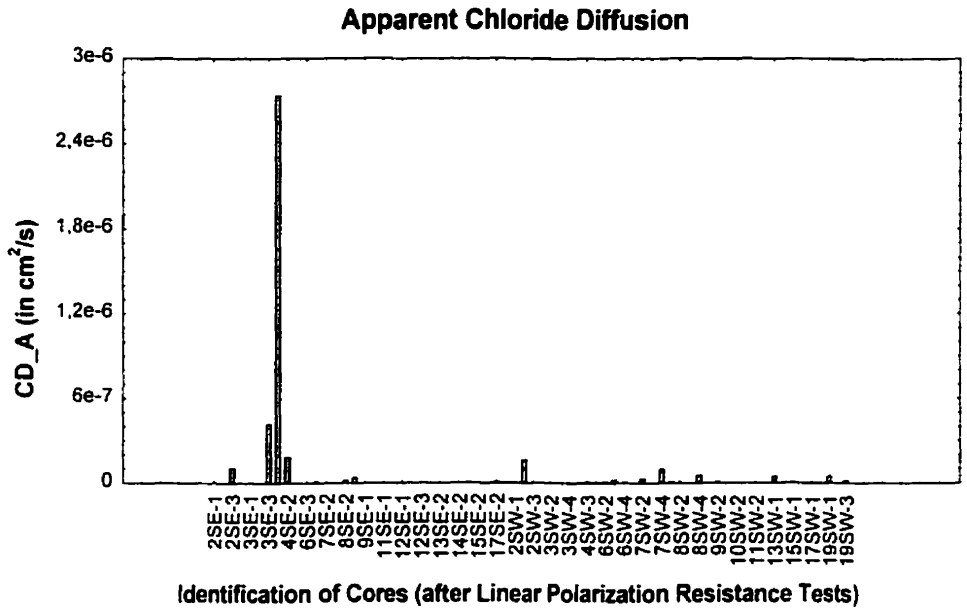

Figure B.15 Bar plot for the apparent chloride diffusion (CD_a).

Appendix C Univariate analysis and results

Appendix C presents the results of the univariate analysis performed on the remaining 14 variables of interest, since the results for the chloride diffusion migration were presented in Chapter Five. The normality and residual plots are presented for all variables, with additional plots being also presented in the cases where the variable was transformed to the log-normal format. Figure C1 to C13 follow :

C.1 In-situ water permeability (WP)

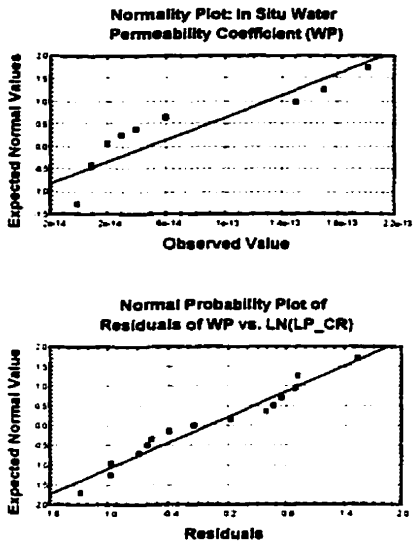

Figure C.1 Normal probability plots of variable (top) and of residuals (bottom). No variable transformation was performed for the in-situ water permeability (WP).

C.2 Electrical resistance (ER)

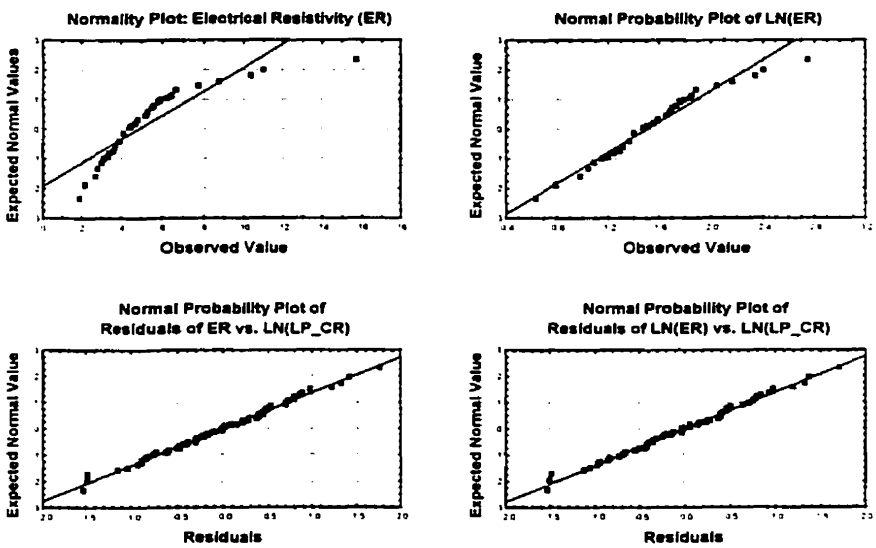

Figure C.2 Normal probability plots of variable (top) and of residuals (bottom) before (left) and after (right) the variable transformation for the electrical resistance (ER).

C.3 Pulse velocity (PV)

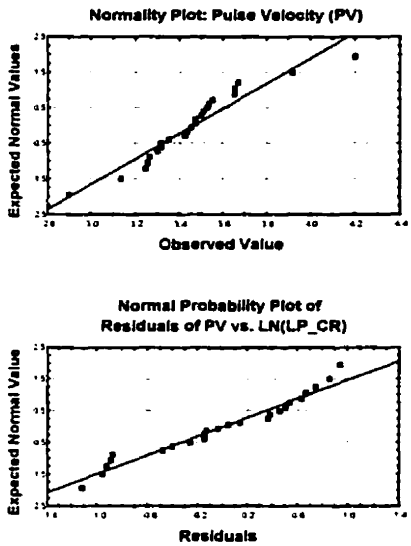

Figure C.3 Normal probability plots of variable (top) and of residuals (bottom). No variable transformation was performed for the pulse velocity (PV).

C.4 Absorptivity after immersion (AB_astm)

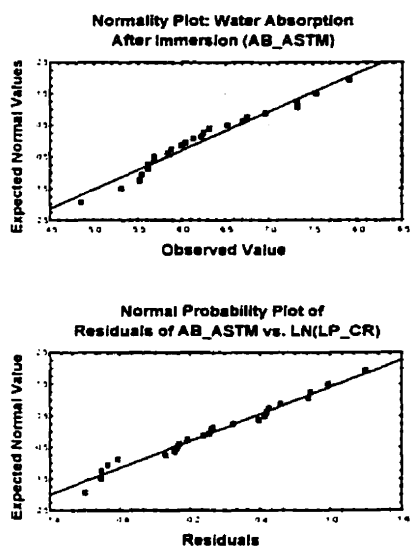

Figure C.4 Normal probability plots of variable (top) and of residuals (bottom). No variable transformation was performed for the absorptivity after immersion (AB_astm).

C.5 Dry density (SD_b)

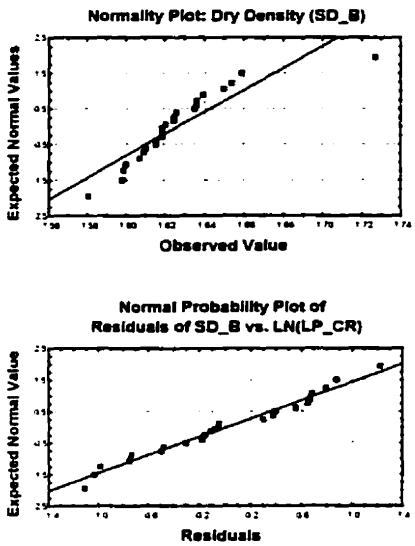

Figure C.5 Normal probability plots of variable (top) and of residuals (bottom). No variable transformation for the dry density (SD_b).

C.6 Volume of permeable voids (VV)

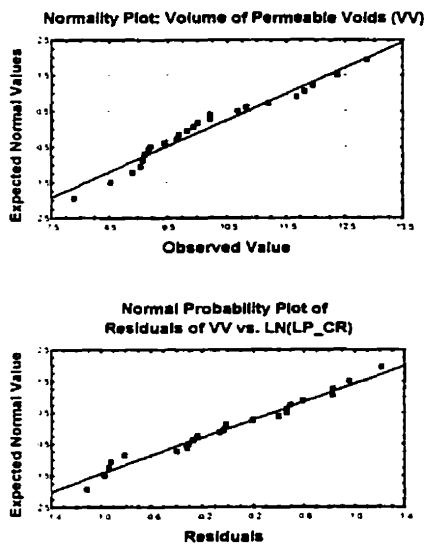

Figure C.6 Normal probability plots of variable (top) and of residuals (bottom). No variable transformation was performed for the volume of permeable voids (VV).

C.7 Compressive strength (CS)

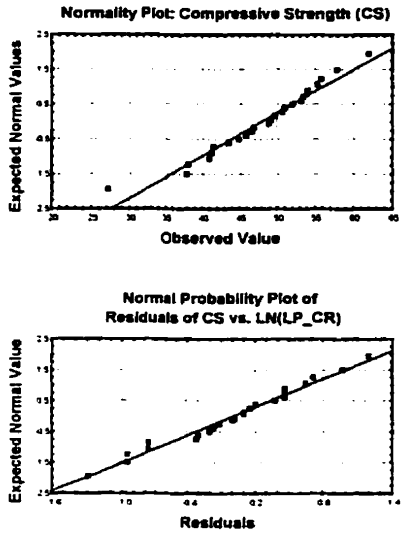

Figure C.7 Normal probability plots of variable (top) and of residuals (bottom). No variable transformation was performed for the compressive strength (CS).

C.8 Modulus of elasticity (E_cs)

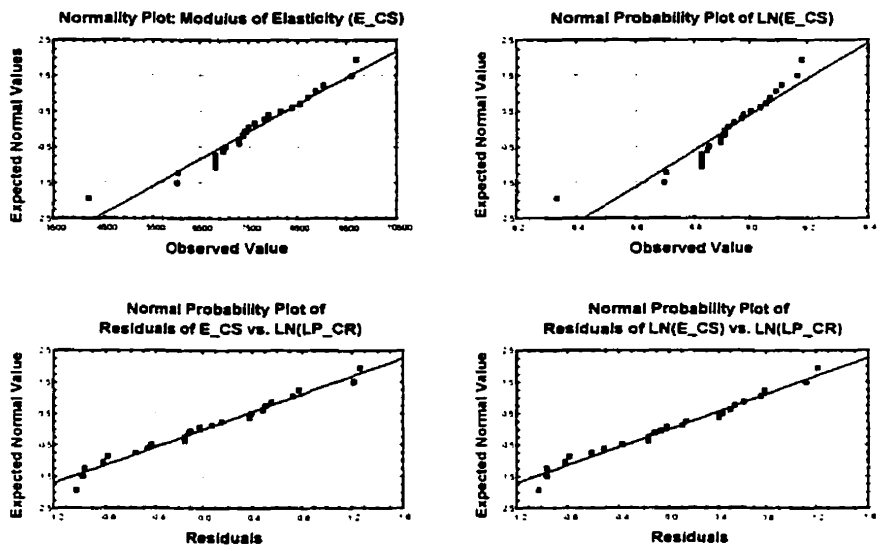

Figure C.8 Normal probability plots of variable (top) and of residuals (bottom) before (left) and after (right) the variable transformation for the modulus of elasticity (E_cs).

C.9 Half-cell potential (HC)

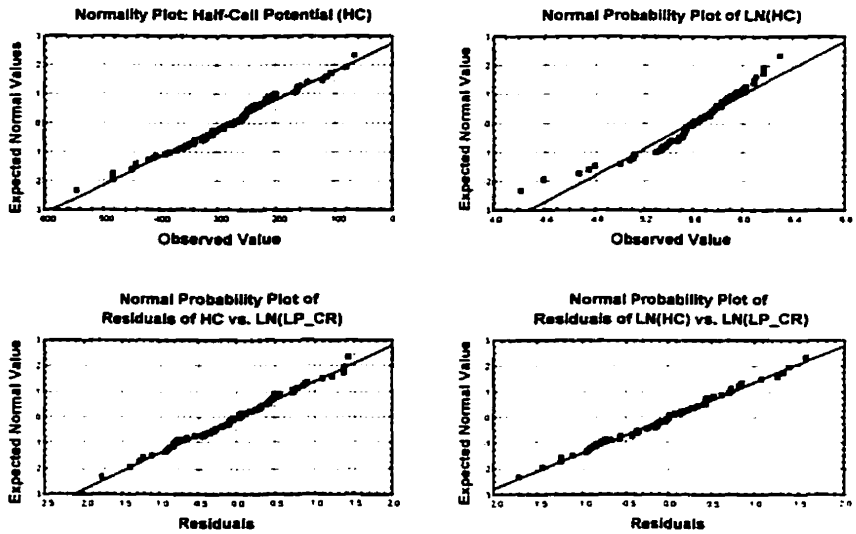

Figure C.9 Normal probability plots of variable (top) and of residuals (bottom) before (left) and after (right) the variable transformation for the half-cell potential (HC).

C.10 Concrete cover (CV)

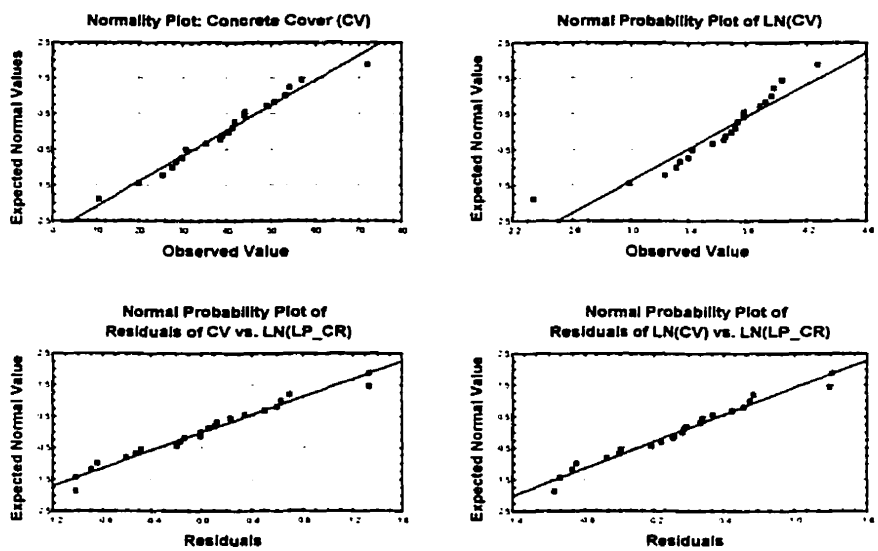

Figure C.10 Normal probability plots of variable (top) and of residuals (bottom) before (left) and after (right) the variable transformation for the concrete cover (CV).

C.11 Corrosion rate (LP_cr)

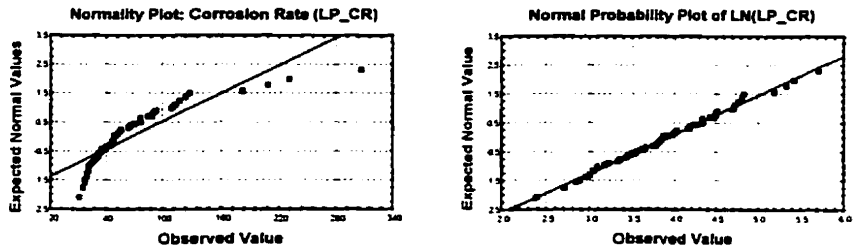

Figure C.11 Normal probability plots of variable (top) before (left) and after (right) the variable transformation for the corrosion rate (LP_cr).

C.12 Carbonation depth (CR)

For the carbonation depth, since no trace of carbonation was found on any of the cores tested, it was not possible to perform the univariate analysis. The descriptive statistics for the carbonation depth test are presented in Table 4.2 of Chapter Four.

C.13 Chloride ion concentration at rebar (CC_rb)

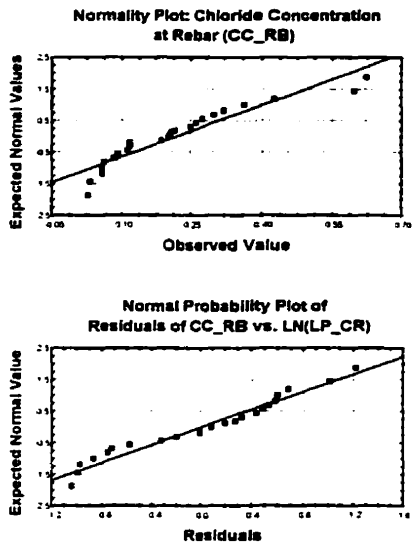

Figure C.12 Normal probability plots of variable (top) and of residuals (bottom). No variable transformation was performed for the chloride ion concentration at rebar (CC_rb).

C.14 Apparent chloride diffusion (CD_a)

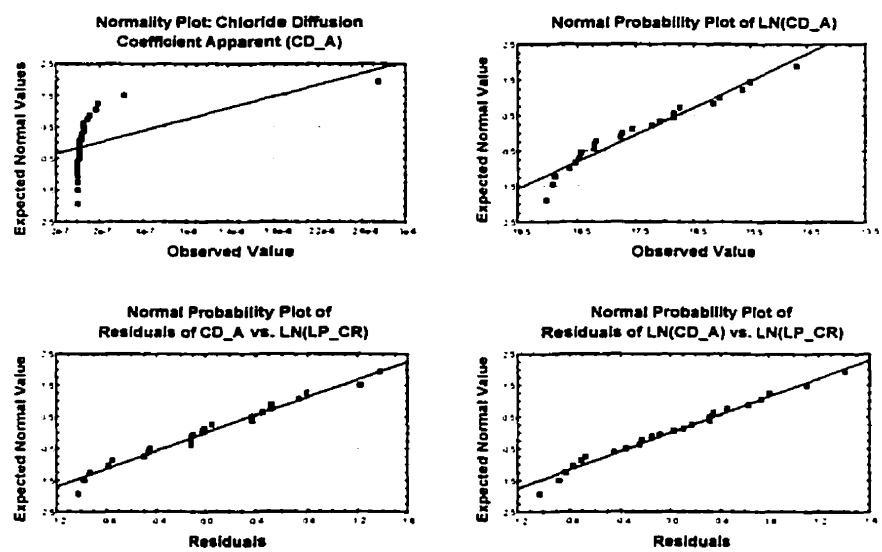

Figure C.13 Normal probability plots of variable (top) and of residuals (bottom) before (left) and after (right) the variable transformation for the apparent chloride diffusion (CD_a).